MICROCOPY RESOLUTION TEST CHART
NATIONAL BUREAU OF STANDARDS-1963-A

FINAL REPORT

AD-A164 514

APPLICATION AND EXTENSION OF AN ANALYTICAL MODEL OF THE CONFINED ACOUSTIC BEAM GENERATED BY A TRANSDUCER

Date: October 1985

Pricipal Investigator

Jerry H. Ginsberg

DTIC
SELECTE
FEB 2 1 1986
D

Sponsored By

**THE OFFICE OF NAVAL RESEARCH
ENVIRONMENTAL SCIENCES DIRECTORATE - CODE 425 UA
GEOPHYSICAL SCIENCES DIVISION**

Under

Contract No. N00014-82-K-0366

GEORGIA INSTITUTE OF TECHNOLOGY
**A UNIT OF THE UNIVERSITY SYSTEM OF GEORGIA
SCHOOL OF MECHANICAL ENGINEERING
ATLANTA, GEORGIA 30332**

DTIC FILE COPY
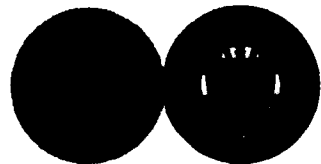
86 2 6 100

FINAL REPORT ON

APPLICATION AND EXTENSION OF

AN ANALYTICAL MODEL OF THE

CONFINED ACOUSTIC BEAM

GENERATED BY A TRANSDUCER

SPONSORED BY

PRINCIPAL INVESTIGATOR:

JERRY H. GINSBERG

PROFESSOR OF MECHANICAL ENGINEERING

GEORGIA INSTITUTE OF TECHNOLOGY

ATLANTA, GEORGIA 30332

TABLE OF CONTENTS

Accesion For	
NTIS CRA&I	☑
DTIC TAB	☐
U announced	☐
Justification	
By *ltr. on file*	
Distribution /	
Availability Codes	
Dist	Avail a d / or Special
A-1	

1

I. BACKGROUND

Numerous evaluations of the acoustic field radiating from a baffled transducer have appeared in the published literature. An important feature is that these theories are applicable for a wide range of parameters. Approximations, such as those describing an axisymmetric sound beam in the far field (Fraunhofer zone) can substantially reduce computational cost, but they are not necessary. Linear theory is valid when the source level is sufficiently low. Even then, diffraction effects in the near field, which lead to localized cancellations and reinforcements, complicate the task of correlating near field measurements to far field propagation properties.

The situation becomes more complicated when one tries to increase the propagation range by raising the source level. It is logical to try to overcome effects such as dissipation and scattering by generating higher level signals. Such attempts inevitably lead to a greater role for nonlinear effects. One of the effects of nonlinearity is to divert energy from the fundamental signal to higher harmonics, which is equivalent to lowering the efficiency of the transducer. In the face of these concurrent effects it is apparent that developing a unified theory for nonlinear effects in sound beams is a challenging matter. However, such a theory is necessary if understanding of the distortion phenomena is to be enhanced. A prime example of the prior lack of insight is the observed differences between the distortion of the compression and rarefaction phases of a signal, which had no analog in simpler types of acoustic waves.

A variety of approaches have been employed to study the effects of nonlinearity in this system. One approach has relied on a conventional perturbation solution of an approximate nonlinear wave equation. Such an analysis seems to give very good results near the transducer face. However, it quickly breaks down with increasing range due to assumptions that are made in the perturbation steps.

An investigation of properties in the far field was developed based on an approximation as a quasi-spherical wave. Such a formulation assumes that the wave arrives at the transition to the far field (e.g. the Rayleigh distance) without substantial prior distortion. Hence, the spherical wave description is inherently limited to cases where the transducer excitation is comparitively low level. This type of analysis also leads to certain anomalies, such as the fact that the level of distortion is dependent on the choice for the spherical transition distance, which may be arbitrarily chosen beyond the Rayleigh distance.

Another approach that has been widely employed in the Russian literature is founded on a version of Burgers' equation that has been modified to account for spreading and diffraction. This nonlinear partial differential equation has been solved numerically for several types of boundary motion. The primary

limitation of this approach are the approximations on which the model equation are based, and computational difficulties stemming from rapid transition due to diffraction. An alternative treatment of this nonlinear parabolic equation based on Fourier series expansions has reduced the computational problems, but quaestions regarding the adequacy of the model equation still remain.

II. RESEARCH TECHNIQUE

The primary goal of this project was to develop an analytical description of transducer radiation in which finite amplitude effects, diffraction, and spherical spreading are treated consistently, without limitation to a speciific spatial domain. The technique employed singular perturbation theory in conjunction with asymptotic analysis.

The general approach uses the King integral in linear theory, which is a Fourier-Bessel integral transform, to develop the second order source terms that generate nonlinearities in the response. There are two kinds of nonlinear effects that arise at the second order. Some produce terms that remain bounded as the signal propagates. (One such effect is associated with the fact that the input from the transducer originates from a moving boundary, rather than the much simpler description, $z = 0$.) The smallness of the acoustic Mach number leads to the conclusion that these fixed magnitude effects cannot account for measured levels of distortion. The other group of nonlinear effects arise from resonance-like phenomena. These terms lead to distortion that grows with increasing distance. Shocks ultimately form from this effect, unless dissipation is adequate to overcome the nonlinear distortion process. It is this cumulative growth effect that needs to be evaluated.

The growth effects in the second order terms are evaluated by using asymptotic integration techniques to identify the portion of the second order terms that grow most rapidly with increasing range. The aforementioned breakdown of conventional (i.e. regular) perturbation solutions is avoided by introducing coordinate transformations that essentially are based on recognition that cumulative growth is a singularity.

This approach was the basis for a variety of studies. Some were devoted to developing efficient numerical algorithms for quantitative evaluation. Others increased the generality of the transducer vibration, including linkage with the effects of elastic behavior. Another group of studies endeavored to obtain insight into the nature of physical processes. These efforts are surveyed below.

III. RESEARCH ACHIEVEMENTS

A. Axisymmetric Monochromatic Excitation

The analysis described in the previous section involved a large effort to place some of the steps on a firm mathematical foundation. This effort has also clarified the physical under-standing of the manner in which a continuous spectrum of modes interact to create distortion. The initial presentation [2] was improved substantially in the published version [6, 7]. Those works compared the analytical results to series of independent measurements. The predictions for amplitude levels of the har-monics were well within the identifiable experimental error. Furthermore, a comparison of waveforms showed that the analysis does describe the different shape of the waveform in the compres-sion and arefaction phases. The comparison also confirmed a change in this asymmetry associated with the transition from the near field to the far field. No prior analysis had anticipated this phenomenon.

The original version of the computer program for this model was quite inefficient. It required a relatively large amount of computer memory and long execution times. Of even greater con-cern was the dependence of the analysis on a hypothesis regarding the nature of the distortion process far from the axis in com-parison to very close to the axis. Both matters were effectively treated by a recently completed Ph. D. thesis [12, 14]. That work developed independent solutions in each region by using different asymptotic approximations. The signal in the paraxial region was found to behave like a spectrum of quasi-planar waves, whereas the off-axis signal was found to consist of spectra of inward and outward propagating conical waves. The individual responses were then matched to obtain uniformly accurate expressions. Significantly, the results agreed with the earlier mathematical forms. A key benefit of the analysis was that the new perspec-tive led to a Fourier series representation that decreased computational time by as much as a factor of one hundred.

This improved computational power was exploited to test the theoretical predictions against several prior series of measurements. The agreement was generally very close, with one exception. Experiments by Gould in the late 1960's investigated the signal very close to the transducer face at a high reduced frequency, $ka = 114$. The measured second harmonic distribution was quite different from the theory. This discrepancy is now under investigation. Current indications are that the dis-crepancies between theory and measurement correspond to the second order terms that are discarded in the analysis because they have minor influence far from the transducer.

The ease with which computations could be performed made it possible to generalize the nature of the excitation. A study of particular interest considered the case where the transducer is actually a membrane that is subjected to steady-state harmonic excitation [11]. The response of the membrane and the surface

4

pressure are fully coupled in this situation. The analysis of the finite amplitude sound beam was combined with a vibration analysis of the membrane to determine all aspects of the response. It was shown that the vibration analysis could be safely performed without recourse to nonlinear theories for the acoustic signal, but that the acoustic signal required knowledge of the effects of nonlinear elasticity when the excitation was at a system resonance.

B. Nonsymmetric Monochromatic Excitation

The recent analysis of axisymmetric waves [12] also considered a situation in which the transducer vibration consists of the superposition of an axisymmetric component and an azimuthally travelling nonsymmetric part. The latter corresponds to a spatially phased rocking motion that resembles the wobbling of a rolling coin as it falls to the ground. The analysis was much like that for the axisymmetric case. One benefit of the greater generality was a clarification in the task of matching the off-axis and paraxial signals. This study is apparently the first to address nonsymmetric finite amplitude sound beams. Indeed, nonsymmetric situations have not been extensively explored in the linear case. It was shown that because azimuth dependent signals must vanish along the beam axis, the interaction with axisymmetric effects cannot affect the signal on-axis.

C. Dual Frequency Axisymmetric Excitation

A major generalization was achieved in analyses of the propagation of a signal generated by axisymmetric excitation at two arbitrary frequencies. In the limit as the difference between these primary frequencies decreases, one obtains a parametric array. The analysis followed the line of investigation originally developed for the single frequency case. The initial study of harmonic formation [5] identified the mechanism by which the primary signals interact, but it was limited to very short ranges. The innovative aspects of the subsequent research [13, 15] was in the identification of the approrpriate set of coordinate transformations. It is such properties that represent the actual interaction effects. It was shown that the distortion of each primary signal is dependent in equal part on the signal in both primaries.

The analytical results were prohibitive for extensive numerical evaluation, particularly at long ranges. For this reason, an interface with a spherical propagation model was developed. The same type of interface had been explored earlier for monochromatic waves [4], but had been abandoned when the Fourier series form of that signal was identified. The remarkable aspect of the dual frequency study was that it showed far better agreement than earlier theories with a variety of prior experiments on parametric arrays. It even reproduced features in

5

the difference frequency signal that had earlier seemed to be anomolous.

D. Validation

An initial series of experiments was performed by Dr. Mark Moffett in July 1982 at the NUSC facility at Newport, Rhode Island in order to obtain data for a comparison with the theoretical model [1]. Agreement between theory and experiment for amplitudes of the harmonics was reasonably good. The hydrophones employed for measurement showed substantial irregularity in their frequency response and no phase calibration was performed. The discrepancies between theory and experiment were shown to be less than the uncertainty in the response of the transducer.

In September 1983, Moffett endeavored to improve his measure ments by resurrecting the special purpose transducers that were utilized by Browning and Mellen. The data was sent to Georgia Tech in its original digital form in order to provide a complete data base for comparison. There was a great deal of difficulty in reading the tapes due to limitations of the available equipment. Eventually, the data were displayed as waveforms and analyzed for frequency content.

As the data was being analyzed, it became apparent that the receiving hydrophone exhibited extremely anamolous behavior at high sound pressure levels, such as third harmonic levels that execeeded the second, and fourth harmonics that exceeded the third. The causes of this behavior that have not yet been identified. However, an extremely important verification was obtained at a far field location. The signal there had decayed to a level that seemed to be within the tolerance of the receiver, even though the source was being driven to a high amplitude--it was found that the measured and predicted signals coincided at that location [8].

E. Other Viewpoints

A key aspect of the King integral for linear radiation is that it treats the signal as a superposition of a continuous spectrum of modes. The physical significance of the nonlinear interaction of these modes is obscured by the lack of a discrete mode that could be traced through the anaalysis. The continuous spectrum of modes in the King integral arises because the baffled system is essentially a circular wave guide of infinite diameter.

A finite diameter waveguide has a discrete spectrum of modes. By exciting only one such mode in a linear sense, it would be possible to follow closely the manner in which resonant interactions take place nonlinearly. Analyses of this problem in circular [3] and two-dimensional waveguides [9, 10] followed steps that were suggested by the analysis of sound beams. In the

circular geometry the modes excited by the nonlinearities were similar to the directly excited one. As a result, all of the harmonics were in phase. This is manifested by identical types of distortion for the compression and rarefaction phases of a signal.

The two-dimensional study disclosed the existence of an internal resonance that had not been identified in earlier investigations. Specifically, it was found that the transverse variation nonlinearly excites the planar mode, as well as second and higher spatial harmonics. At high frequencies, the phase speeds of the various modes coalesce, which results in nonlinear dispersive interaction between the modes. Significantly, the signal in this case was shown to be display waveform distortion of the type observed in sound beams. This verifies the nonlinear King integral approach to sound beams, which treats the signal as the dispersive interaction of neighboring modes in an infinite waveguide.

F. Parameter Studies

The main computer program for sound beams was modified to provide predictive capabilities for an assortment of transducer vibration patterns $f(R)$. Propagation curves showing the dependence of the amplitudes and phase angles in the region from the transducer to the far field have been carried out [8, 11, 14] for a piston transducer, in which the particle velocity across the piston face is uniform. Results for a hypothetical transducer, in which the pressure is uniform across the face, were also obtained, because that had been the basis for studies using the modified Burgers' equation. Another configuration receiving consideration was the elastic membrane, in which case the pattern for the transducer vibration is a Bessel function.

The effect of diffraction decreases with the progression from the piston to the membrane configuration because spatial transitions are less severe. It was found that, although the fundamental frequency signal inside the Rayleigh length is substantially different between the cases of uniform particle velocity and pressure, the second and higher harmonics were quite close. In the membrane case, the rapid spatial variations in the fundamental were substantially reduced, and the higher harmonics varied quite smoothly. This could prove to be useful for applications requiring near field measurements.

A noteworthy aspect of this study is the fact that there had been no prior extensive evaluations of phase shifts for the higher harmonics in the near field and the transition region. The evaluations revealed an interesting trend for the phase angles. The higher harmonics are close in phase to the fundamental near the source. As the wave propagates, each harmonic tends to lag further behind its predecessor, until there is a 90° phase difference in the far field. This is significant because a true spherical wave also undergoes a 90° phase shift in the transition

from the near field to the far field. The implication of this observation is that asymmetrical distortion results from spherical transitions for higher harmonics which are delayed by the higher frequencies.

IV. CHRONOLOGICAL LISTING OF PROJECT PUBLICATIONS AND PRESENTATIONS

1. M. B. Moffett and J. H. Ginsberg, "Finite amplitude waveforms produced by a piston projector," J. Acoust. Soc. Am. 72 , S40 (1982); presented at the 104th Meeting of the Acoustical Society of America, Orlando, Florida (9-12 November 1982).

2. J. H. Ginsberg, "An Improved King integral for finite amplitude sound beams", J. Acoust. Soc. Am. 73 , S82 (1983); presented at the 105th Meeting of the Acoustical Society of America, Cincinnati, Ohio (9-13 May 1983).

3. J. H. Ginsberg and H. C. Miao, "Finite amplitude wave propagation in a cylindrical waveguide," 11th International Congress on Acoustics, Paris, France (19-27 July 1983).

4. J. H. Ginsberg, "Transition from the nonlinear King integral to spherical propagation for a finite amplitude sound beam," J. Acoust. Soc. Am. 74, , S24 (1983); presented at the 106th Meeting of the Acoustical Society of America, San Diego, California (7-11 November 1983).

5. M. A. Foda and J. H. Ginsberg, "Analysis of nonlinear harmonic generation for arbitrary dual frequency transducer excitation," J. Acoust. Soc. Am. 75 , S92 (1984); presented at the 107th Meeting of the Acoustical Society of America, Norfolk, Virginia (7-10 May 1984).

6. J. H. Ginsberg, "Nonlinear King integral for arbitrary sound beams at finite amplitude - I. Asymptotic evaluation of the velocity potential," J. Acoust. Soc. Am. 76 , 1201-1207, 1984).

7. J. H. Ginsberg, "Nonlinear King integral for arbitrary sound beams at finite amplitude - II. Derivation of uniformly accurate expressions," J. Acoust. Soc. Am. 76 , 1208-1214, 1984).

8. J. H. Ginsberg, "Evaluation of the Overall Sound Field Properties of Finite Amplitude Sound Beam," 108th Meeting of the Acoustical Society of America, Minneapolis, Minnesota (8-12 October 1984).

9. H. C. Miao and J. H. Ginsberg, "Finite Amplitude Distortion and Dispersion in a Hard-Walled Waveguide," 109 th Meeting of the Acoustical Society of America, Austin, TX, April 9-12, 1985.

10. H. C. Miao and J. H. Ginsberg, "Finite Amplitude Distortion and Dispersion of a Symmetric Mode in a Waveguide", submitted to J. Acoust. Soc. Am., 1985.

11. J. H. Ginsberg, "Finite Amplitude Sound Beams Resulting from Nonlinear Vibration of a Circular Membrane Undergoing Axisymmetric Resonant Excitations," Proc. of IUTAM Symposium on Aero and Hydro-elasticity, Lyon, France, July, 1985.

12. H. C. Miao, "Analysis of Nonsymmetric Effects in Finite Amplitude Sound Beams," Ph.D. thesis, Georgia Inst. of Tech., 1985.

13. M. A. Foda, "Propagation and Interaction of Finite Amplitude Acoustic Waves Generated by a Dual Frequency Transducer," Ph.D. thesis, Georgia Inst. of Tech., 1985.

14. H. C. Miao and J. H. Ginsberg, "Fourier Series Representation of Finite Amplitude Sound Beams," 110 th Meeting of the Acoustical Society of America, Nashville, TN, November 4-8, 1985.

15. M. A. Foda and J. H. Ginsberg, "Finite Amplitude Acoustic Waves Generated by a Baffled Dual Frequency Transducer", 110 th Meeting of the Acoustical Society of America, Nashville, TN, November 4-8, 1985.

THE JOURNAL

of the

Acoustical Society of America

Program of the
104th Meeting

WEDNESDAY MORNING, 10 NOVEMBER 1982

DADE AND FLORIDA KEYS ROOMS, 8:45 TO 10:50 A.M.

Session V. Physical Acoustics IV: Nonlinear Acoustics

9:35

V4. Finite-amplitude waveforms produced by a circular piston projector.
Mark B. Moffett (Naval Underwater Systems Center, New London, CT
06320) and Jerry H. Ginsberg (Georgia Institute of Technology, Atlanta,
GA 30332)

Measurements were made of the waveforms produced at six different
locations on the axis of a 0.51-m-diam projector driven at 60 kHz in the
NUSC/Newport large acoustic tank facility. The locations were at the
last three pressure maxima in the nearfield, a quasifarfield point at 5 m,
and two farfield positions at 10 m and 15 m. The projector was driven at
several levels, and yielded waveforms ranging from sinusoidal at the low-
est levels and shortest ranges to shock formation at the highest levels and
longer ranges. Two different hydrophones were used, but neither had a
flat enough response to avoid ringing when shocks were present. The
waveforms exhibit the asymmetry (sharp pressure peaks and rounded
pressure troughs) previously observed by Browning and Mellen [J.
Acoust. Soc. 44, 644–646 (1968)] and predicted by recent work of Gins-
berg which accounts for diffraction as well as nonlinear propagation ef-
fects. [Work supported by ONR Code 425 UA.]

Sheraton Twin Towers
Orlando, Florida
8–12 November 1982

FINITE AMPLITUDE WAVEFORMS PRODUCED
BY A CIRCULAR PISTON PROJECTOR

MARK B. MOFFETT
Naval Underwater Systems Command
New London, CT 06320

JERRY H. GINSBERG
Georgia Institute of Technology
School of Mechanical Engineering
Atlanta, Georgia 30332

presented at the

104 th Meeting of

THE ACOUSTICAL SOCIETY OF AMERICA

Orlando, Florida
November 9 - 12, 1982

I would like to describe some work Mark Moffett and I have been doing with finite-amplitude waveforms in cases where diffraction occurs. No doubt you are all aware of what happens to one-dimensional finite amplitude waves, such as plane waves or spherically-spreading waves. In such cases, the pressure peaks travel slightly faster than the troughs, and it is an easy matter to predict the waveform via weak-shock theory. For example, a waveform which is initially sinusoidal distorts in an antisymmetric way and eventually can become a sawtooth shape because the peaks move as far ahead as the troughs lag behind. A much more difficult problem is the prediction of the waveforms resulting when diffraction is present, as in the nearfield of a piston projector. The propagation is not one-dimensional. It is no longer a simple matter to follow a pressure signal as it propagates from one point in space to another, because the diffracted field at any point results from contributions from several source regions.

Diffracted fields are normally calculated via linear theory, and so nonlinear effects like distortion can't be handled readily. We have been working at Georgia Tech on a new approach which can account for diffraction and nonlinear distortion simultaneously, under an ONR contract. We needed some experimental data for comparison with the theory for the case of a circular piston projector. Mark Moffett was asked to see if he could provide some data. I will show you some of those results shortly.

<< Viewgraph 1 - Browning and Mellen Waveforms >>

First, I'd like to show the kind of thing that happens when
diffraction and distortion operate together. These pictures are
from a 1962 letter to the editor by Browning and Mellen. They used
a tiny, 8/10ths-of-a-millimeter-diameter microprobe as a hydrophone
and looked at the waveforms on the axis of a 40-centimeter square
projector driven at 150 kHz. The top left picture shows the
waveforms measured at three different levels at the longest range,
which was 8 meters. Then the next two photos down the left hand
side and the three down the right hand side show the progressive
distortion of the pressure waveform as the range was increased from
1 meter to 5 meters.

Positive pressure is up in these pictures, and so you can see
that the pressure peaks are sharp while the troughts become rounded.
In other words, we are not evolving toward the sawtooth shape which
would be expected for plane or spherical waves. Diffraction and
geometric dispersion shift the phase of the harmonics relative to
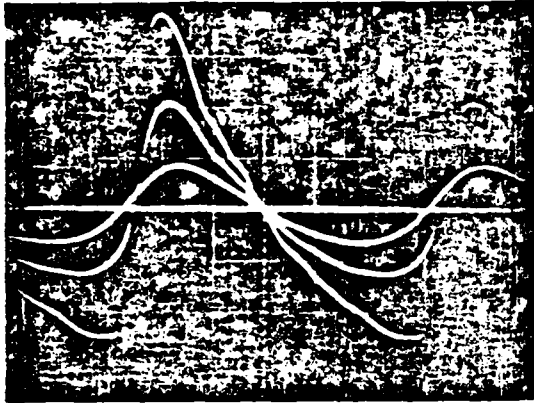the fundamental.

Slide 1

FIG. 4. Pressure waveform at 8 m as a function of P_0. $P_0 = 1$ bar max.
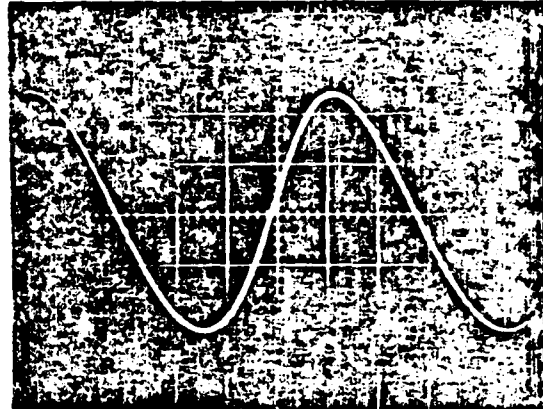

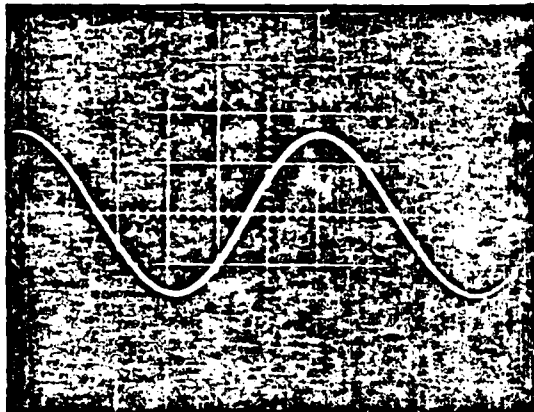FIG. 7. Waveform at 3 m ($P_0 = 0.5$ bar).

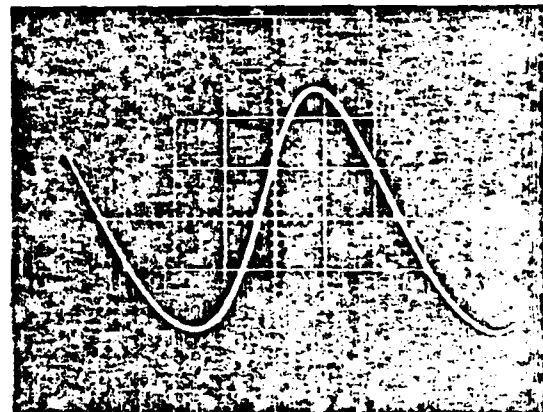FIG. 5. Waveform at 1 m ($P_0 = 0.5$ bar).

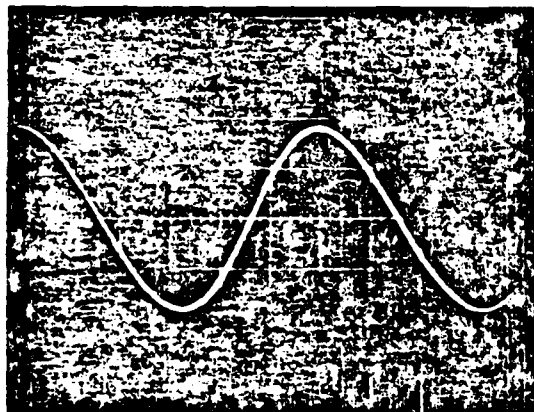FIG. 8. Waveform at 4 m ($P_0 = 0.5$ bar).

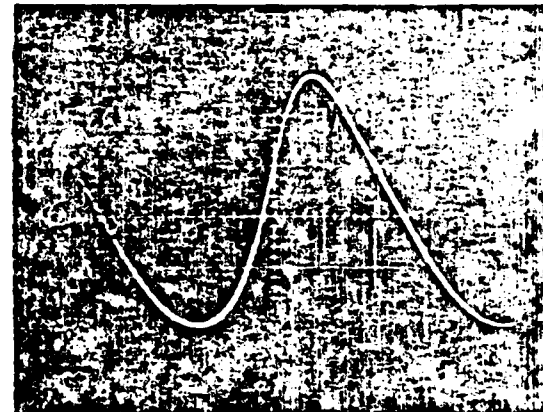FIG. 6. Waveform at 2 m ($P_0 = 0.5$ bar).

FIG. 9. Waveform at 5 m ($P_0 = 0.5$ bar).

so as to minimize wall reflections. For the projector dimensions and wavelength of this experiment, the Fresnel zone extends to about 4 m but the Fraunhofer zone spreading is quite insignificant over the remaining tank length.[1] The hydrophone is then set on the projector axis, and waveform observations are made at appropriate distances.

Figure 3 gives a comparison of two waveforms; the more sinusoidal one was measured at 2 m and the more distorted, at 8 m. The initial peak pressure P_0 measured at 1 m was approximately 1 bar. The oscillations on the trailing side of the 8-m trace are artifacts caused by "shock" excitation of hydrophone resonances that fall above the useful frequency range.

<< Viewgraph 2 - Block Diagram >>

Unfortunately, we couldn't use the Browning and Mellen data for comparison with the theory, because the theory hasn't been worked out yet for a square projector, which is a three-dimensional problem. We therefore decided to repeat the experiment using a circular projector. The projector was a 20-inch-diameter array of 60-kHz tonepiltz elements made by Raytheon Sub Signal Division. The projector was driven with 60-kHz pulses which were amplified with one of Bill Konrad's 20-kilowatt drivers. The hydrophone output was captured with a Biomation transient recorder, which is actually a digital machine containing an A-to-D converter. After capturing and storing the waveform, it was plotted on an X-Y recorder. The experiment was done at NUSC/s large tank facility at Newport, Rhode Island.

It would have been nice if we could have used one of the Browning and Mellen microprobe hydrophones, but we would have had to operate the projector just below the surface. Also, we weren't sure any of the probes were still working. We tried three different hydrophones, hoping that one of them would have a flat enough response to accurately reproduce the waveform. The first was an LC-5 hydrophone, made by Celesco, or what used to be Atlantic Research. The LC-5 is a 1/16th-inch cylinder. It is just about the smallest commercially-available hydrophone there is. The second was lent to us by Gerry Harris of the Bureau of Radiological Health. It consisted of a polymer membrane stretched over a metal hoop. This hydrophone turned out not to be useful below a megahertz, apparently, because of resonances involving the supporting hoop.
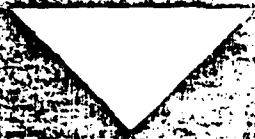
X-Y recorder

transient recorder

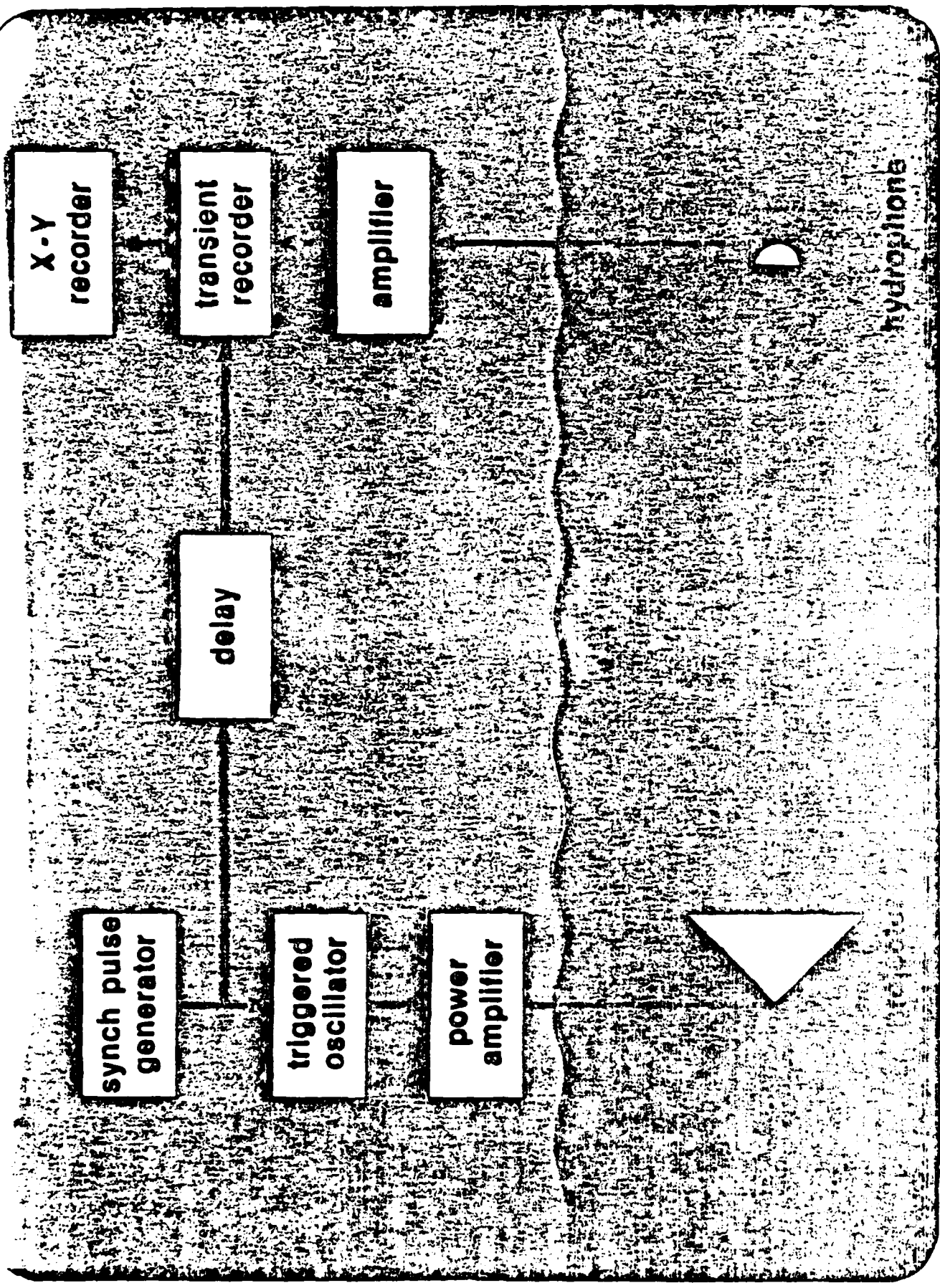amplifier

delay

synch pulse generator

triggered oscillator

power amplifier

hydrophone

The third hydrophone we had was also a polymer-type used in
medical ultrasonics, but in this case the polymer is backed with
a silicone rubber absorber. This hydrophone was made by the
Raytheon Research Division and lent to us by Roger Tancrell and
Dave Wilson. This is a plot of its sensitivity and you can see
that it's not bad, but it's not really flat either. Nevertheless,
the Raytheon hydrophone turned out to be the best of the three.

Slide 3
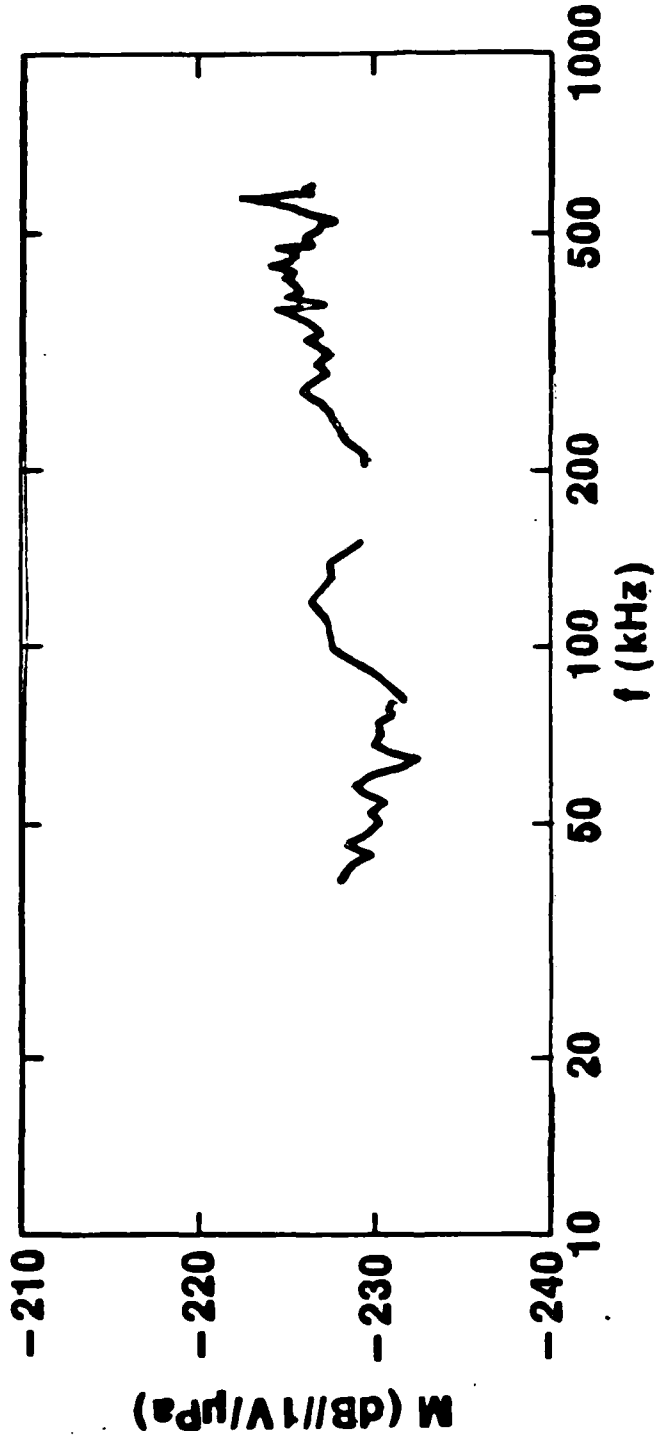
<< Viewgraph 4 - Waveforms at $2.63\,m$>>

Here are some typical results. They are waveforms on the
projector axis at 5 meters. The waveforms correspond to
approximately 10-dB increments in drive. The receiving amplifier
was also changed in 10-dB steps to make the signal levels
comparable. Positive pressure is up in these plots.

You can see that the waveform goes from nearly sinusoidal
at the lowest level (shown in black) to a form with sharp peaks
and rounded troughs (shown in red).

You can also see that the zero crossings on the ascending
part of the wave shifts back as the level increases. In contrast,
zero crossings are unchanged in one-dimensional waves. The rise
in the peak pressure which accompanies the narrowing of the
compression phase is consistent with conservation of momentum,
as is the broader and shallower form of the rarefaction phase.

Slide 4
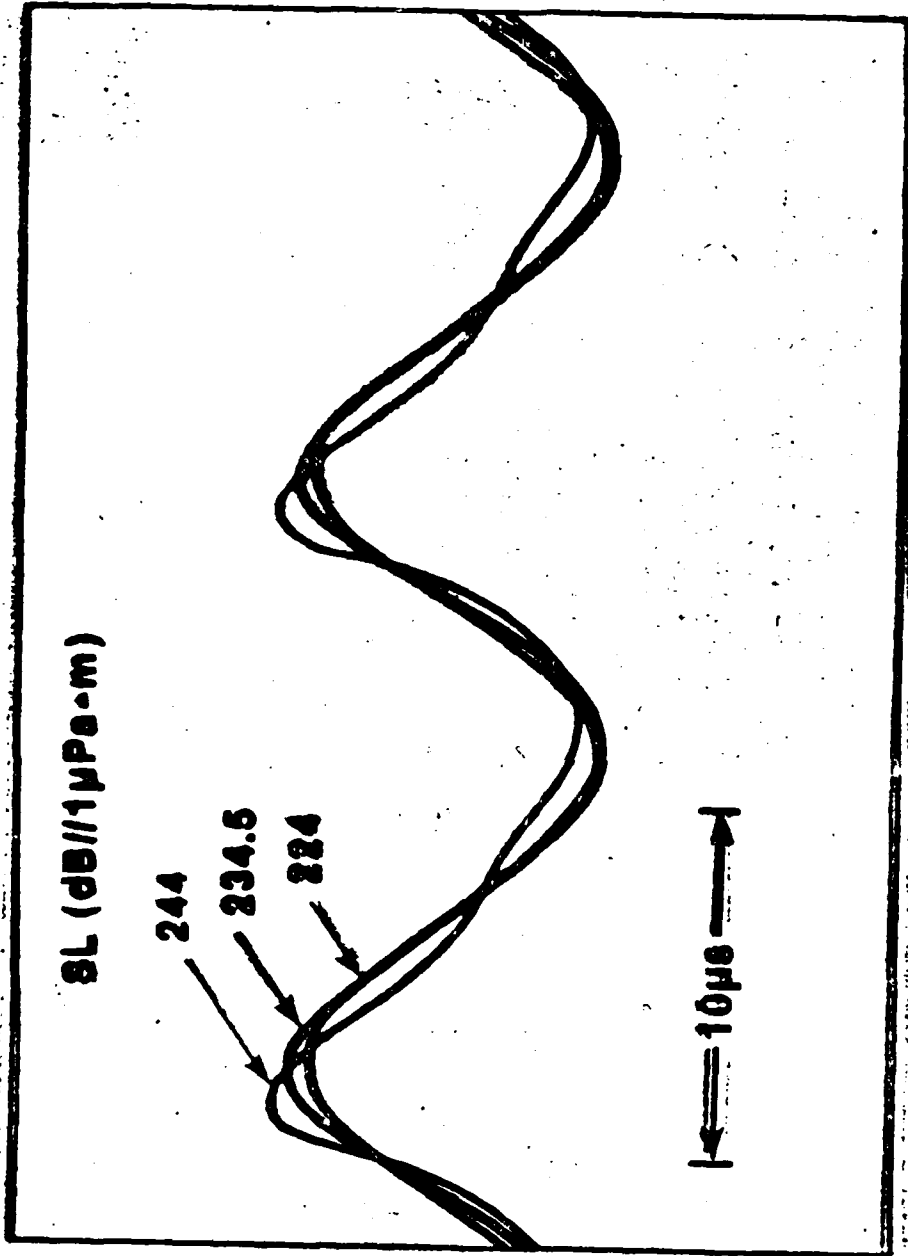
This shows how the waveform evolves with increasing range
from half a meter to a little over 15 meters from the projector.
All measurements were made on the projector axis. The upper
three waveforms were taken at axial maxima. (Probing was done
to make sure that they were maxima). The 5-meter point is
beyond the last axial maximum at 2.63 meters, but is not yet
in the true farfield. The 10 and 15 meter distances do qualify
as genuine farfield measurements.

These plots are for a source level of approximately 243 dB
with respect to one micropascal-meter. You can again see the
sharpening of the peaks and the rounding of the troughs as the
propagation distance is increased. Each plot begins at an
instant where the pressure is zero. You can see that the first
zero crossing moves back in retarded time as the range increases.
I should explain that the zero of the retarded time was determined
by referring to the signal at a very low drive level, where it was
sinusoidal.

In order to be sure that the nonlinear distortion we measured
was not due to hydrophone nonlinearity, we determined the second
order sentitivity in a subsequent measurement. It was low enough
that we didn't have to worry about it. Also, we can see that the
waveform close to the projector is nearly sinusoidal. Since the
highest levels were measured at short ranges, the short-range
waveforms would be more distorted than those farther away if the
hydrophone were behaving in a nonlinear way.

Slide 5
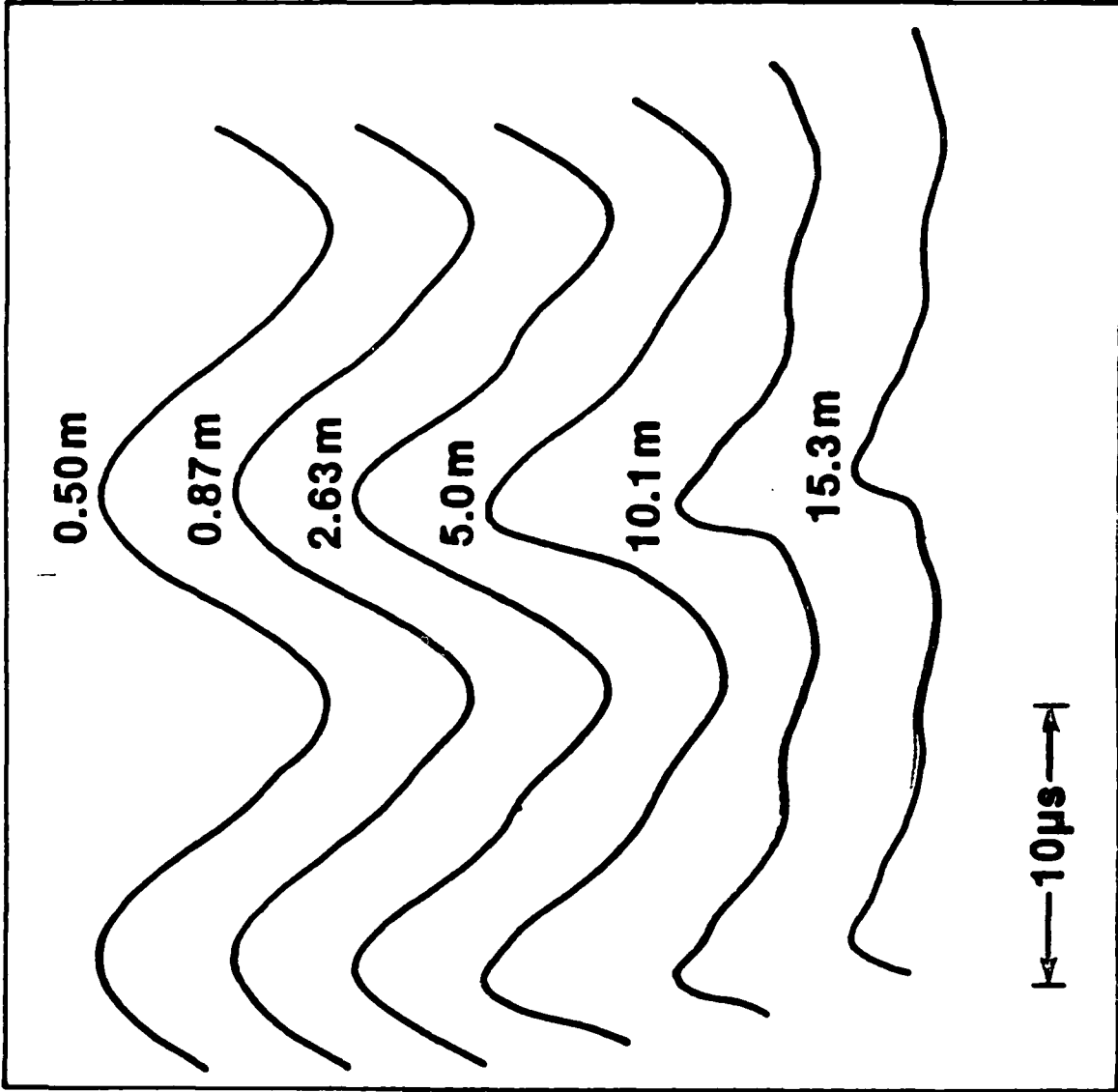
<< Viewgraph 6 - Raytheon and LC - 5 Waveforms >>

Unfortunately, since we did not have a hydrophone with a flat
response from 60 kHz to 600 kHz or so, we did not know that the
hydrophone did not introduce some artifacts into the signal. Here
is a comparison of the Raytheon hydrophone (the solid curve) and
the LC-5 (the dotted curve) at the highest source level and longest
range.

The sharp rise corresponds to the formation of a shock. There
is some ringing just after the shocked portion of the LC-5, so the
Raytheon seems to have done a better job. However, the analytical
results indicate that the secondary lump on the Raytheon hydrophone
waveform is a result of the second harmonic (120 kHz) emphasis in
the hydrophone response.

In computing results of the analytical model, we found that
the computational time to evaluate the diffraction integral
became excessive at the larger distances. Also we encountered
convergence difficulties at the larger distances. Accordingly,
we focused on the predictions for the smaller ranges.

Slide 6

HYDROPHONE OUTPUT

TIME

10μs
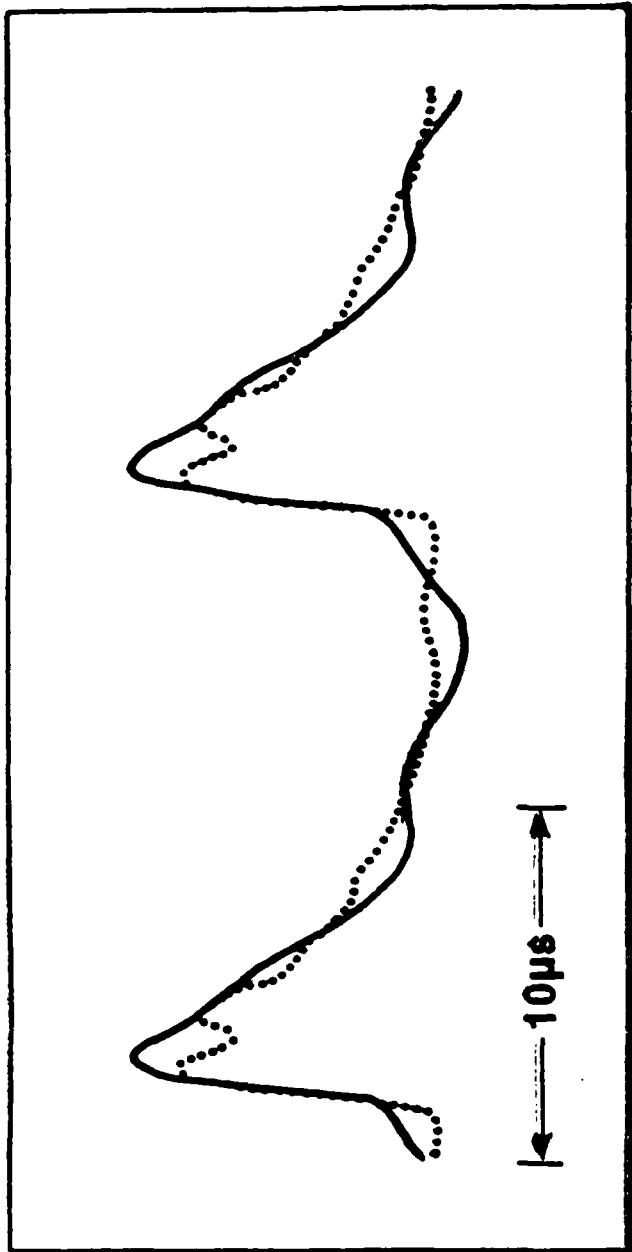
<< Viewgraph 7 - Computed Waveform >>

Here is a comparison of the computed waveform (shown in black) and the measured one (shown in red) at 2.63 meters. The irregularities in the analytical result arise from nonconvergence, but the results are reliable at most time instants. I should mention that this is pretty much the worst case. The other computed waveforms were much more regular.

When we compare this result to the measured waveform we note some significant discrepancies. However, we must also account for the hydrophone response. We did not have a phase calibration for the Raytheon. Instead, we wrote a microcomputer program that describes the analytical result in terms of its frequency response.

Analytical Prediction
Raytheen probe @ 2.63m

―― Measured
━━ **Computed**
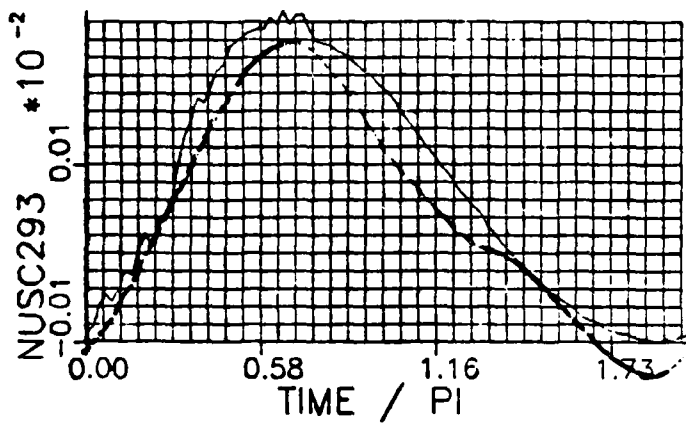
<< Viewgraph 8 - Frequency Response >>

A Fourier analysis of the computed waveform was used to
reconstruct the signal from the lowest five harmonics. This is
the green curve. Using the known amplitude sensitivity and
modifying the relative phases of the harmonics yielded the
result shown in black. For comparison, the experimental result
is shown in red. The agreement with the measured signal is remarkably
good.

Similar analyses for the other cases indicated that the
theory over-predicts the distortion very close to the source,
but it seems to be quite accurate beyond one transducer
diameter.

Correction for Frequency Response

NUSC 2.9.3

#	ORIG AMPL	CORR FACTOR	ORIG LAG	ADDED LAG
1	1.821E-04	1	135.183	-43
2	3.8496E-05	1.41253755 3 dB	200.552	-92
3	1.0379E-05	.891250938 -1 dB	251.197	-30
4	3.6679E-06	1.25892541 2 dB	344.974	-75
5	1.6637E-06	1.49623566 3.5 dB	55.1545	-40

POLARITY = 1
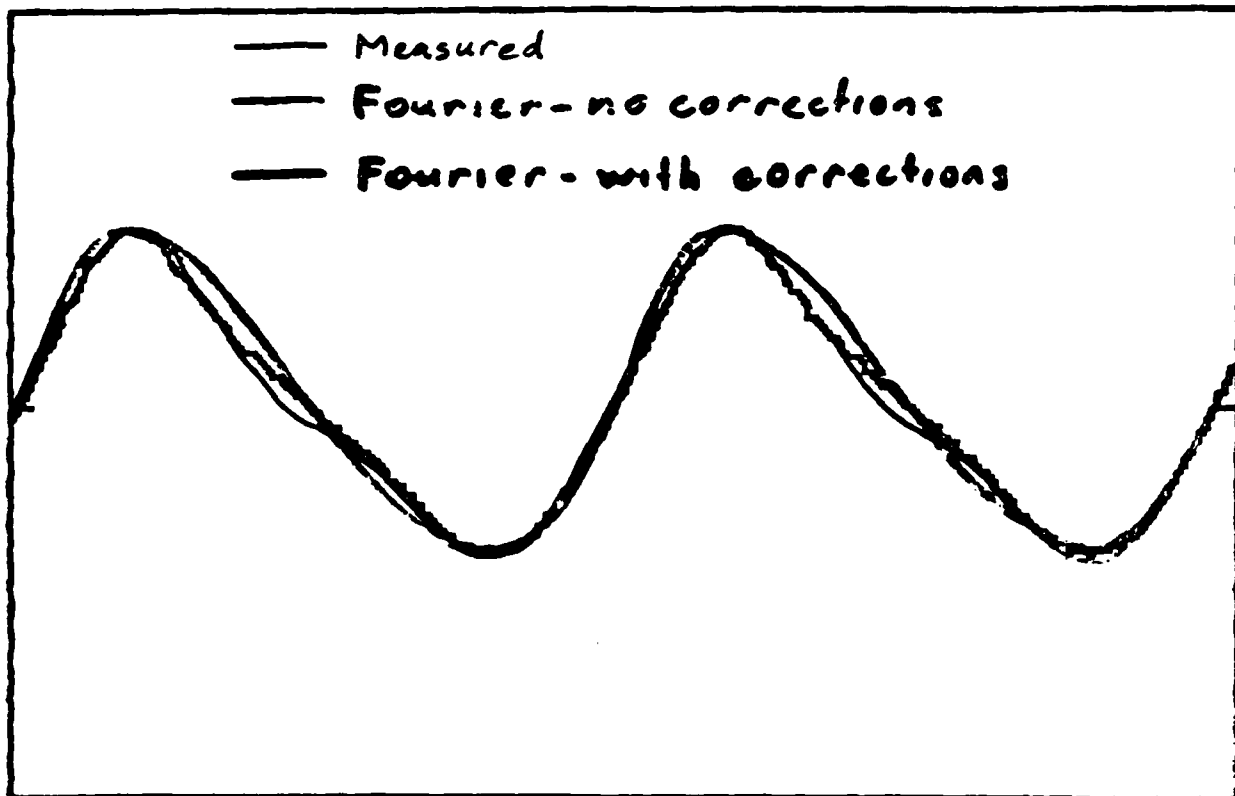
—— Measured

—— Fourier-no corrections

—— Fourier-with corrections

NUSC FILE # 920619.dat
MAX. SPL (LINEAR) ON-AXIS = 222.600 DB
k a = 64.3380 BETAO=3.6 SOUND SPEED = 1488 m/s
z (nondim.) = 2533.03 POLAR ANGLE = 0 (deg)

———— : NONLINEAR THEORY; — — — : MEASURED; ········· : LINEAR

PRESSURE (nondim.) × 10⁵

TIME (nondim.) / 2π
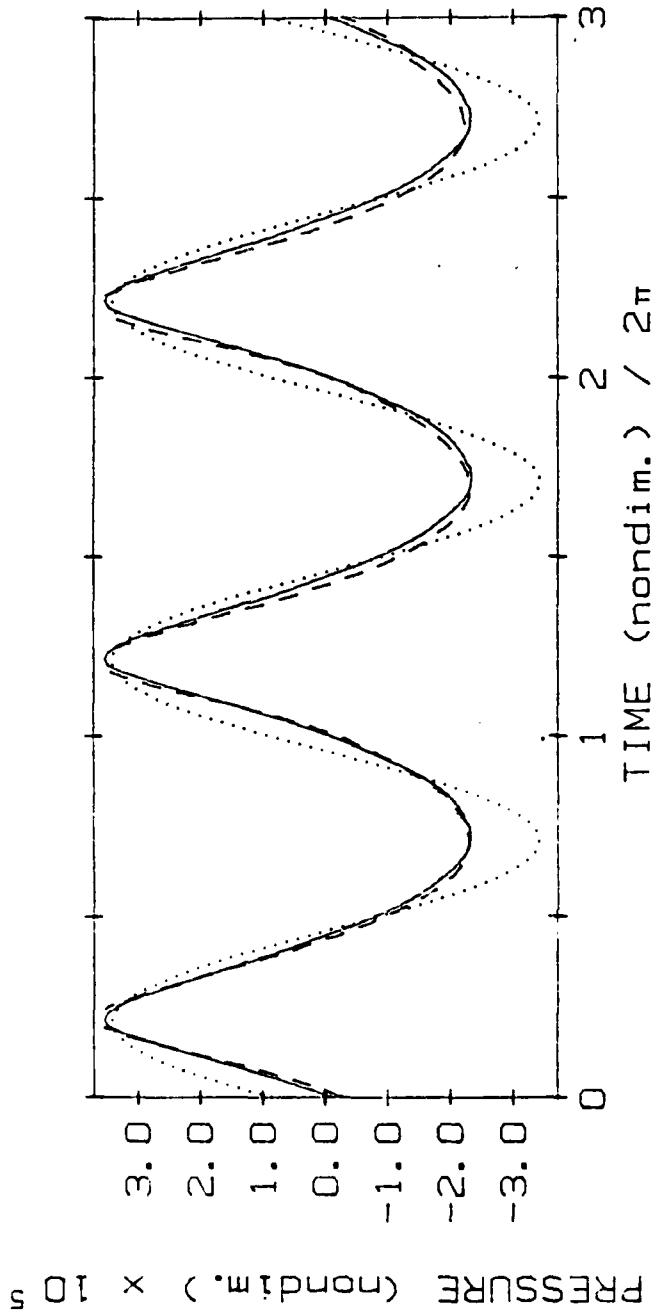
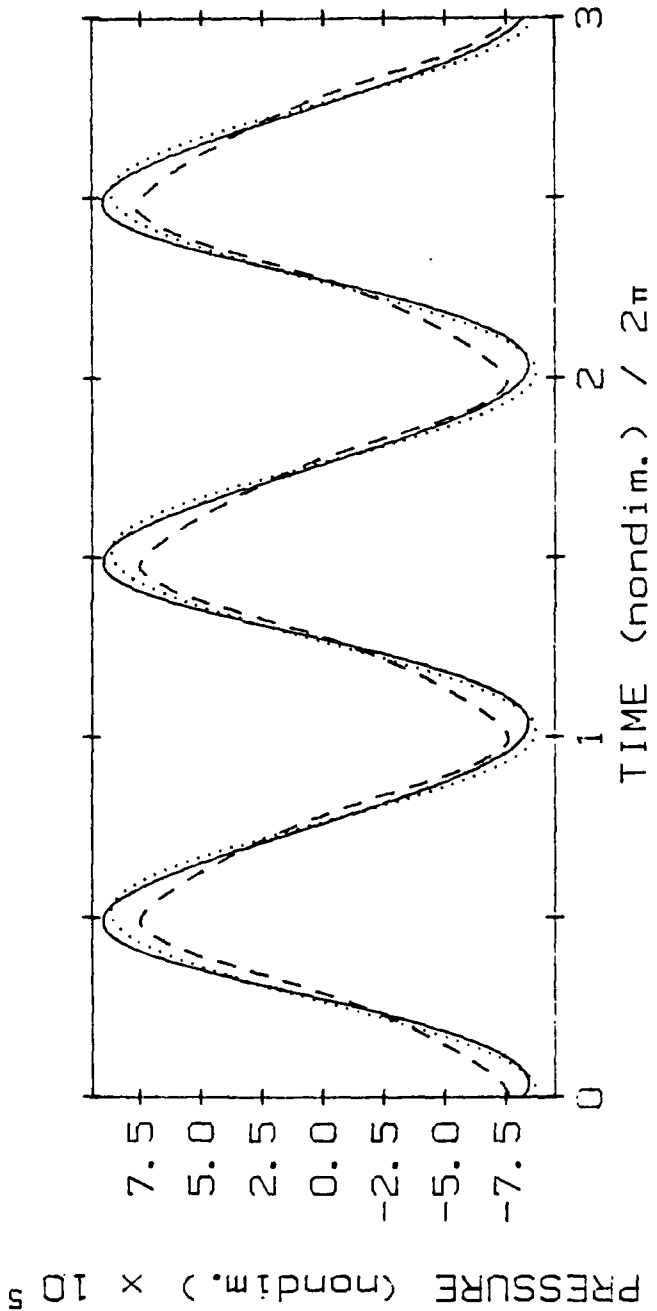NUSC FILE # 920005.DAT
MAX. SPL (LINEAR) ON-AXIS = 222.600 DB
k a = 64.3380 BETA0=3.6 SOUND SPEED = 1488 m/s
z (nondim.) = 215.31 POLAR ANGLE = 0 (deg)

————— :NONLINEAR THEORY; — — — :MEASURED; ········· :LINEAR.

NUSC FILE # 920015.dat   *Plotted to match peak*

MAX. SPL (LINEAR) ON-AXIS = 222.600 DB

k a = 64.3280 BETAO=3.6   SOUND SPEED = 1488 m/s

z (nondim.) = 73.46 POLAR ANGLE = 18 (deg)

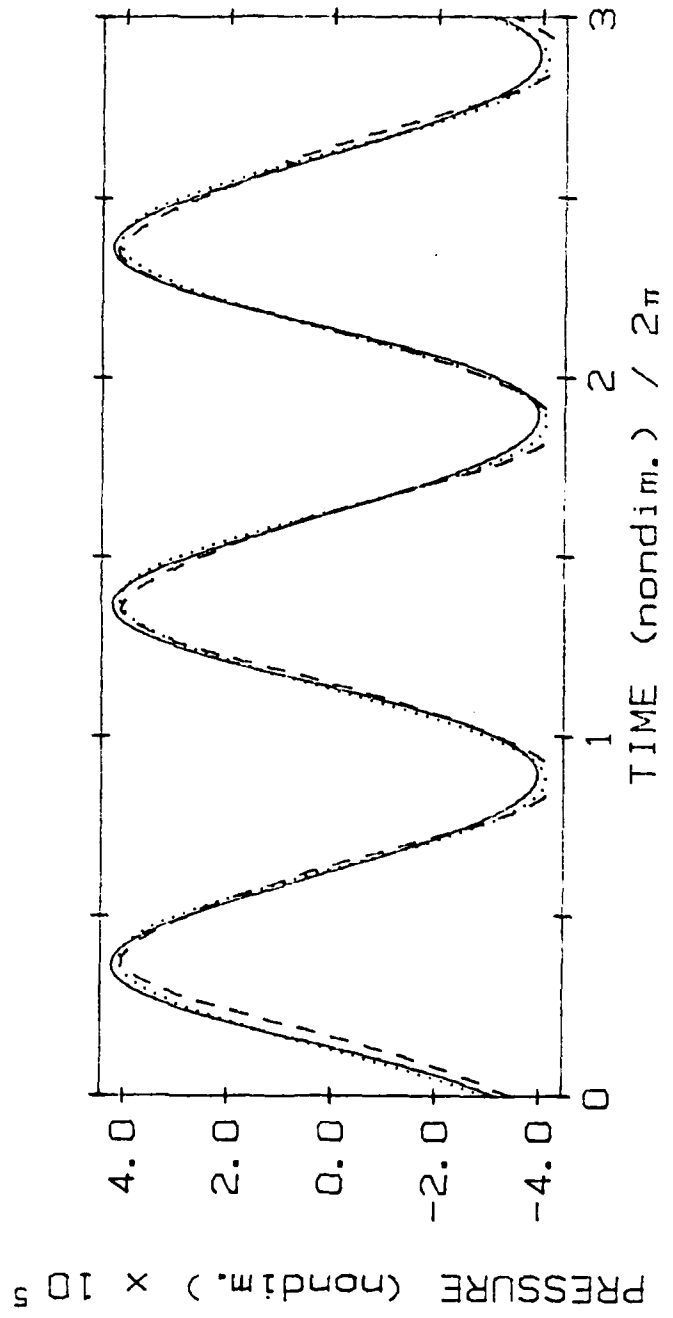———— : NONLINEAR THEORY;   – – – : MEASURED;   .... : LINEAR

PRESSURE (nondim.) x 10⁵

TIME (nondim.) / 2π

THE JOURNAL

of the

Acoustical Society of America

Program of the
105th Meeting

THURSDAY AFTERNOON, 12 MAY 1983   IVORY ROOM A, 2:00 TO 3:50 P.M.

Session LL. Physical Acoustics VIII: Nonlinear Acoustics

3:05

LL5. An improved King integral algorithm for finite amplitude sound beams. Jerry H. Ginsberg (School of Mechanical Engineering, Georgia Institute of Technology, Atlanta, GA 30332)

This paper supercedes the previous analysis [J. H. Ginsberg, J. Acoust. Soc. Am. Suppl. 1 71, S30 (1982)] of the infinite baffle problem for an axisymmetric harmonic excitation, which derived a nonlinear King integral describing the distortion associated with finite acoustic Mach numbers. That analysis was shown [M. B. Moffett and J. H. Ginsberg, J. Acoust. Soc. Am. Suppl. 1 72, S40 (1982)] to exhibit excessive nearfield distortion in comparison to experiment. Using the linear King integral in its conventional complex function form, as opposed to the real function analysis employed previously, leads to formulation of the second order potential in terms of complex functions. Asymptotic integration of this potential function reveals that there may be significant contribution from the evanescent spectrum (small transverse wavenumbers), as well as from the propagating spectrum. A coordinate straining transformation describing the full spectrum is deduced. From it, the previous analysis is shown to be only asymptotically correct. The new analysis reveals that the distortion is governed by a transformation that involves Fresnel integrals for the propagating spectrum and the error function for the evanescent spectrum. Some comparisons of the analytical prediction and the results of Moffett and Ginsberg are presented [Work supported by ONR, Code 420.]

●

Stouffer's Cincinnati Towers
Cincinnati, Ohio
9–13 May 1983

Axisymmetric Sound Radiation from a Planar Surface –

Finite Amplitude Effects

axis of symmetry

compressible inviscid fluid

$\hat{R}$

$\hat{z}$
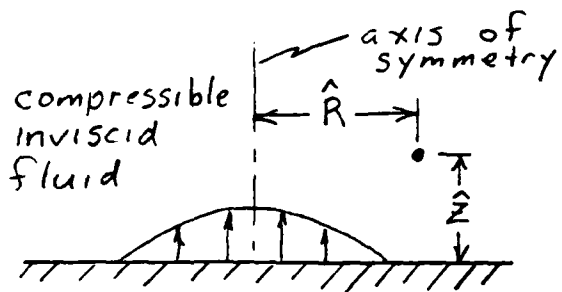
Cylindrical coordinates

$$\hat{R} = c_o R / \omega$$

$$\hat{z} = c_o z / \omega$$

$$\hat{t} = t / \omega$$

Harmonic excitation

Either pressure or axial velocity is specified on $z = 0$. example:

$$v_z = \varepsilon c_o f(R) \sin[t + g(R)]$$

where $|\varepsilon| \ll 1$ but finite.

Other Approaches

1. J.C. Lockwood, T.G. Muir, D.T. Blackstock (1973)
   a. <u>Far field analysis</u>
   b. <u>Signal treated as a non-uniform spherical wave</u>

2. E.A. Zabolotskaya, R.V. Khokhlov, et al (1969-1980)
   a. <u>Near field analysis - non-uniform planar waves</u>
   b. <u>Burgers' equation</u> modified by adding a Laplacian operator for the transverse direction
   c. <u>Finite differences</u> in space and time.

Foundations of Present Analysis

Potential Function

$$V_z = c_0 \frac{\partial \phi}{\partial z} \qquad V_R = c_0 \frac{\partial \phi}{\partial R}$$

$$p = -\rho_0 c_0^2 \frac{\partial \phi}{\partial t} + O(\phi^2)$$

Combination of Techniques

(1) <u>Direct method</u> using perturbation series - previously employed for non-uniform Cartesian, cylindrical and spherical waves (1974-1980)

(a) <u>Nonlinear wave equation</u>

$$\nabla^2 \phi - \frac{\partial^2 \phi}{\partial t^2} = (\gamma - 1) \frac{\partial \phi}{\partial t} \nabla^2 \phi$$
$$+ \frac{\partial}{\partial t} (\nabla \phi \cdot \nabla \phi) + O(\phi^3)$$

(b) <u>Perturbation series</u>

$$\phi = \varepsilon\,\phi_1 + \varepsilon^2 \phi_2 + \cdots$$

(c) Method of <u>renormalization</u> -

Require $\dfrac{\phi_2}{\phi_1} \leq O(1)$ everywhere

(2) <u>Integral transform</u> - used to form ϕ_1 (1980)

(3) <u>Stationary phase integration</u> - used to determine the most significant part of ϕ_2 (1981)

First Order Terms

Hankel transform (cylindrical coordinates)

$$\phi_1(z, R, t) = \int_0^\infty \Phi_1(z, k, t)\, k\, J_0(kR)\, dk$$

Transform d.e. & b.c.

$$\frac{\partial \phi_1}{\partial z}\bigg|_{z=0} = \int_0^\infty V_k \sin(t + \Theta_k)\, k\, J_0(kR)\, dk$$

transformed velocity amplitude

transformed phase angle

Result

$$\phi_1 = \int_0^1 \frac{k V_k}{\lambda_k}(\cos \Psi_k)\, J_0(kR)\, dk$$

$$- \int_1^\infty \frac{k V_k}{\bar{\lambda}_k}\left[\sin(t + \Theta_k)\right] \exp(-\bar{\lambda}_k z)\, J_0(kR)\, dk$$

where

$$\lambda_k = (1 - k^2)^{1/2} \qquad \bar{\lambda}_k = (k^2 - 1)^{1/2}$$

$$\Psi_k = t + \Theta_k - \lambda_k z : \underline{\text{axial phase variable}}$$

Interpretation

1. $J_o(kR)$ is oscillatory in $R \Rightarrow$ the <u>transverse wavelength</u> is essentially $1/k$.

2. The response consists of a <u>continuous spectrum</u> of transverse wavelengths.

3. <u>Large transverse wavelengths</u> $(k<1)$ <u>propagate dispersively</u> — $1/\lambda_k$ is the phase speed.

4. <u>Small transverse wavelengths</u> $(k>1)$ <u>evanesce</u> — <u>negligible</u> influence for large z.

Second Order Terms

1. Primary goal: Identify terms in ϕ_2 which can make $|\epsilon^2 \phi_2|$ comparable to $|\epsilon \phi_1|$.

2. Use ϕ_1 to form source terms for ϕ_2 — neglect evanescent terms.
   General form:

$$\nabla^2 \phi_2 - \frac{\partial^2 \phi_2}{\partial t^2} = \int_0^1 \int_0^1 \left[f_1(z,t,k,n) J_0(kR) J_0(nR) + f_2(z,t,k,n) J_0'(kR) J_0'(nR) \right] n k \, dn \, dk$$

3. Earlier work in curvilinear coordinates:
   a. Consider ϕ_2 in the domain where asymptotic expansions of Bessel functions are valid.

   b. Examine the asymptotic solution for ϕ_2. Examine it to deduce the form that features Bessel functions.

Procedure

1. Assume that ϕ_2 has the form of the source terms.

$$\phi_2 = \int_0^1 \Phi_2(k, z, R, t)\, dk$$

$$\Phi_2 = \left[\int_0^1 \bar{\Phi}_2^{(1)}\, n\, J_0(nR)\, dn\right] k\, J_0(kR)$$

$$+ \left[\int_0^1 \Phi_2^{(2)}\, n\, J_0'(nR)\, dn\right] k\, J_0'(kR)$$

2. Use asymptotic expansions for kR & $nR \gg 1$.

$$\nabla^2 \Phi_2 - \frac{\partial^2 \Phi_2}{\partial t^2} = \frac{1}{R} \int_0^1 C(k,n) \sin(\psi_k \pm \psi_n) \cos\left[(kR - \pi/4)\right.$$

$$\left. \pm (nR - \pi/4)\right] dn$$

a. $\underline{Secularity}$ when $n \approx k$ if both $\underline{alternative}$ signs are alike.

b. Let $\underline{n = k + q\Delta}$, $|\Delta| \ll 1$

c. Difference signs $\Rightarrow$ integrand is essentially a function of z only

3. <u>Try</u> $\quad \Phi_2 = \frac{1}{R} \int_0^1 [a(k,n,z) \sin(\psi_k + \psi_n)$

$\qquad\qquad + b(k,n,z) \cos(\psi_k + \psi_n)] \cos(kR$

$\qquad\qquad + nR - \pi/2) \, dn \quad + \frac{F(z)}{R} \; ; \; \underline{kR \gg 1}$

4. <u>Harmonic balance</u>

$$a'' + 2\alpha_{kn} b' + \beta_{kn} a_{kn} = \gamma_{kn}$$
$$b'' - 2\alpha_{kn} a' + \beta_{kn} b_{kn} = 0$$

$\left.\right\}$ JASA, vol. 69 (1981)

where $\underline{\beta_{kn} \to 0}$ if $n \to k$.

5. With $\underline{n = k + q\Delta}$, determine the solution for $|\Delta| \ll 1$. <u>Match</u> it to the particular <u>solution</u> for $n \equiv k$.

6. Method of <u>stationary phase</u> — integrate over <u>all values of q</u>.

Asymptotic Result:

When $\underline{kR >> 1}$

$$\Phi_2 = (\gamma+1)\frac{1}{2R}\left(\frac{z}{2\pi}\right)^{1/2}\int_0^1 \frac{V_k^2}{\lambda_k^{3/2}} k \left[\sin 2\Psi_k \right.$$

$$\left. + \cos 2\Psi_k \right] \cos(2kR - \pi/2) + \frac{F(z)}{R}$$

Matching:

1. Assumed <u>general solution</u> for Φ_2 was

$$\Phi_2 = \left[\int_0^1 \Phi_2^{(1)} n \, J_0(nR)\,dn\right] J_0(kR)$$

$$+ \left[\int_0^1 \Phi_2^{(2)} n \, J_0'(nR)\,dn\right] J_0'(kR)$$

2. <u>Expand</u> this for $\underline{n=k}$ & $\underline{kR >> 1}$.

3. Deduce $\Phi_2^{(1)}$ & $\Phi_2^{(2)}$ (both are independent of R) such that asymptotic form of general solution matches the asymptotic result.

Resulting Potential Function

1. Evaluate $F(z)$:

    a. Conservation of mass

    b. Axial velocity $\equiv \partial\phi/\partial z \Rightarrow$ average over a plane $z = $ constant for one period

    c. Average value must vanish

    d. Conclusion $\underline{F(z) \equiv 0}$

2. Combine results.

$$\phi = \varepsilon \int_0^1 \frac{k V_k}{\lambda_k} \left\{ (\cos \Psi_k) J_0(kR) \right.$$

$$+ \frac{1}{4} \varepsilon (\gamma+1) \left(\frac{\pi z}{2\lambda_k}\right)^{1/2} k V_k \left(\sin 2\Psi_k \right.$$

$$\left. + \cos 2\Psi_k \right) \left[J_0(kR)^2 - J_0'(kR)^2 \right] \right\} dk$$

$$+ \varepsilon (\phi_1)_{ev} + \underline{O(\varepsilon^2)} \quad \text{at all } R \text{ \& } z$$

Physical Response

Particle velocity:

$$v_x = c_0 \frac{\partial \phi}{\partial x} \qquad v_z = c_0 \frac{\partial \phi}{\partial z}$$

Pressure:

$$p = -\rho_0 c_0^2 \frac{\partial \phi}{\partial t} + O(\phi^2)$$

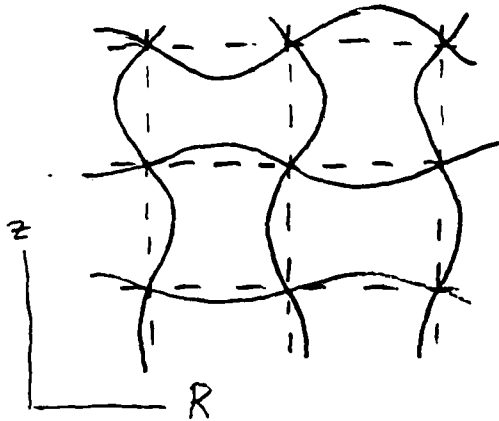Denote response variables as u_i.

General form:

$$u_i = \int_0^1 \left[\varepsilon \, u_{i_1}(k, z, R, t) \right.$$
$$\left. + \varepsilon^2 z^{1/2} u_{i_2}(k, z, R, t) \right] dk$$
$$+ (u_i)_{ev} + O(\varepsilon^2)$$

<u>Significance</u> of the second
order term <u>increases</u>
as z increases

Non - Uniform Accuracy

G. B. Whitham: Moderate nonlinearity

1. <u>Linear form</u> of solution is essentially <u>correct</u>

2. <u>Location</u> corresponding to a specific phase <u>is shifted</u> due to nonlinearity

dashed line is linear grid
solid line is nonlinear grid

3. <u>Grid distortion</u> is <u>dependent</u> on the <u>wave number</u> n.

Method of Renormalization

Change the independent variables:

Linear	Nonlinear
$\lambda_k z$	α_k
kR	β_k

Discrepancies grow as $z^{1/2}$. Try:

$$\lambda_k z = \alpha_k + \varepsilon z^{1/2} F_z \, (k, \alpha_k, \beta_k, t)$$

$$kR = \beta_k + \varepsilon z^{1/2} F_R \, (k, \alpha_k, \beta_k, t)$$

Choose F_z & F_R to <u>remove all $O(\varepsilon^2)$</u> <u>terms that are not uniformly</u> <u>accurate.</u>

Procedure

Substitute transformation into each u_i and $\underline{expand\ in\ \varepsilon}$.

$$u_i = \int_0^1 \left\{ \varepsilon\, u_{i,1}(k, \alpha_k, \beta_k, t) \right.$$

$$+ \varepsilon^2 z^{1/2} \left[F_z \frac{\partial}{\partial \alpha_k} u_{i,1}(k, \alpha_k, \beta_k) \right.$$

$$\left. \left. + F_R \frac{\partial}{\partial \beta_k} u_{i,1}(k, \alpha_k, \beta_k, t) + u_2(k, \alpha_k, \beta_k, t) \right] \right\} dt$$

There are no functions F_z and F_R which $\underline{cancel\ all\ O(\varepsilon^2 z^{1/2})\ terms} \Rightarrow$ a non-oscillatory term is retained.

Response grows with increasing z if this term is omitted

Reason: Coordinate straining generates a $\underline{non\text{-}zero\ mean}$ $\underline{value}$ which is $\underline{canceled\ by}$ $\underline{the\ remainder}$.

Results

1. Coordinate straining

$$\lambda_k z = \alpha_k + \varepsilon(\gamma+1)\left(\frac{\pi z}{\lambda_k}\right)^{1/2} k V_k \sin\left(t + \theta_k - \alpha_k - \frac{\pi}{4}\right) J_0(\beta_k)$$

$$k R = \beta_k + \varepsilon(\gamma+1)\left(\frac{\pi z}{\lambda_k}\right)^{1/2} k V_k \cos\left(t + \theta_k - \alpha_k - \frac{\pi}{4}\right) J_0'(\beta_k)$$

2. Pressure

$$P = \rho_0 c_0^2 \varepsilon \int_0^1 \frac{k V_k}{\lambda_k} \left\{ \sin\left(t + \theta_k - \alpha_k\right) J_0(\beta_k) \right.$$

$$\left. + \frac{1}{2}(\gamma+1)\varepsilon\left(\frac{\pi z}{2\lambda_k}\right)^{1/2} k V_k \left[J_0(\beta_k)^2 + J_0'(\beta_k)^2 \right] \right\} dk$$

$$+ \rho_0 c_0^2 \varepsilon \int_0^1 \frac{k V_k}{\lambda_k} \cos\left(t + \theta_k\right) \exp\left(-\bar{\lambda}_k z\right) J_0(k R) \, dk$$

Explanation

1. Each transverse wave number k gives a _non-uniform planar wavelet_ resembling one in a circular cylindrical waveguide.

2. Each wavelet _propagates dispersively_ in the axial direction

3. The _distortion_ (i.e. the coordinate transformation) of each wavelet is _unaffected by the other wavelets._

4. The coordinate transformation suggests _self-refraction._

Self-Refraction

1. <u>Phase of the response</u> in a wavelet:

Response variable	Axial: $t + \theta_k - \alpha_k$	Transverse: β_k
pressure: $(p)_k$	$\sin(\ )$	$J_0(\ )$
axial velocity: $(V_z)_k$	$\sin(\ )$	$J_0(\ )$
transverse velocity: $(V_R)_k$	$\cos(\ )$	$J_0'(\ )$

(proportional)

2. <u>Phase of the transformation</u> for a wavelet:

Position parameter	Axial: $t + \theta_k - (\alpha_k + \frac{\pi}{4})$	Transverse: β_k
Axial: $\lambda_k z$	$\sin(\ )$	$J_0(\ )$
Transverse: kR	$\cos(\ )$	$J_0'(\ )$

3. <u>Combined influence:</u>

Position Parameter	Response Type	Affecting Transformation	
		Axial Location	Transverse Location: β_k
$\lambda_k z$	$(V_z)_k$	$\alpha_k + \frac{\pi}{4}$ (i.e. $\frac{1}{8}$ period earlier)	β_k
kR	$(V_R)_k$		

4. <u>Geometric viewpoint</u> (selected k)

	Linear	Nonlinear
Wavefront	Constant $\lambda_k z$	Constant α_k
Ray	Constant kR	Constant β_k

<u>Picture of wavefronts and rays</u> (time t fixed)

direction of propagation

transverse shift

$(V_z)_k$

$(V_R)_k$

$\alpha_k + \frac{\pi}{4}$: intersected point P at time $t - \frac{\pi}{4}$

constant $\lambda_k z$

transverse shift

constant α_k

constant kR

constant β_k
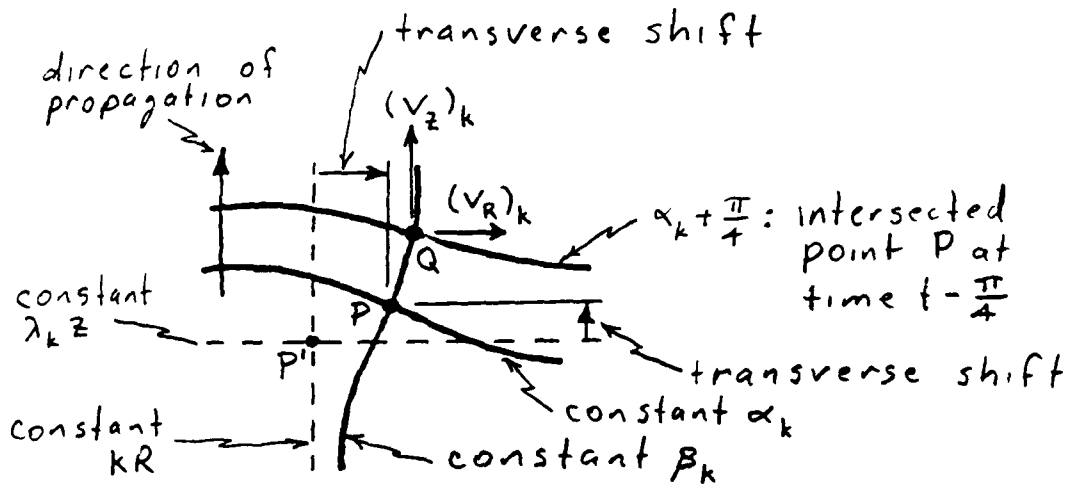
5. (a) Nonlinear response at P = linear at P'

   (b) Axial shift $\sim (V_z)_k$ at Q

   (c) Radial shift $\sim (V_R)_k$ at Q

Quantitative Analysis

1. Numerical integration

   (a) <u>Discretize</u> $k: k_0 = 0, k_1, k_2, \ldots; k_{i+1} - k_i \ll 1$

   (b) <u>Weighting coefficients</u>
   $$\int_a^b f(k) \, dk = \sum_i W_i f(k_i) + error$$
   $\uparrow$ independent of $f(k)$

   (c) <u>Equal spacing</u> (not necessary)
   $$k_{i+1} - k_i = h$$

   (d) Interpolating polynomials – n point rule
   (Newton - Cotes formulae)
   $$\underline{error} = \begin{cases} O\left(h^{n+1} \dfrac{d^{n+1} f}{dk^{n+1}}\right) & \text{if } n \text{ is odd} \\[2mm] O\left(h^n \dfrac{d^n f}{dk^n}\right) & \text{if } n \text{ is even} \end{cases}$$

   (e) <u>Criteria</u> affecting choice
   Note that <u>$f(k)$ oscillates rapidly</u>
   when z or R is large.

   (1) Higher derivatives of $f(k)$ are large

   (2) Decrease h as $r = (z^2 + R^2)^{1/2}$ increases

   (f) Conclusion
   <u>Trapezoidal rule; $h \leq 1/50$</u>

2. <u>Numerical algorithm</u> : $N = 1/h$

$$p = \rho_0 c_0^2 \varepsilon \sum_{i=0}^{N} W_i \left\{ \frac{k V_k}{\lambda_k} \sin(t + \theta_k - \chi_k) J_0(\beta_k) \right.$$

$$+ \frac{1}{2} \varepsilon (\gamma+1) \left(\frac{\pi z}{2\lambda_k} \right)^{1/2} \frac{k^2 V_k^2}{\lambda_k} \left[J_0(\beta_k)^2 + J_0'(\beta_k)^2 \right] \right\} \bigg|_{k=k_i}$$

$$+ \rho_0 c_0^2 \varepsilon \sum_{i=N}^{\infty} W_i \left\{ \frac{k \bar{V}_k}{\bar{\lambda}_k} \cos(t \right.$$

$$+ \theta_k) \exp(-\bar{\lambda}_k z) J_0(kR) \right\} \bigg|_{k=k_i}$$

$$\Downarrow \text{rapid convergence}$$

3. <u>Evaluation of coordinate transformation</u>

Specify $k = k_i$, & $(z, R, t) \Rightarrow$ Find α_k & β_k

<u>Newton - Raphson method</u>

    (a) <u>Guess</u> a root $\alpha_k = \alpha^{(1)}$, $\beta_k = \beta^{(1)}$

    (b) True root is at

$$\alpha_k = \alpha^{(1)} + \Delta\alpha, \quad \beta_k = \beta^{(1)} + \Delta\beta$$

    (c) Coordinate transformation:

$$\lambda_k z = f(\alpha_k, \beta_k) ; \quad kR = g(\alpha_k, \beta_k)$$

(d) <u>Taylor series</u>

$$\lambda_k z = f(\alpha^{(1)} + \Delta\alpha, \beta^{(1)} + \Delta\beta)$$

$$= f(\alpha^{(1)}, \beta^{(1)}) + \Delta\alpha \left(\frac{\partial f}{\partial \alpha}\right)^{(1)} + \Delta\beta \left(\frac{\partial f}{\partial \beta}\right)^{(1)} + \ldots$$

$$k R = g(\alpha^{(1)} + \Delta\alpha, \beta^{(1)} + \Delta\beta)$$

$$= g(\alpha^{(1)}, \beta^{(1)}) + \Delta\alpha \left(\frac{\partial g}{\partial \alpha}\right)^{(1)} + \Delta\beta \left(\frac{\partial g}{\partial \beta}\right)^{(1)} + \ldots$$

(e) <u>Solve</u>

$$\begin{bmatrix} \left(\frac{\partial f}{\partial \alpha}\right)^{(1)} & \left(\frac{\partial f}{\partial \beta}\right)^{(1)} \\ \left(\frac{\partial g}{\partial \alpha}\right)^{(1)} & \left(\frac{\partial g}{\partial \beta}\right)^{(1)} \end{bmatrix} \begin{Bmatrix} \Delta\alpha \\ \Delta\beta \end{Bmatrix} = \begin{Bmatrix} \lambda_k z - f(\alpha^{(1)}, \beta^{(1)}) \\ k R - g(\alpha^{(1)}, \beta^{(1)}) \end{Bmatrix}$$

Then $\quad \alpha^{(2)} = \alpha^{(1)} + \Delta\alpha$
$\qquad \beta^{(2)} = \beta^{(1)} + \Delta\beta$ $\Big\}$ <u>iterate</u>

(f) <u>Shocks</u>

$$\begin{vmatrix} \left(\frac{\partial f}{\partial \alpha}\right)^{(1)} & \left(\frac{\partial f}{\partial \beta}\right)^{(1)} \\ \left(\frac{\partial g}{\partial \alpha}\right)^{(1)} & \left(\frac{\partial g}{\partial \beta}\right)^{(1)} \end{vmatrix} = \underline{\text{Jacobian}} \text{ of the transform-}$$
$$\text{ation at point } (\alpha^{(1)}, \beta^{(1)})$$

<u>Jacobian</u> $= 0$ means a <u>shock</u>
(e.g. $\Delta\alpha$ & $\Delta\beta$ are not <u>unique</u>).

Newton-Raphson <u>convergence slows</u> as a
shock is approached.

Pressure Boundary Condition

1. Pressure given on boundary:
$$p|_{z=0} = \rho_0 c_0^2 \varepsilon \, f_p(R) \sin\left[t + g_p(R)\right]$$

2. Hankel transform and inversion:
$$p|_{z=0} = \rho_0 c_0^2 \varepsilon \int_0^\infty k P_k \sin(t + \eta_k) J_0(kR) \, dk$$

3. Evaluate earlier solution on $z=0 \Rightarrow \alpha_k = 0$ & $\beta_k = kR$
$$p|_{z=0} = \rho_0 c_0^2 \varepsilon \int_0^1 \frac{k V_k}{\lambda_k} \sin(t + \Theta_k) J_0(kR) \, dk$$
$$+ \rho_0 c_0^2 \varepsilon \int_1^\infty \frac{k V_k}{\bar{\lambda}_k} \cos(t + \Theta_k) J_0(kR) \, dk$$

4. Match boundary equations:

   $\underline{k < 1}$: Replace $\dfrac{V_k}{\lambda_k}$ by P_k & replace Θ_k by η_k

   $\underline{k > 1}$: Replace $\dfrac{V_k}{\bar{\lambda}_k}$ by P_k & replace Θ_k by $\eta_k - \dfrac{\pi}{2}$

5. $\underline{\text{Singularity}}$: $\lambda_k = \bar{\lambda}_k = 0$ when $k = 1$

   Pressure b.c. : Integrands are analytic

   Velocity b.c.: Integrands are singular, but integrable.

Example
Uniform Pressure Distribution

$$p|_{z=0} = \begin{cases} \rho_0 c_0^2 \, \varepsilon \, \sin t & 0 \le R < \frac{a\omega}{c_0} \quad (\hat{R} < a) \\ 0 & R > \frac{a\omega}{c_0} \end{cases}$$

For a <u>piston</u> (i.e. velocity b.c.)
   Beam forming: $a\omega/c_0 > 1$
   Far field: $r = (R^2 + z^2)^{1/2} = O\left(\frac{a^2\omega^2}{c_0^2}\right)$

<u>Hankel transforms</u>:
$$P_k = \frac{a\omega}{c_0} \frac{1}{k} J_1\left(\frac{a\omega}{c_0} k\right), \quad \Theta_k = 0$$
$$P_k \to \frac{1}{2}\left(\frac{a\omega}{c_0}\right)^2 \quad \text{as} \quad k \to 0$$

<u>Input parameters</u>:
  At specified (z, R, t):

    $\frac{P}{\varepsilon}$, $\frac{V_z}{\varepsilon}$, $\frac{V_R}{\varepsilon}$ depend only on $\frac{a\omega}{c_0}$ & $\varepsilon(\gamma+1)$

<u>Air</u>: $\gamma = 1.4 \impliedby$ value used

<u>Water</u>: $\frac{B}{A} = \gamma - 1 = 5.5$

<u>Similarity</u>: $\left(\frac{P}{\varepsilon}\right)_{water} = \left(\frac{P}{\varepsilon}\right)_{air}$ when

$$\varepsilon_{water} = \frac{(\gamma+1)_{air}}{\left(\frac{B}{A}+2\right)_{water}} \, \varepsilon_{air} = 0.32 \, \varepsilon_{air}$$

Velocity B. C.
Unresolved Singularity

1. Coordinate transformation

$$\lambda_k z = \alpha_k + \varepsilon(\gamma+1)\left(\frac{\pi z}{\lambda_k}\right)^{1/2} kV_k \sin(t+\theta_k-\alpha_k-\tfrac{\pi}{4}) J_0(\beta_k)$$

$$kF = \beta_k + \varepsilon(\gamma+1)\left(\frac{\pi z}{\lambda_k}\right)^{1/2} kV_k \cos(t+\theta_k-\alpha_k-\tfrac{\pi}{4}) J_0'(\beta_k)$$

2. When $k \approx 1$, $\lambda_k \approx 0$.

  (a) Both $O(\varepsilon)$ terms are large at all z.

  (b) A shock forms at small z $\Rightarrow$ not physically acceptable.

3. Note:

  (a) $\pi/4$ phase angle

  (b) $\lambda_k z = \alpha_k + O(\varepsilon z^{1/2}) \Rightarrow \left(\frac{\pi z}{\lambda_k}\right)^{1/2} = z\left(\frac{\pi}{\alpha_k}\right)^{1/2} + O(\varepsilon)$

4. Hypothesis

  The above transformation is the asymptotic expansion for large z of a _Bessel function form_

$$\lambda_k z = \alpha_k + \frac{\pi}{2^{1/2}} \varepsilon(\gamma+1)kV_k z\left[\sin(t+\theta_k)J_0'(\alpha_k) - \cos(t+\theta_k)J_0(\alpha_k)\right]J_0(\beta_k)$$

$$kR = \beta_k + \frac{\pi}{2^{1/2}} \varepsilon(\gamma+1)kV_k z\left[\sin(t+\theta_k)J_0(\alpha_k) + \cos(t+\theta_k)J_0'(\alpha_k)\right]J_0'(\beta_k)$$
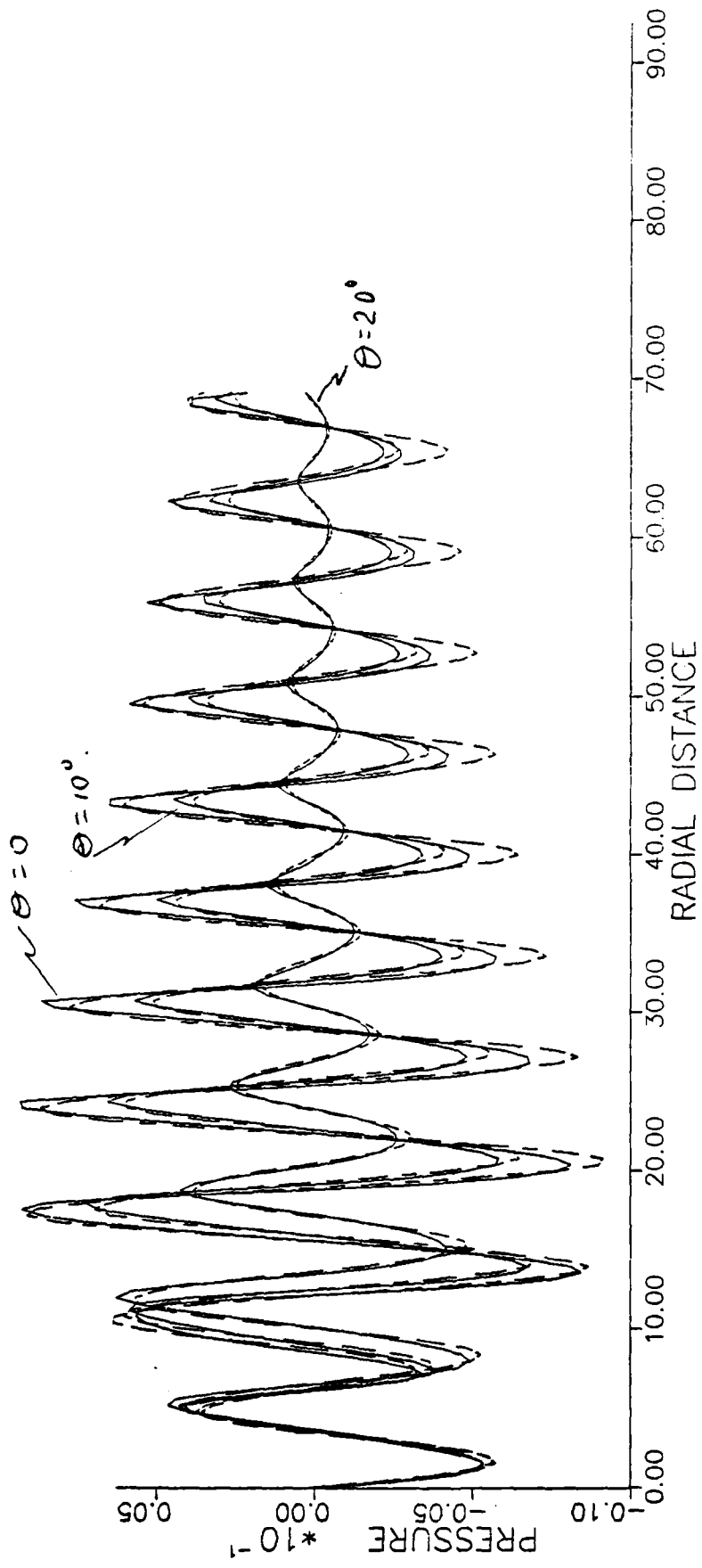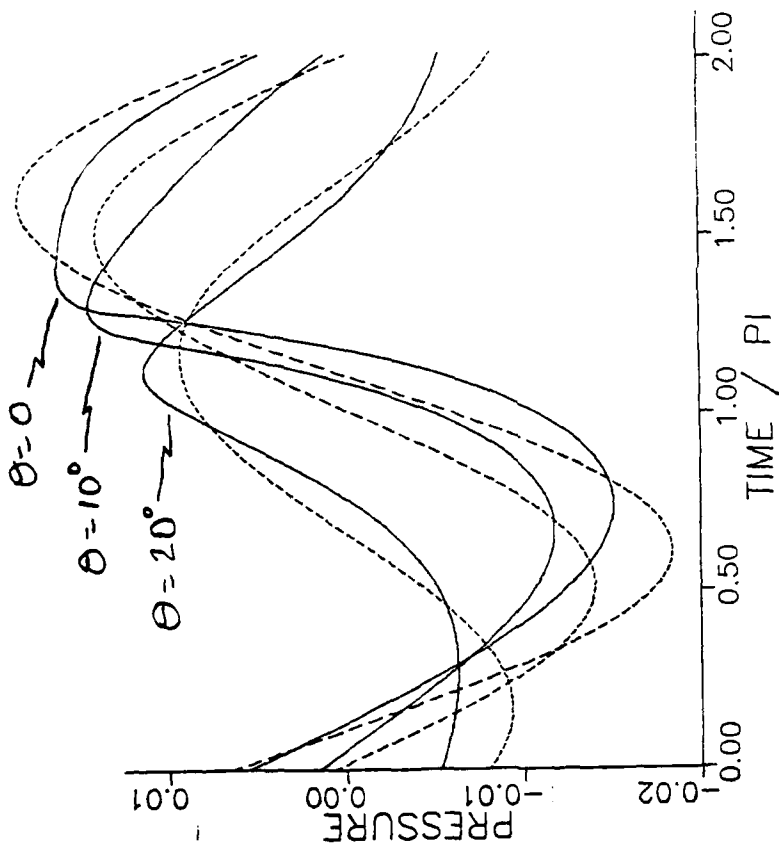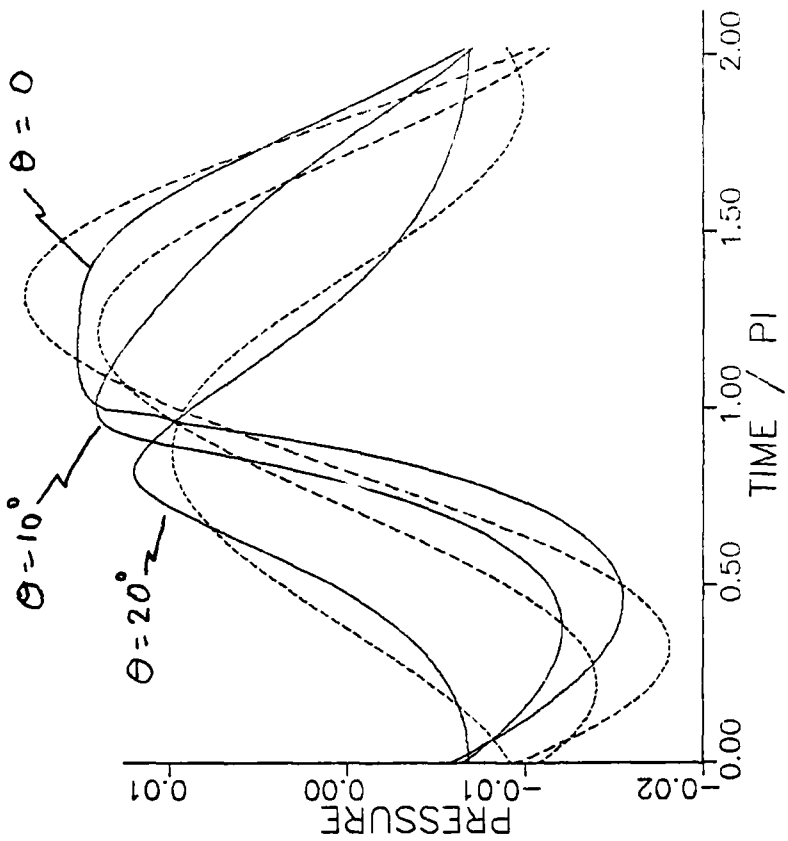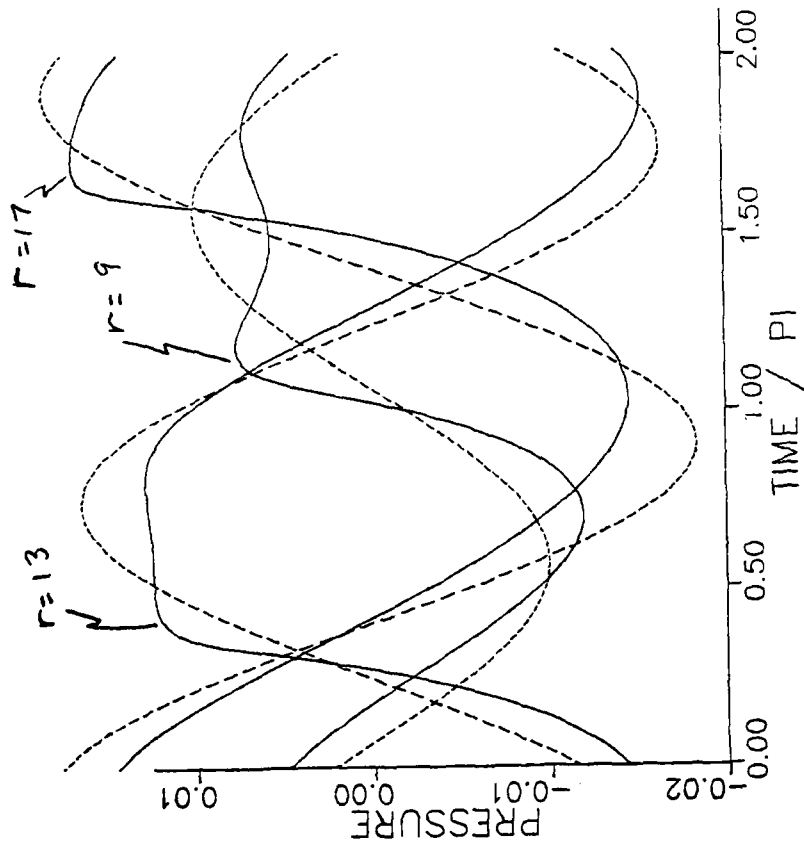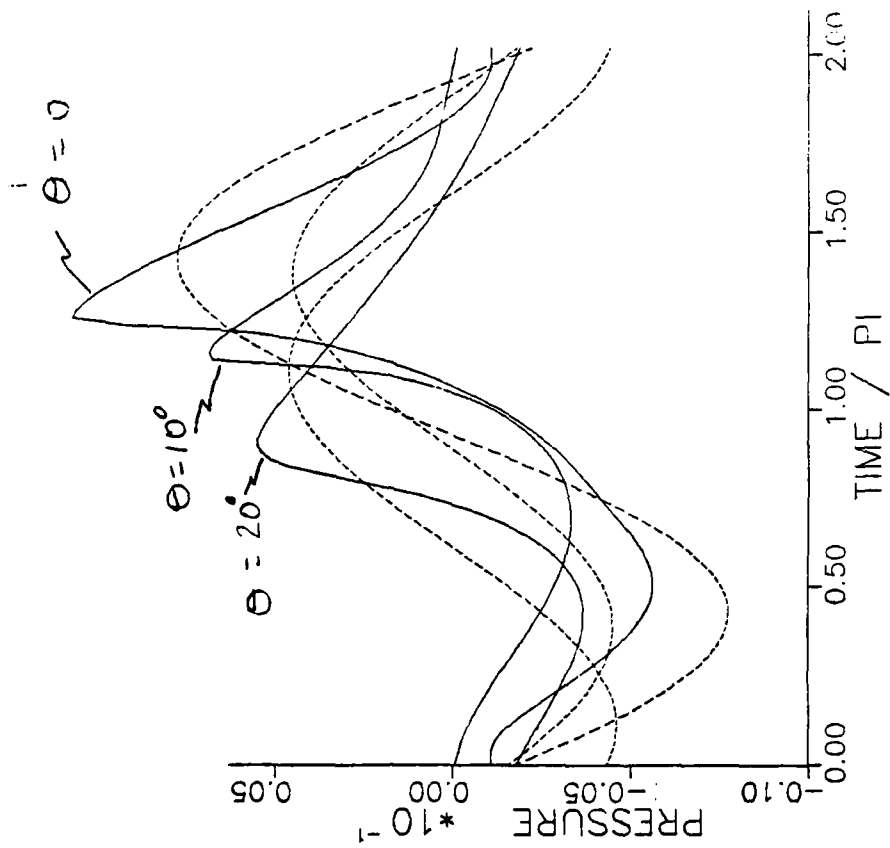
Figure 1
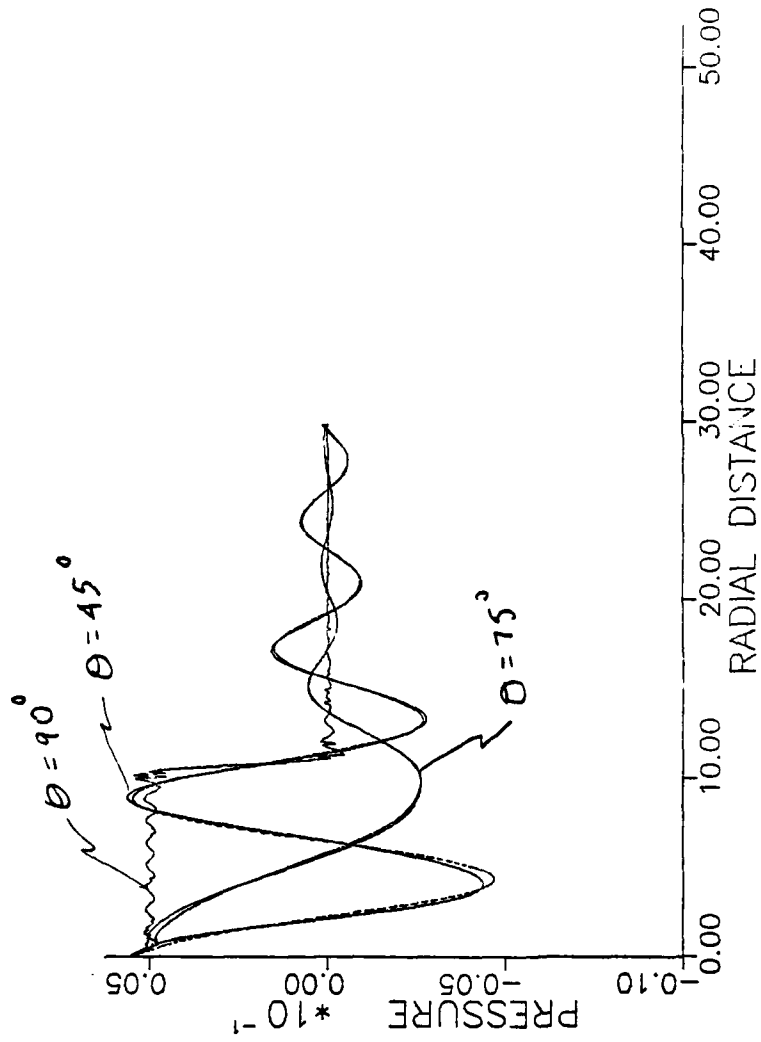
Figure 2
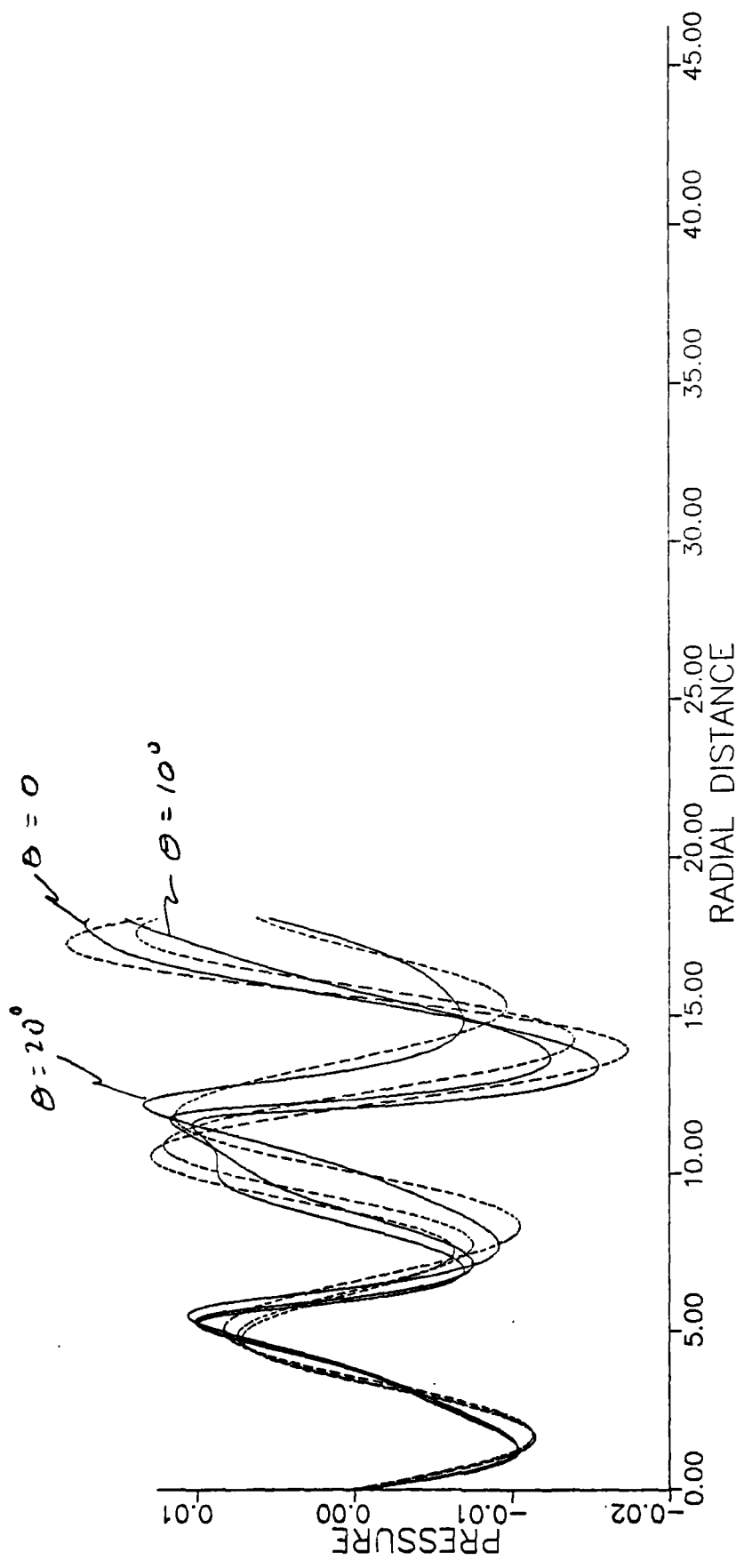
Figure 3
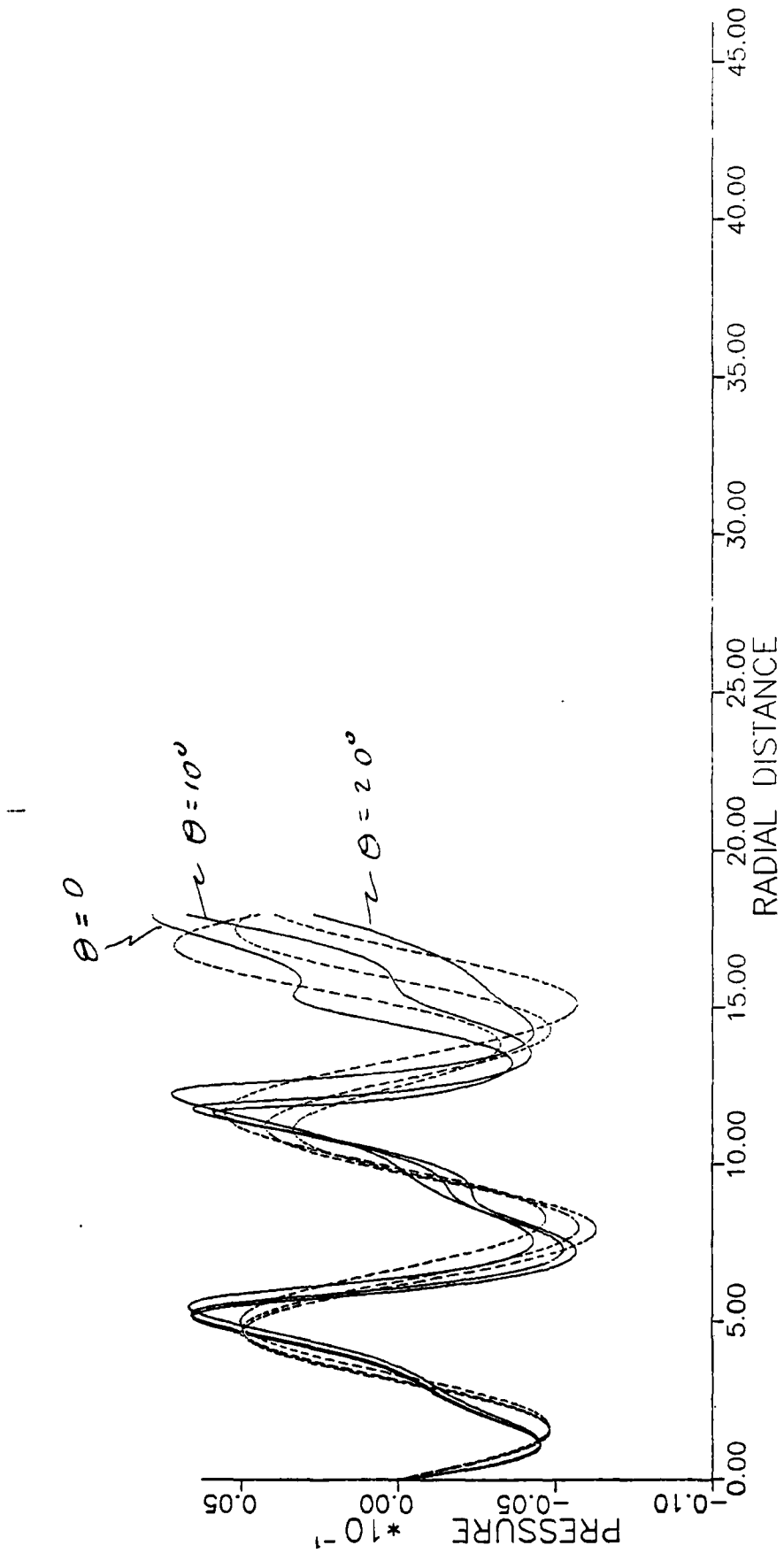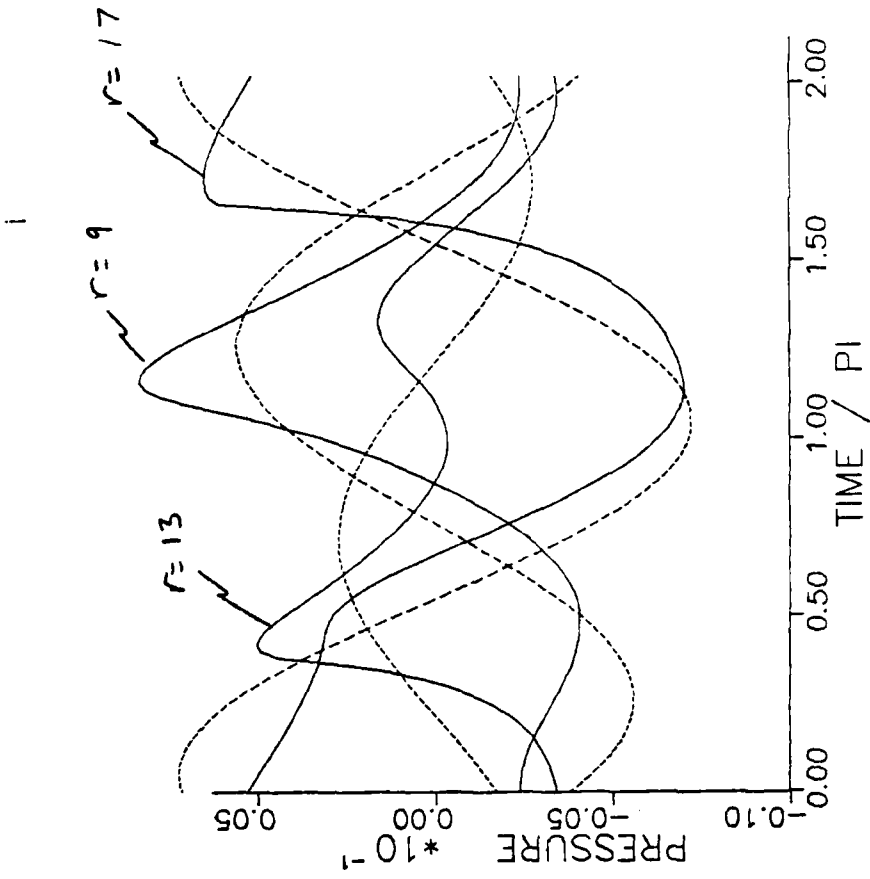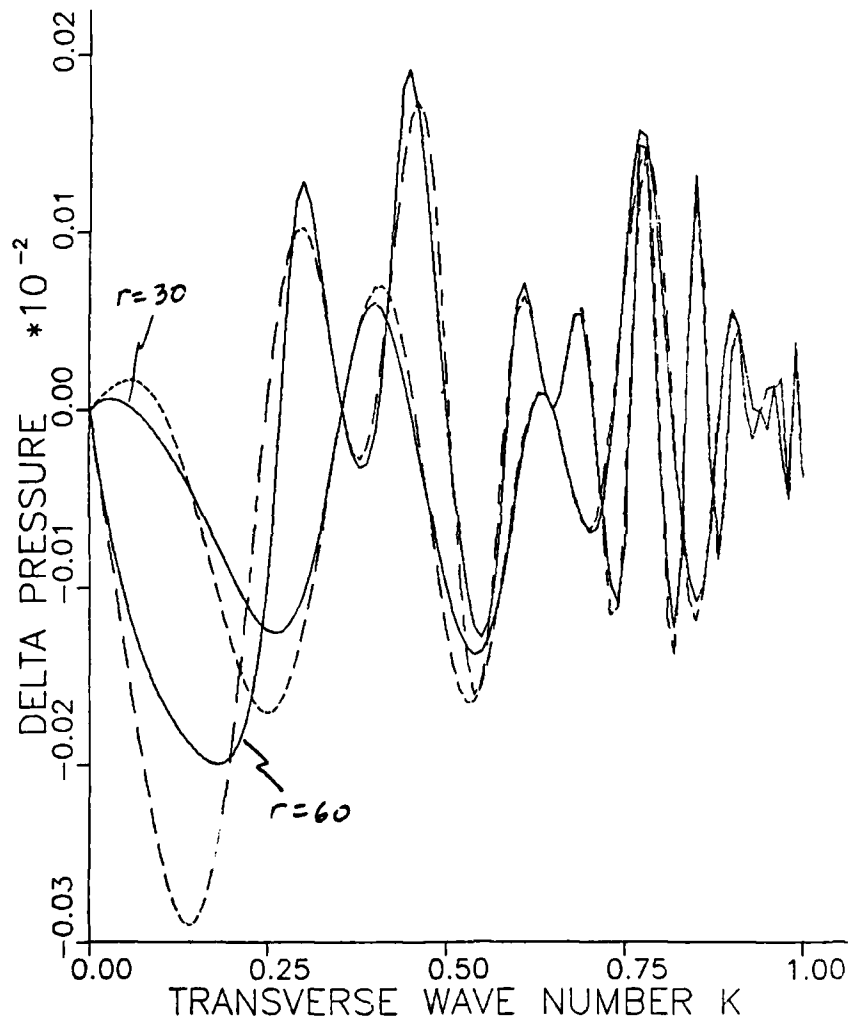
Figure 4
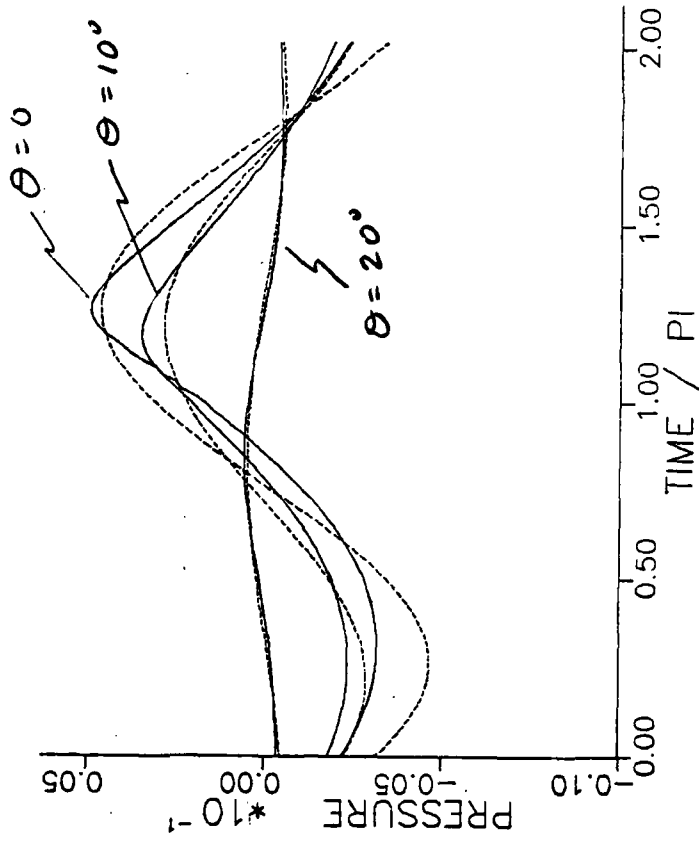
Figure 5
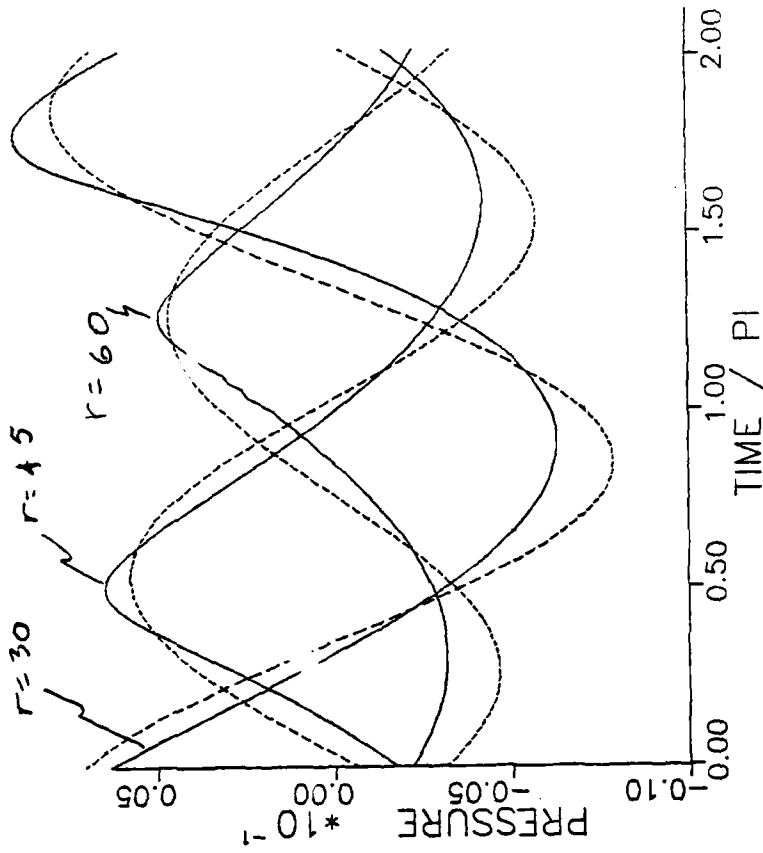
Figure 6

Figure 7

Figure 8

Figure 9

Figure 10

Figure 11

Figure 12
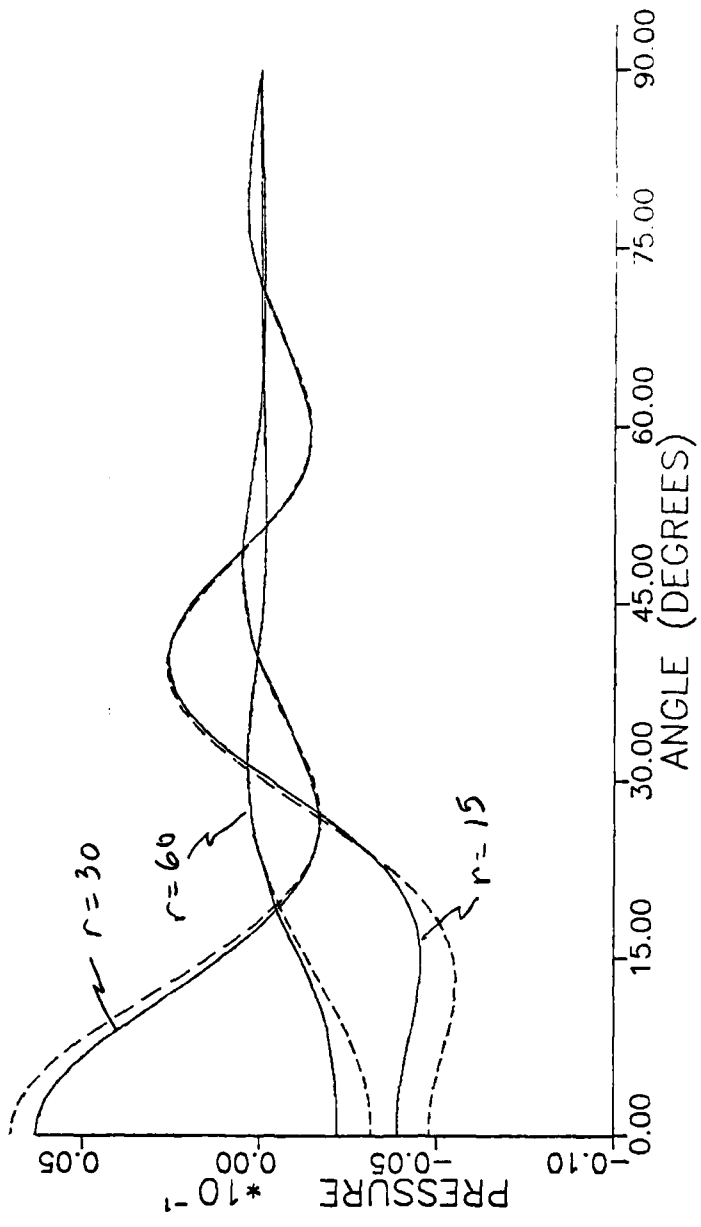
Figure 13
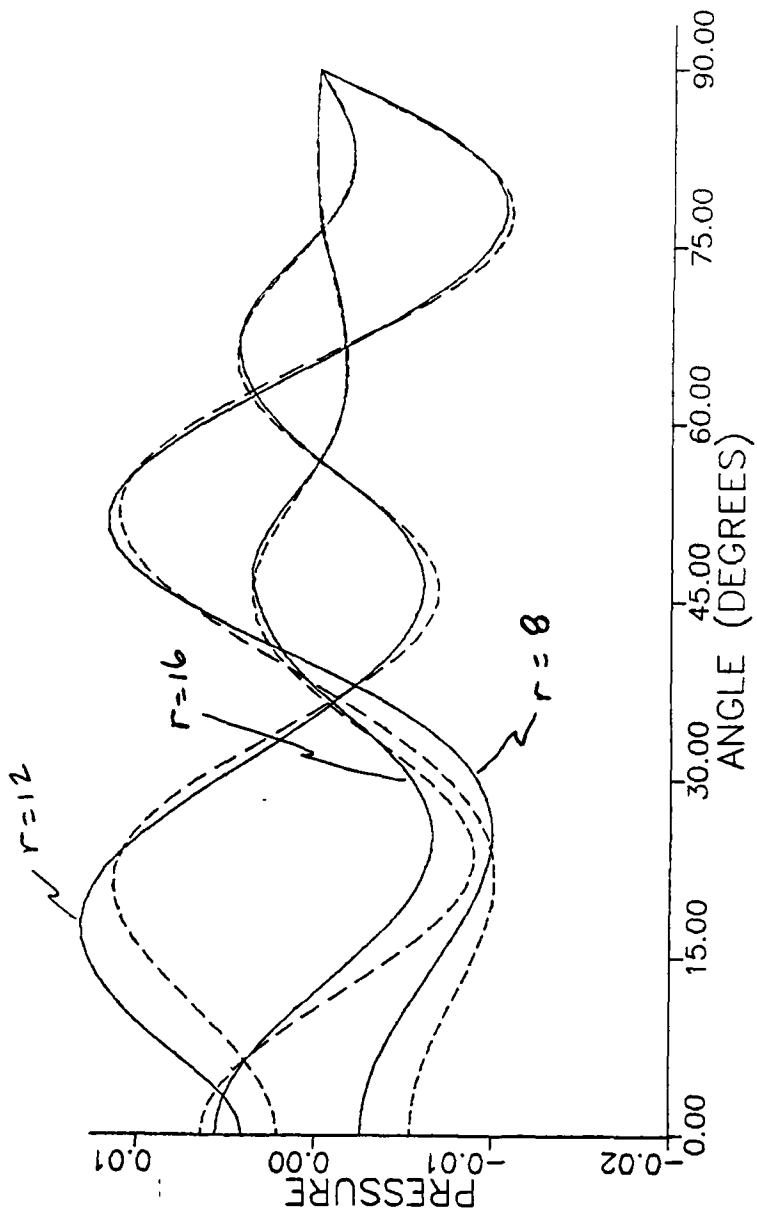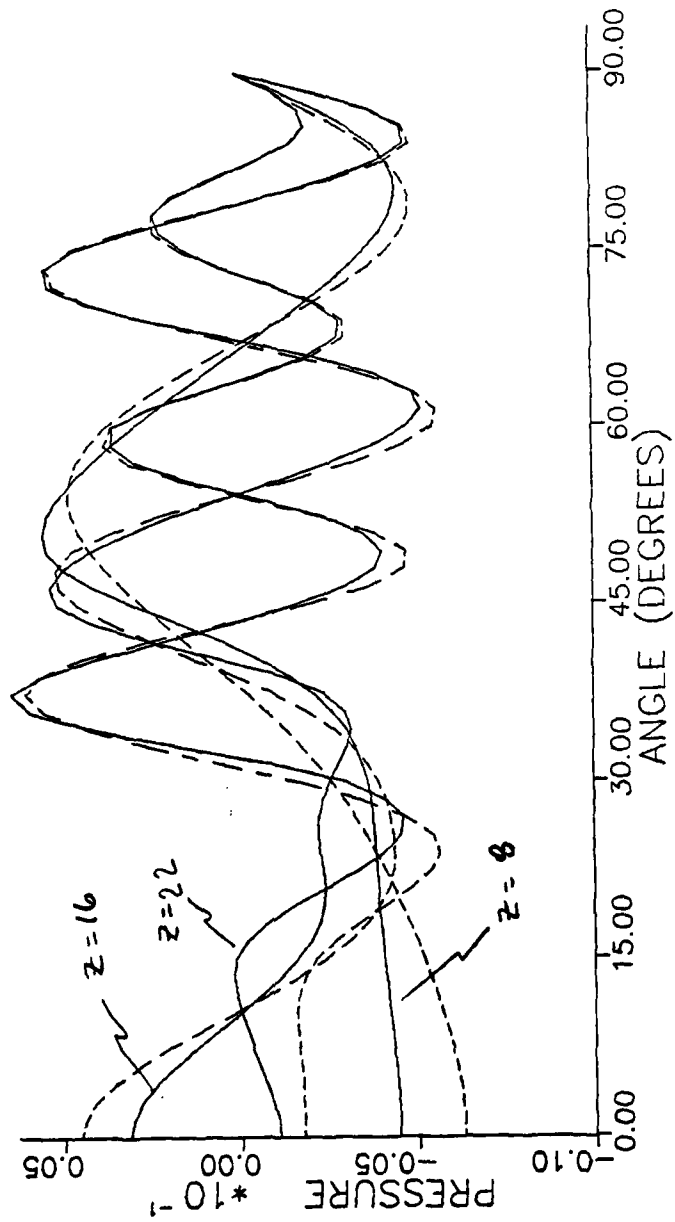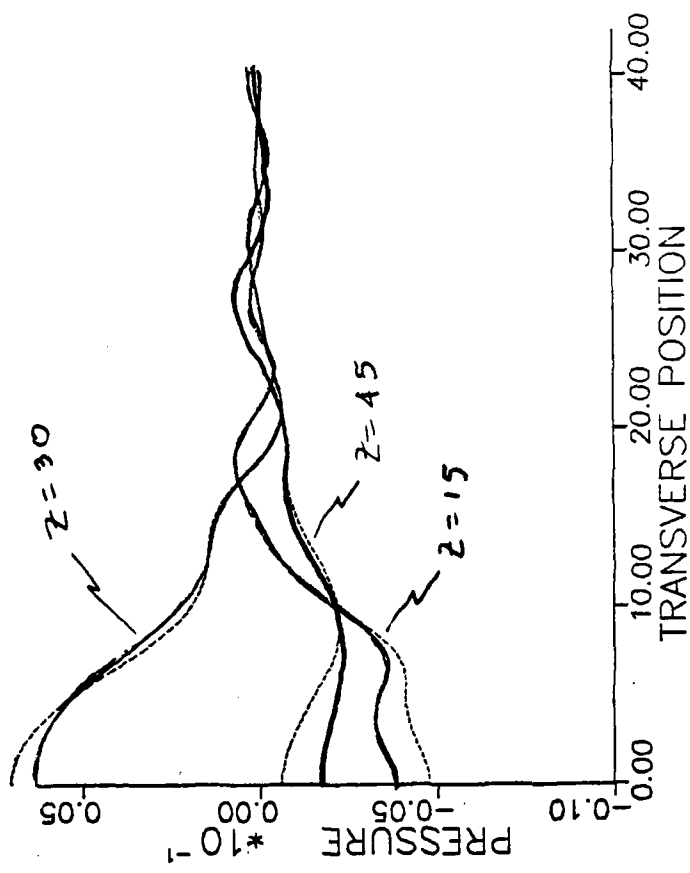
Figure 14

Figure 15

Figure 16

11e CONGRÈS INTERNATIONAL D'ACOUSTIQUE

11th International Congress on Acoustics

11 Internationaler Kongress für Akustik

Paris
19 - 27 juillet
1983

11 ICA

HORS SÉRIE   vol. 1

FINITE AMPLITUDE ACOUSTIC WAVE PROPAGATION IN A CYLINDRICAL WAVEGUIDE

GINSBERG, Jerry H. and MIAO, H. C.

Georgia Institute of Technology
School of Mechanical Engineering
Atlanta, Georgia   30332
USA

Introduction

A signal propagating through a hard-walled circular duct can undergo significant nonlinear distortion, even if the acoustic Mach number is a small fraction. Keller and Millman [1] and Nayfeh [2] investigated this problem under the assumption that other duct modes are not resonantly excited by driven modes. The present work discloses that there is a nonlinear mechanism in which cumulative distortion is generated. The method for analyzing this phenomenon is a direct perturbation scheme using coordinate straining transformations. Much of the development draws on techniques used by the first author to analyze cylindrically propagating waves [3,4]. For simplicity, only axisymmetric duct modes are considered here.

Analytical Formulation

Let $(z/k, R/k)$ denote <u>dimensional</u> axial and transverse coordinates, respectively, for the cylindrical duct, and let <u>dimensional</u> time be t/Ω, where Ω is the frequency of an excitation at $z = 0$ and $k = \Omega/c_0$, with c_0 being the speed of sound in the reference state.

The nonlinear wave equation governing the potential function in this case is

$$\nabla^2\phi - \frac{\partial^2\phi}{\partial t^2} = 2(\beta_0 - 1)\frac{\partial\phi}{\partial t}\nabla^2\phi + \frac{\partial}{\partial t}(\nabla\phi \cdot \nabla\phi) + 0(\phi^3) \qquad (1)$$

where β_0 is the coefficient of nonlinearity ($= 1 + B/2A$ for a liquid). For a hard-walled duct the potential function must satisfy

$$v_R\Big|_{R=ka} = c_0\frac{\partial\phi}{\partial R}\Big|_{R=ka} = 0 \qquad (2)$$

where a is the dimensional radius of the duct. The harmonic excitation considered here gives rise to only one duct mode in a linearized analysis, which is the case when

$$v_z\Big|_{z=0} = c_0\frac{\partial\phi}{\partial z}\Big|_{z=0} = \epsilon c_0 J_0(\mu R)\cos t; \quad J_0'(\mu ka) = 0 \qquad (3)$$

J. H. Ginsberg, Wave Propagation in a Cylindrical Waveguide

---

where J_0 denotes the Bessel function of the first kind of order zero. Note that $\mu k a > 0$ can be any of the zeroes of J_0'.

The acoustic Mach number ϵ is much less than unity. It is used as the perturbation parameter for the potential function.

$$\phi = \epsilon\phi_1 + \epsilon^2\phi_2 + \dots \tag{4}$$

The leading term in this expansion is

$$\phi_1 = -\frac{1}{\alpha} \sin(t - \alpha z) \, J_0(\mu R) \tag{5}$$

where the wave number α is found by satisfying the linear wave equation to be

$$\alpha = (1 - \mu^2)^{\frac{1}{2}} \tag{6}$$

Second Order Analysis

Using the first order solution ϕ_1 to form the source terms exciting the second order potential ϕ_2 obviously leads to products of Bessel functions. Such terms are not amenable to conventional techniques for finding particular solutions. Consider instead the region off-axis where μR is sufficiently large to replace the Bessel function by its asymptotic expansion. Such a region exists if ka is sufficiently large. In cases where ka is not large, the analysis may be conceptualized as temporarily removing the walls of the duct, thereby converting the system to an infinite half plane in $z > 0$. Carrying out the analysis in the fictitious region where μR is large nevertheless leads to a response which satisfies the boundary conditions for the original problem.

When $\mu R \gg 1$, eq. (5) may be represented as

$$\phi_1 = -\frac{1}{\alpha} \left(\frac{2}{\pi\mu R}\right)^{\frac{1}{2}} \sin(t - \alpha z) \cos(\mu R - \frac{\pi}{4}) + 0[(\mu R)^{-3/2}] \tag{7}$$

Substituting this expression into the second order part of the wave equation yields

$$\nabla^2\phi_2 - \frac{\partial^2\phi_2}{\partial t^2} = -\frac{1}{\pi\alpha^2\mu R} \left[(\beta_0 - 2\mu^2) + \beta_0 \sin(2\mu R) \right] \sin(2t - 2\alpha z) + 0[(\mu R)^{-2}] \tag{8}$$

Only the part of the particular solution which exhibits growth with increasing z need be evaluated. The remainder of the particular solution, as well as the complementary solution, remain very small in the entire domain. The result is that in the region where $\mu R \gg 1$, for all z,

$$\phi_2 = -\frac{\beta_0}{4\pi\alpha^3\mu R} z \cos(2t - 2\alpha z) \sin(2\mu R) + 0[(\mu R)^{-1}] \tag{9}$$

The foregoing is recognizable as the asymptotic expansion for large μR of

$$\phi_2 = -\frac{\beta_0}{8\alpha^3} z \cos(2t - 2\alpha z) [J_0(\mu R)^2 - J_0'(\mu R)^2] + 0(1) \tag{10}$$

J. H. Ginsberg, Wave Propagation in a Cylindrical Waveguide

---

where $0(1)$ represents terms that are bounded for all z. This expression is descriptive of the most significant part of the second order potential at <u>all</u> μR.

Renormalization

Expressions for the particle velocity components v_z, v_R and the pressure p may be obtained by taking the appropriate derivatives of the potential function as obtained from eqs. (4), (5), and (9). The general form of these variables is

$$U_1 = \epsilon f_1(t - \alpha z, \mu R) + \epsilon^2 z \, f_2(t - \alpha z, \mu R) + 0(\epsilon^2) \qquad (11)$$

where f_1 and f_2 denote bounded functions. These expressions lose validity when $z = 0(1/\epsilon)$, where the second order term is no longer small. This situation is corrected by replacing the independent variables by a set of strained coordinates. Because time appears only in combination with αz, no separate transformation of t is required. The general form of this transformation is

$$\alpha z = \xi + \epsilon z g_1(\xi, \eta), \quad \mu R = \eta + \epsilon z g_2(\xi, \eta) \qquad (12)$$

Equations (12) are substituted into the expressions described by eqs. (11). Then the functions g_1 and g_2 may be determined by requiring that the $0(\epsilon^2)$ terms in a Taylor series expansion remain bounded for all z. The result of this procedure is that

$$\alpha z = \xi + \frac{\epsilon \beta_0}{2\alpha^2} z \, \cos(t - \xi) J_0(\eta R)$$

$$\mu R = \eta - \frac{\epsilon \beta_0}{2\alpha^2} z \, \sin(t - \xi) J_0'(\eta R) \qquad (13)$$

The particle velocity and pressure resulting from this transformation are

$$p = \frac{\rho_0 c_0}{\mu} \quad v_z = \epsilon \frac{\rho_0 c_0^2}{\mu} \, \cos(t - \xi) J_0(\eta) + 0(\epsilon^2)$$

$$v_R = - \epsilon c_0 \frac{\mu}{\alpha} \sin(t - \xi) J_0'(\eta) + 0(\epsilon^2) \qquad (14)$$

Discussion and Example

Equations (13) and (14) jointly describe the signal. For the purpose of interpreting the results it is instructive to first observe that the coordinate transformation may be rewritten as

$$\alpha z = \xi + \frac{\beta_0}{2\alpha^2} z \, (\frac{v_z}{c_0}) \; ; \quad \mu R = \eta + \frac{\beta_0}{2\mu\alpha} z (\frac{v_R}{c_0}) \qquad (15)$$

Lines of constant ξ and η represent wavefronts and rays of constant phase, respectively, for the signal described by eqs. (14). Thus eq. (15) describes a process of self-refraction, in which rays (constant η) are bent by the transverse velocity. This is in addition to the amplitude dispersion which shifts the wavefronts (constant ϵ) in one-dimensional waves.

The waveforms in Figure 1 describe a signal in air when the fundamental nonplanar duct mode is excited. The corresponding sound pressure level at the source is 156.5 dB (re 20 μPa) and $ka = 9.5$. Each waveform is plotted in retarded time, such that the linearized signal for each case would appear in the figure as one period of a sine curve having essentially the same amplitude as that for the nonlinear signal. The signal at $R = 6.0$ shows a predominant second harmonic because the position is near a nodal ray for the linear signal. This is one of the effects of self-refraction.

Figures 2 and 3 describe the amplitudes P_n of the first six harmonics as a function of the source amplitude P_0. Figure 2 (on-axis) is reminiscent of the result for planar waves. Figure 3 is for an off-axis location near a nodal line for the linear theory. The higher harmonics grow much more rapidly than the fundamental here, as a result of self-refraction of the nodal ray. The gap in the plot of P_1 corresponds to a thus far unexplained null when $P_0 = 156$ dB.

References

1. J. B. Keller and M. H. Millman, J. Acoust. Soc. Am., 49, 329-333 (1971).
2. A. H. Nayfeh, J. Acoust. Soc. Am., 57, 803-810 (1975).
3. J. H. Ginsberg, J. Acoust. Soc. Am., 64, 1671-1678 (1978).
4. J. H. Ginsberg, J. Acoust. Soc. Am., 64, 1679-1687 (1978).
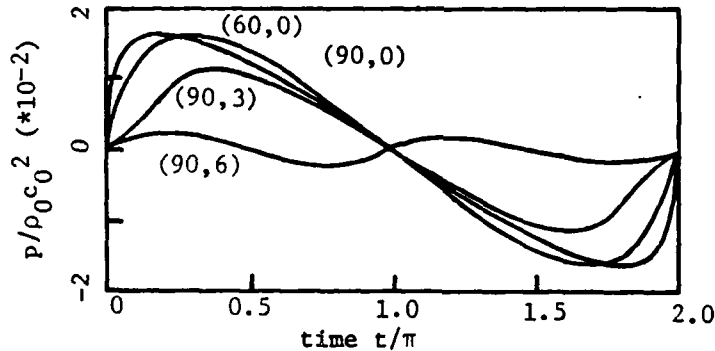
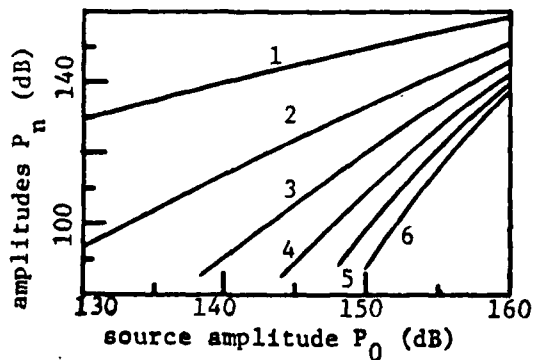Fig 1. Waveform at position (z,r), as indicated

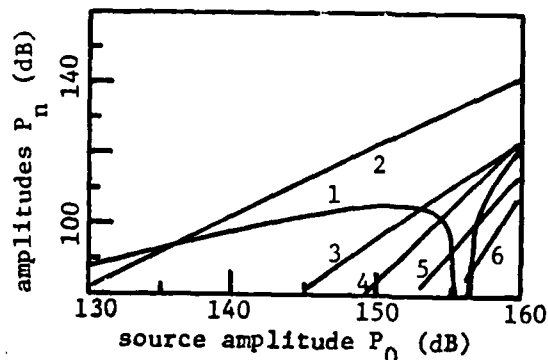Fig 2. Frequency response, $z=90, R=0$

Fig 3. Frequency response, $z=90, R=6$

Finite Amplitude Acoustic
Wave Propagation in a
Cylindrical Waveguide

by

J. H. Ginsberg and H. C. Miao
School of Mechanical Engineering
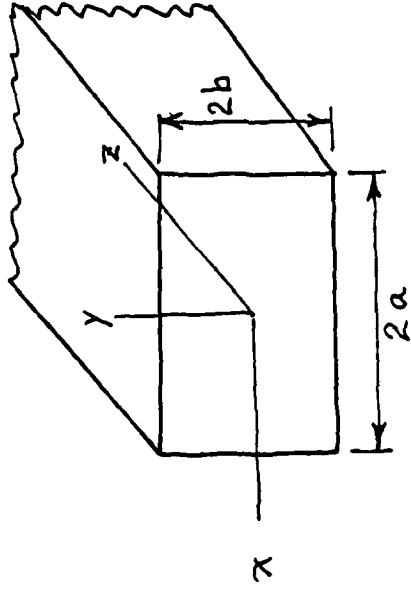Georgia Institute of Technology

Linear Theory

Hard Walled Waveguides

Rectangular

Eigenmode

$$p = e^{i\lambda_3(z-ct)}(\cos \lambda_1 x)(\cos \lambda_2 y)$$

$$\lambda_1 a = m\pi, \quad \lambda_2 b = n\pi$$

$$c^2 = c_0^2\left(1 + \frac{\lambda_1^2}{\lambda_3^2} + \frac{\lambda_2^2}{\lambda_3^2}\right)$$

Groups having same λ_1/λ_3 and λ_2/λ_1 have the same c.
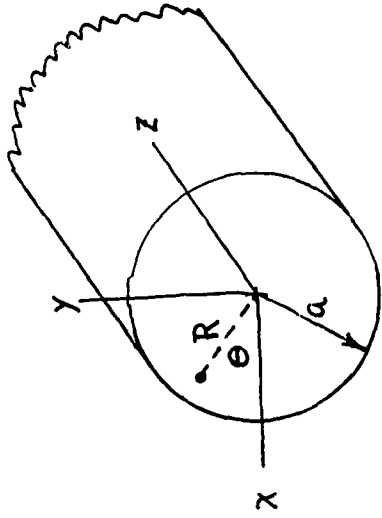
Circular Waveguide

Eigenmode

$$p = e^{i\lambda_3(z-ct)} J_n(\lambda_1 R)(\cos n\theta)$$

$$J_n'(\lambda_1 a) = 0$$

$$c^2 = c_0^2\left(1 + \frac{\lambda_1^2}{\lambda_3^2}\right)$$

Eigenvalues λ_1 do not occur in integer multiples $\Rightarrow$ Distinct c

Question? If $\lambda_1 a >> 1$, then

$$J_n'(\lambda_1 a) \approx \left(\frac{2}{\pi \lambda_1 a}\right)^{1/2} \sin\left(\lambda_1 a - n\frac{\pi}{2} - \frac{\pi}{4}\right) = 0$$

i.e. $\lambda_1 a$ approaches integer multiples

Are there jointly propagating groups?

Finite Amplitude Effects

Circular Cross Section

Axisymmetric - Harmonic

$k = \omega/c_0$: axial wave number - planar modes

$R/k, z/k$: (dimensional) cylindrical coordinates

Nonlinear wave equation:

$$\nabla^2 \phi - \frac{\partial^2 \phi}{\partial t^2} = 2(\beta_0 - 1) \frac{\partial \phi}{\partial t} \nabla^2 \phi + \frac{\partial}{\partial t}(\nabla \phi \cdot \nabla \phi) + O(\phi^3)$$

$$\boxed{\varepsilon \ll 1}$$

Modal excitation:

$$\frac{\partial \phi}{\partial z} = \varepsilon J_0(\mu R) \cos(t) \quad \text{on} \quad z = 0$$

Hard walls:

$$J_0'(\mu k a) = 0$$

Harmonic Formation

Perturbation series: $\phi = \varepsilon \phi_1 + \varepsilon^2 \phi_2 + \cdots$

First order: ϕ_1 is linear solution

$$\phi_1 = -\frac{1}{\alpha} \sin(t - \alpha z) J_0(\mu R)$$

$$\alpha = (1 - \mu^2)^{1/2}$$

Second order:

$$\nabla^2 \phi_2 - \frac{\partial^2 \phi_2}{\partial t^2} = -\left\{ \frac{(\beta_0 - \mu^2)}{\alpha^2} J_0(\mu R)^2 - \frac{\mu^2}{\alpha^2} J_0'(\mu R)^2 \right\} \sin(2t - 2\alpha z)$$

Complementary solution never grows

Distortion results from growth of ϕ_2

$$\boxed{\text{Find particular solution}}$$

Useful identities:

$$\left(\frac{\partial^2}{\partial R^2} + \frac{1}{R}\frac{\partial}{\partial R}\right) J_0(\mu R)^2 = -2\mu^2\left[J_0(\mu R)^2 - J_1(\mu R)^2\right]$$

$$\left(\frac{\partial^2}{\partial R^2} + \frac{1}{R}\frac{\partial}{\partial R}\right) J_1(\mu R)^2$$

$$= 2\mu^2\left[J_0(\mu R)^2 - \left(1-\frac{2}{\mu^2 R^2}\right) J_1(\mu R)^2\right]$$

$$-\frac{2}{\mu R} J_0(\mu R) J_1(\mu R)$$

Hypothesis:
1. If $ka \gg 1$ there is a region where $1/\mu R \ll 1$
2. If ka not large, ignore b.c. at wall $\Rightarrow$ consider infinite half-plane $\Rightarrow$ find solution for $1/\mu R \ll 1$ and verify that b.c. at $R = ka$ is satisfied

Particular solution - variation of parameters

$$\phi_2 = -\frac{\beta_o}{8\alpha^3} z \cos(2t - 2\alpha z)\left[J_o(\mu R)^2 - J_o'(\mu R)^2\right]$$

+ terms bounded at all z

Check boundary condition at wall

Is $\left.\frac{\partial \phi_2}{\partial R}\right|_{R=ka} = 0$?

$\frac{d}{dR}\left[J_o(\mu R)^2 - J_o'(\mu R)^2\right] = 2\mu J_o'(\mu R)\left[J_o(\mu R) - J_o''(\mu R)\right]$

but $\left.J_o'(\mu R)\right|_{R=ka} = J_o'(\mu ka) \equiv 0$

State Variables

Form $\quad \phi = \varepsilon \phi_1 + \varepsilon^2 \phi_2$

Then $\quad v_z = c_o \dfrac{\partial \phi}{\partial z}, \quad v_R = c_o \dfrac{\partial \phi}{\partial R}$

$\qquad p = -\rho_o c_o^2 \dfrac{\partial \phi}{\partial t} + \zeta(\phi^2)$

General form:

$$u_i = \varepsilon f_{i1}(t - \alpha z, \mu R)$$
$$+ \varepsilon^2 z \, f_{i2}(t - \alpha z, \mu R) + O(\varepsilon^2)$$

$\qquad\qquad\qquad\qquad \Uparrow \qquad\qquad\qquad \Uparrow$
$\qquad\qquad\text{non-uniform} \qquad\quad \text{always}$
$\qquad\qquad\text{accuracy} \qquad\qquad\quad \text{bounded}$

Method of Renormalization

1. Near-identity transformation

$$\alpha Z = \xi + \varepsilon \xi \xi g_z (t-\xi, \eta)$$
$$\mu R = \eta + \varepsilon \xi \xi g_R (t-\xi, \eta)$$

2. Taylor series expansions

Powers of ε

Each u_i

3. Cancel terms that are proportional to ξ

Defines g_z and g_R functions

Results

$$P = \frac{\rho_o c_o}{\mu} v_z = \frac{\rho_o c_o^2}{\mu} \epsilon \cos(t-\xi) J_o(\eta)$$

$$v_R = -c_o \frac{\mu}{\alpha} \epsilon \sin(t-\xi) J_o'(\eta)$$

where $\quad \alpha z = \xi + \frac{\beta_o}{2\alpha^2} z \approx \frac{v_z}{c_o}$

$\qquad \mu R = \eta + \frac{\beta_o}{2\mu\alpha} z \approx \frac{v_R}{c_o}$

Self-refraction:

Lines of constant ξ: wavefronts of constant phase

Lines of constant η: rays tracing signal back to excitation

Wavefronts and rays are bent by velocity component transverse to them

Typical Waveforms

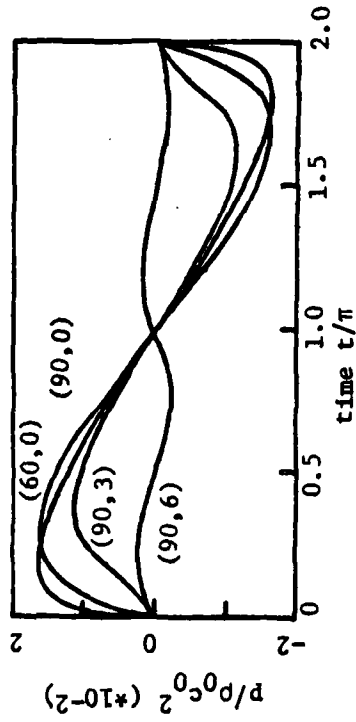Air: 156.5 dB re 20 μPa, ka = 9.5

Distance/ka = units of cylinder radius

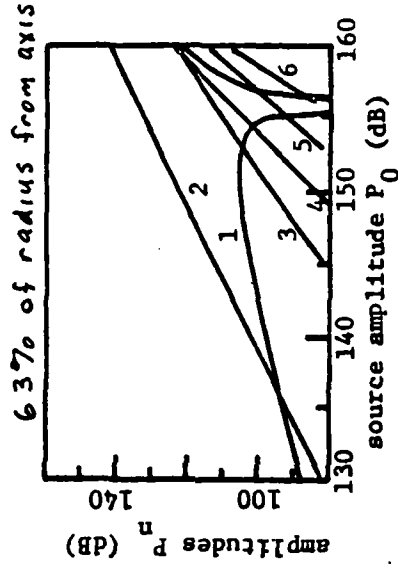Fig 1. Waveform at position (z,r), as indicated

Frequency Response
ka = 9.5
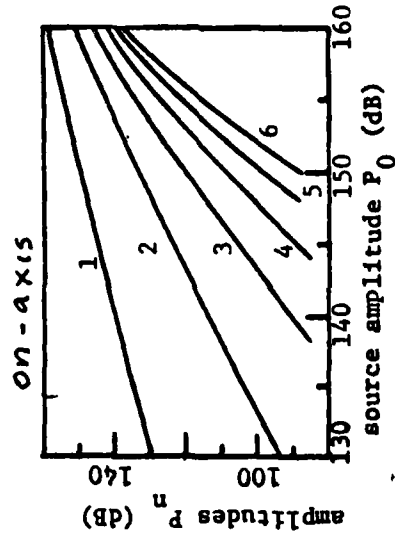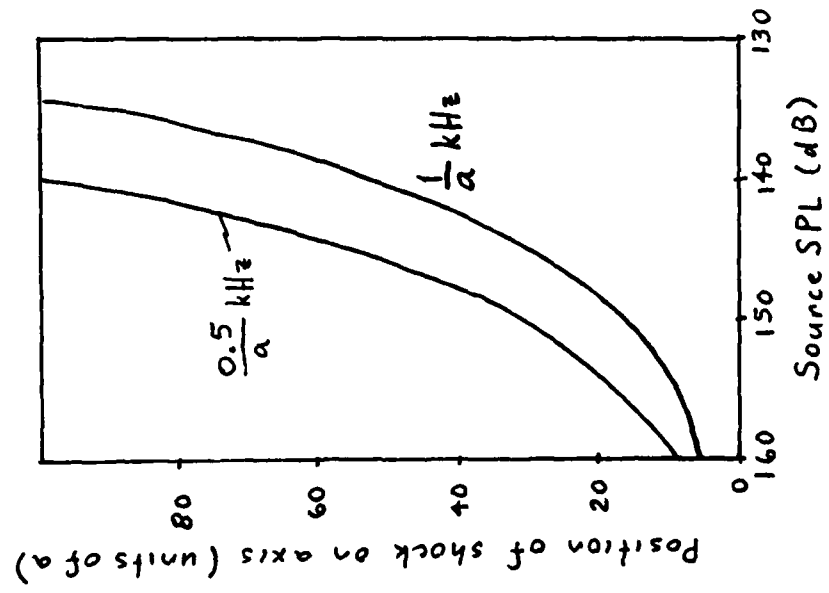

Fig 2. Frequency response, z=90,R=0

Fig 3. Frequency response, z=90,R=6

Shocks - multi-valued solution

First occurrence - Jacobian vanishes

$$\begin{vmatrix} \dfrac{\partial \xi}{\partial z} & \dfrac{\partial \eta}{\partial z} \\[2mm] \dfrac{\partial \xi}{\partial R} & \dfrac{\partial \eta}{\partial R} \end{vmatrix} = 0$$

$$z^* = \frac{2\alpha^2}{\epsilon \beta_0}$$

Graph: vertical axis "Position of shock on axis (units of a)" with values 80, 60, 40, 20; horizontal axis "Source SPL (dB)" with values 130, 140, 150, 160. Curves labeled $\dfrac{0.5}{a}$ kHz and $\dfrac{1}{a}$ kHz.

Nonlinear King integral for arbitrary axisymmetric sound beams at finite amplitudes. I. Asymptotic evaluation of the velocity potential

Jerry H. Ginsberg

School of Mechanical Engineering, Georgia Institute of Technology, Atlanta, Georgia 30332

This paper initiates the derivation of a general analytical model for nonlinear effects in sound beams driven at high source pressure levels. The excitation is generated by a planar transducer that is in harmonic motion in an arbitrary axisymmetric pattern. The analysis develops a perturbation solution of a nonlinear equation for the velocity potential. The first-order term, which is derived with the aid of a Hankel transform to represent the transverse dependence, is the King integral for a linear sound beam. Using this integral to form the source terms exciting the second-order potential leads to a dual Hankel transform. Reduction to a single integral is achieved with the aid of an asymptotic integration following Laplace's method. The second-order term that is derived in this manner describes the tendency for the second harmonic to grow with increasing distance from the source. This result is an intermediate step in the overall development, because the integrand loses validity in the spectrum of transverse wavenumbers near the transition between evanescent and propagating wavelets, as well as for increasing distance from the transducer.

PACS numbers: 43.25.Cb

INTRODUCTION

Recent surveys[1,2] have noted that the "infinite baffle" problem has been described by several alternative formulations. The specific concern in this subject is the signal generated within a fluid by small amplitude oscillations of a transducer which is contained within an infinite planar boundary. Such results are valid for very weak signals, in which case material and convective nonlinearities are negligible effects. Two basic formulations of the linear problem are the Rayleigh and King integrals.

The Rayleigh integral[3] treats the signal as a superposition of spherical wavelets which are generated by infinitesimal sources on the transducer face. In contrast, the King integral[4] results from a Hankel (Fourier–Bessel) integral transform transverse to the axis of symmetry. The acoustical medium in such an analysis becomes a waveguide of infinite diameter. The transducer then seems to generate a spectrum of guided planar mode wavelets whose strength varies with the transverse position. The significant aspect of both quadrature solutions is that they provide a convenient framework for quantitative evaluations of the signal at any location. They also lead to analytical approximations that are valid in certain ranges, such as the Fraunhofer (farfield) region.

The same is not true for treatments of nonlinear effects which arise when the transducer is driven to large amplitudes. One type of analysis of this question was performed by Lockwood *et al.*[5] They considered the case where the excitation is reasonably small, so that nonlinearity is not significant in the nearfield. Such a restriction leads to a farfield description based on Lockwood's analysis of nonuniform spherical waves.[6] Obviously, such an analysis provides no information regarding nonlinear effects in the nearfield.

The nearfield was the specific concern of the analysis performed by Ingenito and Williams.[7] They employed a perturbation series for the potential function, in which the leading term was described by the Rayleigh integral. That result was then used to evaluate the source terms exciting the second-order potential. Neglecting backscattering at the second order and introducing some additional approximations then led to a description of second harmonic formation that had a quadrature form.

One limitation of that analysis is that it is valid only for very high frequencies: $ka > 100$ according to Ref. 7. Another shortcoming is one that is often encountered in perturbation analyses. Specifically, if a dependent variable is expanded in a perturbation series, then the results are only valid when the second-order terms are very small compared to the first order ones. The analysis performed by Ingenito and Williams indicated that the second harmonic grows with increasing axial distance, whereas the first harmonic (i.e., linear result) shows no such growth. It follows that these results shed light on how harmonics begin to form, but further extrapolation might lead to errors. (This seems to be the case for their Fig. 1.)

Another formulation of finite amplitude sound beams, which has been prominent in the Soviet literature, employs a modified Burgers' equation. The basic assumption made in the derivation of this equation[8,9] is that there are three spatial scales for the signal. The shortest scale is the axial wavelength and the longest scale describes the development of nonlinear effects axially. The intermediate scale describes the variation transverse to the axis of symmetry.

These approximations seem reasonable for the high-frequency limit. Unfortunately, solutions for monochromatic transducer motion have only been obtained by finite-difference techniques. Typical of such investigations are Refs. 10–

12, which all seem to have employed the same (incompletely described) computer code. It is significant that this group of investigations have only considered situations where the boundary excitation is a prescribed pressure. Extending those analyses to cases where the particle velocity on the boundary is known, as is the case for most transducers, requires a relation between pressure and velocity that is not contained in the basic theory. Also, it should be noted that the small scale of some diffraction effects[13] introduces some doubt regarding the length scales assumed to derive the modified Burgers' equation.

The present investigation is a perturbation analysis, as was the work by Ingenito and Williams, although the King integral is used here to describe the first-order term. The analysis is founded on the recognition that nonlinearities arise in two forms when the signal level is moderately high. Some nonlinear effects maintain their level or die out as the signal propagates away from the transducer. Typical of such an effect is the fact that the transducer face represents a moving, rather than a fixed boundary, for satisfying continuity of particle velocity.

Order of magnitude considerations indicate that such effects are too small to describe the levels of higher harmonics that have been measured.[14,15] As is the case for planar and other one-dimensional waves,[16] significant distortion phenomena stem from cumulative growth of higher harmonics. Such action is a result of the fact that the acoustic medium is nondispersive, so that higher harmonics propagate with, and resonantly interact with, the primary signal.

The present analysis consistently accounts for cumulative growth effects. The sole assumption introduced in the course of the analysis is that the nonlinear mechanism causing harmonic generation has the same behavior at all locations in the acoustic field. The first part of the investigation, described in this paper, obtains an expression for the first two orders of approximation of the velocity potential. The second part of the investigation[17] will employ coordinate straining transformations to correct irregularities in the response associated with the derived potential function. The acoustic signal will be described in a quadrature form that is reminiscent of the linear King integral. A quantitative example will compare the harmonic content of the waveform to measurements recently reported by Gallego-Juarez and Gaete-Garreton.[15]

The overall analytical procedure may be traced back to the author's previous investigation of two-dimensional radiation from a boundary.[18,19] However, the use of complex functional forms and the introduction of Hankel transforms to treat the axisymmetrical geometry require substantial alterations from previous work.

I. FUNDAMENTAL EQUATIONS

The propagation speed of infinitesimal planar waves is denoted as c_0, and $(\beta_0 - 1)$ is the nonlinearity parameter in the pressure-density relation at fixed entropy[3]

$$p = \rho_0 c_0^2 \left[\left(\frac{\rho - \rho_0}{\rho_0} \right) + (\beta_0 - 1) \left(\frac{\rho - \rho_0}{\rho_0} \right)^2 + \cdots \right]. \quad (1)$$

Thus $\beta_0 = (\gamma + 1)/2$ for an ideal gas, where γ is the ratio of specific heats. Let (R, z) denote nondimensional cylindrical coordinates (axisymmetric), with $R = 0$ corresponding to the center of the transducer which is on the boundary $z = 0$. Also, denote the nondimensional time variable as t. The corresponding dimensional position coordinates are $(R/k, z/k)$ and the dimensional time is t/ω, where ω is the frequency of the monochromatic excitation and $k = \omega/c_0$ is the wavenumber for a nominal planar wave.

The dimensionless velocity potential ϕ is related to the particle velocity components by

$$v_z = c_0 \frac{\partial \phi}{\partial z}, \quad v_R = c_0 \frac{\partial \phi}{\partial R}. \quad (2)$$

The boundary condition corresponding to the axisymmetric motion of an arbitrary transducer may then be written in complex form as

$$\left. \frac{\partial \phi}{\partial z} \right|_{z=0} = \frac{\epsilon}{2i} f(R) \exp(it) + \text{c.c.}, \quad (3)$$

where $f(R)$ is any complex function whose magnitude approaches zero with increasing R. In general, c.c. will be used to denote the complex conjugate of the preceding term. (Forming products of complex functions necessitates retaining conjugate parts, rather than identifying only real parts.) For weakly nonlinear waves, the acoustic Mach number ϵ is a finite parameter with $|\epsilon| \ll 1$. The nonlinear wave equation governing ϕ is[20]

$$\nabla^2 \phi - \frac{\partial^2 \phi}{\partial t^2} = 2(\beta_0 - 1) \frac{\partial \phi}{\partial t} \nabla^2 \phi + \frac{\partial}{\partial t} (\nabla \phi \cdot \nabla \phi) + O(\phi^3), \quad (4a)$$

where

$$\nabla^2 \phi = \frac{\partial^2 \phi}{\partial R^2} + \frac{1}{R} \frac{\partial \phi}{\partial R} + \frac{\partial^2 \phi}{\partial z^2}, \quad (4b)$$

$$\nabla \phi \cdot \nabla \phi = \left(\frac{\partial \phi}{\partial R} \right)^2 + \left(\frac{\partial \phi}{\partial z} \right)^2.$$

In addition to Eq. (3), the other boundary condition for ϕ is that the signal should be either an outgoing wave or an evanescent wave at large z, and that it show suitable decay with increasing R.

The velocity potential is expanded in a perturbation series

$$\phi = \epsilon \phi_1 + \epsilon^2 \phi_2 + \cdots. \quad (5)$$

The equations governing ϕ_1 and ϕ_2 are found by collecting like powers of ϵ in Eqs. (3) and (4a). The first-order equations are

$$\nabla^2 \phi_1 - \frac{\partial^2 \phi_1}{\partial t^2} = 0,$$

$$\left. \frac{\partial \phi_1}{\partial z} \right|_{z=0} = \frac{1}{2i} f(R) \exp(it) + \text{c.c.} \quad (6)$$

Equations (6) are the statement of the linearized problem. The nonlinear effects are contained in ϕ_2 and succeeding terms. A complete solution for ϕ_2 requires satisfaction of the boundary conditions, which involves evaluation of the

complementary solution, as well as of the particular solution associated with the source terms arising from ϕ_1. However, the complementary solution is bounded and therefore represents a noncumulative $O(\epsilon^2)$ contribution to the signal at all locations. As noted earlier such effects are usually insignificant compared to the observed levels of nonlinear distortion. Thus it is only necessary to find a particular solution of the second-order equation. The first of Eqs. (6) provides a simple identity for $\nabla^2 \phi_1$. The resulting second-order equation arising from Eq. (4a) is

$$\nabla^2 \phi_2 - \frac{\partial^2 \phi_2}{\partial t^2} = \frac{\partial}{\partial t}\left[(\beta_0 - 1)\left(\frac{\partial \phi_1}{\partial t}\right)^2 + \nabla \phi \cdot \nabla \phi \right]. \quad (7)$$

II. LINEARIZED SOLUTION

Two approaches that have been employed to solve the linearized problem, Eqs. (6), are the Rayleigh integral and the King integral. The latter, which is essentially an inversion of a Hankel (Fourier–Bessel) transform, is more suitable for the task of evaluating ϕ_2. Hence let

$$\phi_1 = \int_0^\infty n\Phi_1(n,z,t)J_0(nR)\,dn + \text{c.c.} \quad (8)$$

Substituting this expression into Eqs. (6) and using the fact that $J_0(nR)$ is a solution of Bessel's equation leads to

$$\frac{\partial^2 \Phi_1}{\partial z^2} - \frac{\partial^2 \Phi_1}{\partial t^2} - n^2 \Phi_1 = 0,$$

$$\frac{\partial \Phi_1}{\partial z}\bigg|_{z=0} = F_n \exp(it), \quad (9)$$

where

$$F_n = \frac{1}{2i}\int_0^\infty R f(R) J_0(nR)\,dR \quad (10)$$

is the transform of the (complex) spatial excitation function $f(R)$.

The solution of Eqs. (9) is a propagating wave when $0 < n < 1$, or an evanescent wave when $n > 1$. This solution is

$$\Phi_1 = -(F_n/\mu_n)\exp(it - \mu_n z), \quad (11)$$

where

$$\mu_n^2 = n^2 - 1. \quad (12a)$$

Satisfying the radiation condition as $z \to \infty$ leads to the following choice for the branch cuts:

$$\mu_n = \begin{cases} i(1 - n^2)^{1/2}, & 0 < n < 1, \\ (n^2 - 1)^{1/2}, & n > 1. \end{cases} \quad (12b)$$

The result of substituting Eq. (11) into Eq. (8) is

$$\phi_1 = -\int_0^\infty \left(\frac{nF_n}{\mu_n}\right)\exp(it - \mu_n z)J_0(nR)\,dn + \text{c.c.} \quad (13)$$

This is the King integral representation of the potential function for the linearized sound beam.

III. SECOND-ORDER POTENTIAL

The first-order solution ϕ_1 in Eq. (13) is used to form the source terms driving ϕ_2 in Eq. (7). Forming quadratic products of ϕ_1 requires that different symbols be used to represent the transverse wavenumber forming each term in the product. Also, care must be taken to include the complex conjugate parts in the product. A quadratic product of sinusoidal terms generally leads to a term having a nonzero mean value, but the time derivative appearing on the right side of Eq. (7) removes such an effect. The result is

$$\nabla^2 \phi_2 - \frac{\partial^2 \phi_2}{\partial t^2}$$
$$= -4i\int_0^\infty \int_0^n \left(\frac{mnF_m F_n}{\mu_m \mu_n}\right)[(\beta_0 - 1 - \mu_m \mu_n)$$
$$\times J_0(mR)J_0(nR) - mnJ_1(mR)J_1(nR)]$$
$$\times \exp[2it - (\mu_m + \mu_n)z]\,dm\,dn + \text{c.c.}, \quad (14)$$

where the symmetry of the integrand has been exploited to reduce the integration over the first wavenumber to a finite range. (This introduces an additional factor of two.)

It is consistent with the form of Eq. (14) to try to construct the particular solution for ϕ_2 as the sum of two dual Hankel transforms. The kernel of one transform would be $mn J_0(mR)J_0(nR)$ and the kernel of the second would be $mn J_1(mR)J_1(nR)$. The following equivalent form, which utilizes linear combinations of the aforementioned kernel functions, leads to significant analytical simplifications.

$$\phi_2 = \int_0^\infty \Phi_2\,dn, \quad (15a)$$

where

$$\Phi_2 = n\int_0^n m\Phi_{21}(z,t,m,n)[J_0(mR)J_0(nR)$$
$$- J_1(mR)J_1(nR)]dm + n\int_0^n m\Phi_{22}(z,t,m,n)$$
$$\times [J_0(mR)J_0(nR) + J_1(mR)J_1(nR)]dm. \quad (15b)$$

The following identities, which are derived from the recursion relations for Bessel functions,[21] are useful for evaluating the transverse derivatives of ϕ_2:

$$\left(\frac{\partial^2}{\partial R^2} + \frac{1}{R}\frac{\partial}{\partial R}\right)J_0(mR)J_0(nR)$$
$$= -(m^2 + n^2)J_0(mR)J_0(nR) + 2mnJ_1(mR)J_1(nR),$$

$$\left(\frac{\partial^2}{\partial R^2} + \frac{1}{R}\frac{\partial}{\partial R}\right)J_1(mR)J_1(nR) \qquad (16)$$
$$= 2mnJ_0(mR)J_0(nR) - (m^2 + n^2 - 4/R^2)J_1(mR)$$
$$\times J_1(nR) - 2(m/R)J_0(mR)J_1(nR)$$
$$- 2(n/R)J_1(mR)J_0(nR).$$

In view of these relations, the result of substituting Eqs. 15 into Eq. (14) and matching the integrands on either side of the equality sign is
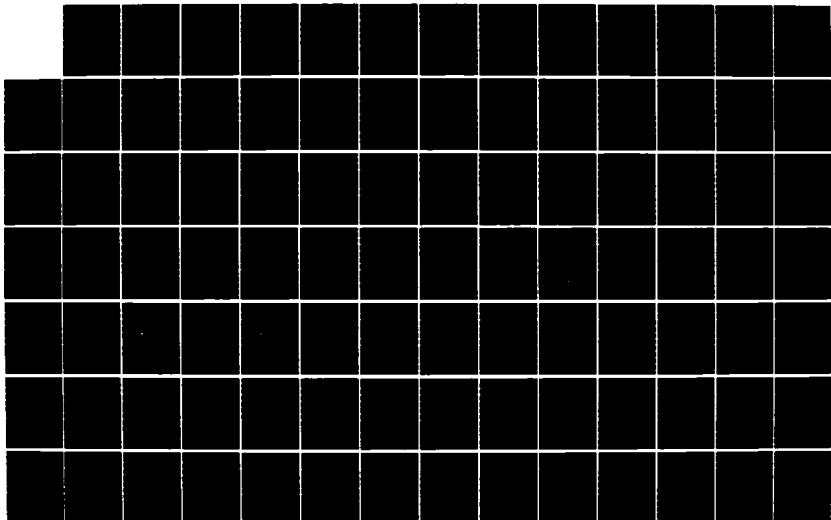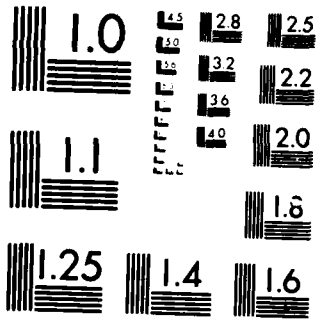
MICROCOPY RESOLUTION TEST CHART
NATIONAL BUREAU OF STANDARDS 1963-A

$$\left[\frac{\partial^2 \Phi_{21}}{\partial z^2} - \frac{\partial^2 \Phi_{21}}{\partial t^2} - (m+n)^2 \Phi_{21}\right][J_0(mR)J_0(nR) - J_1(mR)J_1(nR)]$$

$$+ \left[\frac{\partial^2 \Phi_{22}}{\partial z^2} - \frac{\partial^2 \Phi_{22}}{\partial t^2} - (m-n)^2 \Phi_{22}\right][J_0(mR)J_0(nR) + J_1(mR)J_1(nR)]$$

$$- [(4/R^2)J_1(mR)J_1(nR) - 2(m/R)J_0(mR)J_1(nR) - 2(n/R)J_1(mR)J_0(nR)](\Phi_{21} - \Phi_{22})$$

$$= -4i(F_m F_n/\mu_m \mu_n)[(\beta_0 - 1 - \mu_m \mu_n)J_0(mR)J_0(nR) - mnJ_1(mR)J_1(nR)]\exp[2it - (\mu_m + \mu_n)z] + \text{c.c.} \qquad (17)$$

If the last bracketed term on the left side of this equation was not present, it would be a simple matter to match like functions of R on either side. In order to address this matter, note that the functions Φ_{21} and Φ_{22} are independent of R. Conditions governing them in a specific region of R should be applicable for all R. This is significant because the bracketed term causing difficulty in Eq. (17) decreases at a rate $1/R$ faster than the other terms as R increases. The foregoing argument suggests that because the term is negligible at large R, it should be negligible in the evaluation of Φ_{21} and Φ_{22} at any R.

The validity of this hypothesis might be questioned for situations where n and m are small. In that case, the asymptotic decay of Bessel functions having arguments mR or nR might be approached at unacceptably large values of R. This question may be examined by using the series expansions of the Bessel functions for small arguments. Specifically, when $mR \ll 1$ and $nR \ll 1$, it may be shown that

$$\frac{4}{R^2}J_1(mR)J_1(nR) - 2\frac{m}{R}J_0(mR)J_1(nR) - 2\frac{n}{R}J_1(mR)$$

$$\times J_0(nR) = -mn[1 - \tfrac{1}{4}(m^2 + n^2)R^2$$
$$+ \tfrac{1}{64}(5m^2n^2 - m^4 - n^4)R^4 - \cdots] . \qquad (18)$$

Thus the third bracketed term in Eq. (17) is $O(mn)$ when mR and nR are small, whereas other terms in that equation are order unity. Thus the troublesome bracketed term should have negligible influence in this region also.

Neglecting the aforementioned term has a physical justification. Recall that in the King integral formulation, the acoustic signal is viewed as a spectrum of modes in an infinite waveguide. The wavenumbers m and n are merely parameters characterizing the transverse rate of variation of these modes. It is reasonable to expect that the nonlinear mechanism generating the second-order contributions to these modes are described by the same differential equations at all values of R, and for all values of m and n.

When the third bracketed term in Eq. (17) is ignored, matching like functions of R in that equation leads to

$$\frac{\partial^2 \Phi_{21}}{\partial z^2} - \frac{\partial^2 \Phi_{21}}{\partial t^2} - (m+n)^2 \Phi_{21}$$

$$= -2i\frac{F_n F_m}{\mu_n \mu_m}(\beta_0 - 1 - \mu_n \mu_m + nm)$$

$$\times \exp[2it - (\mu_n + \mu_m)z] + \text{c.c.},$$

$$\frac{\partial^2 \Phi_{22}}{\partial z^2} - \frac{\partial^2 \Phi_{22}}{\partial t^2} - (m-n)^2 \Phi_{22}$$

$$= -2i\frac{F_n F_m}{\mu_n \mu_m}(\beta_0 - 1 - \mu_n \mu_m - nm)$$

$$\times \exp[2it - (\mu_n + \mu_m)z] + \text{c.c.} \qquad (19)$$

The virtue of constructing the solution for ϕ_2 in the form of Eqs. (15) is now evident; any other form would not have resulted in uncoupling of the equations for the transform variables Φ_{21} and Φ_{22}.

The form of the solution of Eqs. (19) is suggested by the physical implication of the linear King integral, which consists of a continuous spectrum of modes in a circular waveguide of infinite extent. The axis of the sound beam (i.e., the z axis) is the direction in which these modes propagate. In general, nonlinear generation of harmonics increases with increasing propagation distance. Hence the particular solutions may be written as

$$\Phi_{21} = a(z,m,n)\exp[2it - (\mu_n + \mu_m)z] + \text{c.c.},$$
$$\qquad (20)$$
$$\Phi_{22} = b(z,m,n)\exp[2it - (\mu_n + \mu_m)z] + \text{c.c.},$$

where cumulative growth will be manifested by increasing values of the amplitudes a and b. Substitution of Eqs. (20) into Eqs. (19) leads to a set of uncoupled ordinary differential equations for these amplitudes.

$$\frac{d^2a}{dz^2} - 2(\mu_n + \mu_m)\frac{da}{dz} + [(\mu_n + \mu_m)^2 - (m+n)^2 + 4]a$$

$$= -2i\frac{F_n F_m}{\mu_n \mu_m}(\beta_0 - 1 - \mu_n \mu_m + nm), \qquad (21a)$$

$$\frac{d^2b}{dz^2} - 2(\mu_n + \mu_m)\frac{db}{dz} + [(\mu_n + \mu_m)^2 - (m-n)^2 + 4]b$$

$$= -2i\frac{F_n F_m}{\mu_n \mu_m}(\beta_0 - 1 - \mu_n \mu_m - nm). \qquad (21b)$$

At this stage, it is appropriate to recall that the analysis of ϕ_2 requires evaluation of only the portion that exhibits growth. If the values of m and n are such that the coefficient of a or b in Eqs. (21) does not vanish, then the particular solution is independent of z. In contrast, if this coefficient should vanish, then the corresponding particular solution for a or b is proportional to z. (Vanishing of the coefficient is equivalent to secularity in perturbation analyses of nonlinear vibrations.) It is found with the aid of Eq. (12b) that the condition of a vanishing coefficient only occurs when $m = n$ in Eq. (19a). Therefore only the contribution of a needs to be evaluated. The magnitude of b is bounded at all z, which means that b does not represent a cumulative distortion effect.

IV. INTEGRATION BY LAPLACE'S METHOD

The condition where the solution to Eq. (21a) grows with increasing z has been shown to arise as $m \to n$. In contrast, regions far from $m = n$ represent contributions that do not change in overall magnitude with increasing distance.

The contribution of the region around $m = n$ may be determined by following Laplace's asymptotic integration method[22] based on an expansion using

$$m = n - q\Delta, \quad \Delta \ll 1, \quad q = O(1), \quad (22a)$$

where Δ and q are positive because $m < n$ for the integrals in Eqs. (15). Note that Δ is a fixed parameter indicating the scale of the difference between m and n. The Taylor series for the coefficient μ_m defined in Eq. (12b) is found to be

$$\mu_m = \mu_n(1 - nq\Delta/\mu_n^2 - q^2\Delta^2/2\mu_n^4 + \cdots). \quad (22b)$$

These expressions for m and μ_m lead to the following representation of Eq. (21a) in the region where $m \approx n$:

$$\frac{d^2a}{dz^2} - 2\mu_n\left(2 - \frac{nq\Delta}{\mu_n^2} - \frac{q^2\Delta^2}{2\mu_n^4} + O(\Delta^3)\right)\frac{da}{dz}$$

$$- [q^2\Delta^2/\mu_n^2 + O(\Delta^3)]a_1 = -2i\beta_0 F_n^2/\mu_n^2. \quad (22c)$$

Now observe that when $q = 0$ $(m = n)$, the particular solution of this equation is

$$a|_{q=0} = (i\beta_0 F_n^2/2\mu_n^3)z. \quad (23)$$

In contrast, the general solution for a when $q \neq 0$ has the form

$$a = A_1 \exp(\sigma_1 z) + A_2 \exp(\sigma_2 z) + 2i\beta_0 F_n^2/q^2\Delta^2, \quad (24)$$

where the coefficients σ_1 and σ_2 are the roots of the characteristic equation governing the complementary solution:

$$\sigma^2 - 2\mu_n(2 - nq\Delta/\mu_n^2 - q^2\Delta^2/2\mu_n^4)\sigma - q^2\Delta^2/\mu_n^2 = 0. \quad (25)$$

Solving this quadratic equation yields

$$\sigma_1 = -q^2\Delta^2/4\mu_n^3 + O(\Delta^3), \quad \sigma_2 = 4\mu_n + O(\Delta). \quad (26)$$

As $q \to 0$, Eq. (24) must approach Eq. (23). Because σ_2 is $O(1)$ and Eq. (23) has no term that varies exponentially in z, set $A_2 = 0$. Also, because σ_1 is $O(\Delta^2)$, $\exp(\sigma_1 z)$ may be replaced by the leading terms in a series. The condition that Eq. (24) approach Eq. (23) then leads to

$$\lim_{q \to 0} [A_1(1 + \sigma_1 z) + 2i\beta_0 F_n^2/q^2\Delta^2] = (i\beta_0 F_n^2/2\mu_n^3)z. \quad (27)$$

The first of Eqs. (26) shows that this condition is satisfied at all values of z by

$$A_1 = -2i\beta_0 F_n^2/q^2\Delta^2. \quad (28)$$

Substituting this expression into Eq. (24) yields the general solution

$$a = (2i\beta_0 F_n^2/q^2\Delta^2)[1 - \exp(-q^2\Delta^2 z/4\mu_n^3)]. \quad (29)$$

The next step is to evaluate the total contribution to Φ_2 of the value of a associated with all wavenumbers m. For this determination the first wavenumber n is held constant at an arbitrary value. The combined effect is defined by Eqs. (15) and (20) to be

$$\Phi_2 = n\int_0^n m\{a(z,m,n)\exp[2it - (\mu_n + \mu_m)z] + c.c.\}$$

$$\times [J_0(mR)J_0(nR) - J_1(mR)J_1(nR)]dm + O(1). \quad (30)$$

Equation (29) gives the behavior of a in the region where $m \approx n$. According to Laplace's integration technique, the behavior at large z may be found by using that relation only. In order to demonstrate this feature, the region of integration is broken into two intervals. The boundary between these intervals is defined to be $m = n - \delta$, where δ is a small finite quantity. Then

$$\Phi_2 = \int_0^{n-\delta} d\Phi_2 + \int_{n-\delta}^n d\Phi_2. \quad (31)$$

Because the first domain of integration does not contain the secularity condition, the oscillatory nature of the integrand results in boundedness of the first integral for all z.[23] This term, like comparable effects that occurred earlier, does not contribute to the cumulative distortion process, so it is discarded. In essence, this region features destructive interference between the m and n waves.

In order to evaluate the second integral, Eqs. (22) and (29) are substituted into Eq. (30). The difference between m and n is less than δ in the region of integration, so m may be replaced by n in the Bessel function. Similarly, μ_m may be replaced by μ_n in the exponential term in Eq. (30). The integral arising from Eq. (31) then simplifies to

$$\Phi_2 = \{2i\beta_0 n^2 F_n^2 E(\delta,\Delta,z/\mu_n^3)\exp(2it - 2\mu_n z) + c.c.\}$$

$$\times [J_0(nR)^2 - J_1(nR)^2], \quad (32)$$

where

$$E(\delta,\Delta,z/\mu_n^3) = \int_0^{\delta/\Delta}\left(\frac{1 - \exp(-q^2\Delta^2 z/4\mu_n^3)}{q^2\Delta^2}\right)(\Delta dq). \quad (33)$$

Evaluation of the function E introduces a square root of z/μ_n^3, for which it is important to account for the fact that μ_n is imaginary when $n < 1$. Specifically,

$$\left(\frac{z}{\mu_n^3}\right)^{1/2} = \left(\frac{\mu_n z}{|n^2 - 1|^2}\right)^{1/2} = \frac{(\mu_n z)^{1/2}}{\mu_n\overline{\mu_n}}, \quad (34)$$

where an overbar denotes the complex conjugate of the marked quantity. Integration by parts of Eq. (33) then gives

$$E(\delta,\Delta,z/\mu_n^3) = \left(\frac{(\pi\mu_n z)^{1/2}}{2\mu_n\overline{\mu_n}}\right)\text{erf}\left(\frac{\delta(\mu_n z)^{1/2}}{2\mu_n\overline{\mu_n}}\right)$$

$$- (1/\delta)[1 - \exp(-\delta^2 z/4\mu_n^3)], \quad (35)$$

where erf denotes the error function.

One noteworthy feature of Eqs. (32) and (35) is that the only remaining parameter associated with the asymptotic integration is the integration limit δ, which is finite value. Consider Eq. (35) as z increases while δ is held fixed. An expansion of the error function for large arguments leads to

$$\text{erf}\left(\frac{\delta(\mu_n z)^{1/2}}{2\mu_n\overline{\mu_n}}\right) \sim 1 - \frac{2\mu_n\overline{\mu_n}}{\delta(\pi\mu_n z)^{1/2}}\exp\left(\frac{-\delta^2 z}{4\mu_n^3}\right), \quad (36)$$

$$E(\delta,\Delta,z/\mu_n^3) \sim [(\pi\mu_n z)^{1/2}2\mu_n\overline{\mu_n}] - 1/\delta.$$

The growth effect comes from the first term in E above. In general, the behavior as $z \to \infty$ is said to be the "dominant term."[22] The dominant term in Φ_2 originates from the portion of the particular solution associated with the region of

secularity, $m \simeq n$. Subdominant terms, such as the particular solution associated with $m = n$, have already been neglected because they do not represent a growth effect. Thus the function E in Eq. (32) may be replaced by its dominant term, as given by Eq. (36) when $1/\delta$ is neglected. When the resulting expression for Φ_2 is used to form the second-order potential according to Eq. (15a), and then combined with the first-order potential in Eq. (13), the result is

$$\phi = \int_0^x \Phi \, dn, \tag{37a}$$

where

$$\Phi = -\epsilon \frac{nFn}{\mu_n} \exp(it - \mu_n z) J_0(nR) + \epsilon^2 i \beta_0 \frac{n^2 F_n^2}{\mu_n \mu_n} (\pi \mu_n z)^{1/2}$$
$$\times \exp(2it - 2\mu_n z)[J_0(nR)^2 - J_1(nR)^2]$$
$$+ \text{c.c.} + \text{subdominant terms.} \tag{37b}$$

V. CLOSURE

An expression for the pressure may be obtained by differentiating Eqs. (37) with respect to time, but the result has some problematical aspects. First, it is clear that the $O(\epsilon^2)$ term grows as $z^{1/2}$, while the $O(\epsilon)$ term remains bounded. Thus the second-order term satisfies the smallness assumptions inherent to a perturbation series only when z is small compared to $1/\epsilon^2$.[24] From a practical viewpoint this limits the validity of the result to distances that are very small compared to the shock formation distance.

Another aspect relating to the validity of the result is less obvious. Consider the situation where $n \to 1$, in which case $\mu_n \to 0$. The expression for pressure derived from Eq. (37) has μ_n in the denominator, so it is singular at $n = 1$. The key aspect of the singularity is that the $O(\epsilon)$ term will contain a factor $1/\mu_n$, while the $O(\epsilon^2)$ term will contain a factor $1/\mu_n \mu_n^{1/2}$. Thus, the $O(\epsilon^2)$ term grows more rapidly than the $O(\epsilon)$ term as $n \to 1$. This is another instance where the magnitude of the second-order term grows relative to the first-order term. As was true for the $z^{1/2}$ dependence, nonuniform accuracy limits the usefulness of the pressure derived from Eqs. (37).

The lack of uniform accuracy in z is not surprising, because it is the equivalent of secular terms in nonlinear vibration analyses. The nonuniform accuracy in the wavenumber n is a result of the analytical procedure that was followed. The integration by Laplace's method assumed that $|\mu_n|$ is not very small. This is most clearly indicated in Eq. (22b), where the truncation of the series expansion is appropriate only if $q\Delta/\mu_n^2 \ll 1$. Only very small values of q satisfy this criterion when $n \to 1$ ($\mu_n \to 0$). Therefore, the contribution to the second-order potential from the region around $n = 1$ is not well described asymptotically.

There are other shortcomings in the form of Eq. (37b). First, the $O(\epsilon)$ term is the same as that obtained from linear theory, i.e., it is the conventional King integral. Thus the relation does not indicate that there is depletion of the fundamental harmonic as energy is transferred to higher harmonics.[25] Another important limitation is that Eq. (37b) describes only the second harmonic, but higher harmonics are known to be significant to the distortion process.

The aforementioned items lead to concern regarding the validity of any prediction of pressure. This would certainly be the case if Eqs. (37) were to be used directly. The analysis in the next part of this investigation[17] overcomes these difficulties. It treats the response obtained from Eqs. (37) as the asymptotic representation for small $\epsilon z^{1/2}$ and $n \neq 1$ of functional forms that are uniformly accurate. Such an analysis is not applied directly to the velocity potential because there are situations where a portion of the potential may exhibit nonuniform growth while the pressure and other state variable do not.[26]

[1] G. R. Harris, "Review of transient field theory for a baffled planar piston," J. Acoust. Soc. Am. 70, 10–20 (1981).
[2] R. New, R. I. Becker, and P. Wilhelmij, "A limiting form for the nearfield of the baffled piston," J. Acoust. Soc. 70, 1518–1526 (1981).
[3] A. D. Pierce, Acoustics (McGraw- Hill, New York, 1981), Chap. 5.
[4] E. Skudrzyk, The Foundations of Acoustics (Springer-Verlag, New York, 1971), pp. 429–430.
[5] J. C. Lockwood, T. G. Muir, and D. T. Blackstock, "Directive harmonic generation in the radiation field of a circular piston," J. Acoust. Soc. Am. 53, 1148–1153 (1973).
[6] J. C. Lockwood, "Two problems in high-intensity sound," Univ. Texas at Austin, Appl. Res. Lab., ARL-TR-71-26 (1971).
[7] F. Ingenito and A. O. Williams, "Calculation of second-harmonic generation in a piston beam," J. Acoust. Soc. Am. 49, 319–328 (1971).
[8] E. A. Zabolotskaya and R. V Khokhlov, "Quasi-plane waves in the nonlinear acoustics of confined beams," Sov. Phys. Acoust. 15, 35–40 (1969).
[9] E. A. Zabolotskaya and R. V. Khokhlov, "Convergent and divergent sound beams in nonlinear media," Sov. Phys. Acoust. 19, 39–42 (1970).
[10] N. S. Bakhvalov, Ya. M. Zhileikin, E. A. Zabolotskaya, and R. V Khokhlov, "Nonlinear propagation of a sound beam in a nondissipative medium," Sov. Phys. Acoust. 22, 272–274 (1976).
[11] N. S. Bakhvalov, Ya. M. Zhileikin, E. A. Zabolotskaya, and R. V. Khokhlov, "Propagation of finite amplitude sound beams in a dissipative medium," Sov. Phys. Acoust. 24, 271–275 (1978).
[12] N. S. Bakhvalov, Ya. M. Zhileikin, E. A. Zabolotskaya, and R. V Khokhlov, "Harmonic generation in sound beams," Sov. Phys. Acoust. 25, 101–106 (1979).
[13] J. Zemanek, "Beam behavior within the nearfield of a vibrating piston," J. Acoust. Soc. Am. 49, 181–191 (1971).
[14] M. B. Moffett, "Measurement of fundamental and second harmonic pressures in the field of a circular piston source," J. Acoust. Soc. Am. 65, 318–323 (1979).
[15] J. A. Gallego-Juarez and L. Gaete-Garreton, "Experimental study of nonlinearity in free progressive acoustic waves in air at 20 kHz," J. Physique 40 (C8), 336–340 (1978); "Propagation of finite-amplitude ultrasonic waves in air —I. Spherically diverging waves in the free field," J. Acoust. Soc. Am. 73, 761–765 (1983).
[16] D. T. Blackstock, "On plane, spherical, and cylindrical sound waves of finite amplitude in lossless fluids," J. Acoust. Soc. Am. 36, 217–219 (1964).
[17] J. H. Ginsberg, "Nonlinear King integral for arbitrary axisymmetric sound beams at finite amplitudes—II. Derivation of uniformly accurate expressions," J. Acoust. Soc. Am. 76, 1208–1214 (1984).
[18] J. H. Ginsberg, "On the nonlinear generation of harmonics in sound radiation from a vibrating planar boundary," J. Acoust. Soc. Am. 69, 60–65 (1981).
[19] J. H. Ginsberg, "Uniformly accurate description of finite amplitude sound radiation from a harmonically vibrating planar boundary," J. Acoust. Soc. Am. 69, 929–936 (1981).
[20] S. Goldstein, Lectures in Fluid Mechanics (Wiley-Interscience, New York, 1960), Chap. 4.

1206   J. Acoust. Soc. Am., Vol. 76, No. 4, October 1984

Jerry H. Ginsberg: Beams at finite amplitudes. I. Potential   1206

[21]*Handbook of Mathematical Foundations*, edited by M. Abramowitz and I. A. Stegun (Dover, New York, 1965), Chap. 7.

[22]C. M. Bender and S. A. Orszag, *Advanced Mathematical Methods for Scientists and Engineering* (McGraw-Hill, New York, 1978), pp. 261–267.

[23]I. N. Sneddon, *Fourier Transforms* (McGraw-Hill, New York, 1951), Chaps. 1–2.

[24]A. H. Nayfeh, *Perturbation Methods* (Wiley-Interscience, New York, 1973), pp. 16–18.

[25]W. Keck and R. T. Beyer, "Frequency spectrum of finite amplitude ultrasonic waves in liquids," Phys. Fluids 3, 346–352 (1960).

[26]A. H. Nayfeh and A. Kluwick, "A comparison of three perturbation methods for non-linear waves," J. Sound Vib. 48, 293–299 (1976).

Nonlinear King integral for arbitrary axisymmetric sound beams at finite amplitude. II. Derivation of uniformly accurate expressions

Jerry H. Ginsberg

School of Mechanical Engineering, Georgia Institute of Technology, Atlanta, Georgia 30332

The first part of this investigation [J. Acoust. Soc. Am. 76, 1201–1207 (1984)] derived a perturbation representation of the velocity potential for an axisymmetric, monochromatic sound beam in the form of a complex function. That result, which used Hankel transforms to describe the dependence on transverse position, lacked uniform validity in the corresponding wavenumber, as well as the distance from the transducer. Expressions for the state variables derived from the potential have the same behavior. The example of a planar wave is used to adapt the singular perturbation method of renormalization to the case where the potential is in complex form. The resulting technique is used to obtain a coordinate straining transformation that makes the state variables uniformly accurate. The expression for the pressure is similar to the King integral in linear theory, except that the integrand is a function of the strained coordinates. Comparison of the predicted waveform properties with experimental data [Gallego-Juarez and Gaete-Garreton, J. Acoust. Soc. Am. 73, 761–765 (1983)] shows good correlation. Further evaluations disclose some new features of the distortion phenomena in both the time and frequency domains.

PACS numbers: 43.25.Cb

INTRODUCTION

A general analysis of axisymmetric sound beams was initiated in Part I of this study.[1] The overall goal of the investigation is to develop a theory that can be used to evaluate how various features of harmonic transducer motion are manifested within the entire acoustic field. This intent obviates the use of theories founded on effects that arise only in the near- or farfield.

It was found in Part I that combining a consistent nonlinear wave equation with a Hankel integral transform and an asymptotic integration technique led to a representation of the velocity potential in the form of a perturbation series. The second part of the analysis, presented here, will utilize that potential function to derive an integral expression for the acoustic pressure. This integral reduces to the King integral of linear theory[2] in the limit of an infinitesimal source pressure level.

Numerical evaluation of this integral permits comparison of the theoretical predictions to those in one series of experiments. In addition to providing validation, the example will yield some insight into the unusual distortion phenomena that have been observed in sound beams.[3]

I. NONUNIFORMLY ACCURATE EXPRESSIONS

In the first part of this investigation z and R were nondimensional cylindrical coordinates for a transducer centered at $z = R = 0$, and t was nondimensional time. The corresponding dimensional quantities are obtained by using $1/\omega$ to define the time scale and $1/k = c_0/\omega$ to define the length scale, where ω is the frequency of the monochromatic motion of the transducer and c_0 is the linearized speed of sound. The transducer motion was written in complex form as

$$v_z = (\epsilon/2i)c_0 f(R)\exp(it) + \text{c.c.}, \tag{1}$$

where $f(R)$ is an arbitrary complex function whose magnitude goes to zero as $R \to \infty$. The acoustic Mach number ϵ is small compared to unity, so it is a convenient parameter for a perturbation series. In general, c.c. will denote the complex conjugate of the preceding terms.

A Hankel transform was used to describe the first-order effects transverse to the axis of the sound beam. For a specified transverse wavenumber n, which is the parameter for the transform, there is a corresponding Hankel transform F_n of the shape function $f(R)$,

$$F_n = \frac{1}{2i}\int_0^\infty R f(R) J_0(nR)\,dR \tag{2}$$

as well as a (nondimensional) axial wavenumber μ_n, where the radiation condition is satisfied by

$$\mu_n = i(1 - n^2)^{1/2}; \quad 0 < n < 1,$$
$$\mu_n = (n^2 - 1)^{1/2}; \quad n > 1. \tag{3}$$

As a result of employing a Hankel transform, the first-order velocity potential was expressed in terms of the King integral. This first-order result led to an inhomogeneous wave equation for the second-order potential. An asymptotic integration by Laplace's method was crucial to the evaluation of second-order effects. The expression for the velocity potential that was derived by this method retained only the part of the second-order terms that displayed cumulative growth of higher harmonics. Thus, it did not evaluate any term whose magnitude is $O(\epsilon^2)$ at all values of z. The derived velocity potential was written as

$$\phi = \int_0^\infty \Phi\,dn, \tag{4}$$

where, for $|\mu_n|^{3/2} > O(\epsilon)$,

$$\Phi = -\epsilon\frac{nF_n}{\mu_n}\exp(it - \mu_n z)J_0(nR) + i\epsilon^2\beta_0\frac{n^2F_n^2}{\mu_n\bar\mu_n}(\pi\mu_n z)^{1/2}$$
$$\times \exp(2it - 2\mu_n z)[J_0(nR)^2 - J_1(nR)^2] + c.c. + SDT, \tag{5}$$

where SDT represents *subdominant terms* that do not grow with increasing z, and an overbar denotes the complex conjugate. Note that β_0 is the coefficient of nonlinearity, equal to $\frac{1}{2}(\gamma + 1)$ for an ideal gas, where γ is the ratio of specific heats.

The limitation on the value of μ_n for Eq. (5) means that the expression is not applicable in the vicinity of $n = 1$. This is a consequence of the asymptotic expansion that led to Eq. (5), for which it was assumed that $\mu_n = O(1)$. Equation (5) is said to lack uniform accuracy in both n and z, because the magnitude of the second-order term grows relative to the first-order term as $n \rightarrow 1$ and as $z \rightarrow \infty$. The primary task here is to obtain from Eq. (5) expressions that are uniformly accurate.

Differentiating Eqs. (4) and (5) yields expressions for the particle velocity components and pressure. As suggested by the form of Eq. (4), let V_z, V_R, and P denote the contribution of a specific wavenumber n to the axial velocity v_z, transverse velocity v_R, and pressure p, according to

$$v_z = c_0\int_0^\infty V_z\, dn, \quad v_R = c_0\int_0^\infty V_R\, dn, \tag{6}$$

$$p = \rho_0 c_0^2\int_0^\infty P\, dn. \tag{7}$$

In the evaluation of the expression for V_z, the factor $z^{1/2}$ in the $O(\epsilon^2)$ term of Φ may be considered to be constant, because its derivative leads to an $O(\epsilon^2 z^{-1/2})$ term, which decreases in importance as z increases. The physical variables associated with Eqs. (5) and (6) are then found to be, for n not close to 1,

$$V_z = \frac{\partial\Phi}{\partial z}$$
$$= \epsilon nF_n\exp(it - \mu_n z)\{J_0(nR) - 2i\epsilon\beta_0(nF_n/\bar\mu_n)$$
$$\times (\pi\mu_n z)^{1/2}\exp(it - \mu_n z)[J_0(nR)^2 - J_1(nR)^2]\}$$
$$+ c.c + SDT, \tag{8}$$

$$V_R = \frac{\partial\Phi}{\partial R} = -\epsilon(n^2F_n/\mu_n)\exp(it - \mu_n z)\{J_0'(nR)$$
$$- 2i\epsilon\beta_0(nF_n/\bar\mu_n)(\pi\mu_n z)^{1/2}\exp(it - \mu_n z)$$
$$\times [J_0(nR)J_0'(nR) - J_1(nR)J_1'(nR)]\}$$
$$+ c.c. + SDT, \tag{9}$$

$$P = (i/\mu_n)V_z. \tag{10}$$

It is convenient for later operations to denote the derivatives of Bessel functions by primes, rather than making use of identities for derivatives.

II. CORRECTION OF THE DEPENDENCE ON THE TRANSVERSE WAVENUMBER

Equations (8)–(10) suffer from the same lack of uniform accuracy as that associated with Eq. (5). Such behavior is not acceptable for state variables such as particle velocity and

pressure.[4] The recognition that the integration regarded $|\mu_n|$ to be substantially larger than zero is crucial to correcting the dependence on n. It leads to the conclusion that Eqs. (8)–(10) are the asymptotic representation for nonsmall μ_n of alternative functional forms that behave properly as $\mu_n \rightarrow 0$. Note that each $O(\epsilon^2)$ term contains a factor $\mu_n^{-1/2}$ higher than the corresponding $O(\epsilon)$ term. It follows that the alternative forms must feature a function whose expansion for large $\mu_n z$ is proportional to $\mu_n^{-1/2}$.

A variety of functions, such as Bessel functions, are possible candidates in this regard. However, recall that μ_n is either real or imaginary, depending on the value of n. Most functions whose asymptotic behavior is appropriate for real μ_n introduce new singularities for imaginary μ_n, or vice versa. The only function that was found to be acceptable for all values of n was the complementary error function. Specifically, it is known[5] that for large $\mu_n z$,

$$erfc[(\mu_n z)^{1/2}]$$
$$= (\pi\mu_n z)^{-1/2}\exp(-\mu_n z)[1 + O(1/\mu_n z)]. \tag{11}$$

Using Eq. (11) to recast the $O(\epsilon^2)$ terms in Eqs. (8)–(10) leads to

$$V_z = \epsilon nF_n\exp(it - \mu_n z)\{J_0(nR) - 2i\pi\epsilon\beta_0(\mu_n/\bar\mu_n)$$
$$\times nF_n z\, erfc[(\mu_n z)^{1/2}]\exp(it)[J_0(nR)^2 - J_1(nR)^2]\}$$
$$+ c.c. + SDT, \tag{12}$$

$$V_R = -\epsilon\frac{n^2F_n}{\mu_n}\exp(it - \mu_n z)\{J_0'(nR) - 2i\pi\epsilon\beta_0(\mu_n/\bar\mu_n)$$
$$\times nF_n z\, erfc[(\mu_n z)^{1/2}]\exp(it)[J_0(nR)J_0'(nR)$$
$$- J_1(nR)J_1'(nR)]\} + c.c. + SDT, \tag{13}$$

$$P = (i/\mu_n)V_z. \tag{14}$$

Note that the coefficient $\mu_n/\bar\mu_n$ is merely $+1$ or -1 depending on whether μ_n is real ($n > 1$) or imaginary ($n < 1$). Thus Eqs. (12)–(14) have the same degree of singularity in μ_n for the first- and second-order terms; they are descriptive of the response for all n.

III. DERIVATION OF RENORMALIZATION USING COMPLEX VARIABLES

Although Eqs. (12)–(14) are valid for all n, they still are not uniformly accurate for all z. One method for correcting this situation is the renormalization version of the method of strained coordinates.[6] The general basis for this method is the argument that nonuniform behavior relative to one of the independent variables (space or time) is the result of improper truncation of a Taylor series expansion in powers of ϵ. A much simpler example is to expand $\sin(z + \epsilon z)$ in powers of ϵ, and to truncate such an expansion. The original function is periodic, but the truncated representation shows cumulative growth in ϵz.

As a consequence of the foregoing argument, it may be anticipated that there is a transformation of the space–time variables for which the response does not exhibit cumulative growth. The difference between the magnitude of the physical variables and the transformed ones will grow cumulatively in the same manner as the $O(\epsilon^2)$ terms in Eqs. (12)–(14).

The transformed variables therefore represent a straining of the physical space–time grid.

All prior applications of the renormalization technique seem to have employed real functional forms. In order to adapt the method to the complex functions in Eqs. (12)–(14), it is useful to consider the analogous steps for a finite amplitude planar wave. Consider such a wave propagating in the z direction, due to a harmonic particle velocity imposed at $z = 0$. The potential function in this case is governed by

$$\frac{\partial^2 \phi}{\partial z^2} - \frac{\partial^2 \phi}{\partial t^2} = 2(\beta_0 - 1)\frac{\partial \phi}{\partial t}\frac{\partial^2 \phi}{\partial z^2} + 2\frac{\partial \phi}{\partial z}\frac{\partial^2 \phi}{\partial z \partial t} + O(\phi^3),$$
(15)

$$\left.\frac{\partial \phi}{\partial z}\right|_{z=0} = \left(\frac{\epsilon}{2i}\right)\exp(it) + \text{c.c.},$$

where the scales for nondimensionalizing position and time are the same as those for the sound beam.

Carrying out a perturbation analysis based on

$$\phi = \epsilon \phi_1 + \epsilon^2 \phi_2 + \cdots$$
(16)

yields a homogeneous wave equation for ϕ_1, which is solved for a wave propagating in the positive z direction. This solution is used to form the source terms in an inhomogeneous wave equation for ϕ_2. The particular solution of the latter is readily obtained by elementary methods, with the result that

$$\phi = \tfrac{1}{2}\epsilon \exp[i(t-z)] + \tfrac{1}{4}\epsilon^2 \beta_0 z \exp[2i(t-z)]$$
$$+ \text{c.c} + O(\epsilon^2),$$
(17)

where the $O(\epsilon^2)$ terms not appearing explicitly are bounded for all z.

The expressions for particle velocity and pressure corresponding to Eq. (17) are

$$v_z = c_0\frac{\partial \phi}{\partial z} = \frac{1}{2i}\epsilon c_0 \exp[i(t-z)]$$
$$\times \{1 + \tfrac{1}{2}\epsilon \beta_0 z \exp[i(t-z)]\} + \text{c.c.} + O(\epsilon^2),$$
(18)

$$p = -\rho_0 c_0^2 \frac{\partial \phi}{\partial t} = \rho_0 c_0 v_z.$$

These are not uniformly accurate because the $O(\epsilon^2)$ term grows with increasing z relative to the $O(\epsilon)$ term. It is postulated that the dependence on the strained coordinate variables is uniformly accurate. Because t only occurs in conjunction with z, it is adequate to strain only the space variable. The strained coordinate ζ approaches z when $\epsilon \to 0$, so the transformation is considered to have the form

$$z = \zeta + \epsilon[S(\zeta,t) + \overline{S}(\zeta,t)] + \cdots.$$
(19)

The task now is to evaluate the function S. The first new feature of the complex variable formulation of the planar wave is that S is considered to be complex, in agreement with the form of Eq. (18). It is necessary to introduce the complex conjugate of S in Eq. (19) because the transformation must be real.

Presumably, expressing v_z and p in terms of ζ rather than z leads to uniform accuracy. This should be the result of substituting Eq. (19) into Eq. (18). Because the earlier analysis considered only the first two orders of ϵ, enforcing uniformity will involve considering only those powers in a series expansion. First note that for $\epsilon \ll 1$,

$$\exp(-iz) = \exp[-i(\zeta + \epsilon S + \epsilon \overline{S})]$$
$$= \exp(-i\zeta)[1 - i\epsilon(S + \overline{S})] + O(\epsilon^2) \quad (20)$$

Substitution of Eq. (19) into Eq. (18) in conjunction with Eq. (20) leads to the following ϵ and ϵ^2 terms:

$$p/\rho_0 c_0^2 = v_z/c_0$$
$$= (1/2i)\epsilon \exp[i(t-\zeta)]\{1 - i\epsilon(S + \overline{S})$$
$$+ \tfrac{1}{2}\epsilon \beta_0 \zeta \exp[i(t-\zeta)]\} + \text{c.c.} + O(\epsilon^2), \quad (21)$$

where $O(\epsilon^2)$ means terms having that order of magnitude at all z.

Equation (21) will be nonuniform in ζ unless the $\epsilon \zeta$ term is canceled. This is the criterion for the straining function S. Thus, set

$$S = (1/2i)\beta_0\zeta \exp[i(t-\zeta)].$$
(22)

The terms remaining in Eq. (21) are

$$\frac{p}{\rho_0 c_0^2} = \frac{1}{2i}\epsilon \exp[i(t-\zeta)](1 - i\epsilon \overline{S}) + \text{c.c.} + O(\epsilon^2)$$
$$\equiv \frac{1}{2i}\epsilon \exp[i(t-\zeta)] + \frac{1}{4i}\epsilon^2\beta_0\zeta + \text{c.c.} + O(\epsilon^2). \quad (23)$$

Note that the ϵ^2 term appearing above is imaginary. Accounting for the complex conjugate of each term yields

$$\frac{p}{\rho_0 c_0^2} = \frac{v_z}{c_0} = \epsilon \sin(t - \zeta) + O(\epsilon^2)$$
(24)

and the transformation obtained by substituting S and $\overline{S}$ into Eq. (19) is

$$z = \zeta + \epsilon\beta_0\zeta \sin(t - \zeta).$$
(25)

In order to demonstrate the correctness of the wave described by Eqs. (24) and (25), Eq. (24) is used to eliminate the sine term in Eq. (25):

$$z = \zeta(1 + \beta_0 v_z/c_0).$$
(26)

Solving this relation for ζ and substituting the result back into Eq. (24) then yields

$$\frac{p}{\rho_0 c_0^2} = \frac{v_z}{c_0} = \epsilon \sin\left(t - \frac{z}{(1 + \beta_0 v_z/c_0)}\right).$$
(27)

Except for the fact that z and t are nondimensional here, Eq. (27) is *identical* to Earnshaw's closed form solution for finite amplitude planar waves[7] in the case of harmonic excitation at a boundary. The same result using real functions was obtained previously.[4]

The perturbation analysis of the velocity potential provided an indication of how higher harmonics tend to be formed. Although the expressions that resulted were not uniformly accurate, the information the analysis provided was sufficient to permit the coordinate straining procedure to identify the more general signal. The exactness of the result in this case was fortuitous. In general, all that can be expected from the procedure is that the error in the uniformly accurate prediction will be no larger than $O(\epsilon^2)$ at any location.

IV. APPLICATION OF RENORMALIZATION TO THE SOUND BEAM

Only a few modifications are required to apply the method in the preceding section to Eqs. (12)–(14). As was true for the planar wave, t only occurs in combination with z, so no transformation of the time scale shall be introduced. However, R is an independent coordinate, so a straining transformation for that spatial variable is also needed. Thus the coordinate straining to be tried is

$$z = \zeta_n + \epsilon[S_z(\zeta_n,\alpha_n,t,n) + \text{c.c.}],$$

$$R = \alpha_n + \epsilon[S_R(\zeta_n,\alpha_n,t,n) + \text{c.c.}].$$

(28)

Note that a subscript n has been associated with the strained coordinates in order to emphasize that the strained coordinate describes only one transverse wavenumber in a continuous spectrum.

In order to focus on the conceptual aspects of renormalization, Eqs. (12) and (13) are written in the standard form,

$$V_j = \epsilon f_j(z,R,t,n) + \epsilon^2 z g_j(z,R,t,n) + \text{c.c.} + O(\epsilon^2);$$
$$j = 1,2.$$

(29)

Substituting Eqs. (28) into Eq. (29) and retaining the ϵ and ϵ^2 terms in a Taylor series expansion leads to

$$V_j = \epsilon f_j(\zeta_n,\alpha_n,t,n) + \epsilon^2\Big((S_z + \overline{S}_z)\frac{\partial}{\partial \zeta_n}f_j(\zeta_n,\alpha_n,t,n)$$

$$+ (S_R + \overline{S}_R)\frac{\partial}{\partial \alpha_n}f_j(\zeta_n,\alpha_n,t,n)$$

$$+ \zeta_n g_j(\zeta_n,\alpha_n,t,n) \Big) + \text{c.c.} + O(\epsilon^2); \quad j = 1,2.$$

(30)

The foregoing is analogous to Eq. (21) for the case of planar waves. The straining functions S_z and S_R must annihilate the nonuniform $\zeta_n g_j$ term in Eq. (30). Hence, set

$$S_z\frac{\partial}{\partial \zeta_n}f_j(\zeta_n,\alpha_n,t,n) + S_R\frac{\partial}{\partial \alpha_n}f_j(\zeta_n,\alpha_n,t,n)$$

$$= -\zeta_n g_j(\zeta_n,\alpha_n,t,n); \quad j = 1,2.$$

(31)

It is necessary to find functions S_z and S_R that satisfy Eq. (31) for both values of j. This is achieved by using trial forms that are suggested by comparing the functions g_j to the derivatives of f_j. The actual transformation obtained by satisfying Eq. (31) and then forming Eqs. (28) is

$$z = \zeta_n - 2\pi\epsilon\beta_0\zeta_n\{i(nF_n/\bar{\mu}_n)\exp(it)$$

$$\times \text{erfc}[(\mu_n\zeta_n)^{1/2}] + \text{c.c.}\}J_0(n\alpha_n),$$

(32)

$$R = \alpha_n + 2\pi\epsilon\beta_0\zeta_n\{i(F_n\mu_n/\bar{\mu}_n)\exp(it)$$

$$\times \text{erfc}[(\mu_n\zeta_n)^{1/2}] + \text{c.c.}\}J_1(n\alpha_n).$$

In general, the terms remaining in Eq. (30) when Eq. (31) holds are

$$V_j = \epsilon f_j(\zeta_n,\alpha_n,t,n) + \epsilon^2\Big(\overline{S}_z\frac{\partial}{\partial \zeta_n}f_j(\zeta_n,\alpha_n,t,n)$$

$$+ \overline{S}_R\frac{\partial}{\partial \alpha_n}f_j(\zeta_n,\alpha_n,t,n) \Big) + \text{c.c.} + O(\epsilon^2).$$

(33)

This expression is comparable to Eq. (23) for a planar wave. The ϵ^2 term in that case was imaginary, so that no such terms appeared explicitly when the real form of the solution was written. The expressions for the sound beam are more complicated, primarily due to the presence of Bessel functions describing the transverse variation of the sound beam. Here, renormalization removes any $O(\epsilon^2)$ terms in V_j that depend explicitly on time.

In other words, the coordinate straining transformation derived from Eq. (31) is based on matching the tendency for generation of higher harmonics. Such a transformation introduces a mean value over one period. The ϵ^2 terms appearing in Eq. (33) cancel that mean value at all locations.

All of the state variables may be obtained from Eq. (33). The quantity of primary interest is the pressure, for which the proportionality in Eq. (14) is used to determine P. The contribution of all transverse wavenumbers n is obtained by integrating according to Eq. (6), with the result that

$$p = \rho_0 c_0^2\epsilon\int_0^\infty \Big(\frac{inF_n}{\mu_n}\Big)\exp(-\mu_n\zeta_n)\{\exp(it)J_0(n\alpha_n)$$

$$- 2i\pi\epsilon\beta_0 n\overline{F}_n\zeta_n\ \text{erfc}[(\bar{\mu}_n\zeta_n)^{1/2}]$$

$$\times[J_0(n\alpha_n)^2 - (\bar{\mu}_n/\mu_n)J_1(n\alpha_n)^2]\}dn + \text{c.c.} \quad (34)$$

Equations (32) and (34) jointly describe the pressure at specified values of z, R, and t. Because of the complicated nature of these relations, quantitative evaluations require numerical algorithms for solving the coordinate transformation, and for integrating over all values of n. When $n < 1$, in which case μ_n is imaginary, evaluating the pressure according to Eqs. (32) and (34) requires computing the complement of the error function for complex arguments. Useful identities[5] for this task are

$$\text{erfc}[(i\sigma)^{1/2}]$$

$$\equiv 2^{1/2}\exp(-i\pi/4)\{[\tfrac{1}{2} - S_2(\sigma)] + i[\tfrac{1}{2} - C_2(\sigma)]\},$$

(35)

$$\text{erfc}[-(i\sigma)^{1/2}]$$

$$\equiv 2^{1/2}\exp(-i\pi/4)\{[\tfrac{1}{2} - C_2(\sigma)] + i[\tfrac{1}{2} - S_2(\sigma)]\},$$

where $S_2(\sigma)$ and $C_2(\sigma)$ denote Fresnel integrals, defined as

$$S_2(\sigma) = \frac{1}{(2\pi)^{1/2}}\int_0^\sigma \frac{\sin x}{x^{1/2}}dx,$$

$$C_2(\sigma) = \frac{1}{(2\pi)^{1/2}}\int_0^\sigma \frac{\cos x}{x^{1/2}}dx.$$

(36)

The occurrence of Fresnel integrals here is intuitively appealing, because such functions are known to enter into the evaluation of diffraction effects in the linear infinite baffle problem.[8]

V. RESULTS FOR A PISTON

Expressions describing the response in terms of *real* functions may be obtained from Eqs. (32) and (34). In view of Eqs. (35), different expressions are required for the propagating modes $(n < 1)$ and the evanescent modes $(n > 1)$. The singularity in Eq. (34) at $n = 1$ is regular. Numerical evaluation of the pressure integral therefore presents no unforeseen dif-

ficulties. As is usual for diffraction integrals, the pressure integrand in Eq. (34) oscillates rapidly as a function of n at large distances from the transducer (large z or R). The transcendental nature of the coordinate transformation, Eqs. (32), at a specified n makes the usual numerical algorithms for efficiently evaluating such integrals unsuitable. However, a Gauss–Chebychev integration formula[9] is particularly well-suited to the $1/\mu_n$ singularity. This matter, as well as the algorithm by which the coordinate transformation is evaluated at discrete values of n, will be described elsewhere.

The net result is an algorithm that is relatively costly for extensive computation. Nevertheless, it yields a prediction of the instantaneous acoustic pressure that can be utilized to generate waveforms or spatial profiles of the signal.

Such predictions are limited to locations where shocks do not form in the individual duct modes. Shocks are manifested by a vanishing value of the Jacobian of the coordinate transformation, corresponding to a multivalued solution. Selecting the appropriate solution in the presence of a shock requires considerations not addressed in the present study.

The experiments recently reported by Gallego-Juarez and Gaete-Garreton[10] for propagation in air provide useful data for validating the analysis. The transducer for those experiments was a circular plate whose spatial vibration pattern was combined with steps on the plate in order to simulate a piston. For a piston of diameter $2a$, the shape function $f(R)$ in Eq. (1) is

$$ f(R) = \begin{cases} 1, & R < ka, \\ 0, & R > ka, \end{cases} \tag{37} $$

which leads to the following Hankel transform amplitude:

$$ F_n = (ka/2in)J_1(n\,ka). \tag{38} $$

The transducer diameter in the aforementioned study was 200 mm and the frequency was 20.4 kHz. This corresponds to $ka = 37.1$ when $c_0 = 345$ m/s. (The ambient conditions were not specified.) Only measurements beyond a distance $z/k = 900$ mm were reported, whereas the last axial maximum on axis occurred at $z/k = 218$ mm. Comparing the experimental and computed results will therefore indicate how well farfield propagation properties are predicted.

Figures 1–3 reproduce the amplitude response curves in Ref. 10 for the fundamental frequency and the first three

FIG. 2. Amplitude response at 2 m on-axis. Harmonic number as indicated. $k = 371$ m^{-1}, $a = 0.1$ m, $\beta_0 = 1.2$. ------: Theory for source SPL = 132.5 dB. ———: Ref. 10. ······: Linearized response.

higher harmonics obtained at three locations on the axis of symmetry. The sloping dotted line is the closed form linear solution of the Rayleigh integral for the pressure amplitude on-axis.[2,8] Comparing the measured fundamental at low source pressure levels with the Rayleigh prediction for Fig. 2 causes concern. Mechanisms such as dissipation which affect the fundamental at very low source levels, where linear theory is valid, do not explain why the measured amplitude should be higher than the theoretical one. Also, increasing the source level in the linear domain (< 115 dB) did not exactly increase the received fundamental SPL in the experiments by the same amount.

Because of this uncertainty regarding the measurements, comparisons with the present analysis based on source SPL might be erroneous. The method used for comparison was to evaluate the analytical waveform at a nominal source level. The waveform was then Fourier analyzed to determine the corresponding amplitude levels (and phase angles) for all harmonics. The comparable experimental data point was selected by matching the predicted and measured amplitudes of the fundamental. This matching is indicated by the dotted horizontal lines marked by the number 1.

Figure 1, which is for the most remote location, shows that the second and third harmonic levels agree to within 2 dB between theory and experiment, while the fourth har-
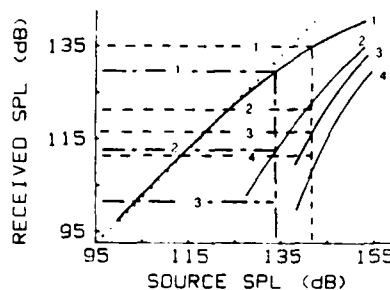

FIG 1. Amplitude response at 3.2 m on-axis. Harmonic number as indicated. $k = 371$ m^{-1}, $a = 0.1$ m, $\beta_0 = 1.2$. ------: Theory for source SPL = 132.5 dB. ———: Ref. 10. ······: Linearized response.

FIG. 3. Amplitude response at 1.2 m on-axis. Harmonic number as indicated $k = 371$ m^{-1}, $\beta_0 = 1.2$. ······: Theory for source SPL = 142.5 dB ---·---: Theory for source SPL = 132.5 dB. ———: Ref. 10. ······ Linearized response.

monics are even closer. The discrepancies between theory and experiment are slightly larger in Fig. 2, but they are well within the uncertainty associated with the difference between the measured fundamental and the prediction of linear theory at low levels. It is possible that the disagreement results from the experimental configuration, which employed a stepped transducer face. Even though the fundamental was believed to match well with an ideal piston,[11] minor discrepancies might have a substantial effect on the higher harmonics. Also, it is conceivable that the motion of the transducer face was not exactly axisymmetric. This could substantially alter the on-axis diffraction effects.

Figure 3 presents the response curves for the closest location in the experiments. As indicated by the amount of reduction in the fundamental amplitude, most measurements of the third and fourth harmonics were taken at source levels for which the effects of shock formation are significant. The coordinate transformation for a range of values of the transverse wavenumber n has multiple solutions when shocks are present. The theory is not formally valid in this case, but the numerical algorithm was implemented to select the value of the strained coordinate ζ_n closest to the value of z when a shocks occurs.

Two source levels were evaluated for Fig. 3. The dashed lines for a theoretical 142.5 dB SPL correspond to significant shocking effects. The agreement between theory and experiment for the lowest three harmonics is remarkable, especially in view of the uncertainty about how shocks should be treated theoretically. The broken line for a theoretical SPL of 132.5 dB show the same degree of agreement for the second harmonic. Extrapolating the curve for the third harmonic back to this level would show that the theory closely predicts this harmonic also.

Figures 1–3 do not provide a complete picture. First, they describe locations which are in the farfield. Furthermore, the response curves do not display the phase angles for the various harmonics. The higher harmonics for planar waves are in-phase with the fundamental, as are cylindrical and spherical waves in the farfield. Asymmetry between the compression and rarefaction phases, which was observed by Mellen and Browning,[3] corresponds in the frequency domain to out-of-phase conditions.

Figures 4 and 5 display waveforms at axial locations in the nearfield and in the farfield, respectively. Reference 10
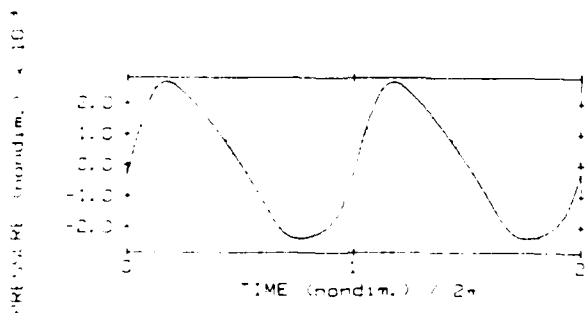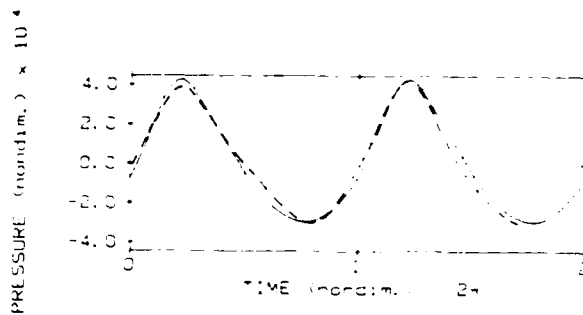
FIG. 5. Waveform at 2.1 m on-axis for 133.5 dB source SPL. $k = 371$ m^{-1}, $a = 0.1$ m, $\beta_0 = 1.2$. ———— : Theory. ······· : Measured in Ref. 10 for 130.5 dB source SPL. ······· : Linearized response.

measured a waveform at the same location as that described by Fig. 5, but for a source level of 130.5 dB. The theoretical waveform obtained from the present analysis for the same source level would show less distortion than the observed one. This discrepancy is consistent with those discussed in regard to Fig. 2, which describes a nearby location. For this reason, the theoretical source SPL was increased by 3 dB for the comparison. The source level for Fig. 4 was selected to give a comparable amount of distortion at the closer location.

Several features of the measured waveform in Fig. 5 must be noted. Although an interval of two periods is shown, the shape for the second period does not duplicate that for the first. Also the null pressure level was not indicated in Ref. 10; the experimental waveform reproduced in Fig. 5 has been plotted to give a zero mean value. Finally, the original waveform was drawn to a very small scale, so its enlargement to obtain Fig. 5 may have introduced additional inaccuracies. In view of these uncertainties, the agreement between the experimental and theoretical waveforms is quite good, particularly for the second period.

The distortion of the waveform in Fig. 4 is the type reported by Browning and Mellen.[3] One effect of nonlinearity is to shift the extrema in the manner that a plane wave distorts. Nonlinearity also enhances and narrows the compression phase, while it has the opposite effect on the rarefaction phase.

The waveform in Fig. 5 is for a lower source level than the one for Fig. 4, so less of the distortion is associated with the nearfield. This gives rise to a phenomenon that is somewhat different from the one appearing in Fig. 4. It is instructive to compare the waveforms in both figures to the corresponding linearized signals. It seems that the maximum compression, which occurs sooner than the linear signal in the nearfield, is retarded as it propagates until it matches the linear maximum. Also, the maximum rarefaction is retarded more in the farfield. Recall that in the Rayleigh formulation, the individual harmonics appear to be nonuniform spherical waves in the farfield. The aforementioned retardation effect might be a consequence of the 90° phase shift that spherical waves undergo in the transition from the nearfield to the farfield. In addition, the fact that Fig. 4 describes a nearfield

FIG. 4. Waveform at 0.184 m on-axis for 142.5 dB source SPL. $k = 371$ m^{-1}, $a = 0.1$ m, $\beta_0 = 1.2$. ———— : Theory. ······· : Linearized response.

1213   J. Acoust. Soc. Am., Vol. 76, No. 4, October 1984

Jerry H. Ginsberg: Beams at finite amplitude. II. Uniform   1213

TABLE I. Fourier series data for the waveforms in Figs. 4 and 5

Location	Harmonic number	$\dfrac{10^3\, p}{\rho_0 c_0^2}$	Amplitude received SPL (dB)	Phase lag ψ re: fundamental
$z/k = 0.184$ m	linear	2.646	142.5	$-4.1°$
	1	2.479	142.0	...
	2	0.426	126.7	$6.9°$
	3	0.208	120.4	$54.8°$
	4	0.083	112.4	$47.2°$
	5	0.055	108.8	$66.6°$
$z/k = 2.1$ m	linear	0.4010	126.1	$-7.0°$
	1	0.3384	124.7	...
	2	0.0623	110.0	$64.2°$
	3	0.0247	101.9	$122.3°$
	4	0.0103	94.3	$-177.1°$
	5	0.0044	86.9	$-129.6°$

location suggests that the asymmetry is produced by diffraction associated with cancellations of the wavelets emanating from the various points on the piston. The generality of these observation needs to be explored further.

The waveforms were Fourier analyzed using a retarded time in which the fundamental is a pure sine. The form of this representation is

$$p = \sum_{j} p_j \sin\left[j(t - t_0) - \psi_j\right],$$

$$\psi_1 \equiv 0, \quad -180° < \psi_j \leqslant 180°.$$

The amplitudes p_j and the phase lags ψ_j of the higher harmonics relative to the fundamental are presented in Table I. There is no obvious pattern to the phase lags in the nearfield case, but the farfield location shows that the increment in the phase lag from a harmonic to next higher one is nearly uniform. This same pattern was observed in the computed waveforms at other farfield locations, with the increments ranging between 40° and 70°. The underlying mechanism for this effect is open to conjecture at this time.

VI. CONCLUSION

The theory for finite amplitude sound beams developed in Part I and here provides a versatile algorithm for evaluating the effects of nonlinearity. The theory has been shown to agree well with experimental data for on-axis responses, both qualitatively and quantitatively. The derived expressions are applicable to off-axis responses, but no such results have been computed thus far.

Comparisons with other available experiments are now underway, but past experiments have been limited in scope. Measurement of amplitude levels in the higher harmonics has received more attention than measurement of the corresponding phase angles and overall waveforms (for understandable reasons). Also, measurements in the true nearfield have been sparse. Hence the theory has not yet been fully confirmed, but insight into basic phenomena has already been gained.

[1]J. H. Ginsberg, "Nonlinear King integral for arbitrary axisymmetric sound beams at finite amplitudes—I. Asymptotic evaluation of the velocity potential," J. Acoust. Soc. Am. 76, 1201–1207 (1984).

[2]E. Skudrzyk, *The Foundations of Acoustics* (Springer-Verlag, New York, 1971), pp. 429–430.

[3]D. G. Browning and R. H. Mellen, "Finite-amplitude distortion of 150-kHz acoustic waves in water," J. Acoust. Soc. Am. 44, 644–646 (1968)

[4]A. H. Nayfeh and A. Kluwick, "A comparison of three perturbation methods for non-linear waves," J. Sound Vib. 48, 293–299 (1976).

[5]*Handbook of Mathematical Foundations*, edited by M. Abramowitz and I. A. Stegun (Dover, New York, 1965), Chaps. 7 and 9.

[6]A. H. Nayfeh, *Perturbation Methods* (Wiley-Interscience, New York, 1973), pp. 95–98.

[7]H. Lamb, *Hydrodynamics* (Dover, New York, 1945), 6th ed., pp. 483–484.

[8]A. D. Pierce, *Acoustics* (McGraw-Hill, New York, 1981), Chap. 5.

[9]L. G. Kelly, *Handbook of Numerical Methods and Applications* (Addison-Wesley, Reading, MA, 1967), pp. 57–61.

[10]J. A. Gallego-Juarez and L. Gaete-Garreton, "Experimental study of nonlinearity in free progressive acoustic waves in air at 20 kHz," J. Physique 40 (C8), 336–340 (1978); "Propagation of finite-amplitude ultrasonic waves in air—I. Spherically diverging waves in the free field," J. Acoust. Soc. Am. 73, 761–765 (1983).

[11]A. Barone and J. A. Gallego-Juarez, "Flexural vibrating free-edge plates with stepped thicknesses for generating high directional ultrasonic radiation," J. Acoust. Soc. Am. 51, 953–959 (1972).

THE JOURNAL

of the

Acoustical Society of America

Program of the
106th Meeting

### Session M. Engineering Acoustics II: Numerical Techniques and Others

3:35

M9. Transition from the nonlinear King integral to spherical propagation for a finite amplitude sound beam. Jerry H. Ginsberg (School of Mechanical Engineering, Georgia Institute of Technology, Atlanta, GA 30332)

The propagation of finite amplitude waves radiating from a baffled piston has been described in terms of directional spherical waves [J. C. Lockwood, T. G. Muir, and D. T. Blackstock, J. Acoust. Soc. Am. 53, 1148–1153 (1973)]. That analysis predicts waveforms at large distances, provided that comparable information is known at a reference location in the farfield. Lockwood *et al.* used this approach based on assuming that linear theory is accurate at the reference location. Such an assumption is inaccurate when the source pressure level is sufficient to generate significant nonlinear effects (growth of higher harmonics and depletion of the fundamental) within the near field. The present work describes the interfacing of the spherical propagation theory and the nonlinear King integral [J. H. Ginsberg, J. Acoust. Soc. Am. Suppl. 1 71, S30 (1982)]. The latter theory is used in this approach to evaluate the nonlinear waveform at the reference location. Comparing the results of interfacing, and of direct propagation according the nonlinear integral formulation, with experimental data provides a strong validation for both theories. The advantage of using directive spherical wave theory lies in its superior computational efficiency and its ability to describe shock formation. [Work supported by ONR, Code 425-UA, and NSF, Grant MEA-8101106.]

Town and Country Hotel
San Diego, California
7–11 November 1983

TRANSITION FROM THE NONLINEAR KING INTEGRAL TO SPHERICAL PROPAGATION FOR A FINITE AMPLITUDE SOUND BEAM

Jerry H. Ginsberg
School of Mechanical Engineering
Georgia Institute of Technology
Atlanta, GA 30338

OBJECTIVES

1. Predict waveform
2. Amplitude and phase of higher harmonics
3. Basic understanding of phenomena
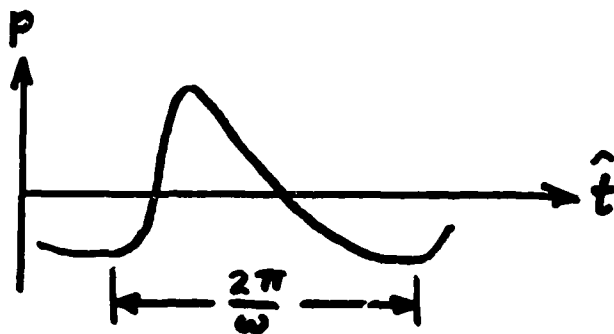
Alternative Analyses

Quasi-spherical propagation

Nonlinear King (diffraction) integral

HIGHER HARMONIC GENERATION IN CW FINITE AMPLITUDE SOUND BEAMS

field point

axial wave number
$k = \omega/c_0$

$\hat{r}$

$\hat{r}_0$

transition
to farfield - is $\hat{r}_0 = \frac{1}{2} k a^2$?

Rayleigh length
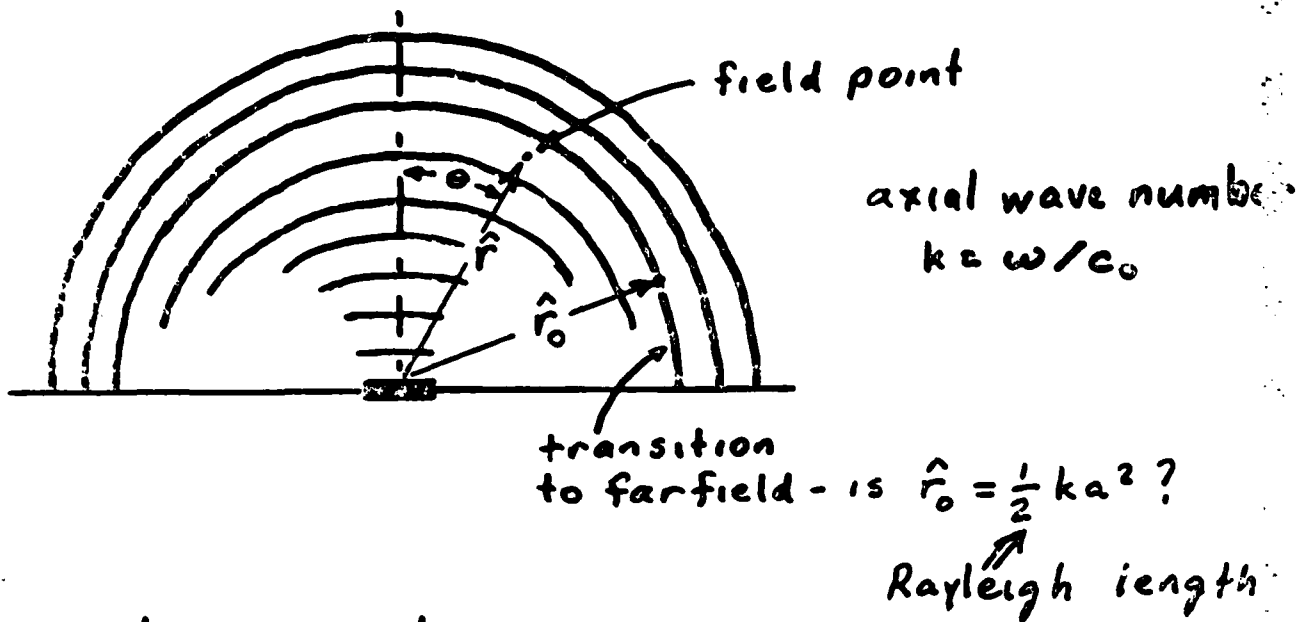
Nondimensional:
  Coordinates:
    cylindrical $R = k\hat{R}$, $z = k\hat{z}$
    spherical: $r = k\hat{r}$
  Time : $t = \omega \hat{t}$

NONLINEAR KING INTEGRAL

Medium is an infinite radius waveguide

Distortion (nearfield & farfield) results
from interaction of duct modes

Perturbation analysis - relate transducer
motion (arbitrary spatial pattern)
directly to signal

Consistent model - uniform description
of distortion, nearfield diffraction,
& spreading

Omit dissipation

Mode Combination

Transverse wave number $= n$

$$p = \rho_0 c_0^2 \, \varepsilon \int_0^\infty \frac{in F_n}{\bar{\mu}_n} \exp(it - \mu_n \xi_n) J_0(n\alpha_n) \, d\eta$$

$+ CC +$ RMS term (cancel RMS

contribution of coordinate straining)

where $\mu_n^2 = (n^2 - 1)$

$v_z = \varepsilon c_0 f(R) e^{it} + CC$ on the boundary

$F_n = \int_0^\infty R f(R) J_0(nR) \, dn$

Coordinate Straining Transformation

$$z = \xi_n - \pi \varepsilon \beta_0 \, \xi_n \left\{ \frac{in F_n}{\bar{\mu}_n} H(n, \xi_n) \right.$$

$$\left. \times \exp(it) \, \text{erfc}\left[(\mu_n \xi_n)^{1/2} \right] + CC \right\} J_0(n\alpha_n)$$

$$R = \alpha_n + \pi \varepsilon \beta_0 \, \xi_n \left\{ \frac{in \bar{\mu}_n F_n}{\mu_n} H(n, \xi_n) \right.$$

$$\left. \times \exp(it) \, \text{erfc}\left[(\mu_n \xi_n)^{1/2} \right] + CC \right\} J_1(n\alpha_n)$$

$\beta_0 = 1 + \frac{1}{2} \frac{B}{A}$: coefficient of nonlinearity

$n < 1$: propagating modes

$n > 1$: evanescent modes

ALGORITHM FOR
FREQUENCY ANALYSIS

A. Input max SPL on-axis, ka, location, medium

B. Transform transducer vibration pattern

C. Select number of integration points

D. Time loop: $0 \leq t < 2\pi$
   1. Propagating mode loop: $0 \leq n < 1$
      a. Select n_i for Guassian integration
      b. Solve coordinate transformation
      c. Sum contribution
   2. Evanescent mode loop: $n > 1$
      a. - c. As above using $m = 1/n$

E. Fourier series analysis - uses only
   one period of the waveform

QUASI- SPHERICAL WAVE

Lockwood - U. Texas, ARL report, 1971

Axisymmetric spherical coordinates (r, θ)

Given $\quad p(r_0, \theta, t) = \rho_0 c_0^2 \varepsilon F(\theta, t)$

then $\quad p(r, \theta, t) = \rho_0 c_0^2 \varepsilon \dfrac{r_0}{r} F(\theta, t - \chi)$

where $\quad \chi = r - r_0 - \beta_0 \varepsilon\, r_0\, \ln\left(\dfrac{r}{r_0}\right) F(\theta, t - \chi)$

i.e. solve a single transcendental equation

APPLICATION TO
SOUND BEAMS

I. Farfield distortion theory

Lockwood, Muir, & Blackstock, JASA, 1971

Use
$$p(r_0, \theta, t) = (A_{lin})_0 \sin\left[t - (\Psi_{lin})_0\right]$$

Make r_0 as small as possible, i.e. r_0 = Rayleigh length

Consequence: higher harmonics generated as the wave propagates are in-phase $\Rightarrow$ symmetry between compression and rarefaction

II. Matched distortion theory

Use
$$p(r_0, \theta, t) = \sum_{j=1}^{M} (A_j)_0 \sin\left[jt - (\Psi_j)_0\right]$$

where $(A_j)_0$ & $(\Psi_j)_0$ are from
the nonlinear King integral

SHOCK FORMATION

Spherical spreading
   Identify where $\partial p / \partial r \to \infty$
   Is it meaningful? $\Longleftrightarrow$ location
      depends on choice for r_0

King integral
   Search for vanishing Jacobian
      of the coordinate transformation
      at any transverse wave number
   Difficult to identify
   What is the physical meaning?
      i.e. duct modes for a small
      band of n exhibit this
      condition.

Results

Define $L = \dfrac{r_o}{\frac{1}{2}(ka)^2}$: spherical boundary parameter

Source SPL = 125 dB in air, $ka = 37.1$, $z = 2115$ on-axis

Type L	Matched distortion			Farfield distortion			Measured JASA, vol 73, p 764
	0.5	1.0	2.0	0.5	1.0	2.0	
A_1	107.6	108.7	108.8	107.7	108.8	109.2	109
Ψ_1	—	—	—	0°	0°	-4°	
A_2	92.0	91.8	89.1	88.6	86.6	79.0	93
Ψ_2	15°	27°	41°	0°	0°	-8°	
A_3	80.0	78.9	73.8	73.0	67.8	52.4	80
Ψ_3	31°	58°	87°	0°	0°	-12°	
A_4	70.0	67.4	61.9	58.8	50.6	27.2	
Ψ_4	46°	92°	147°	0°	0°	-16°	

A_j are dB re 20 μPa for air or 1 μPa for water

Positive Ψ_j means a phase lag re fundamental, $\Psi_1 \equiv 0$ for matched distortion

Source SPL = 125 dB in air, $ka = 37.1$, $r = 2115$, $\theta = 2.5°$

Type L	Matched distortion			Farfield distortion		
	0.5	1.0	2.0	0.5	1.0	2.0
A_1	104.7	105.8	106.1	104.8	105.8	106.1
Ψ_1	—	—	—	0°	0°	0°
A_2	86.6	85.7	85.5	82.7	80.7	72.9
Ψ_2	12°	34°	66°	0°	0°	0°
A_3	72.2	67.5	70.6	64.2	59.1	43.2
Ψ_3	27°	76°	130°	0°	0°	0°
A_4	59.1	55.2	57.3	47.1	39.0	15.0
Ψ_4	43°	124°	-168°	0°	0°	0°

Source SPL = 125 dB in air, ka = 37.1, r = 2115, θ = 5°

Type	Matched distortion			Farfield distortion		
L	0.5	1.0	2.0	0.5	1.0	2.0
A_1	96.4	94.3	93.3	96.4	94.3	93.4
γ_1	—	—	—	0°	0°	0°
A_2	72.6	73.8	67.2	65.9	57.6	47.3
γ_2	56°	56°	54°	0°	0°	-1°
A_3	51.0	53.3	44.6	39.0	24.5	4.9
γ_3	119°	98°	100°	-1°	1°	-1°
A_4	34.6	34.5	21.8	13.6	(noise)	
γ_4	-168°	142°	132°	-1°		

Source SPL = 220 dB in water, ka = 37.1, r = 2115 on-axis

Type L	Matched distortion			Farfield distortion			King *
	0.5	1.0	2.0	0.5	1.0	2.0	
A_1	202.7	203.8	204.0	202.8	203.8	204.2	204.2
Ψ_1	—	—	—	0°	0°	-1°	—
A_2	182.3	182.1	190.	178.6	176.5	168.9	178.7
Ψ_2	15°	27°	42°	0°	0°	-3°	56°
A_3	166.0	164.3	158.2	157.9	152.7	137.2	160.5
Ψ_3	29°	58°	85.8°	0°	1°	-4°	123°
A_4	151.3	145.1	145.6	138.8	130.4	106.9	147.7
Ψ_4	36.7	88.2°	179°	0°	1°	-6°	-153°

Source SPL = 140 dB in air, ka=15, r=675, on-axis

Analysis L	Matched distortion 1.0	2.0	3.0	Farfield distortion 1.0	2.0	3.0	King *
A_1	118.0	118.2	118.5	117.9	118.2	118.4	118.1
ψ_1	—	—	—	0°	-5°	-7°	—
A_2	102.8	100.6	99.1	98.6	95.9	91.7	99.6
ψ_2	20°	32°	35°	1°	-10°	-14°	65°
A_3	90.4	88.6	87.6	83.5	75.7	68.4	88.1
ψ_3	42°	57°	89°	1°	-15°	-21°	94°
A_4	81.0	76.5	63.1	69.5	57.8	46.7	68.1?
ψ_4	59°	121°	67°	1°	-20°	-28°	106°

CONCLUSIONS

1. Farfield distortion underpredicts harmonic generation- best results when $\hat{r}_0 < \frac{1}{2} ka^2$

2. Matched distortion gives best predictions when $\hat{r}_0 > \frac{1}{2} ka^2$ (factor of 2 or more at low frequencies)

3. Predicting phase shifts is much more difficult than predicting amplitudes- farfield distortion is not useful for this task

4. Closeness of matched distortion and King integral validates King integral in the farfield (propagation over a range by independent theories yields similar results)

Program of the
107th Meeting

THURSDAY AFTERNOON, 10 MAY 1984 GREENWAY ROOM, 2:00 TO 3:50 P. M.

Session VV. Physical Acoustics VI: Nonlinear Acoustics

2:50

VV4. Analysis of nonlinear harmonic generation for arbitrary dual frequency transducer excitation. Mosaad A. Foda and Jerry H. Ginsberg (School of Mechanical Engineering, Georgia Institute of Technology, Atlanta, GA 30332)

An earlier study of finite amplitude axisymmetric sound beams [J. H. Ginsberg, J. Acoust. Soc. Am. Suppl. 1 73, S83 (1983)] considered the case of monochromatic excitation. That work featured a singular perturbation analysis combining asymptotic integration and the renormalization version of the method of strained coordinates. The present paper initiates an extension of those techniques to the case of a dual frequency source. The parametric array, in which the primary beams are at closely spaced frequencies, has already received much attention. The system discussed here permits disparate frequencies. Aside from a restriction to axisymmetry, the excitation at each frequency is arbitrary. The analysis thus far has obtained the first two orders of approximation for the velocity potential. This expression describes the manner in which nonlinear effects accumulate for the various sum and difference frequencies. It is the foundation for a future derivation of an expression for the pressure that is descriptive of the entire field. In addition, the trend for harmonic generation indicated by the analysis suggests that conversion efficiency in the parametric array might be improved by altering the transverse vibration pattern of the individual primary beams. [Work supported by ONR, code 425-UA.]

Omni International Hotel
Norfolk, Virginia
6–10 May 1984

Nonlinear Harmonic Generation For

A Dual Frequency Transducer Excitation
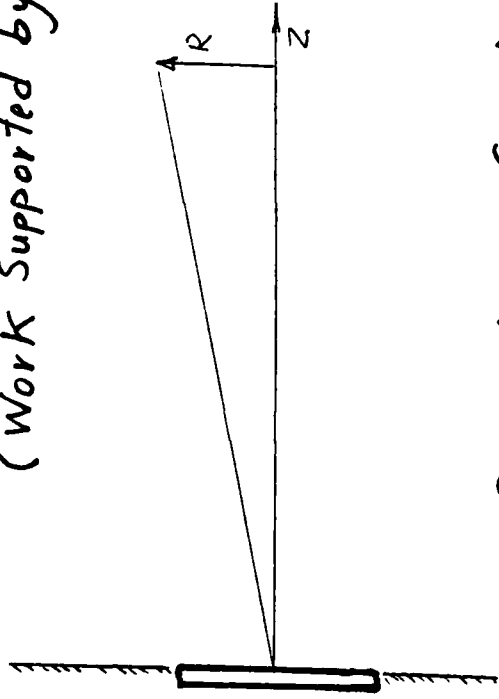
Cylindrical Coordinates:

$$z = K_0 \hat{z}, \quad R = k_0 \hat{R}, \quad t = \omega_0 \hat{t}$$

$$K_0 = \frac{\omega_0}{c_0}, \quad \omega_i = \frac{\hat{\omega}_i}{\omega_0}, \quad i = 1, 2, \quad \omega_0 = \frac{1}{2}(\hat{\omega}_1 + \hat{\omega}_2)$$

Boundary Condition:

$$U_z\big|_{z=0} = \frac{\hat{\epsilon}_1}{2i} f_1(R) e^{i\omega_1 t} + \frac{\hat{\epsilon}_2}{2i} f_2(R) e^{i\omega_2 t} + CC$$

Acoustic Mach numbers

CC ← denotes complex conjugate

$f_i(R)$ arbitrary ($f_i \to 0$ as $R \to \infty$)

Nonlinear Wave Equation For Velocity Potential

$$\nabla^2 \Phi - \frac{\partial^2 \Phi}{\partial t^2} = 2(B_o-1)\frac{\partial \Phi}{\partial t}\nabla^2\Phi + \frac{\partial}{\partial t}(\nabla\Phi\cdot\nabla\Phi) + O(\Phi^3)$$

$$\Phi = \epsilon_o \Phi_1 + \epsilon_o^2 \Phi_2 + O(\epsilon_o^3)$$

where $\quad \epsilon_o = \hat{\epsilon}_1 + \hat{\epsilon}_2$

Dual King Integral – First order terms

Hankel transform for transverse dependence

$$V_n = \epsilon_1 \frac{1}{z_i} \int_0^\infty R f_1(R) J_o(\omega_1 nR)(\omega_1 dR)$$

$$W_n = \epsilon_2 \frac{1}{z_i^2} \int_0^\infty R f_2(R) J_o(\omega_2 nR)(\omega_2 dR)$$

$\Rightarrow$ Helmholtz equation in z, t, n plane

$$\epsilon_i = \frac{\hat{\epsilon}_i}{\epsilon_o}$$

Invert Transform:

$$\Phi_1 = -\int_0^\infty \int \left\{ \frac{n V_n}{\mu_n} \exp[w_1(it - \mu_n z)] \, J_0(w_1 nR) \right.$$
$$\left. + \frac{n W_n}{\mu_n} \exp[w_2(it - \mu_n z)] \, J_0(w_2 nR) \right\} dn$$
$$+ CC$$

$$\mu_n = \begin{cases} (n^2 - 1)^{\frac{1}{2}} & ; \ n > 1 \\ i(1 - n^2)^{\frac{1}{2}} & ; \ n < 1 \end{cases}$$

signs satisfy radiation Condition

Note: Real function form changes type at $n=1$

$\quad n < 1$: Propagating modes

$\quad n > 1$: Evanescent modes

Source terms for the second order potential Φ_2

Inhomogenous Wave equation for Φ_2 ; Source terms are

$$\frac{\partial}{\partial t}\left[\,(B_0-1)\left(\frac{\partial \Phi_1}{\partial t}\right)^2 + \nabla\Phi_1\cdot\nabla\Phi_1\,\right]$$

Source terms are quadratic products of derivatives of Φ_1

General Form – Overbar means Complex conjugate; $\omega^{\pm} = \omega_1 \pm \omega_2$

$$\int\!\!\!\int_0^\infty mn\cdots\left\{\begin{matrix}J_0(\omega_1 mR)\,J_0(\omega_1 nR)\\J_1(\omega_1 mR)\,J_1(\omega_1 nR)\end{matrix}\right\}\exp\left\{\omega_1\left[zit-(\mu_n+\mu_m)z\right]\right\}dm\,dn$$

$$+\int\!\!\!\int_0^\infty mn\cdots\left\{\begin{matrix}J_0(\omega_2 mR)\,J_0(\omega_2 nR)\\J_1(\omega_2 mR)\,J_1(\omega_2 nR)\end{matrix}\right\}\exp\left\{\omega_2\left[zit-(\mu_n+\mu_m)z\right]\right\}dm\,dn$$

$$+\int\!\!\!\int_0^\infty mn\cdots\left\{\begin{matrix}J_0(\omega_1 nR)\,J_0(\omega_2 mR)\\J_1(\omega_1 nR)\,J_1(\omega_2 mR)\end{matrix}\right\}\exp\left\{i\omega^+t-(\omega_1\mu_n+\omega_2\mu_m)z\right\}dm\,dn$$

$$+\int\!\!\!\int_0^\infty mn\cdots\left\{\begin{matrix}J_0(\omega_1 nR)\,J_0(\omega_2 mR)\\J_1(\omega_1 nR)\,J_1(\omega_2 mR)\end{matrix}\right\}\exp\left\{i\omega^-t-(\omega_1\mu_n+\omega_2\bar{\mu}_m)z\right\}dm\,dn$$

$$+\,CC$$

Note : Complementary solution for Φ_z leads to

insignificant higher harmonics ($\epsilon_o \ll 1$).

observed distortion levels can only result

From Cumulative growth $\Rightarrow$ Particular solution

Forming Particular solution from

Combination of Bessel function Products

Variation of parameters - dependence on R

as suggested by source terms.

$$\Phi_2(z,R,t) = \Phi_2^{(1)} + \Phi_2^{(2)} + \Phi_2^{(+)} + \Phi_2^{(-)}$$

$$\Phi_2^{(i)} = \int_0^\infty \!\!\int\!\!\int n\,m \left\{ \Phi_{21}^{(i)}(z,t)\left[J_0(w_{1m}R)\,J_0(w_{1n}R) - J_1(w_{1m}R)\,J_1(w_{1n}R) \right] \right.$$
$$\left. + \Phi_{22}^{(i)}(z,t)\left[J_0(w_{1m}R)\,J_0(w_{1n}R) + J_1(w_{1m}R)\,J_1(w_{1n}R) \right] \right\} dm\,dn$$

$$i = 1, 2$$

$$\Phi_2^{(\pm)} = \int_0^\infty \!\!\int\!\!\int n\,m \left\{ \Phi_{21}^{(\pm)}(z,t)\left[J_0(w_1 nR)\,J_0(w_{2m}R) - J_1(w_1 nR)\,J_1(w_{2m}R) \right] \right.$$
$$\left. + \Phi_{22}^{(\pm)}(z,t)\left[J_0(w_1 nR)\,J_0(w_{2m}R) + J_1(w_1 nR)\,J_1(w_{2m}R) \right] \right\} dm\,dn$$

where: $\Phi_{2j}^{(i)}$ and $\Phi_{2j}^{(\pm)}$ must satisfy the inhomogeneous Helmholtz equation

Note: $\Phi_{2j}^{1,2,+ \text{ or } -}$ — Same governing equation for all R because it is independent of R

Identities:

$$\left(\frac{d^2}{dR^2} + \frac{1}{R}\frac{d}{dR}\right)\left\{\begin{array}{l} J_0(w_{in}R)\, J_0(w_{jm}R) \\ J_1(w_{in}R)\, J_1(w_{jm}R) \end{array}\right\}$$

$$\equiv -(w_{in}^2 + w_{jm}^2)\left\{\begin{array}{l} J_0(w_{in}R)\, J_0(w_{jm}R) \\ J_1(w_{in}R)\, J_1(w_{jm}R) \end{array}\right\}$$

$$+\, 2w_{in}w_{jm}mn \left\{\begin{array}{l} J_1(w_{in}R)\, J_1(w_{jm}R) \\ J_0(w_{in}R)\, J_0(w_{jm}R) \end{array}\right\}$$

$$+ \boxed{zero}$$

$$+ \left\{\frac{4}{R^2}\, J_1(w_{in}R)\, J_1(w_{jm}R) - \frac{2w_{in}}{R}\, J_0(w_{in}R)\, J_1(w_{jm}R) - \frac{2w_{jn}}{R}\, J_1(w_{in}R)\, J_0(w_{jm}R)\right\}$$

(a) Last term is negligible when R is large, and m & n not small

(b) All terms from transverse R derivatives are $O(w_{in}w_{jm}mn)$ when m & n are small and R is not large (near-planar modes)—other terms from Φ_{ij} are $O(w_i w_j)$.

Particular Solution:

$$\Phi_{2j}^{(i)} = a_j^{(i)}(z) \exp\{w_i[z_i t - (\mu n + \mu m)z]\}$$
$$i = 1,2$$

$$\Phi_{2j}^{(+)} = a_j^{(+)}(z) \exp\{iw^+t - (w_1 \mu n + w_2 \mu m)z\}$$

$$\Phi_{2j}^{(-)} = a_j^{(-)}(z) \exp\{iw^-t - (w_1 \mu n + w_2 \bar{\mu}_m)z\}$$

$$a_j''(z) + \alpha_j a_j'(z) + \beta_j a_j(z) = \gamma_j \qquad " \setminus " = \frac{d}{dz}$$

α, β and γ are function of m, n, w_i and β_0.

Uncoupling of a_j equations results from using

Linear combinations of Bessel function products

to form Φ_2

Asymptotic Integration

Particular solution of:

$$a_j''(z) + \alpha_j\, a'(z) + \beta_j\, a(z) = \gamma_j$$

is independent of z unless $\beta_j \longrightarrow 0$

Only case where $\beta_j \longrightarrow 0$ is $m \longrightarrow n$

(which is secularity condition)

Conclusion:

Cumulative growth in ϕ_2 stems from a_j

in the rejon where $m = n + qa$, $\Delta \ll 1$

Procedure

(1) Series expansion of coefficients in powers of qa, Keep leading terms only.

(2) Evaluate general solution (Complementary + Particular) For a_j

(3) Evaluate coefficients of Complementary solution by matching the general solution as $q \to 0$ to the particular solution for $q=0$

(4) Evaluate the integral over $0 < m < \infty$ in Φ_2 using the asymptotic general solution for a_j (Δ fixed)

Integration Procedure

$$\int_0^\infty\!\!\int_0^\infty F(m,n)\,dm\,dn = \int_0^\infty\!\!\int_{n-\delta}^{n+\delta} F(m,n)\,dm\,dn \quad \Leftarrow \text{Secularity}$$

$$+ \int_0^\infty\!\!\int_0^{n-\delta} F(m,n)\,dm\,dn$$

$$+ \int_0^\infty\!\!\int_{n+\delta}^{\infty} F(m,n)\,dm\,dn$$

destructive interference

$$= \int_0^\infty\!\!\int_{-\delta/\Delta}^{\delta/\Delta} F(n+q\Delta,n)\,dq\,dn + \text{Fixed magnitude terms}$$

Seek cumulatively growing part of integral–independent of δ and Δ $\Longrightarrow$ dominant effect. Other terms are subdominant. (other subdominant effects were already omitted, e.g. complementary solution for Φ_2)

Result

$$\Phi_2 = \int_0^\infty \left\{ \left[i B_0 \, w_1^{\frac{3}{2}} \frac{n^2 V_n}{\mu_n \tilde{\mu}_n} (\pi \mu_n z)^{\frac{1}{2}} e^{2w_1(it - \mu_n z)} \left[J_0^2(w_1 nR) - J_1^2(w_1 nR) \right] \right. \right.$$

$$+ i B_0 \, w_2^{\frac{3}{2}} \frac{n^2 W_n}{\mu_n \tilde{\mu}_n} (\pi \mu_n z)^{\frac{1}{2}} e^{2w_2(it - \mu_n z)} \left[J_0^2(w_2 nR) - J_1^2(w_2 nR) \right]$$

$$+ i B_0 (2 w_1 w_2 w^+)^{\frac{1}{2}} \frac{n^2 V_n W_n}{\mu_n \tilde{\mu}_n} (\pi \mu_n z)^{\frac{1}{2}} e^{w^+(it - \mu_n z)} \left[J_0(w_1 nR) J_0(w_2 nR) - J_1(w_1 nR) J_1(w_2 nR) \right]$$

$$+ i B_0 (2 w_1 w_2 w^-)^{\frac{1}{2}} \frac{n^2 V_n \overline{W_n}}{\mu_n \tilde{\mu}_n} (\pi \tilde{\mu}_n z)^{\frac{1}{2}} e^{w^-(it - \mu_n z)} \left[J_0(w_1 nR) J_0(w_2 nR) + J_1(w_1 nR) J_1(w_2 nR) \right] \right\} dn$$

$$+ \, CC \, + \, \text{subdominant terms.}$$

Note: $\mu_n \longrightarrow 0$ as $n \longrightarrow 1$, but terms are

$$O(\mu_n^{-\frac{3}{2}}) = O\left[(n^2 - 1)^{-\frac{3}{4}} \right]$$

integrable singularity

Fig. 3. Propagation curves.

Legend:
- □ MEAN OF THE 418- AND 482-kHz CARRIER FREQUENCY RADIATIONS
- ○ 64-kHz DIFFERENCE FREQUENCY RADIATION
- △ 900-kHz SUM-FREQUENCY RADIATION
- —— THEORY
- --- SPHERICAL SPREADING

Axis: SOUND PRESSURE LEVEL – DB RE 1 μBAR (120, 110, 100, 90, 80, 70, 60, 50, 40, 30, 20, 10)

RANGE – YD (0.2, 0.5, 1, 3, 5, 7, 10, 30, 50, 100, 200)

$\frac{3a^2}{4\lambda c}$ $\frac{2a^2}{\lambda c}$ $\frac{4a^2}{\lambda c}$

Numerical Result

Piston radius $a = .0381\ m$

$\omega_1 = 482\ kHz$, $\omega_2 = 418\ kHz$

Peak SPL $= 110\ dB$

Non uniform accuracy of solution

$\longleftrightarrow$

Diverging values with increasing range
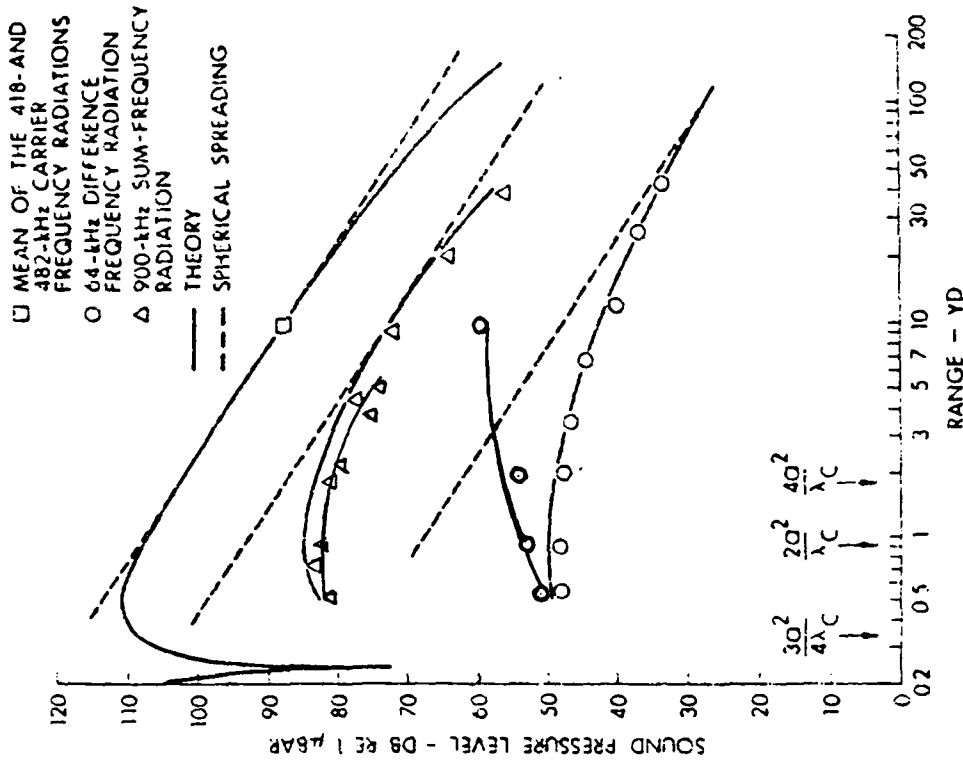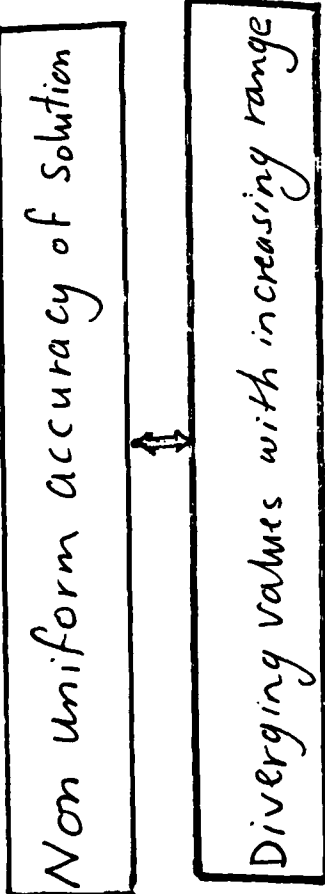
MUIR, T.G. and J.G. WILLETTE
JASA, 52 (5), 1972, P.1482

Possible signal reinforcement

$$\Phi_r \sim \int_0^\infty n V_n W_n \left(\quad \right) dn$$

For a uniform piston velocity

$$nV_n = k_0 a J_1(k_0 a w_1 n)$$

$$nW_n = k_0 a J_1(k_0 a w_2 n)$$

Try making phase of V_n
and W_n coincide

$\longrightarrow \quad a_1 w_1 = a_2 w_2$

(two different radii)
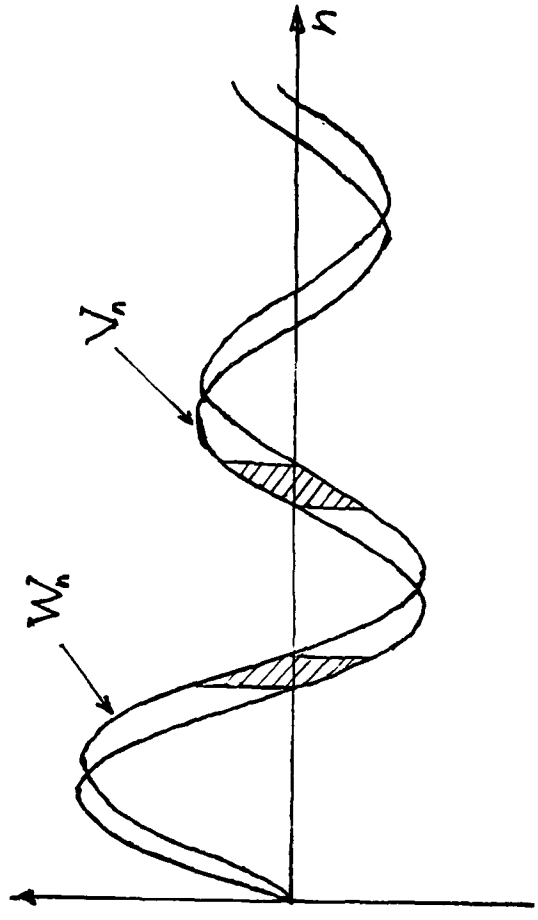
THE JOURNAL

of the

Acoustical Society of America

Program of the
108th Meeting

Leamington Hotel
Minneapolis, Minnesota
8–12 October 1984

K7. Evaluation of the overall sound field properties for a finite amplitude
sound beam. J. H. Ginsberg (School of Mechanical Engineering, Georgia
Institute of Technology, Atlanta, GA 30332)

The nonlinear King integral [J. H. Ginsberg, J. Acoust. Soc. Am. (to
be published)] provides a general algorithm for finite amplitude axisym-
metric waves radiating from a harmonically vibrating transducer. The
derivation of that result was based on asymptotic analyses of the trans-
verse wavenumber spectrum near the axis for almost planar modes and far
off axis. The validity of the analysis is confirmed here by a change of
variables that yields an overall measure of the associated error. Previous
evaluations using the nonlinear King integral provided temporal and fre-
quency spectrum predictions at selected locations, primarily on axis. The
present paper reports on an extensive mapping of the field for a moderate-
ly high frequency in terms of amplitude and relative phase lags for the
fundamental and several higher harmonics. This mapping is cross-refer-
enced to waveform displays that show the changing nature of the asym-
metrical distortion process associated with transition from the nearfield to
the farfield. [Work supported by ONR, Code 425-UA.]

EVALUATION OF THE OVERALL
SOUND FIELD PROPERTIES FOR A
FINITE AMPLITUDE SOUND BEAM

J. H. GINSBERG

School of Mechanical Engineering
Georgia Institute of Technology

Axisymmetric Case
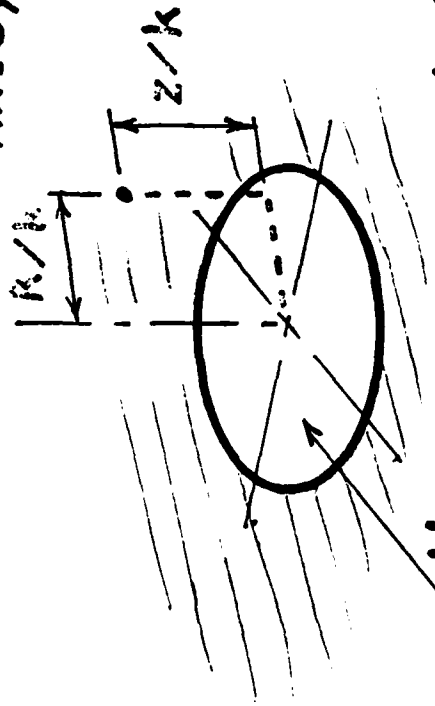
Planar wave number:
$$k = \omega/c_0$$

Units:
$$\frac{z}{2\pi}, \frac{R}{2\pi} \left\{ \begin{array}{l} \text{wavelength} \\ \text{multiples} \end{array} \right.$$

$$\frac{z}{ka}, \frac{R}{ka} \left\{ \begin{array}{l} \text{radius} \\ \text{multiples} \end{array} \right.$$

Harmonic excitation:
frequency $= \omega$

$$v_z = \frac{1}{2i} \epsilon c_0 f(R) \exp(it) \quad \text{on } z=0$$

Hankel transform:

$$V_n = \frac{1}{2i} \int_0^R R\, f(R)\, J_0(nR)\, dR$$

Example: PISTON

$$f(R) = \left\{ \begin{array}{l} 1 : R<a \\ 0 : R>a \end{array} \right. \Rightarrow V_n = \frac{ka}{n} J_1(nka)$$

NONLINEAR KING INTEGRAL

Inversion of Hankel transform:

$$p = \rho_0 c_0^2 \varepsilon i \int_0^\infty \frac{n V_n}{\mu_n} \exp(it - \mu_n \zeta_n) \, J_0(n x_n) \, dn$$

+ mean value correction + CC

$$\mu_n = \begin{cases} i(1-n^2)^{1/2} & n<1 \\ (n^2-1)^{1/2} & n>1 \end{cases}$$

Coordinate straining:

ζ_n & x_n are functions of:

(a) Position coordinates
(b) Time
(c) Transverse wave number

$$\left. \begin{array}{l} \zeta_n \to \lambda_n z \\ x_n \to nR \end{array} \right\} \text{ as } \varepsilon \to 0 \text{ or } z \to 0$$

linear King integral

NUMERICAL ALGORITHM

Angular spectrum: remove singularity

$$n = \begin{cases} \sin X \; ; \; n < 1 \; (propagating \; modes) \\ 1/\sin X \; ; \; n > 1 \; (evanescent \; modes) \end{cases}$$

Integrate over X numerically.

Diffraction integral:

   Propagating spectrum:

$$\exp(it - u_n \, \zeta_n) = \exp(it) \, \exp(-i \, \zeta_n \cos X)$$

   Oscillatory integrand —
   increasing rate as ζ_n increases.

   Decrease integration mesh.

FOURIER ANALYSIS

Define retarded time τ such that the fundamental is a pure sine.

Use King integral to generate waveform.

Evaluate amplitudes and phase lags relative to fundamental:

$$p = p_1 \sin(\tau) + p_2 \sin(2\tau - \psi_2) + p_3 \sin(3\tau - \psi_3) + \cdots$$

Define branch for phase lags:

$$-\pi < \psi_j \leq \pi$$

PHASE ANGLES ALONG R = 0.000

AMPLITUDES ALONG R = 0.000

△ harmonic # 1
▲ harmonic # 2
□ harmonic # 3
▨ harmonic # 4

SPL re 1 uPa

AXIAL DISTANCE z (nondimensional)
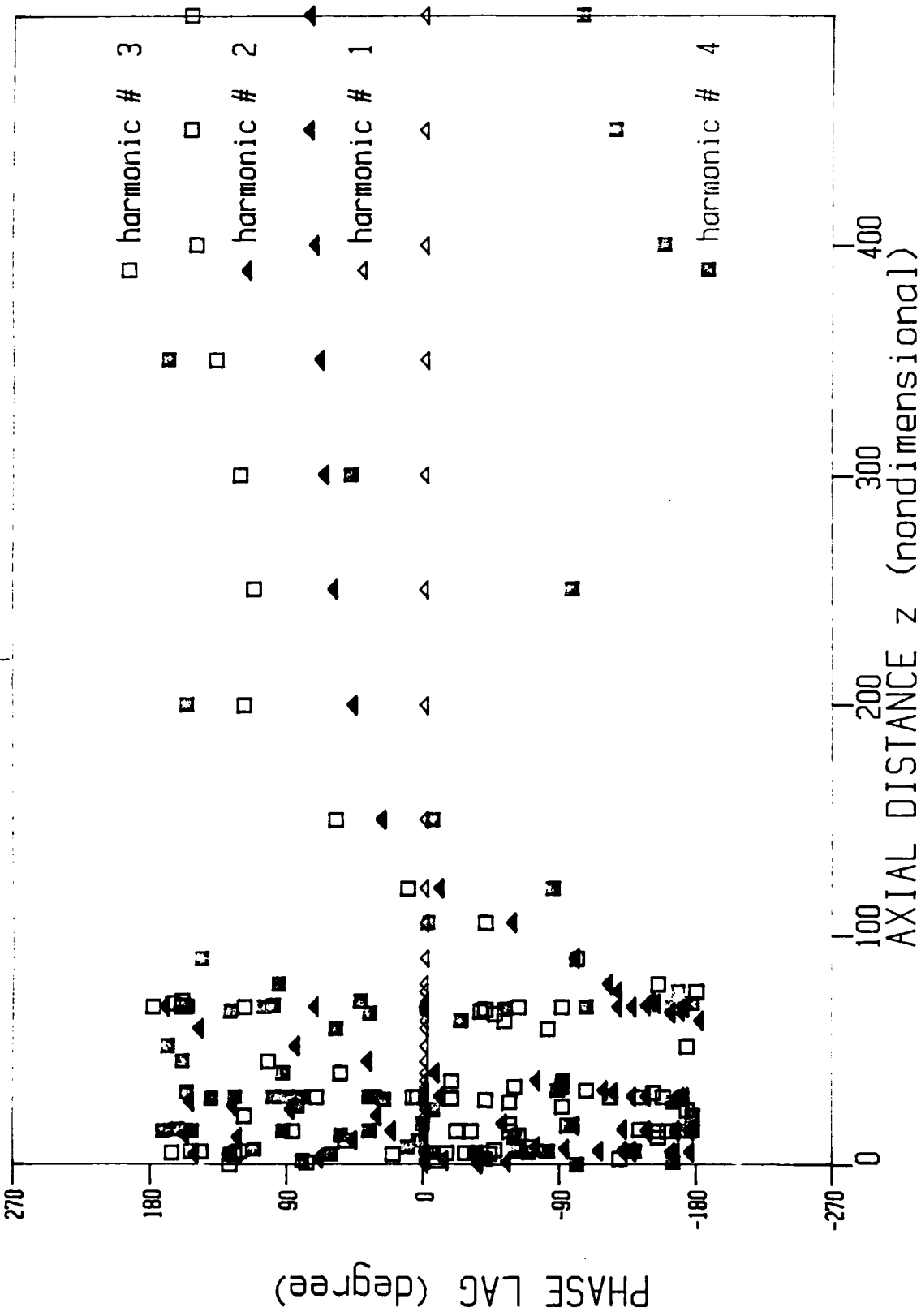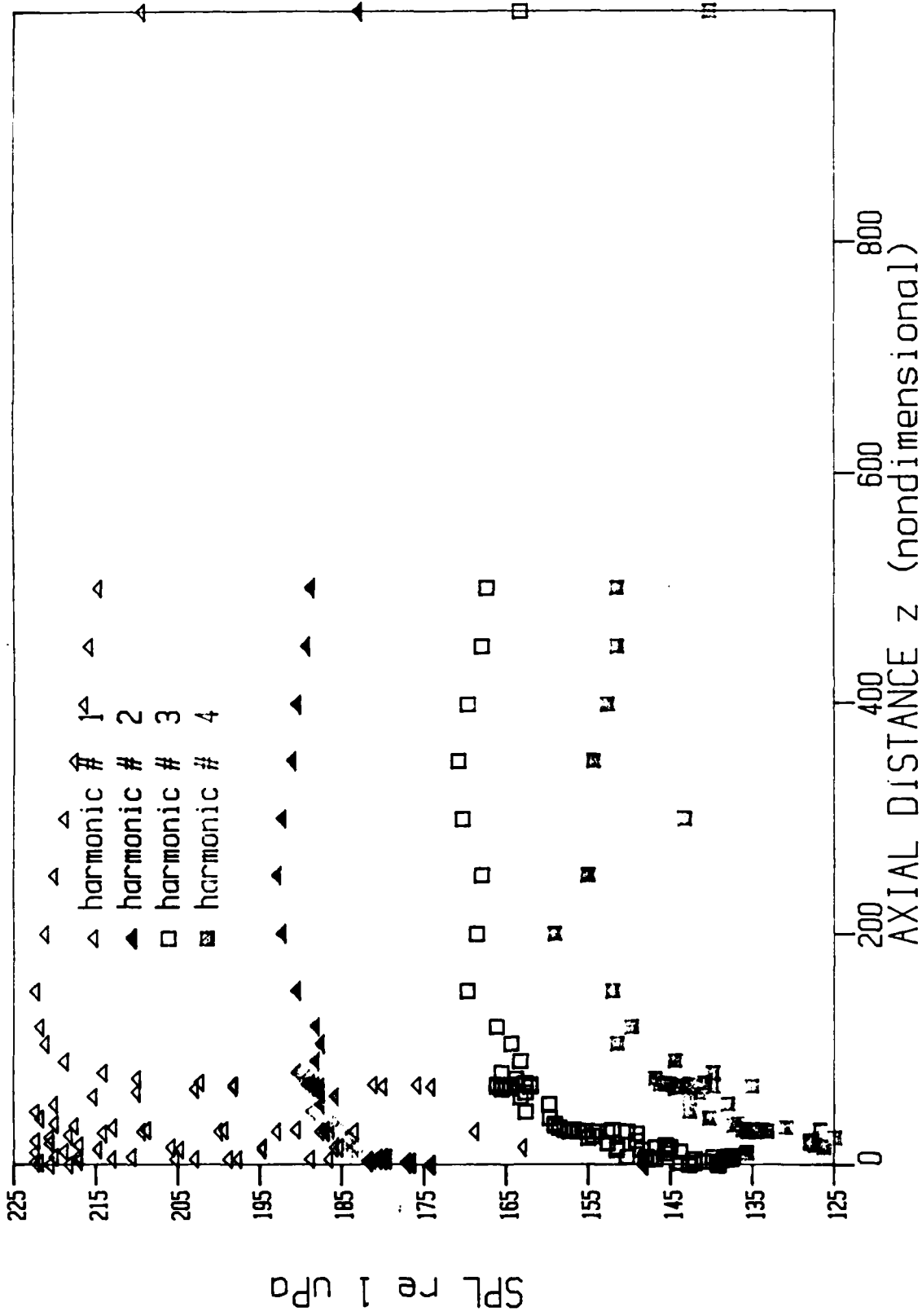
$ka = 64.3$

NUSC FILE # 920005.DAT
MAX. SPL (LINEAR) ON-AXIS = 222.600 DB
ka = 64.3380   BETA0=3.6   SOUND SPEED = 1488 m/s
z (nondim.) = 215.31   POLAR ANGLE = 0 (deg)

——— :NONLINEAR THEORY;   — — — :MEASURED;   ·········· :LINEAR.
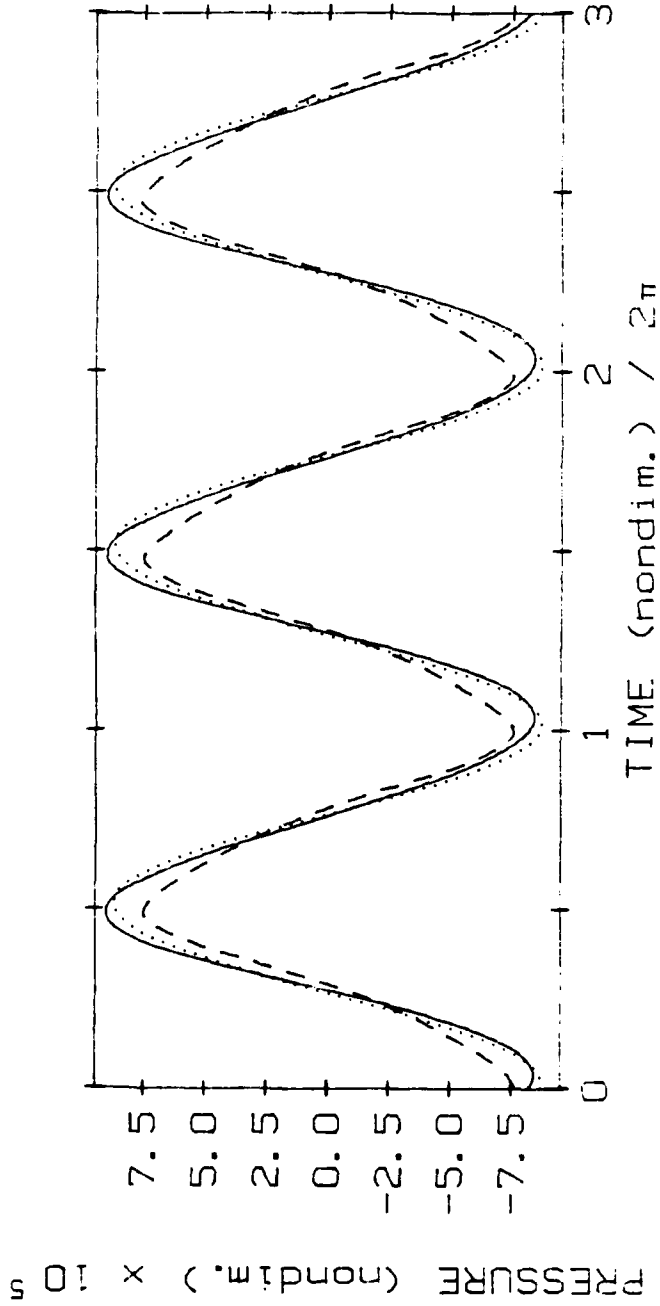
$ka = 64.3$

NUSC FILE # 920019.dat   plotted to match peaks(approx.)
MAX. SPL (LINEAR) ON-AXIS = 222.600 DB
k a = 64.3380 BETA0=3.6   SOUND SPEED = 1488 m/s
z (nondim.) = 2533.03 POLAR ANGLE = 0 (deg)

———— : NONLINEAR THEORY;   — — — : MEASURED;   .... : LINEAR

TIME (nondim.) / 2π

PRESSURE (nondim.) $\times 10^5$

ka = 30

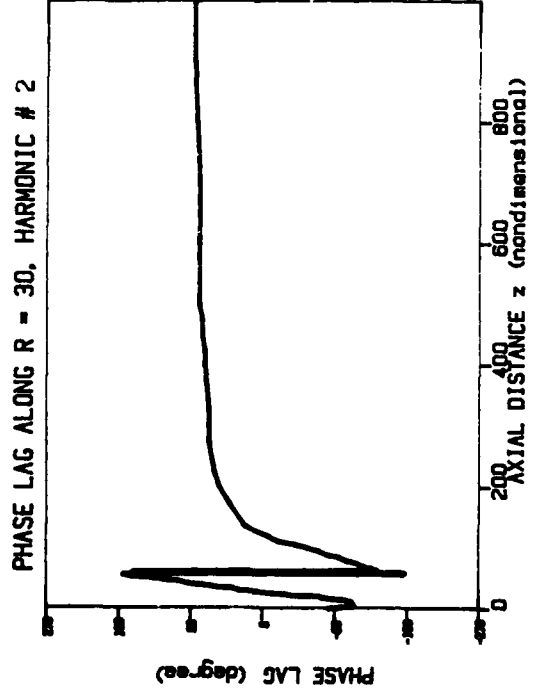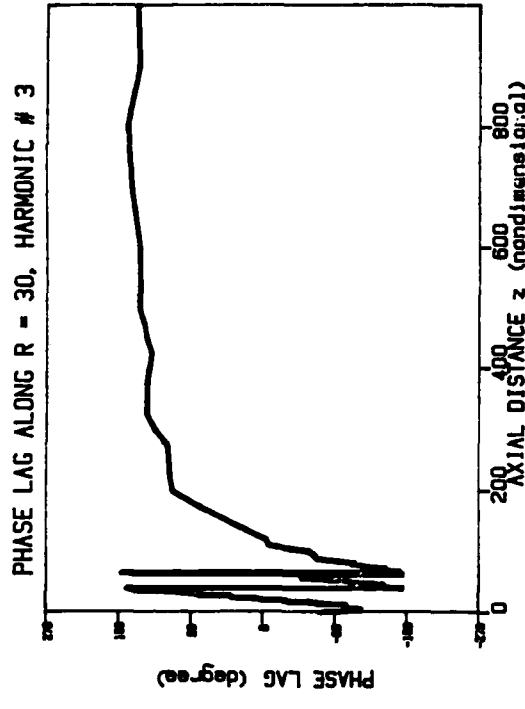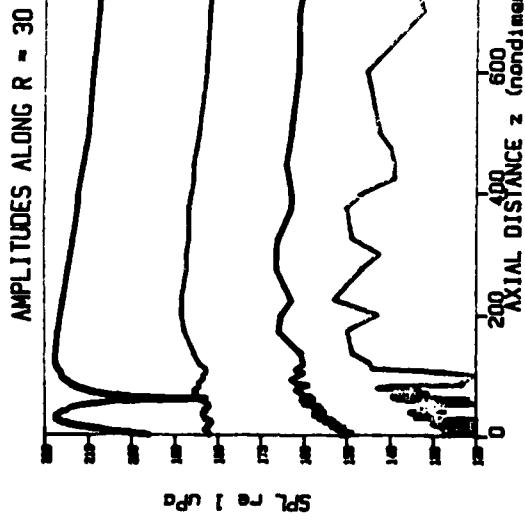

AMPLITUDES ALONG R = 0

PHASE LAG ALONG R = 0, HARMONIC # 3

PHASE LAG ALONG R = 0, HARMONIC # 2
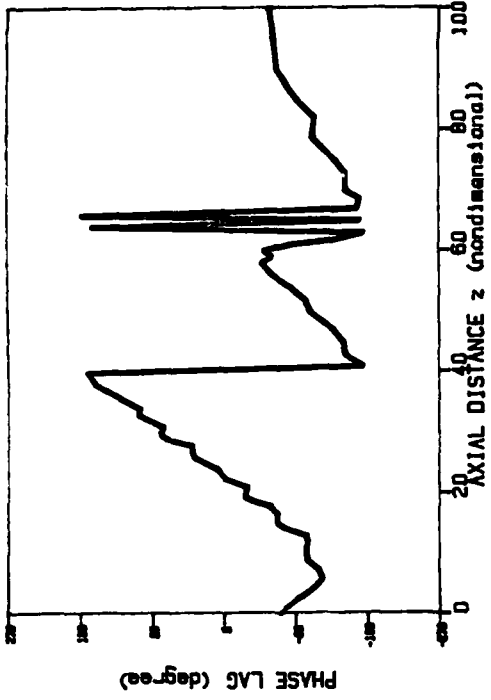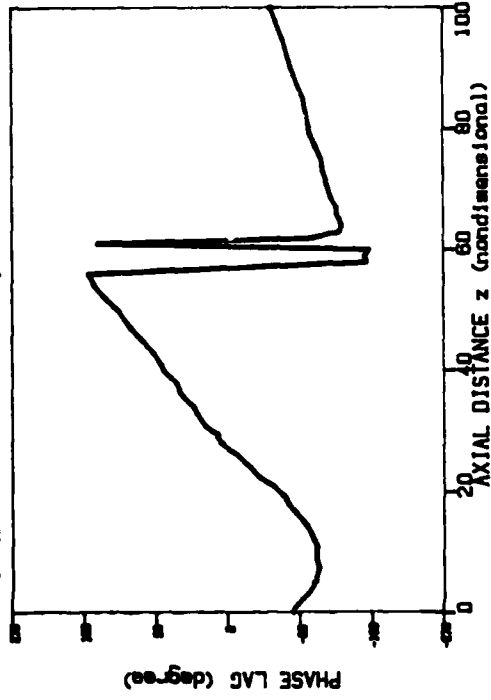
PHASE LAG ALONG R = 0, HARMONIC # 4

ON-AXIS PHASE LAG NEAR A NULL, HARMONIC # 3

ON-AXIS PHASE LAG NEAR A NULL, HARMONIC # 4
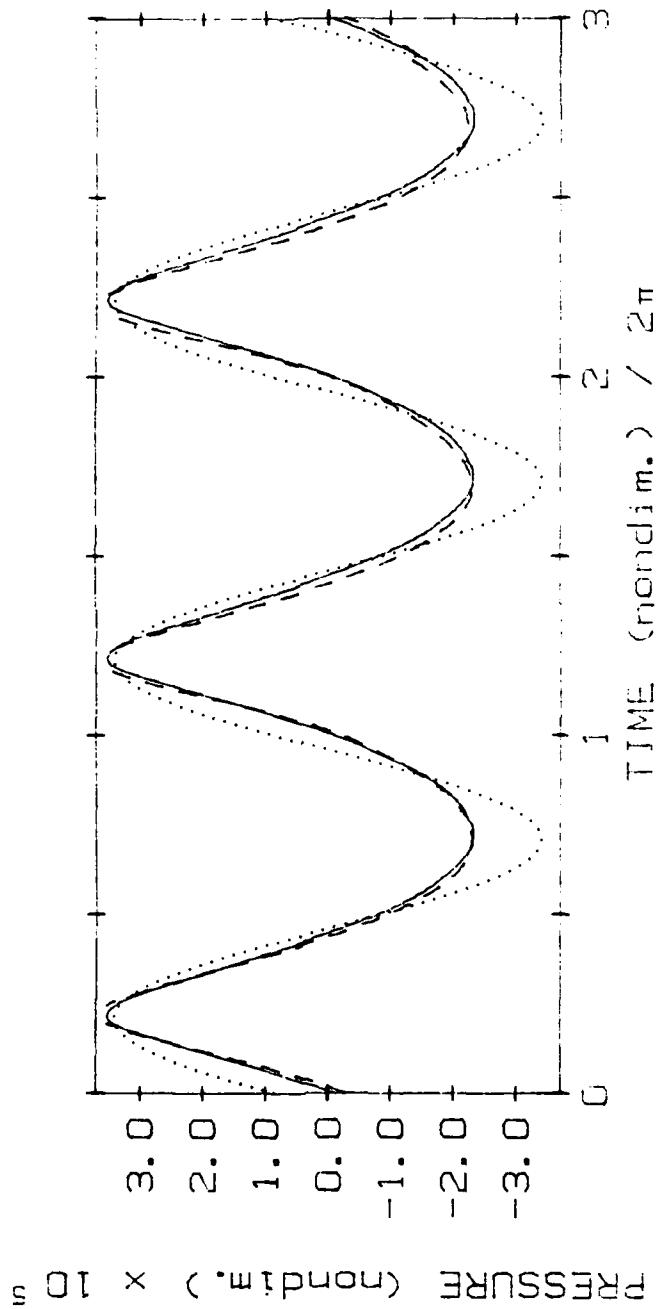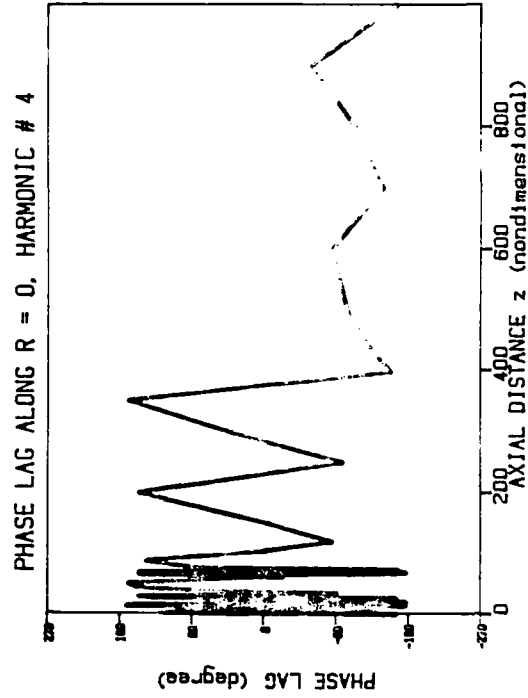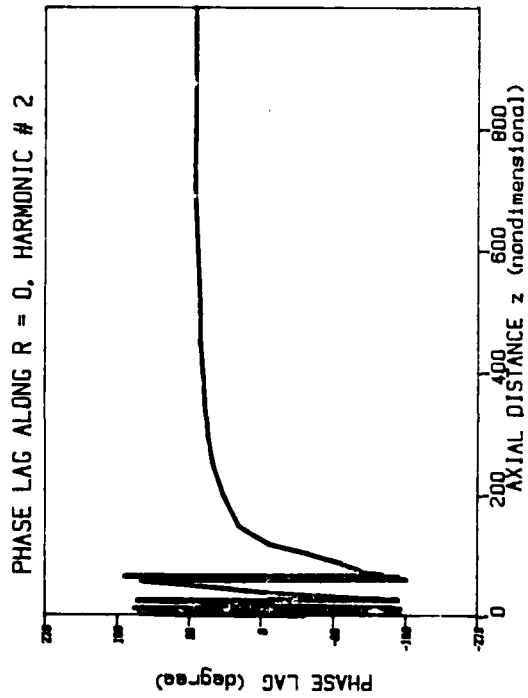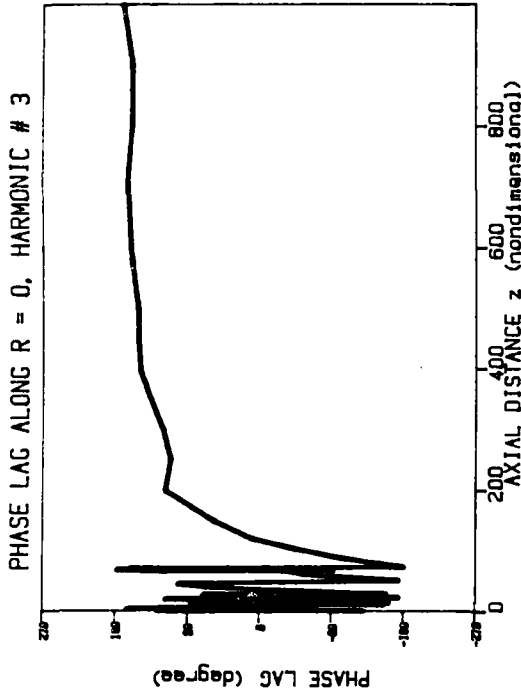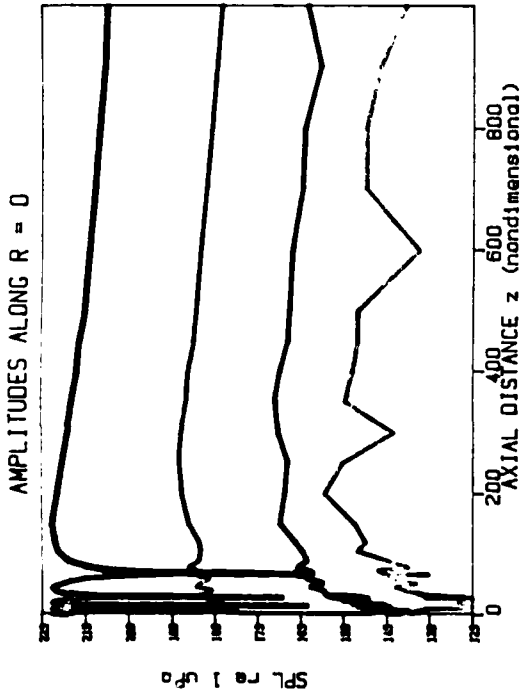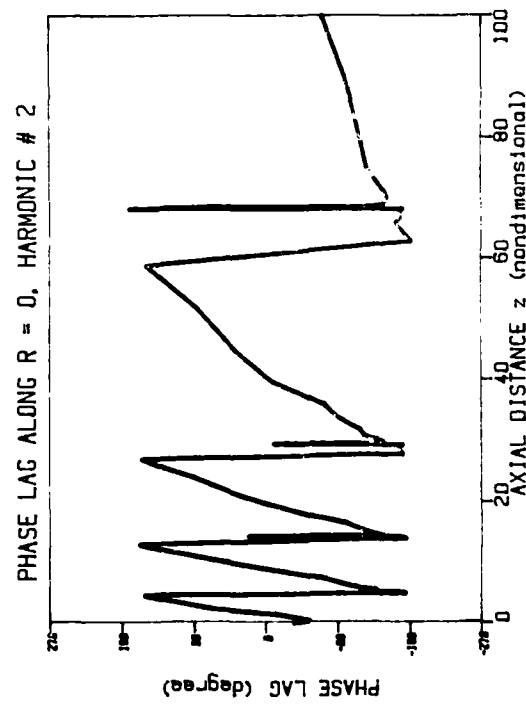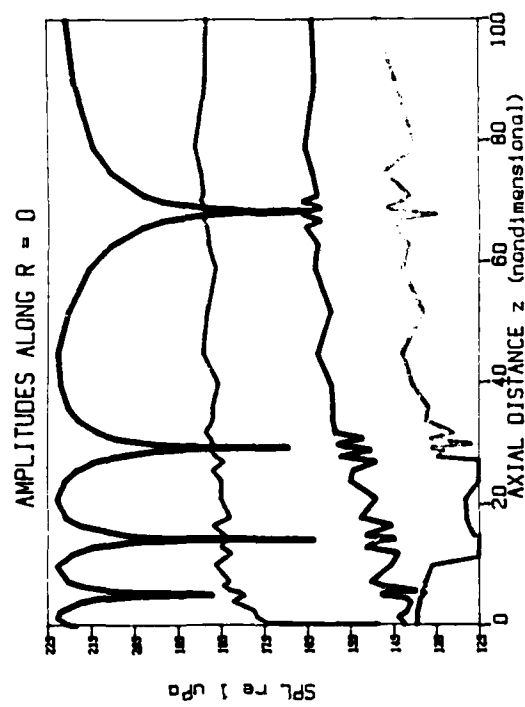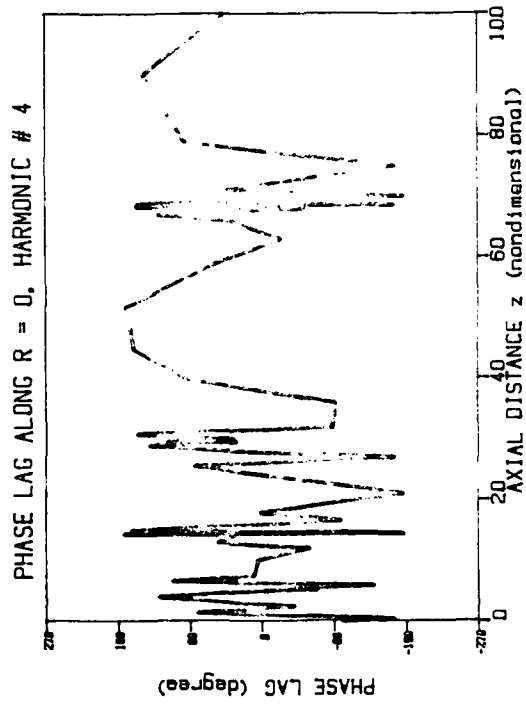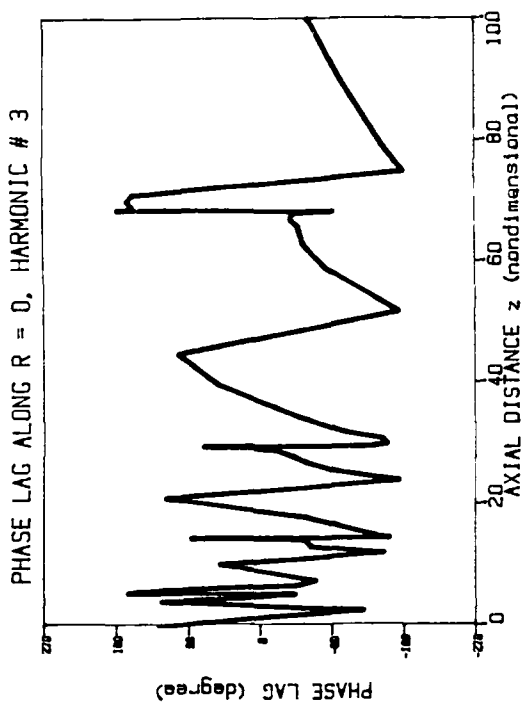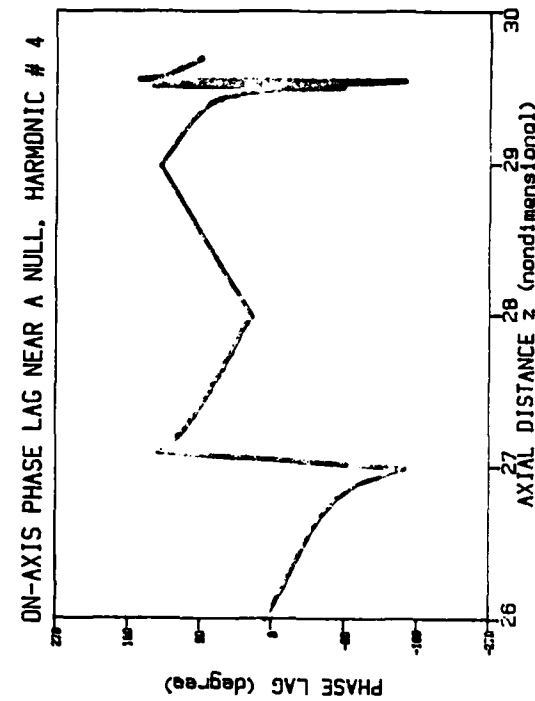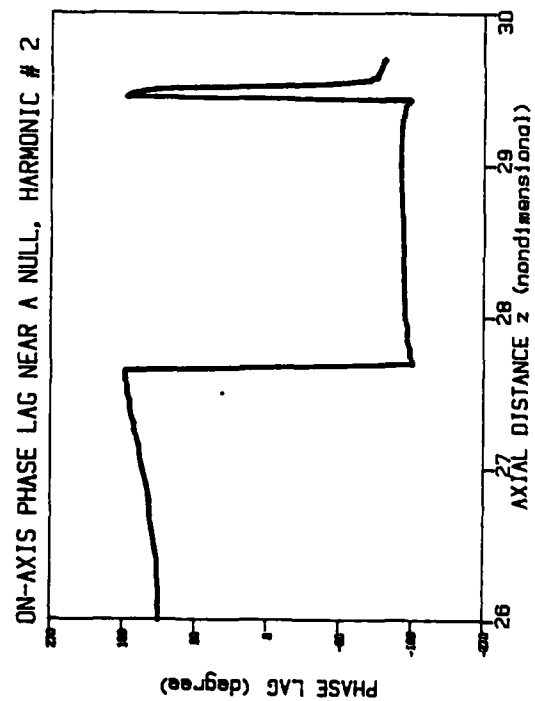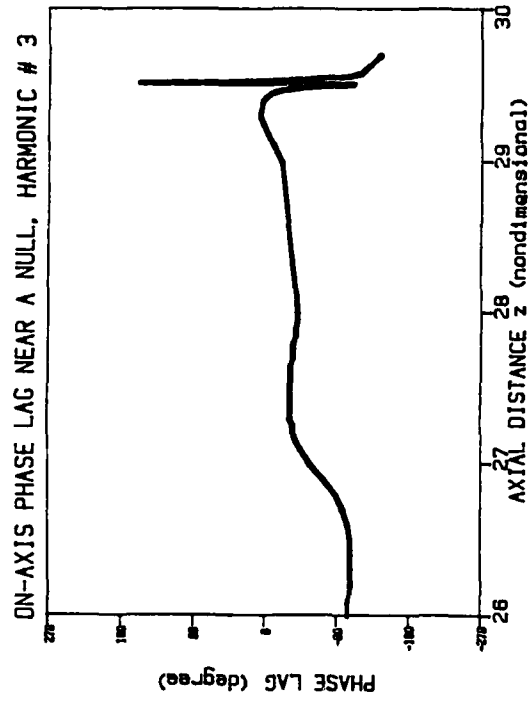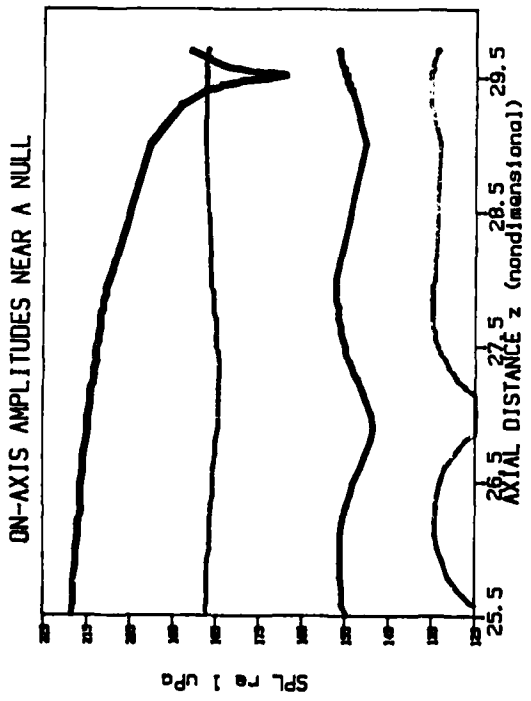
ON-AXIS AMPLITUDES NEAR A NULL

ON-AXIS PHASE LAG NEAR A NULL, HARMONIC # 2
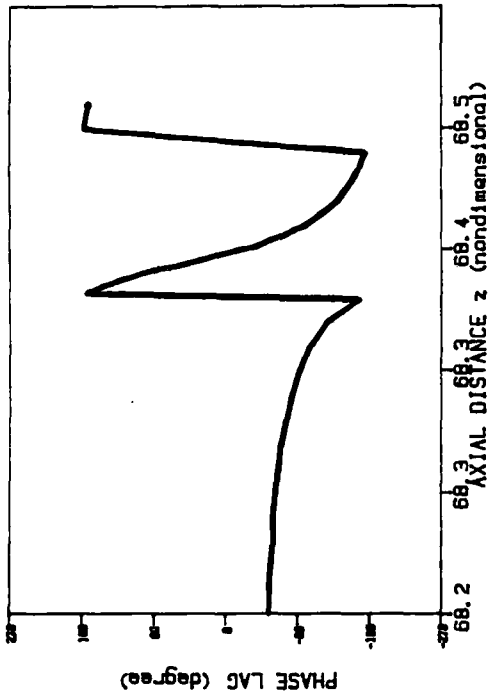
PHASE LAG ALONG R = 10, HARMONIC # 3

AXIAL DISTANCE z (nondimensional)

PHASE LAG (degree)

PHASE LAG ALONG R = 10, HARMONIC # 4

AXIAL DISTANCE z (nondimensional)

PHASE LAG (degree)

AMPLITUDES ALONG R = 10

AXIAL DISTANCE z (nondimensional)

SPL re 1 uPa

PHASE LAG ALONG R = 10, HARMONIC # 2

AXIAL DISTANCE z (nondimensional)

PHASE LAG (degree)
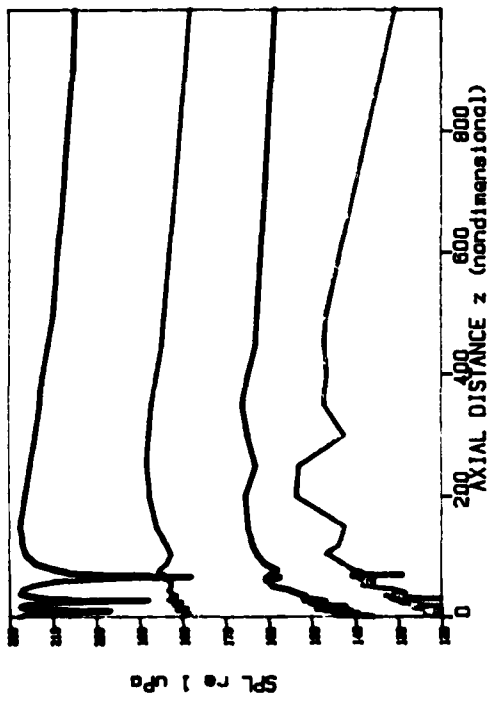
PHASE LAG ALONG R = 10, HARMONIC # 3
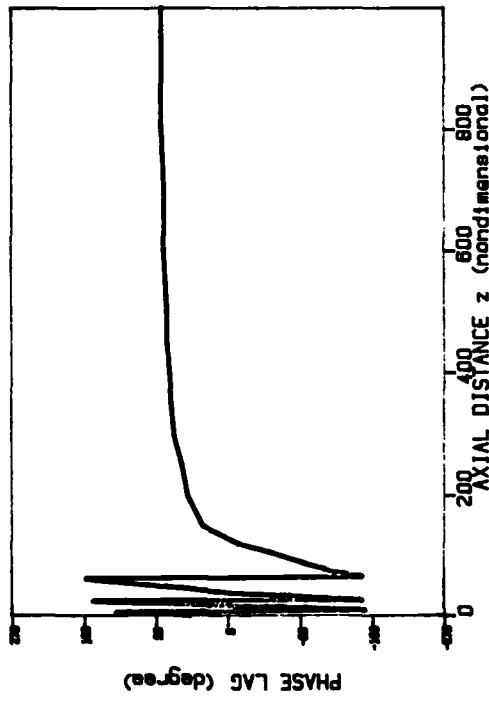
PHASE LAG ALONG R = 10, HARMONIC # 4
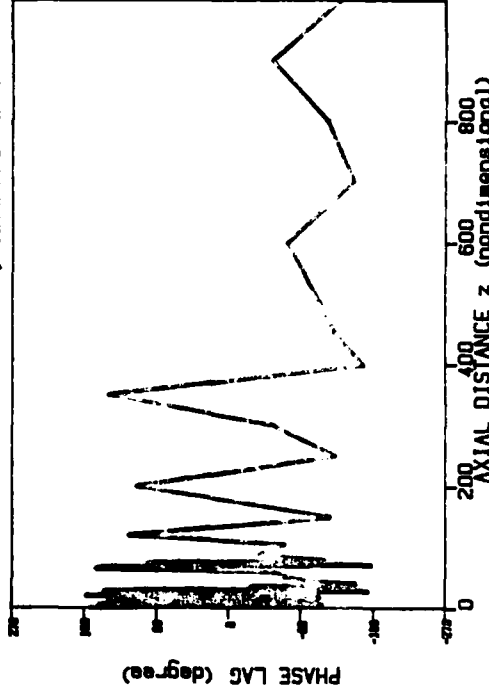
AMPLITUDES ALONG R = 10
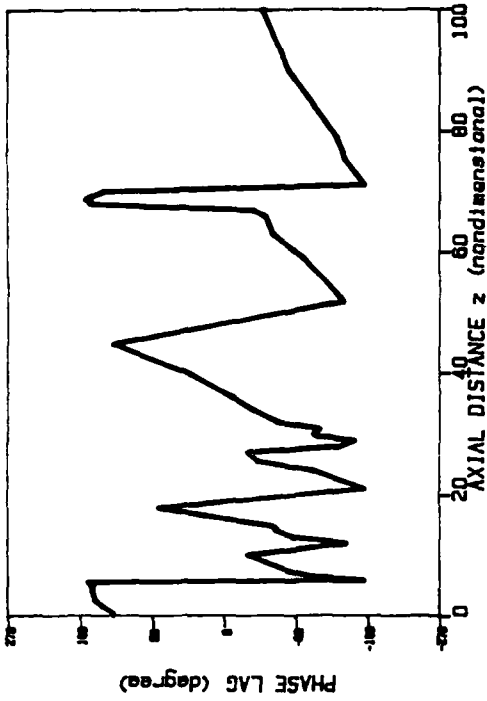
PHASE LAG ALONG R = 10, HARMONIC # 2

PHASE LAG ALONG R = 20, HARMONIC # 3
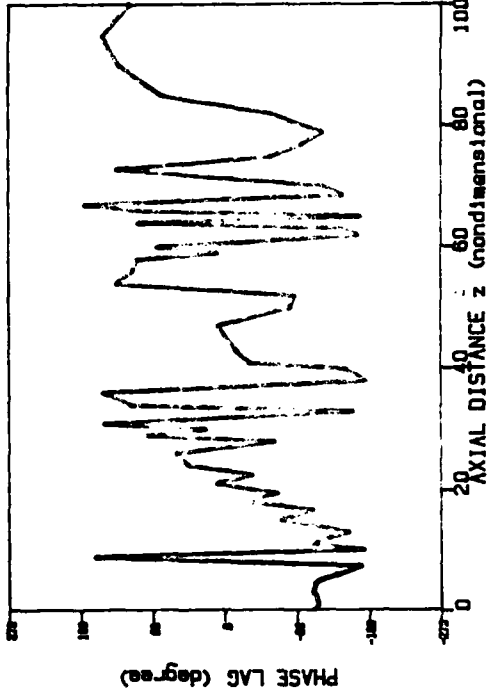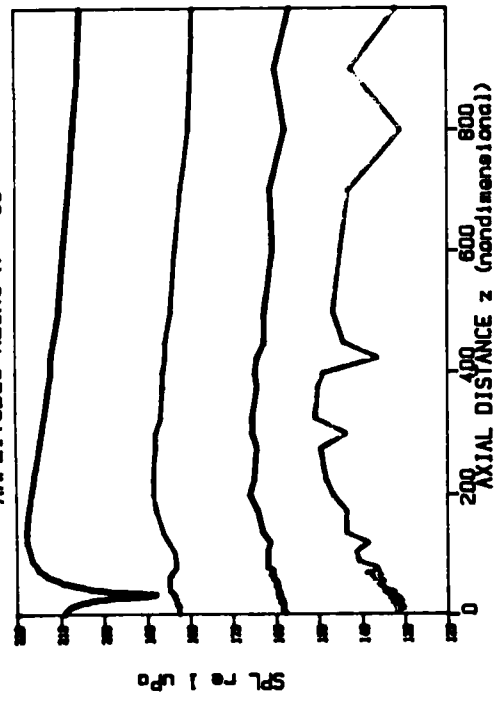
AMPLITUDES ALONG R = 20
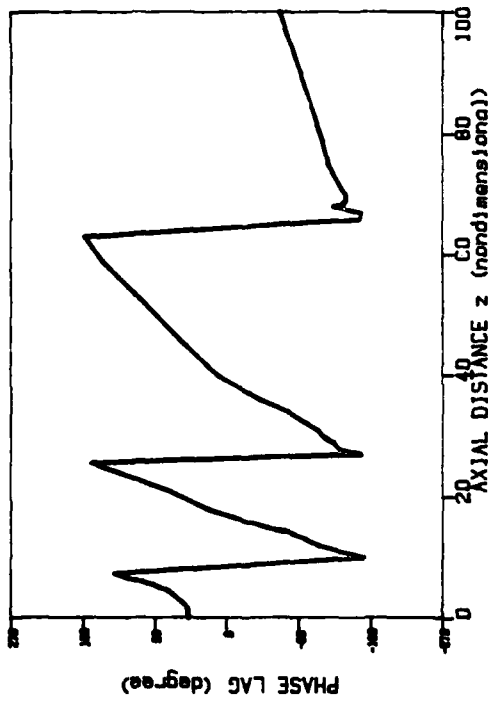
PHASE LAG ALONG R = 20, HARMONIC # 4
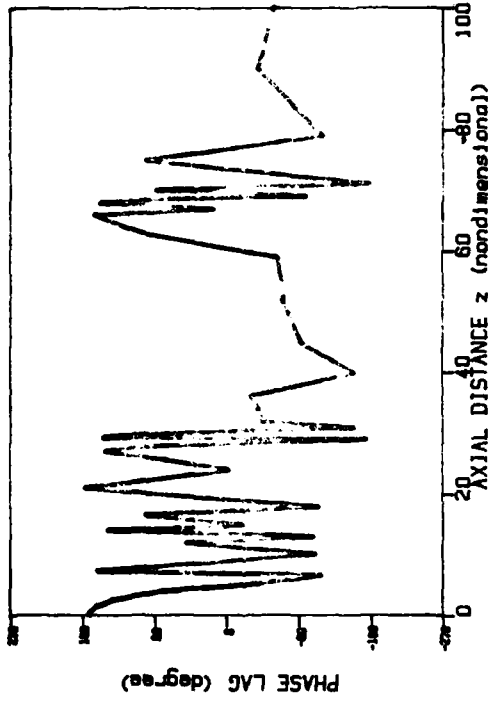
PHASE LAG ALONG R = 20, HARMONIC # 2
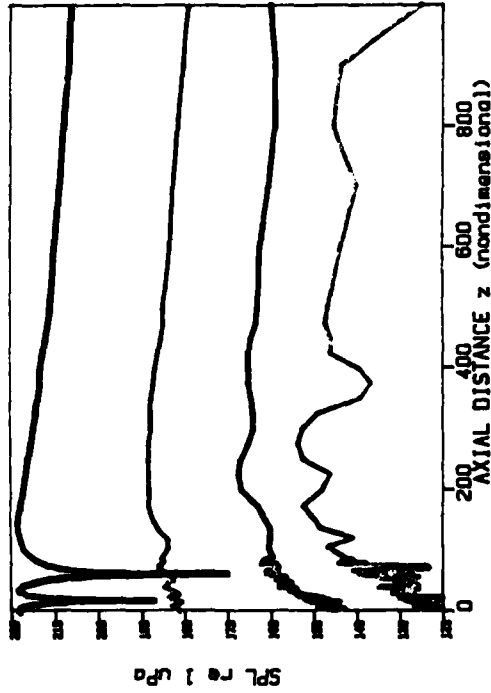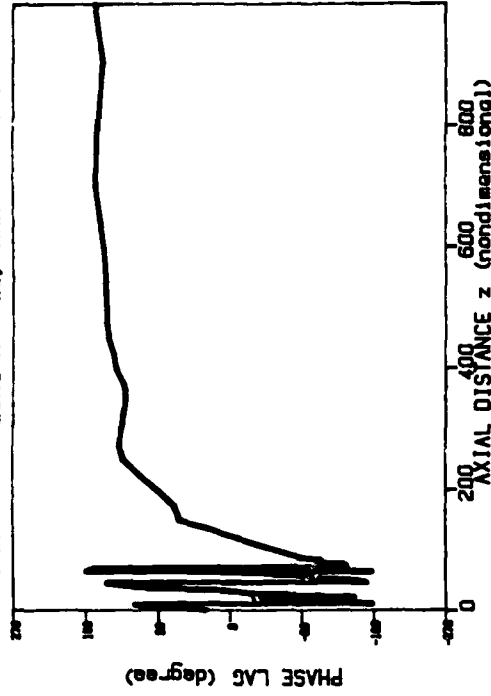
PHASE LAG ALONG R = 20, HARMONIC # 3
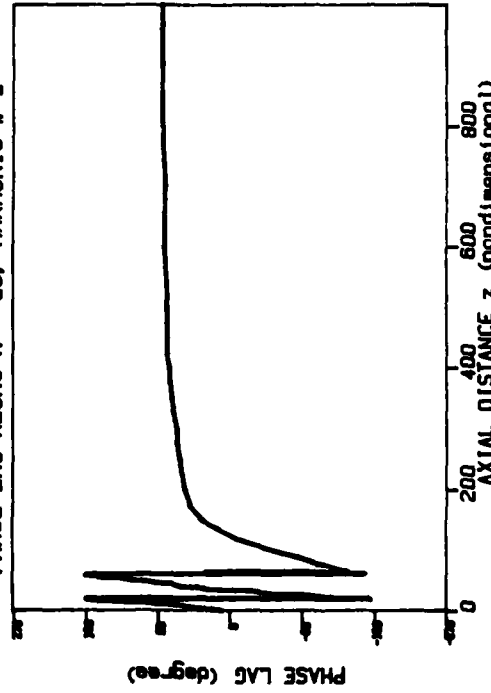
PHASE LAG ALONG R = 20, HARMONIC # 4
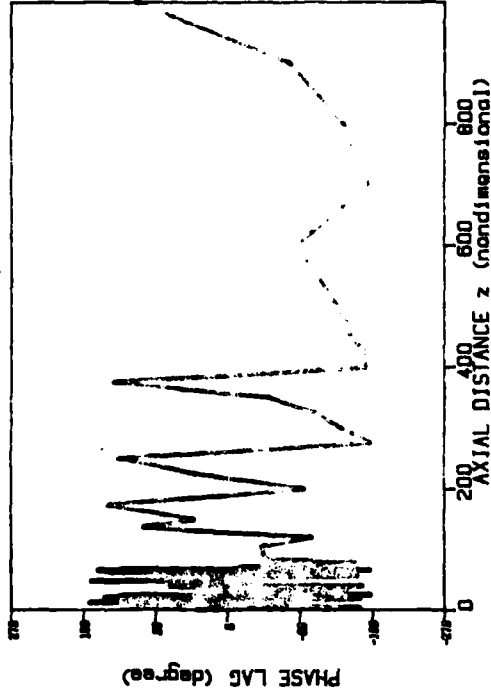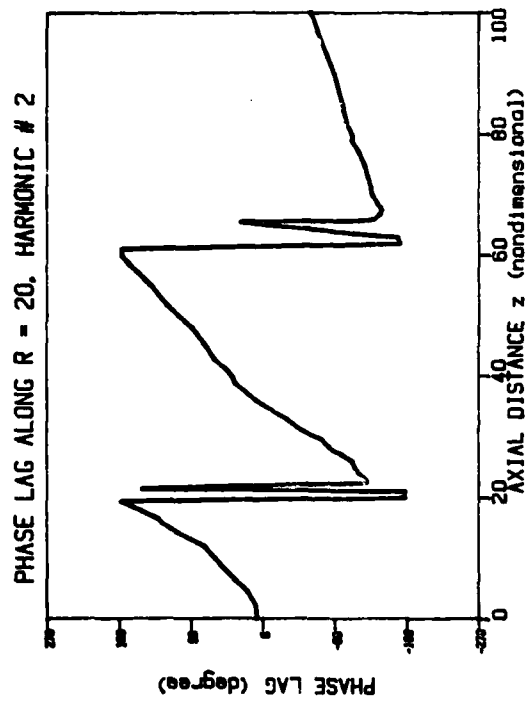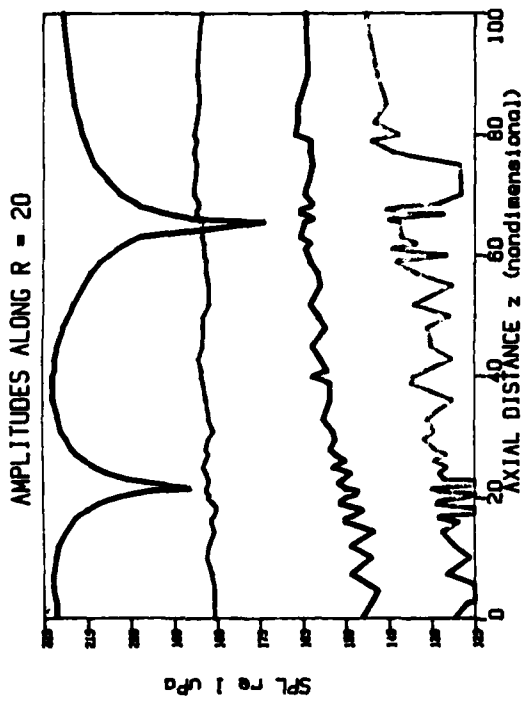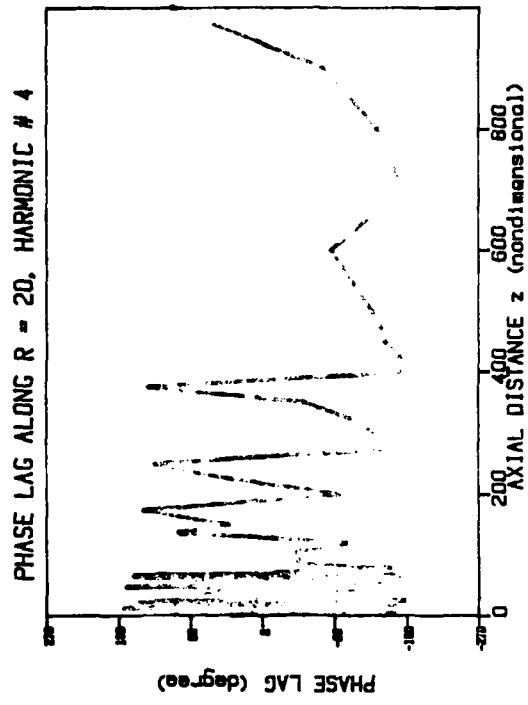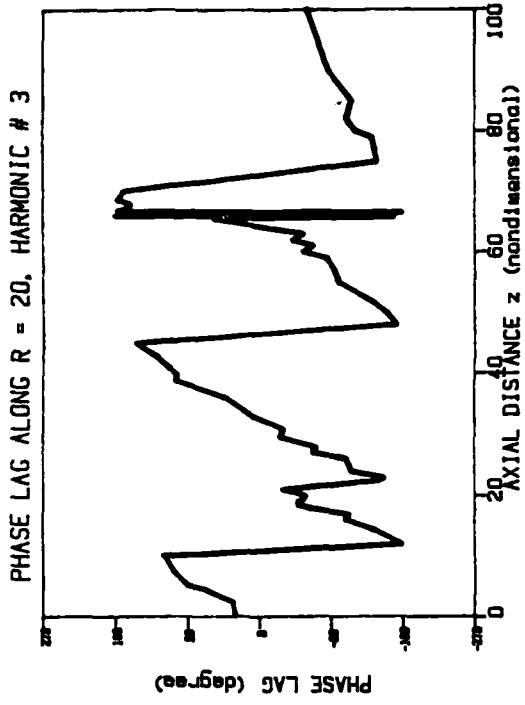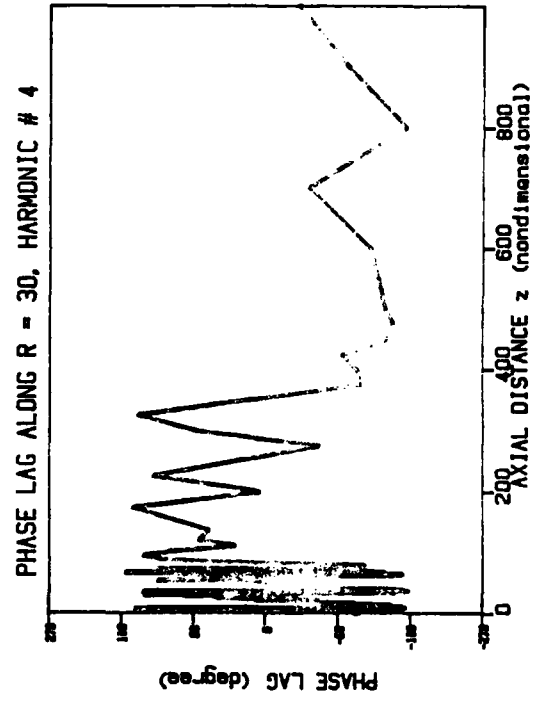
AMPLITUDES ALONG R = 20
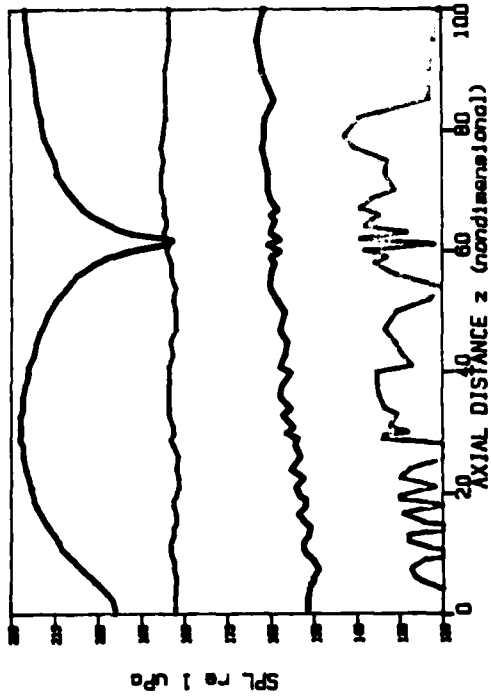
PHASE LAG ALONG R = 20, HARMONIC # 2

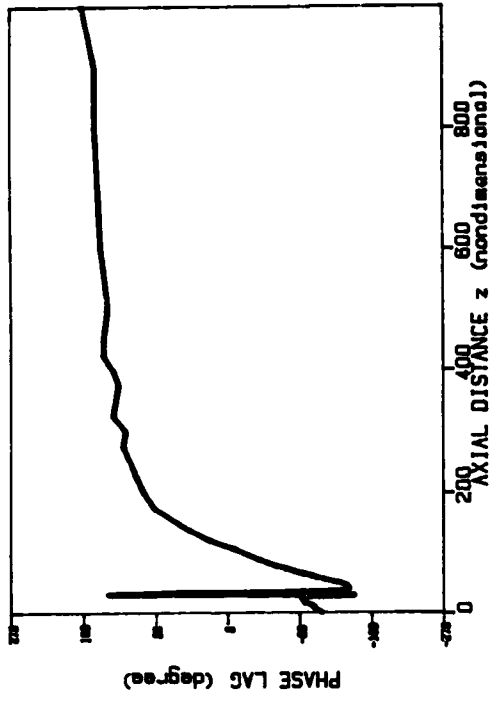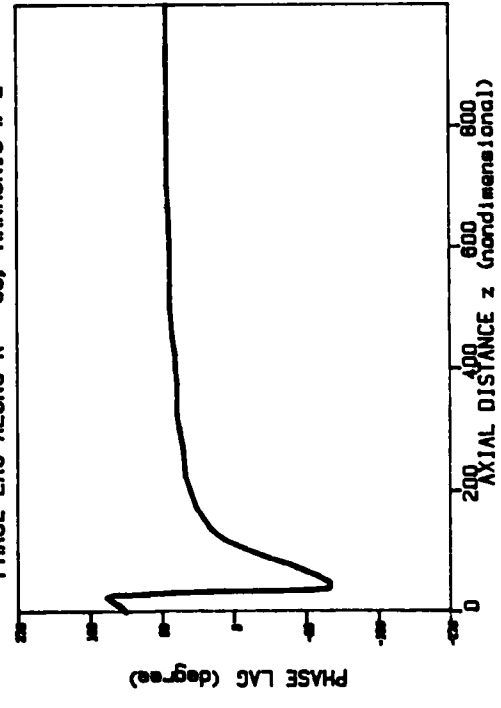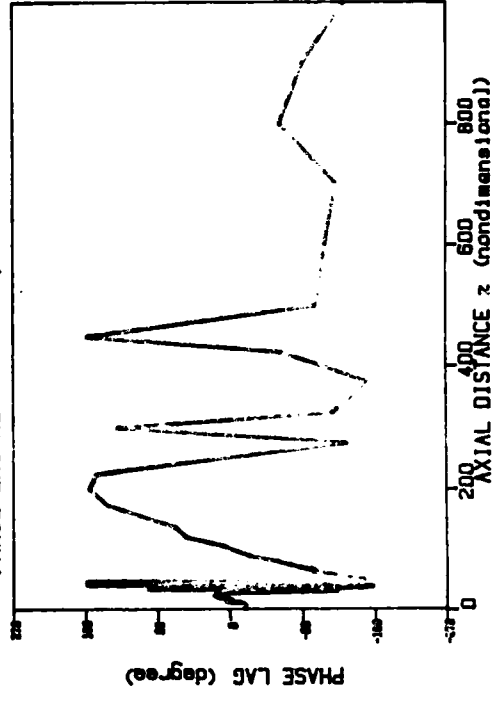PHASE LAG ALONG R = 60, HARMONIC # 3

PHASE LAG ALONG R = 60, HARMONIC # 4
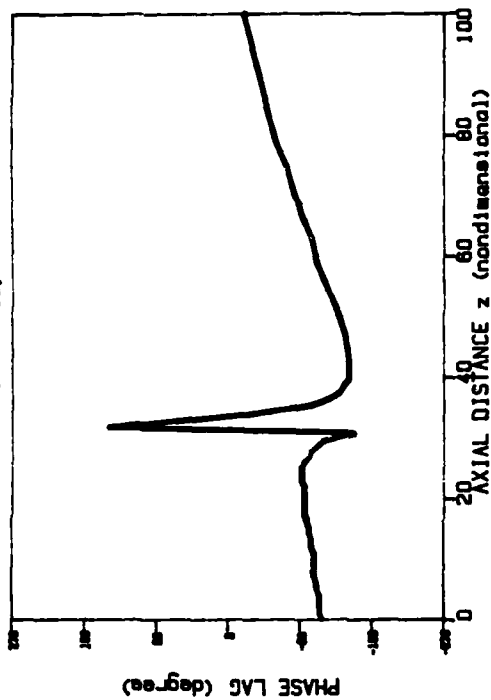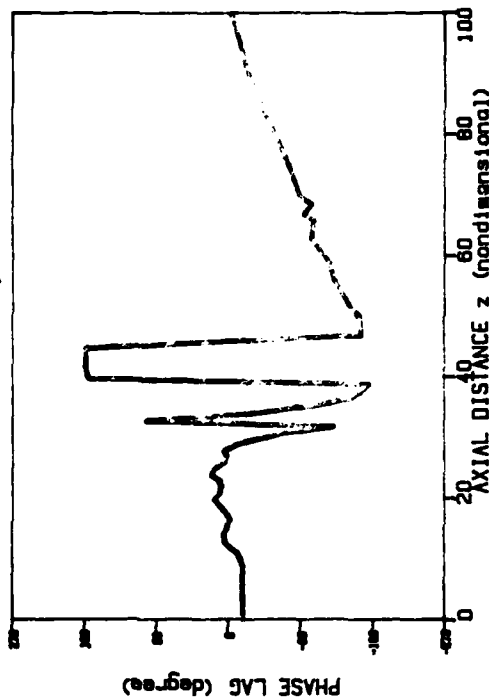
AMPLITUDES ALONG R = 60
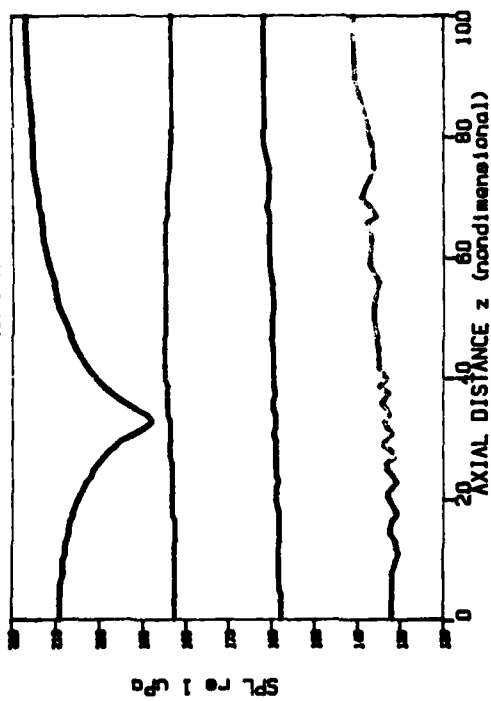
PHASE LAG ALONG R = 60, HARMONIC # 2
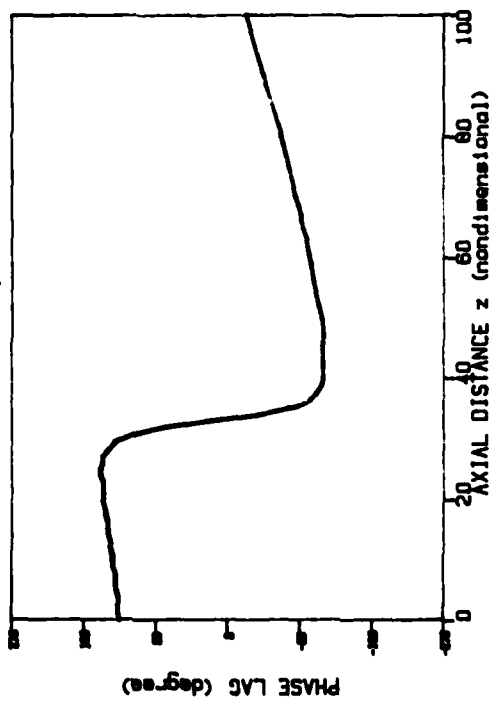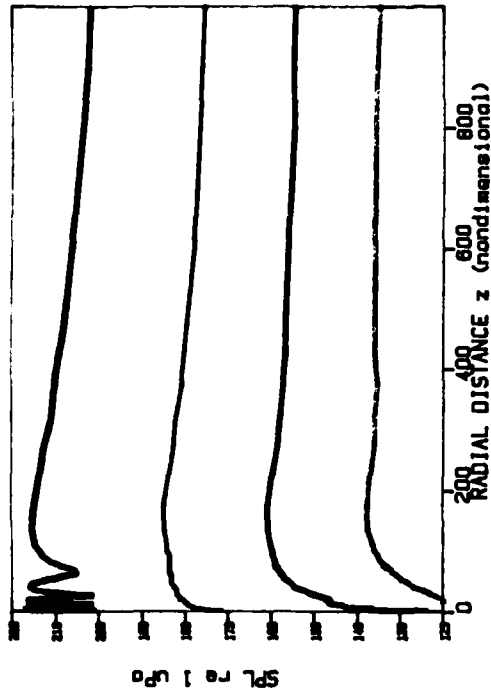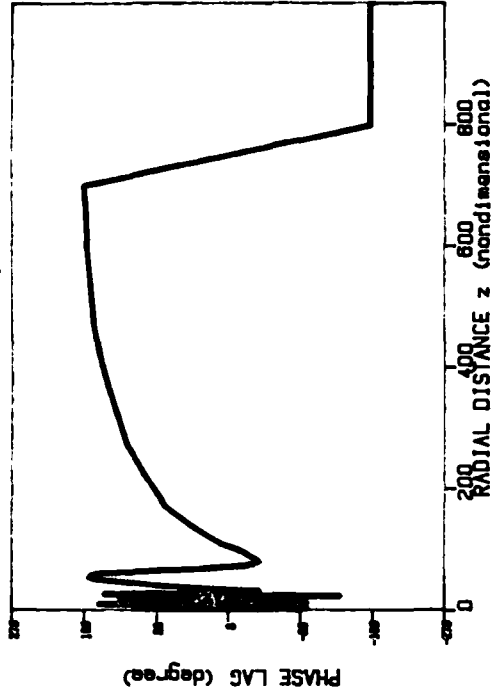
PHASE LAG ALONG θ = 3 , HARMONIC # 3
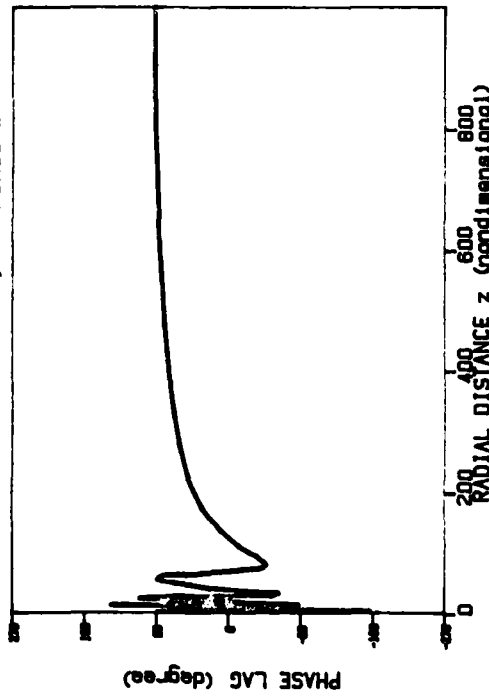
PHASE LAG ALONG θ = 3 , HARMONIC # 4
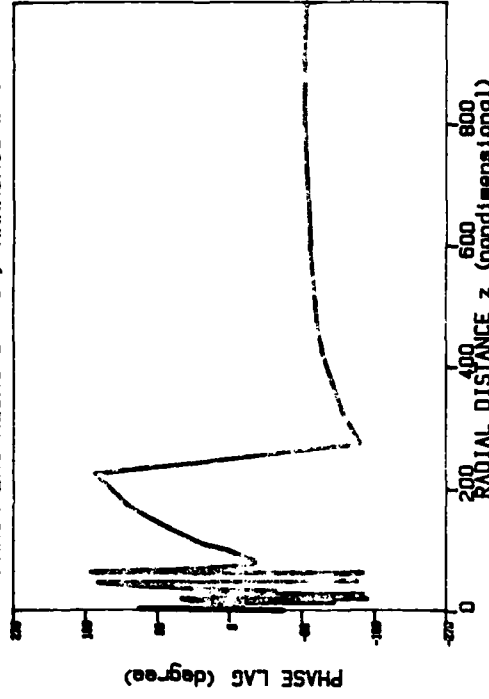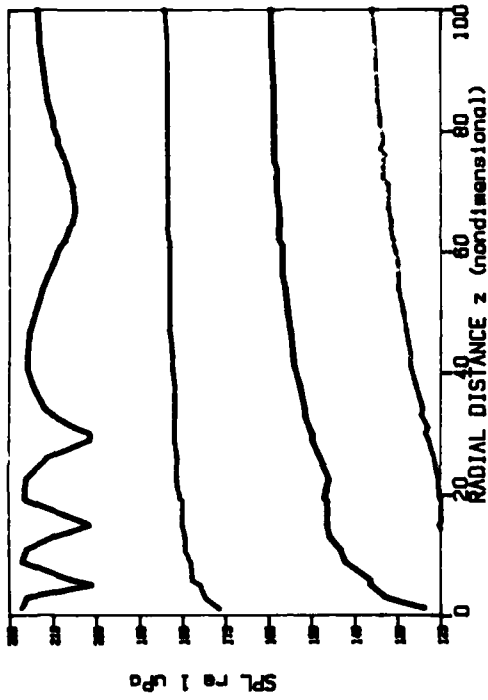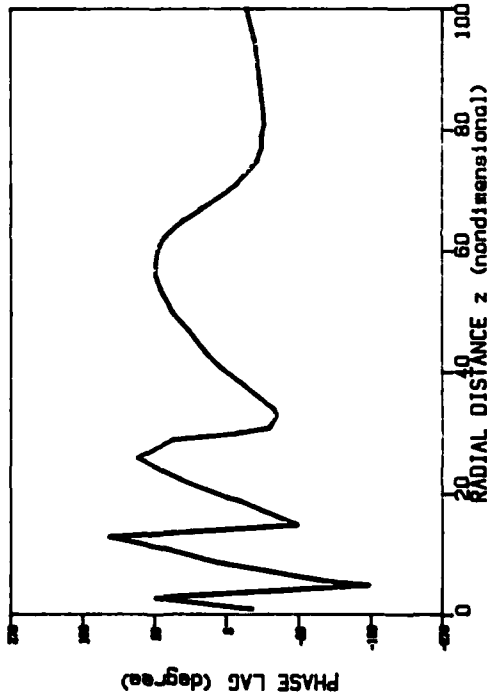
AMPLITUDES ALONG θ = 3

PHASE LAG ALONG θ = 3 , HARMONIC # 2

LINEAR MAX RMS PRESSURE ON-AXIS = 236.500 DB.   k * a = 30.0000

RADIAL DISTANCE = 600.   THETA = 0

TIME (nondim.) / 2π

PRESSURE (nondim.) × 10⁴

LINEAR MAX RMS PRESSURE ON-AXIS = 236.500 DB. k * a = 30.0000
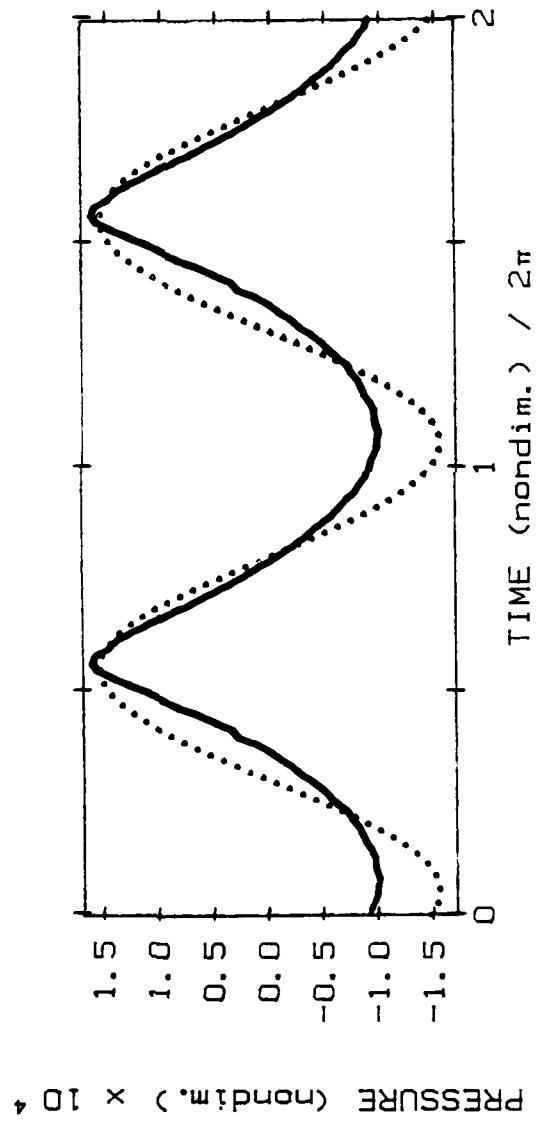
RADIAL DISTANCE = 600. THETA = 3

LINEAR MAX RMS PRESSURE ON-AXIS = 236.500 DB.   k * a = 30.0000

RADIAL DISTANCE = 602.993,   THETA = 5.711
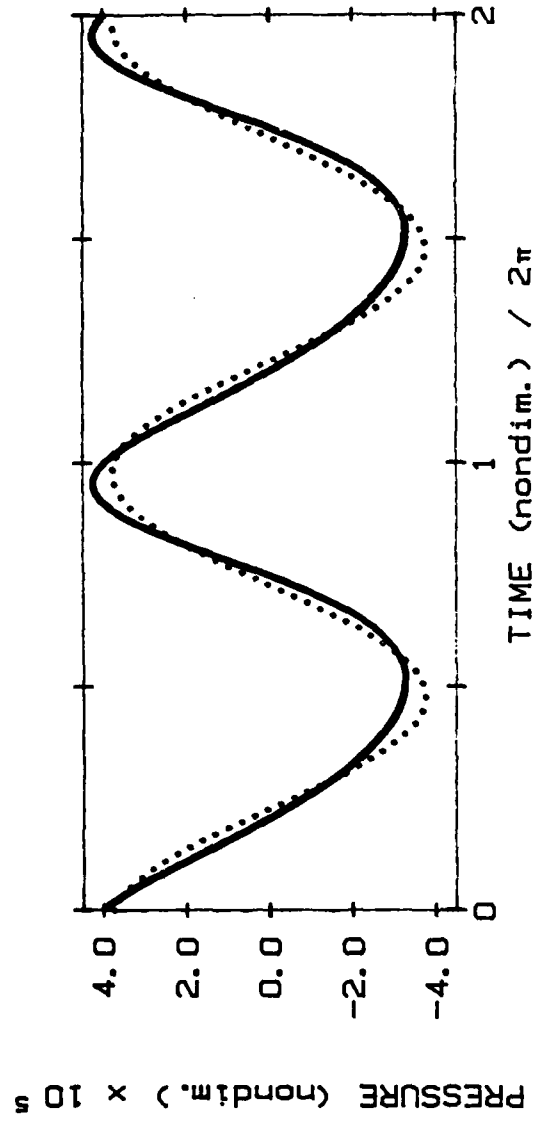
LINEAR MAX RMS PRESSURE ON-AXIS = 246.500 DB.   k * a = 30.0000

RADIAL DISTANCE = 45,   THETA = 0
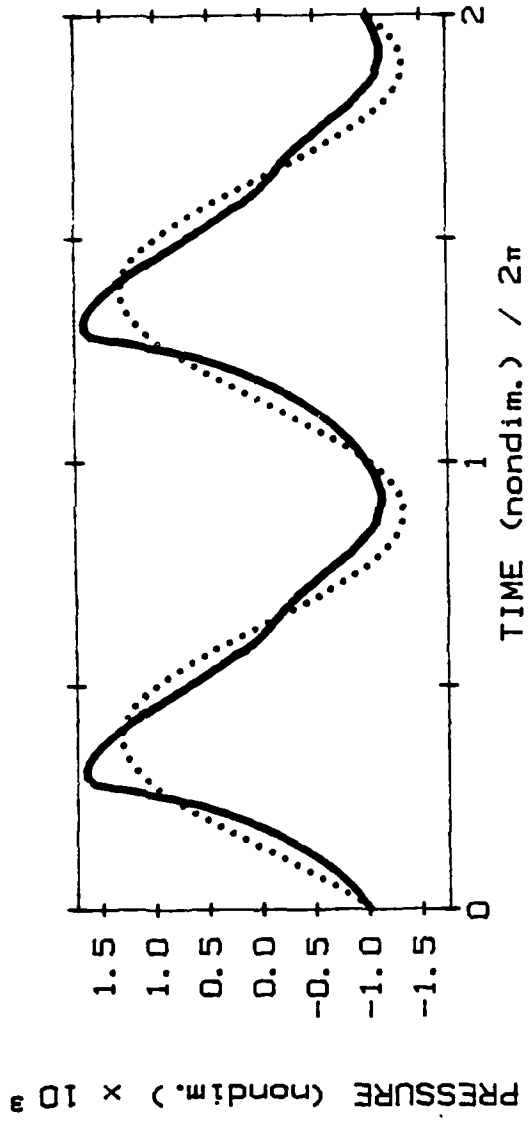
LINEAR MAX RMS PRESSURE ON-AXIS = 246.500 DB.   k * a = 30.0000

RADIAL DISTANCE = 67.082,   THETA = 63.435

LINEAR MAX RMS PRESSURE ON-AXIS = 236.500 DB.   k * a = 30.0000

RADIAL DISTANCE = 45,   THETA = 0

PRESSURE (nondim.) × 10⁴

TIME (nondim.) / 2π
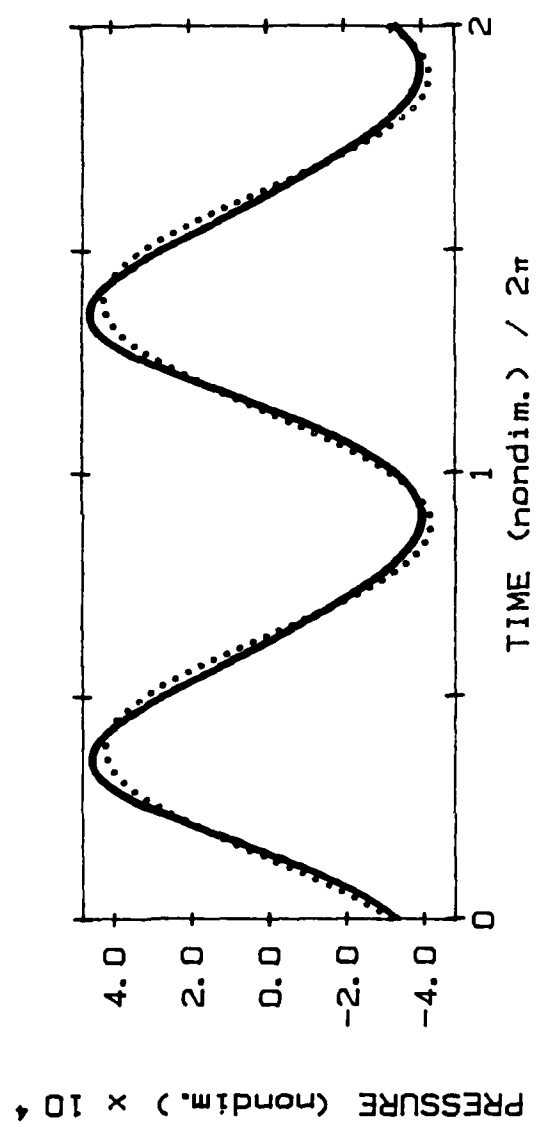
LINEAR MAX RMS PRESSURE ON-AXIS = 236.500 DB.   k * a = 30.0000

RADIAL DISTANCE = 67.082.   THETA = 63.435

THE JOURNAL
of the
Acoustical Society of America

Program of the
109th Meeting

WEDNESDAY AFTERNOON, 10 APRIL 1985

ROOM 3-122, 2:00 TO 4:48 P.M.

Session V. Physical Acoustics IV: Nonlinear Acoustics

3:36

V9. Finite amplitude distortion and dispersion in a hard-walled waveguide. J. H. Ginsberg and H. C. Miao (School of Mechanical Engineering, Georgia Institute of Technology, Atlanta, GA 30332)

The fundamental symmetric two-dimensional mode in a hard-walled rectangular waveguide is decomposed into a pair of obliquely propagating planar waves, in order to treat the effect of nonlinearity. A perturbation analysis of the nonlinear wave equation for the velocity potential identifies amplitude dispersion as one source of singularity. The only interaction between the oblique waves attributable to this effect is a change in the distance parameter affecting the magnitude of the higher harmonics. An-other singularity arises when the frequency ω or width L is large. The oblique waves are then closely aligned with the axis, resulting in resonant interaction with the true planar mode. Harmonic generation in this case has the appearance of a spatial beating pattern. A set of coordinate trans-formations make the representation uniformly valid. Analyses of limiting forms are confirmed by quantitative examples. Small values of ωL are well described by an earlier general solution in terms of groups of nondisper-sive modes [J. H. Ginsberg, J. Acoust. Soc. Am. 65, 1127–1133 (1979)], while large ωL yields a quasiplanar signal. The transition at moderate ωL is characterized by frequency, as well as amplitude, dispersion. The dis-tortion of waveforms then is very close to that obtained in the nearfield of sound beams. [Work supported by ONR.]

Joe C. Thompson Conference Center
The University of Texas at Austin
Austin, Texas
8–12 A...

THE JOURNAL

of the

Acoustical Society of America

Program of the
109th Meeting

WEDNESDAY AFTERNOON, 10 APRIL 1985 ROOM 3-122, 2:00 TO 4:48 P.M.

Session V. Physical Acoustics IV: Nonlinear Acoustics

3:36

V9. Finite amplitude distortion and dispersion in a hard-walled waveguide. J. H. Ginsberg and H. C. Miao (School of Mechanical Engineering, Georgia Institute of Technology, Atlanta, GA 30332)

The fundamental symmetric two-dimensional mode in a hard-walled rectangular waveguide is decomposed into a pair of obliquely propagating planar waves, in order to treat the effect of nonlinearity. A perturbation analysis of the nonlinear wave equation for the velocity potential identifies amplitude dispersion as one source of singularity. The only interaction between the oblique waves attributable to this effect is a change in the distance parameter affecting the magnitude of the higher harmonics. Another singularity arises when the frequency ω or width L is large. The oblique waves are then closely aligned with the axis, resulting in resonant interaction with the true planar mode. Harmonic generation in this case has the appearance of a spatial beating pattern. A set of coordinate transformations make the representation uniformly valid. Analyses of limiting forms are confirmed by quantitative examples. Small values of ωL are well described by an earlier general solution in terms of groups of nondispersive modes [J. H. Ginsberg, J. Acoust. Soc. Am. 65, 1127–1133 (1979)], while large ωL yields a quasiplanar signal. The transition at moderate ωL is characterized by frequency, as well as amplitude, dispersion. The distortion of waveforms then is very close to that obtained in the nearfield of sound beams. [Work supported by ONR.]

Joe C. Thompson Conference Center
The University of Texas at Austin
Austin, Texas
8–12 April 1985

FINITE AMPLITUDE DISTORTION AND
DISPERSION OF THE FUNDAMENTAL SYMMETRIC
MODE IN A WAVEGUIDE

JERRY H. GINSBERG
HSU-CHIANG MIAO

SCHOOL OF MECHANICAL ENGINEERING
GEORGIA INSTITUTE OF TECHNOLOGY

HARD-WALLED WAVEGUIDE

Excite fundamental symmetric mode:
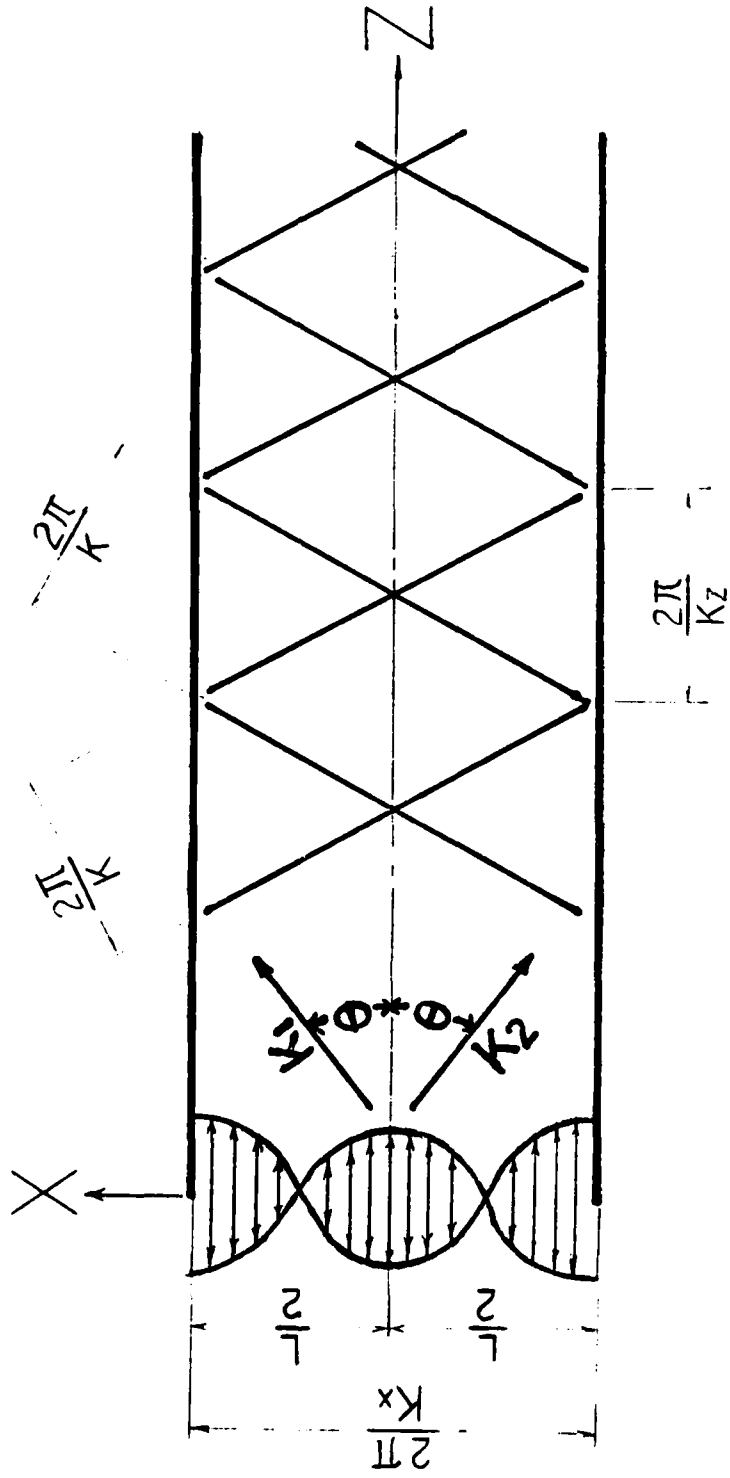
LINEAR SOLUTION

Solve wave equation.

Boundary conditions at wall .

Match pressure input at z = 0.

Radiation condition: propagation in positive z
   frequency above cutoff ==>L > 2 /k

Standing wave in x direction = superposition of
   two planar waves

IMPLICATIONS

1. Waveform is monochromatic.
2. Sinusoidal variation in transverse direction.
3. Constant pressure along any axial line.

FINITE AMPLITUDE EFFECTS

Nonlinear wave equation:

$$C_o^2 \nabla^2 \phi_2 - \frac{\partial^2 \phi_2}{\partial t^2} = \text{quadratic source terms}$$

$$= \begin{cases} 2 \text{ nd harmonic of wave 1} \\ 2 \text{ nd harmonic of wave 2} \\ \underline{\text{sum of wave 1 and wave 2}} \end{cases}$$

No dispersion $\Rightarrow$ 2 nd harmonics resonate

ANOMOLY

Ginsberg 1976, 1979
Nayfeh & Kelly 1978, 1979
Kluwick 1980

Very large L == $k_x \longrightarrow 0$ ==> 2nd harmonics
only give 1/2 the distortion in a true
planar wave.

Explanation:

Sum wave ==> $\frac{1}{K_x^2}$

Singular as $k_x \longrightarrow 0$

Beating response:

Planar driven term: wavelength = $\frac{2\pi}{K_z}$

Planar eigenmode : wavelength = $\frac{2\pi}{K}$

$k_z \longrightarrow k$ as $k_x \longrightarrow 0$

VARIATION OF PARAMETERS

$$\phi_2 = B_1(Z)EXP[2i(\omega t - K_zZ - K_xX)]$$
$$+ B_2(Z)EXP[2i(\omega t - K_zZ + K_xX)]$$
$$+ B_3(Z)EXP[2i(\omega t - K_zZ)]$$

NOTE: B_i depend on z only because:
1. Periodic in time.
2. Hard wall condition on $x = \pm L/2$

Result:

B_1 and B_2 : particular solution only.

B_3 : particular solution $\sim 1/k_x^2$
complementary solution $\Rightarrow$ planar eigenmode

1. 2 nd harmonic $\sim z$ for all k
2. Sum signal is bounded if $k_x = O(1)$,
   but $\sim z$ for $k_x \rightarrow 0$
3. Planar limit now satisfied.

RENORMALIZATION

Evaluate P.

Identify cumulative growth terms.

Change independent variables $\implies$ $K_x X$, $K_z Z$

   coordinate straining

Propagation distance parameters:

  Wave 1: $k_x x + k_z z \implies \alpha_1$

  Wave 2: $- k_x x + k_z z \implies \alpha_2$

  Sum wave: $\alpha_1 + \alpha_2 \, , \; \alpha_1 - \alpha_2$

Result:

$$\frac{P}{\rho_o C_o^2} = \frac{\epsilon}{2}[SIN(\omega t - \alpha_1) + SIN(\omega t - \alpha_2)]$$

$$K_z Z + K_x X - \alpha_1 \sim \begin{cases} \epsilon Z \, SIN(\omega t - \alpha_j) \quad \text{AND} \\ \epsilon(\frac{K^2}{K_z^2} - 2) \, COS[\omega t - \alpha_1 + \nu(\alpha_1 + \alpha_2)] \end{cases}$$

Similar transformation for $- k_x x + k_z z - \alpha_2$

TRENDS

Large kL : $k_x \longrightarrow 0$ $\Rightarrow$ quasiplanar wave

$$\frac{P}{\rho_0 c_0^2} = \mathcal{E} \, \sin(\omega t - k_z z + \beta_0 k_z z \, p) \, \cos(k_x x)$$

Small kL : $k_x = O(1)$ $\Rightarrow$ quasi-independent waves

$$P = P_1 + P_2 \; ; \qquad \frac{P_j}{\rho_0 c_0} = \frac{\epsilon}{2} \, \text{SIN}(\omega t - \alpha_j)$$

$$K_z \pm K_x = \alpha_j + \beta_c \frac{K^2}{K_z} Z P_j$$

Alternate form: standing wave in x direction

Transition: intermediate kL

$N_1 = z / \sigma$ significance of sawtooth distortion

$N_2 = \dfrac{\pi/((k-k_2)}{Z}$ intermodulation of excited and natural modes

N_1 / N_2 measure of which effect predominates

Legend (appearing in figure):
— Interacting waves
– – Independent wave approx.
- - - - Quasi-planar approx.
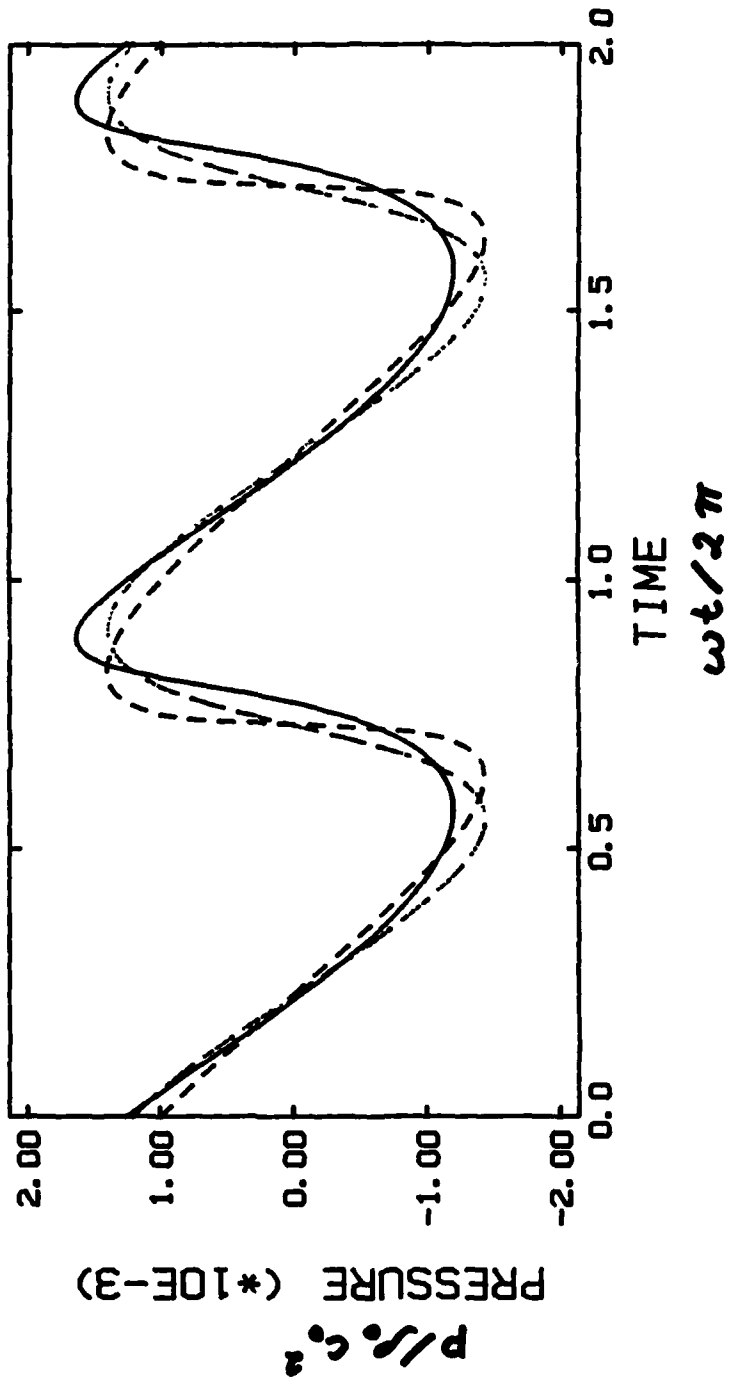
Axes:
TIME $\omega t / 2\pi$
PRESSURE (*10E-3) $p/\rho_o c_o^2$

Finite Amplitude Distortion and Dispersion
of a Symmetric Mode in a Waveguide

Jerry H. Ginsberg

Hsu-Chiang Miao

School of Mechanical Engineering

Georgia Institute of Technology

Atlanta, GA 30332

Abstract

The perturbation method of renormalization is used to study the effect of nonlinearity in a hard-walled waveguide. The excitation would induce only the fundamental symmetric mode if the system was linear. The analysis develops a solution that satisfies a nonlinear wave equation for the velocity potential, as well as all boundary conditions. The response consists of a pair of oblique planar waves that interact through second order excitation of the true planar mode.

The investigation discloses that when the transverse width is much larger than the axial wavelength, the signal has a quasi-planar behavior. In contrast, when the axial wavelength is large, the oblique waves are essentially independent. The distortion is then a result of self-refraction, in which the particle motion shifts the wavefronts and rays. The transition between the long and the short wavelength approximations is marked by the appearance of nonlinear frequency dispersion which produces asymmetrical distortion of the waveform.

(

1. INTRODUCTION

Finite amplitude effects in a waveguide feature multidimensional phenomena involving interacting waves. In linear theory a mode in a hardwalled waveguide may be constructed from pairs of oblique planar waves that are reflected from the walls. The present study will employ the same type of decomposition to show that distortion resulting from nonlinearity displays a phenomenological change as the excitation frequency is increased. This transition is associated with an anomaly contained in previous studies, which only considered the low frequency case.

Initial explorations of finite amplitude nonplanar modes in waveguides employed the perturbation method of multiple scales in a rudimentary fashion that considered selected aspects of wave interaction [1-3]. A different method of vestigation was developed to study waves radiating from a flat plate [4-9]. To a certain extent the latter studies were academic in nature. The system they treated *featured a periodically supported* plate of infinite extent. They assumed periodicity of the signal parallel to the plate, which meant that energy was propagating inward from infinite boundaries. This apparent violation of the uniqueness condition nevertheless proved to be instructive, because the system could be studied by a variety of analytical techniques. The perturbation methods of multiple scales and of renormalization, and the method of characteristics mutually agreed for the case of a spatially sinusoidal excitation. One significant aspect of their result was the prediction of self-refraction, in which the wavefronts and rays of constant phase are distorted by the particle velocity.

Although the plate problem did not treat a physically realizable system, the relevance of these investigations to waveguides was recognized in a subsequent investigation [10]. The basis of that work was that there are

nodal lines in the plate system along which the velocity component parallel to the surface of the plate vanishes. Such lines are perpendicular to the plate, as they are in linear theory. This observation led to the conclusion that the infinite plate analyses had actually derived a single mode in a waveguide.

The treatment of general excitation in a waveguide performed in Reference [10], which was a straightforward extension of the method of renormalization, disclosed a type of superposition principle. Modes having identical phase speed were found to form distinct groups whose distortion in self-refraction was a consequence of only the particle velocity arising from that group. The overall response consisted of a linear combination of the response in each group.

A similar analysis had been used to study waves radiating from cylinders [11-14]. One of those studies [12] identified a paradox associated with very long axial wavelengths. One would expect that if the wavelength along the axis of a cylinder is large, so that the rate of variation in that direction is very gradual, then the response would approach that for the case of a two-dimensional system, in which the axial wavelength is actually infinite. This was found to be the case, except that the distortion phenomena in the limit were found to be too weak by a factor of one half. This dilemma was resolved by noting that distinct modes in the case of axial variation coalesce only when the wavelength is actually infinite.

These observations also apply to the investigation of waveguides [10]. For example, as the width of a waveguide is increased, the earlier analysis predicts that the distortion of the planar mode will be twice as strong as that of the fundamental symmetric (2,0) mode. Although the explanation of coalescing effects for infinite transverse wavelength (i.e., the planar mode) is plausible, it nevertheless is unsettling from a physical viewpoint.

Distortion arises from higher harmonic sources that are generated by nonlinearity in the entire acoustic field. Could it be that minor discrepancies between the long and infinite wavelength cases accumulate to create the discrepancy? Lack of experimental data prevented an earlier response to this question, but discussions with researchers currently involved in such activity [15] sparked the present authors' interest in exploring these concerns.

The analysis presented herein treats an excitation of only the (2,0) mode in a hard-walled waveguide. It will be shown that this mode excites the planar mode in an insignificant fashion, unless $\omega L/c_0 \gg 2\pi$, where L is the transverse width, ω is the (circular) frequency, and c_0 is the linear speed of sound. The phase speed of the (2,0) mode then differs slightly from that of the planar mode. This sets up a spatial beating phenomenon that leads to a smooth transition to the planar mode response in the manner one would expect. The analysis will confirm the earlier theory for waveguides when $\omega L/c_0$ is not large. It will also show that the transition from the earlier theory to the short wavelength case is marked by frequency dispersion, in which the waveforms are remarkably similar to those observed in the nearfield of intense beams of sound [16].

2. FORMULATION

A pressure excitation of the fundamental, symmetric, two-dimensional mode in a hard-walled waveguide may be written as

$$p\big|_{z=0} = \epsilon\rho_0 c_0^2 \sin(\omega t)\cos(k_x x), \quad \epsilon \ll 1, \ -L/2 < x < L/2 \qquad (1)$$

where ρ_0 is the ambient pressure, c_0 is the speed of sound at ambient

conditions, and the transverse wave number k_x is related to the duct width L by

$$k_x = 2\pi/L \tag{2}$$

The question to be addressed here is the effect of nonlinearity associated with the finiteness of ε on the waves that propagate in the positive z direction as a result of this excitation.

The equations of continuity, momentum, and state may be combined to form a single nonlinear wave equation governing the velocity potential [17] under isentropic conditions.

$$c_0^2 \nabla^2 \phi - \frac{\partial^2 \phi}{\partial t^2} = \frac{\partial}{\partial t} \left[\frac{1}{c_0^2} (\beta_0 - 1) \left(\frac{\partial \phi}{\partial t} \right)^2 + \nabla\phi \cdot \nabla\phi \right] + 0(\phi^3) \tag{3}$$

where the nonlinearity coefficient β_0 is the constant associated with the second order term in a polynomial expansion of the pressure perturbation p as a function of the density perturbation ρ at fixed entropy.

$$p/(\rho_0 c_0^2) = \rho/\rho_0 + (\beta_0 - 1) (\rho/\rho_0^2) + \cdots \tag{4}$$

The pressure is related to the potential by

$$\int_0^p \frac{dp}{(\rho_0 + \rho)} + \frac{\partial \phi}{\partial t} + \frac{1}{2} \nabla\phi \cdot \nabla\phi = 0 \tag{5}$$

From equations (4) and (5) p, ρ and ϕ have the same order of magnitude, so elimination of ρ from these relations yields

$$p = -\rho_0 \left[\frac{\partial \phi}{\partial t} + \frac{1}{2} \nabla \phi \cdot \nabla \phi - \frac{1}{2c_0^2} \left(\frac{\partial \phi}{\partial t} \right)^2 \right] + O(\phi^3) \tag{6}$$

The boundary conditions for ϕ are obtained by making the particle velocity normal to the walls vanish,

$$\frac{\partial \phi}{\partial x} = 0 \quad \text{at} \quad x = \pm \frac{L}{2} \tag{7}$$

as well as by matching Eq. (6) at $z = 0$ to Eq. (1). Also, for uniqueness, it is required that the signal consist of a wave propagating in the positive z direction.

The initial stage of the solution technique employs a regular perturbation expansion of the potential in terms of the small parameter ϵ,

$$\phi = \epsilon \, \phi_1 + \epsilon^2 \phi_2 + \tag{8}$$

Matching like powers of ϵ in the differential equation and boundary conditions leads to a sequence of equations in the usual manner. The order ϵ terms are

$$c_0^2 \, \nabla^2 \phi_1 - \frac{\partial^2 \phi_1}{\partial t^2} = 0 \tag{9a}$$

$$\frac{\partial \phi_1}{\partial x} \bigg|_{x = \pm L/2} = 0 \tag{9b}$$

$$\frac{\partial \phi_1}{\partial t}\Bigg|_{z=0} = i \frac{c_o^2}{4} \{ \exp [i(\omega t - k_x x)] $$

$$+ \exp [i(\omega t + k_x x)] \} + CC \qquad (9c)$$

where CC in general shall denote the complex conjugate of all preceding terms. The order ϵ^2 perturbation equations are

$$c_o^2 \nabla^2 \phi_2 - \frac{\partial^2 \phi_2}{\partial t^2} = \frac{\partial}{\partial t} \left[\frac{1}{c_o^2} (\beta_o - 1) \left(\frac{\partial \phi_1}{\partial t} \right)^2 + \nabla \phi_1 \cdot \nabla \phi_1 \right] \qquad (10a)$$

$$\frac{\partial \phi_2}{\partial x}\Bigg|_{x = \pm L/2} = 0 \qquad (10b)$$

$$\frac{\partial \phi_2}{\partial t}\Bigg|_{z=0} = \left[\frac{1}{c_o^2} \left(\frac{\partial \phi_1}{\partial t} \right)^2 - \frac{1}{2} \nabla \phi_1 \cdot \nabla \phi_1 \right]\Bigg|_{z=0} \qquad (10c)$$

3. EVALUATION OF THE POTENTIAL

It is a straightforward matter to solve Eqs. (9) by separation of variables, with the result that

$$\phi_1 = \frac{c_o^2}{4\omega} \{ \exp [i(\omega t - k_x x - k_z z)] $$

$$+ \exp [i(\omega t + k_x x - k_z z)] \} + CC \qquad (11)$$

where

$$k = \omega/c_o , \quad \theta = \sin^{-1} (k_x/k), \quad k_z = k \cos \theta \equiv (k^2 - k_x^2)^{1/2} \qquad (12)$$

Only the case of propagating, rather than evanescent, waves is of interest, which means that $k_x < k$. This condition is obtained whenever ω exceeds the cutoff frequency for the fundamental mode, $\omega > 2\pi c_0/L$.

Equation (11) represents the first order solution as two trains of planar waves propagating symmetrically relative to the centerline $x = 0$. These waves are depicted in Figure 1, where e_1 and e_2 are the individual directions. The angle θ measures the direction in which these waves propagate relative to the centerline. Each wave represents the reflection of the other from the rigid walls. Increasing either the frequency ω or width L decreases θ. In the limit $\theta \to 0$, the two trains of waves merge into the planar mode.

The first step in deriving ϕ_2 is to use Eq. (11) to form the inhomogeneous terms in Eq. (10a). This yields

$$
c_0^2 \, \nabla^2 \phi_2 - \frac{\partial^2 \phi_2}{\partial t^2}
$$

$$
= -\frac{i}{8} c_0^2 \omega \, \beta_0 \, \{ \exp [2i(\omega t - k_x x - k_z z)]
$$

$$
+ \exp [2i (\omega t + k_x x - k_z z)] \}
$$

$$
- \frac{i}{4} c_0^2 \omega (\beta_0 - 2 \frac{k_x^2}{k^2}) \exp [2i(\omega t - k_z z)] \quad + CC \tag{13}
$$

The first two exponentials in Eq. (13) excite second harmonics. Such signals propagate parallel to the two waves forming ϕ_1, which are homogeneous solutions of the linearized wave equation. The corresponding particular solution may be obtained by the method of variation of parameters, in which the amplitude of the homogeneous solution is considered to be an unknown

function. The last inhomogeneous term is a planar second harmonic. Such an excitation matches the planar mode for the waveguide when $k_z = k$. Hence, decreasing k_x brings the planar part of the excitation into close coincidence with the planar mode for that frequency, which means that this excitation is nearly resonant at small k_x. The method of variation of parameters will also yield the solution associated with this term. Thus, let

$$\phi_2 = u(x,z) \exp (2i\omega t) + CC$$

$$u = C(z) \{\exp [- 2i (k_z z + k_x x)] + \exp [-2i (k_z z - k_x x)]\}$$

$$+ D(z) \exp (-2i k_z z) \tag{14}$$

It should be noted that the unknown functions C and D depend on the axial distance only. The periodic nature of the excitation eliminates dependence of these functions on t. Similarly, the rigid wall conditions, Eq. (10b), imposed along $x = \pm \pi/k_x$, could not be satisfied if C or D were functions of x.

The result of requiring that Eq. (14) satisfy Eq. (13) is a set of uncoupled differential equations for the amplitude functions. After Eq. (12) for k_z is applied, these equations are found to be

$$C'' - 4 i k_z C' = - \frac{1}{8} i\beta_0 \omega \tag{15}$$

$$D'' - 4i k_z D' + 4k_x^2 D = - \frac{1}{4} i\omega(\beta_0 - 2 k_x^2/k^2)$$

END
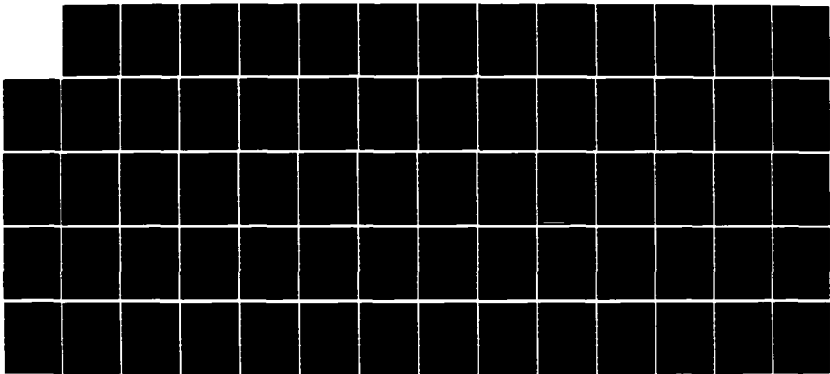
FILMED

DTIC
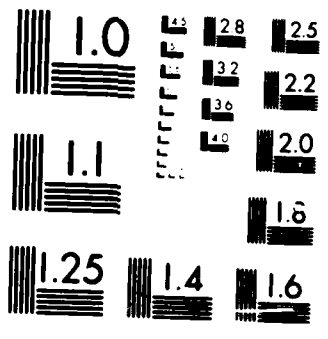
MICROCOPY RESOLUTION TEST CHART

where a prime denotes differentiation with respect to z.

The particular solutions of Eqs. (15) are readily found to be

$$C_p = \frac{\beta_o \, \omega}{32 \, k_z} \, z$$

$$D_p = - \frac{i\omega}{16} \, \left(\frac{\beta_o}{k_x^2} - \frac{2}{k^2} \right) \tag{16}$$

It is convenient to let the constant coefficients of C_p and D_p appear explicitly in the corresponding complementary solutions, which are therefore written as

$$C_c = \frac{\beta_o \omega}{32 \, k_z} \, [C_1 + C_2 \, \exp \, (4ik_z \, z)]$$

$$D_c = - \frac{i\omega}{16} \, \left(\frac{\beta_o}{k_x^2} - \frac{2}{k^2} \right) \, [D_1 \, \exp(\lambda_1 \, z)$$

$$+ \, D_2 \, \exp \, (\lambda_2 \, z)] \tag{17}$$

where λ_1 and λ_2 are roots of the characteristic equation

$$\lambda_{1,2}^2 - 4 \, ik_z \, \lambda_{1,2} + 4 \, k_x^2 = 0 \tag{18a}$$

The roots are found with the aid of Eqs. (12) to be

$$\lambda_1 = 2i(k_z - k), \quad \lambda_2 = 2i(k_z + k) \tag{18b}$$

The expressions for ϕ_2 obtained by substituting Eqs. (16) and (17) into Eqs. (14) must satisfy the radiation condition. In order for ϕ_2 to represent an out-going wave in the z-direction, it must only contain negative imaginary exponentials in the z variable. Satisfaction of this condition requires that $C_2 = D_2 = 0$. The remaining terms yield

$$u = \frac{\beta_0 \omega}{32 k_z} (z + C_1) \{ \exp [- 2i(k_z z + k_x x)]$$

$$+ \exp [-2i(k_z z - k_x x)]\}$$

$$- \frac{i\omega}{16} (\frac{\beta_0}{k_x^2} - \frac{2}{k^2}) [\exp (-2ik_z z) + D_1 \exp(-2ikz)] \qquad (19)$$

Note that C_1 describes complementary solutions of the wave equation associated with second harmonics of the oblique waves, whereas D_1 is the planar eigenmode at the second harmonic frequency.

The case $k_x \equiv 0$ corresponds to a true planar mode, which is governed by the Earnshaw solution for a nonlinear planar wave. However, letting $k_x \rightarrow 0$ in Eq. (19) results in a singularity in the coefficient of the last terms.

Such behavior resembles the case of resonance in a one-degree-of-freedom oscillator whose equation of motion is

$$\ddot{x} + \omega^2 x = F \sin \Omega t \qquad (20)$$

When $\Omega \to \omega$, the amplitude of the particular solution for $\Omega = \omega$ seems to become infinite. This ignores the presence of the complementary solution, which forms a beating response when it is added to the particular solution. In the limit $\Omega = \omega$, the resonant response reduces to a harmonic at frequency ω whose amplitude grows in proportion to t.

In the same manner the singularity of Eq. (19) at $k_x \to 0$ may be removed by an appropriate selection of the coefficient of the homogeneous solutions. The coefficient C_1 is not used for this purpose because the singularity is associated with the planar mode.

In order to study $k_x \to 0$, the troublesome terms in Eq. (19) are expanded in a Taylor series about k_x/k.

$$k_z \equiv (k^2 - k_x^2)^{1/2} = k - \frac{1}{2} \frac{k_x^2}{k} + \cdots$$

$$\exp(-ik_z z) = \exp \left[-i(k - \frac{1}{2} \frac{k_x^2}{k})z + \cdots\right]$$

$$= (1 + \frac{ik_x^2}{2k} z + \cdots) \exp(-ikz) \tag{21}$$

The corresponding asymptotic form of the planar terms in Eq. (19) is

$$-\frac{i\omega}{16} \left(\frac{\beta_0}{k_x^2} - \frac{2}{k^2}\right) [\exp(-2ik_z z) + D_1 \exp(-2ikz)]$$

$$= -\frac{i\omega}{16} \left(\frac{\beta_0}{k_x^2} - \frac{2}{k^2}\right) [1 + \frac{ik_x^2 z}{2k} + D_1] \exp(-2ikz) \tag{22}$$

The singularity for $k_x \to 0$ is cancelled if the leading term in $D_1 = -1$.

Thus let

$$D_1 = -1 + D^* \tag{23a}$$

where the coefficient D^* may depend on k_x in any manner that satisfies the condition

$$\lim_{k_x \to 0} \frac{D^*}{k_x^2} = \delta \tag{23b}$$

where δ is a bounded number. Similarly the coefficient C_1 is restricted to depend on k_x in any manner that is not singular as $k_x \to 0$.

The second order potential is now found from Eqs. (14) and (19) to be

$$\phi_2 = \frac{\beta_0 \omega}{32 k_z} (z + C_1)\exp(2i\omega t)\,[\exp(-2i\psi_1) + \exp(-2i\psi_2)]$$

$$- \frac{i\omega}{16} \left(\frac{\beta_0}{k_x^2} - \frac{2}{k^2}\right)\,\exp(2i\omega t)\,\{\exp[-i(\psi_1 + \psi_2)]$$

$$+ (-1 + D^*)\exp[-i(\psi_1 + \psi_2)k/k_z]\} + CC \tag{24}$$

where

$$\psi_1 = k_z z + k_x x$$

$$\psi_2 = k_z z - k_x x \tag{25}$$

The foregoing expression for ϕ_2 satisfies the wall conditions, Eqs. (10b). At this juncture, ϕ_2 does not satisfy the boundary condition, Eq. (10c),

which specifies that there should be no second order contribution to the pressure at $z = 0$. This condition could be satisfied by appropriate selection of the coefficients C_1 and $D*$. However, both of these describe homogeneous solutions for ϕ_2, and they are not singular as $k_x \to 0$. Thus, they represent effects that are $O(\epsilon^2)$ at all locations. In contrast, observable distortion phenomena are associated with second order terms that grow with increasing distance. Therefore, setting

$$C_1 = D* = 0 \qquad (26)$$

leads to insignificant errors. The corresponding potential function then obtained from Eqs. (8), (11), and (24) is

$$\phi = \epsilon \frac{c_0^2}{4\omega} \exp(i\omega t)[\exp(-i\psi_1) + \exp(-i\psi_2)]$$

$$+ \epsilon^2 \frac{\beta_0 \omega}{32 k_z} z \exp(2i\omega t) [\exp(-2i\psi_1) + \exp(-2i\psi_2)]$$

$$- \epsilon^2 \frac{i\omega}{16} (\frac{\beta_0}{k_x^2} - \frac{2}{k^2}) \exp(2i\omega t) \{\exp[-i(\psi_1 + \psi_2)]$$

$$- \exp[-i(\psi_1 + \psi_2)k/k_z]\} + CC + O(\epsilon^2) \qquad (27)$$

where $O(\epsilon^2)$ refers to terms having that order of magnitude at all locations.

4. EVALUATION OF THE PRESSURE

Prior formulations of nonlinear propagation using the velocity potential have generated the potential in the form of a separation of variables solution. Specifically, the expression was a product of functions of each

space variable and time. In that situation, it was necessary to consider individually the state variables of particle velocity and pressure.

The present case is different because the potential is now represented as two planar waves, each of which is described by a single propagation distance parameter. In general, proper behavior of the expression for pressure in a simple planar wave ensures comparable results for the other state variables. The pressure is related to the potential function by Eq. (6). Omission of the quadratic products in that relation ignores terms that are uniformly $0(\epsilon^2)$, which is comparable to the error in Eq. (27) for ϕ. Thus,

$$\frac{p}{\rho_0 c_0^2} = -\frac{1}{c_0^2} \frac{\partial \phi}{\partial t} + 0(\epsilon^2)$$

$$= -\frac{1}{4} \epsilon i \exp(i\omega t)[\exp(-i\psi_1) + \exp(-i\psi_2)]$$

$$-\frac{1}{16} \epsilon^2 i\beta_0 \frac{k^2}{k_z} z \exp(2i\omega t)[\exp(-2i\psi_1)$$

$$+ \exp(-2i\psi_2)] - \frac{1}{8} \epsilon^2 (\beta_0 \frac{k^2}{k_x^2} - 2) \exp(2i\omega t)$$

$$\times \{\exp[-i(\psi_1 + \psi_2)] - \exp[-i(\psi_1 + \psi_2)k/k_z]\}$$

$$+ CC + 0(\epsilon^2) \tag{28}$$

The first set of $0(\epsilon^2)$ terms grows with increasing z in all cases, and the second set grows when k_x/k is very small. Such functional behavior is a result of using z and x as position variables, neither of which consistently match the spatial scaling of the nonlinear processes. In order to ascertain the correct spatial dependence, a near-identity transformation in the form of

a coordinate straining is employed. A different transformation is introduced for each wave variable ψ_1 and ψ_2.

The presence of $O(\epsilon^2)$ terms in Eqs. (27) that depend on $\psi_1 + \psi_2$ indicates that the waves interact. Further examination of the form of Eq. (27) suggests the trial transformations

$$\psi_j = \alpha_j + \epsilon \, [F_j(\alpha_1,\alpha_2) \, \exp(i\omega t)$$

$$+ \overline{F}_j(\alpha_1,\alpha_2) \, \exp(-i\omega t)] + \ldots; \quad j = 1,2 \qquad (29)$$

where the complex conjugate term, denoted by an overbar, is introduced in order to ensure that the transformation is real. Substitution for ψ_1 and ψ_2 in Eq. (28), followed by expansion in Taylor series in powers of ϵ, yields

$$\frac{p}{\rho_0 c_0^2} = -\frac{1}{4} \epsilon i \, \exp(i\omega t)[\exp(-i\alpha_1) + \exp(-i\alpha_2)]$$

$$-\frac{1}{4} \epsilon^2 [F_1 \, \exp(2i\omega t - i\alpha_1) + \overline{F}_1 \, \exp(-i\alpha_1) \qquad (30)$$

$$+ F_2 \, \exp(2i\omega t - i\alpha_2) + \overline{F}_2 \, \exp(-i\alpha_2)]$$

$$-\frac{1}{16} \epsilon^2 \, i\beta_0 \frac{k^2}{k_z} z \, \exp(2i\omega t) \, [\exp(-2i\alpha_1)$$

$$+ \exp(-2i\alpha_2)] - \frac{1}{8} \epsilon^2 \, (\beta_0 \frac{k^2}{k_x^2} - 2) \, \exp(2i\omega t)$$

$$\times \, \{\exp[-i(\alpha_1 + \alpha_2)] - \exp[-i(\alpha_1 + \alpha_2)k/k_z]\}$$

$$+ CC + O(\epsilon^2)$$

The task now is to determine the functions F_1 and F_2 that cancel all $O(\epsilon^2)$ second harmonic terms which grow with increasing z. For this, the terms that depend on $\alpha_1 + \alpha_2$ are apportioned equally between F_1 and F_2. The appropriate choice is found to be

$$F_1 = -\frac{i\beta_0 k^2}{4 k_z} z \exp(-i\alpha_1) - \frac{1}{4} (\beta_0 \frac{k^2}{k_x^2} - 2) \{\exp(-i\alpha_2) \tag{31}$$

$$- \exp[-i\alpha_1(\frac{k}{k_z} - 1) - i\alpha_2 \frac{k}{k_z}]\}$$

$$F_2 = -\frac{i\beta_0 k^2}{4 k_z} z \exp(-i\alpha_2) - \frac{1}{4} (\beta_0 \frac{k^2}{k_x^2} - 2) \{\exp(-i\alpha_1)$$

$$- \exp[-i\alpha_2 (\frac{k}{k_z} - 1) - i\alpha_1 \frac{k}{k_z}]\}$$

These straining functions do not cancel all $O(\epsilon^2)$ terms in the pressure. The remaining terms, which are created by the complex conjugates of F_1 and F_2, contain combinations of the α_1 and α_2 variables. Their presence is not a problem, because they are independent of t. Their role is to cancel a mean value of the pressure that is created by the cordinate transformation.

It is convenient at this juncture to write the coordinate transformations and pressure resulting from Eqs. (28) - (30) in real functional form. The pressure is governed by

$$\frac{p}{\rho_0 c_0^2} = \frac{\epsilon}{2} \left[\sin(\omega t - \alpha_1) + \sin(\omega t - \alpha_2) \right]$$

$$+ \frac{1}{8} \epsilon^2 (\beta_0 \frac{k^2}{k_x^2} - 2) \{ 2 \cos(\alpha_1 - \alpha_2)$$

$$- \cos \left[2\alpha_1 - \frac{k}{k_z} (\alpha_1 + \alpha_2) \right]$$

$$- \cos \left[2\alpha_2 - \frac{k}{k_z} (\alpha_1 + \alpha_2) \right] \} \tag{32}$$

where

$$\psi_1 \equiv k_z z + k_x x$$

$$= \alpha_1 + \frac{1}{2} \epsilon \beta_0 \frac{k^2}{k_z} z \sin(\omega t - \alpha_1)$$

$$- \frac{1}{2} \epsilon (\beta_0 \frac{k^2}{k_x^2} - 2) \{ \cos(\omega t - \alpha_2)$$

$$- \cos \left[\omega t - \alpha_2 - (\frac{k}{k_z} - 1)(\alpha_1 + \alpha_2) \right] \} \tag{33a}$$

$$\psi_2 \equiv k_z z - k_x x$$

$$= \alpha_2 + \frac{1}{2} \epsilon \beta_0 \frac{k^2}{k_z} z \sin(\omega t - \alpha_2)$$

$$- \frac{1}{2} \epsilon (\beta_0 \frac{k^2}{k_x^2} - 2) \{ \cos(\omega t - \alpha_1)$$

$$- \cos \left[\omega t - \alpha_1 - (\frac{k}{k_z} - 1)(\alpha_1 + \alpha_2) \right] \} \tag{33b}$$

The foregoing relations fully define the pressure. The value of p at specified x, z, and t may be determined by solving Eqs. (33) simultaneously for the values of α_1 and α_2 , and then using those values to compute p. It will be noted that the terms in which α_1 and α_2 couple do not explicitly grow with z. However, their magnitude increases as $k_x/k \to 0$, so the spatial beating phenomena created by this interaction takes on the appearance of growth in the limit. This matter is treated in detail in the next section.

5. ASYMPTOTIC TRENDS

Equations (32) and (33) are generally valid, but examination of the behavior at limiting values of k_x/k provides important insights. For $k_x/k \ll 1$ ($\omega L/c_0 \gg 2\pi$), the coordinate transformation may be expanded in a power series in k_x/k. First, apply the identity for the cosine of a sum to the last term in Eq. (33a).

$$\psi_1 = \alpha_1 + \frac{1}{2} \epsilon\beta_0 \frac{k^2}{k_z} z \sin(\omega t - \alpha_1)$$

$$+ \epsilon(\beta_0 \frac{k^2}{k_x^2} - 2) \sin[\omega t - \alpha_2 - \frac{1}{2} (\frac{k}{k_z} - 1)(\alpha_1 + \alpha_2)]$$

$$x \sin [\frac{1}{2} (\frac{k}{k_z} - 1)(\alpha_1 + \alpha_2)] \quad (34)$$

Since $k/k_z \to 1 + k_x^2/2k^2 + \ldots$, the leading terms in a Taylor series expansion of Eqs. (33) are

$$\psi_1 \sim \alpha_1 + \frac{1}{2} \epsilon\beta_0 kz \sin(\omega t - \alpha_1) + \frac{1}{4} \epsilon\beta_0(\alpha_1 + \alpha_2)\sin(\omega t - \alpha_2) \qquad (35a)$$

When the same operations are performed on Eq. (33b), the result is

$$\psi_2 \sim \alpha_2 + \frac{1}{2} \epsilon\beta_0 kz \, \sin(\omega t - \alpha_2)$$

$$+ \frac{1}{4} \epsilon\beta_0 (\alpha_1 + \alpha_2) \, \sin(\omega t - \alpha_1) \qquad (35b)$$

According to these relations the values of α_1 and α_2 may be estimated as $\alpha_1 = \psi_i + 0(\epsilon \, kz)$. Hence, the factor $\epsilon(\alpha_1 + \alpha_2)$ may be replaced by $\epsilon(\psi_1 + \psi_2) \equiv 2 \, \epsilon \, k_z z$, which is approximately $2\epsilon kz$ because of the smallness of k_x/k. Thus, the coordinate transformations have the common limiting form

$$\psi_i \sim \alpha_i + \frac{1}{2} \epsilon\beta_0 kz \, [\sin(\omega t - \alpha_1) + \sin(\omega t - \alpha_2)]$$

$$\equiv \alpha_i + \epsilon\beta_0 kz \, \sin \left(\omega t - \frac{\alpha_1 + \alpha_2}{2}\right) \, \cos \left(\frac{\alpha_1 - \alpha_2}{2}\right) \qquad (36)$$

from which it follows that

$$\psi_1 - \psi_2 \equiv 2 \, k_x x \sim \alpha_1 - \alpha_2$$

$$\psi_1 + \psi_2 \equiv 2 \, k_z z \sim \alpha_1 + \alpha_2 + 2\epsilon\beta_0 kz \, \sin \left(\omega t - \frac{\alpha_1 + \alpha_2}{2}\right) \, \cos \left(\frac{\alpha_1 - \alpha_2}{2}\right) \qquad (37)$$

The same analysis is now applied to Eq. (32). Series expansion in powers of k_x/k yields

$$\frac{p}{\rho_0 c_0^{\,2}} = \frac{\varepsilon}{2} \left[\sin(\omega t - \alpha_1) + \sin(\omega t - \alpha_2) \right]$$

$$+ \frac{1}{8}\, \varepsilon^2 \left(\beta_0 \frac{k^2}{k_x^2} - 2 \right) \{ 2 \cos(\alpha_1 - \alpha_2) - \cos[(\alpha_1 - \alpha_2)$$

$$- \frac{k_x^2}{2k^2}(\alpha_1 + \alpha_2)] - \cos\left[(\alpha_1 - \alpha_2) - \frac{k_x^2}{2k^2}(\alpha_1 + \alpha_2) \right] \}$$

$$\sim \varepsilon \sin\left(\omega t - \frac{\alpha_1 + \alpha_2}{2} \right) \cos\left(\frac{\alpha_1 - \alpha_2}{2} \right) \tag{38}$$

The next step is to substitute the first of Eqs. (37) into the foregoing, and to use the resulting expression for p to eliminate $\alpha_1 + \alpha_2$ between the second of Eqs. (37) and Eq. (38). The pressure expression that is derived in this manner is

$$\frac{p}{\rho_0 c_0^{\,2}} \sim \varepsilon \sin\left(\omega t - k_z z + \beta_0 kzp \right) \cos\left(k_x x \right) \tag{39}$$

If $k_x \equiv 0$, this expression reduces to the well known solution for a planar finite amplitude wave at moderate amplitudes [18]. For very small k_x/k, the signal described by equation (39) is a quasi-planar wave. The distortion is measured by the value of $\beta_0 kzp$, the change in the axial phase variable from its value $\omega t - k_z z$ in linear theory. The wave is not truly planar because the amplitude varies with transverse position as $\cos(k_x x)$. Comparable phenomena are encountered in the far field of cylindrical and spherical waves whose amplitude is not uniform in the transverse direction [11,19].

Suppose that the limits of Eqs. (32) and (33) for small k_x/k had been derived without considering the interaction terms (those containing both α_1 and α_2). The result would have been the same, except that β_0 in such an expression would have been replaced by $\frac{1}{2}\beta_0$. In other words, half the

nonlinear effect when $k_x \ll k$ is due to interaction between the oblique waves.

The situation for comparatively low frequencies (exceeding cutoff) can also be examined asymptotically. Suppose that $k_x/k = 0(1)$ (recall that $k_x < k$ for propagating modes). In that case the interactive terms in Eqs. (32) and (33) are not associated with beating interactions, so they remain $0(\epsilon^2)$ at all locations. Such effects may be ignored. The remaining terms may be written as

$$p = p_1 + p_2, \quad \frac{p_j}{\rho_0 c_0^2} = \frac{1}{2} \epsilon \sin(\omega t - \alpha_j); \quad j = 1,2 \qquad (40a)$$

where

$$\psi_j = \alpha_j + \beta_0 \frac{k^2}{k_z} z \, p_j \qquad (40b)$$

The coordinate straining for each wave p_j is reminiscent of that for a planar wave, with an important exception. The nonlinear effect is measured by the difference between the nonlinear and linear spatial phases, $\alpha_j - \psi_j$. In an isolated planar wave, this difference is proportional to the propagation distance, which would be $(k_z z \pm k_x x)/k$ for waves propagating in the direction of either oblique wave. Instead, the distance parameter for each wave in Eq. (40b) is $z \, k/k_z$. It follows that although Eqs. (39) specify a superposition of the oblique waves, the presence of one affects the other by altering the spatial dependence for the distortion phenomena.

Another viewpoint for the low frequency (long axial wavelength) case may be obtained from a different resolution. Define new strained coordinates η, ξ such that

$$\alpha_1 = \xi + \eta, \quad \alpha_2 = \xi - \eta \qquad (41)$$

Return now to Eqs. (32) and delete the second $O(\epsilon)$ term in each, because those terms are not growth effects when $k_x/k = O(1)$. The variables α_1 and α_2 are removed from the functional dependence by forming the sum and difference of those equations after substitution of Eqs. (41). This yields

$$k_z z = \xi + \frac{1}{2} \epsilon\beta_0 \frac{k^2}{k_z} z \sin(\omega t - \xi) \cos(\eta)$$

$$k_x x = \eta - \frac{1}{2} \epsilon\beta_0 \frac{k^2}{k_z} z \cos(\omega t - \xi) \sin(\eta) \qquad (42)$$

The corresponding expression for pressure obtained from Eq. (32) is

$$\frac{p}{\rho_0 c_0^2} = \epsilon \sin(\omega t - \xi) \cos(\eta) + O(\epsilon^2) \qquad (43)$$

The significance of this representation of the signal becomes apparent when the particle velocity is evaluated. For this, the oblique planar wave decomposition is useful. The approximation $v = p/\rho c_0$ is applicable to weakly nonlinear, as well as linear, planar waves. The propagation directions $\bar{e}_1$ and $\bar{e}_2$ in Figure 1 may be used in conjunction with Eqs. (32) and (41) to represent the individual contributions. Thus

$$\underline{v} = \frac{1}{2} c_0 \epsilon [\underline{e}_1 \sin(\omega t - \xi - \eta) + \underline{e}_2 \sin(\omega t - \xi + \eta)] + O(\epsilon^2) \qquad (44a)$$

The components of particle velocity are therefore

$$v_z = \underline{v} \cdot \underline{e}_z = c_0 \epsilon \frac{k_z}{k} \sin(\omega t - \xi)\cos(\eta) \qquad (44b)$$

$$v_x = \underline{v} \cdot \underline{e}_x = - c_0 \epsilon \frac{k_x}{k} \cos(\omega t - \xi) \sin(\eta)$$

These expressions may be substituted into Eqs. (41), with the result that the new strained coordinates are found to be governed by

$$k_z z = \xi + \frac{1}{2} \beta_0 \frac{k^3}{k_z^2} z \frac{v_z}{c_0}$$

$$k_z x = \eta + \frac{1}{2} \beta_0 \frac{k^3}{k_x k_z} z \frac{v_x}{c_0} \qquad (45)$$

This form was derived in the earlier analysis that assumed noninteracting modes [10]. Constant values of ξ and η are wavefronts and rays, respectively, for the phase of the wave in Eq. (43). The velocity components transverse to these lines are v_z and v_x, respectively. Hence, the dependence of the wavefronts on v_z, and of the rays on v_x, was ascribed to self-refraction in the earlier work.

6. EXAMPLE

The trends identified in the previous section indicate that at low frequencies ($k_x = O(k)$) the distortion process involves only the harmonics of the fundamental mode for the waveguide. In contrast, at high frequencies ($k_x \ll k$) the tendency is to form a quasiplanar wave that propagates like the true planar mode. Identification of these trends leaves the questions of when the transitions to each situation occur, and what happens in the intermediate regime?

These matters may be addressed by numerical examples. Quantitative results in general are obtained by solving the coupled transcendental Eqs. (33) for the strained coordinates α_1 and α_2 corresponding to specified values of x, z, and t. These values then yield the pressure according to Eq. (32). If desired, a waveform may be generated by incrementing ωt through an interval 2π, and that result may be Fourier analyzed to determine the

frequency response. One simplification in performing a numerical evaluation is that, for specified properties of the fluid, the value of $p/\rho_0 c_0{}^2$ obtained from Eqs. (32) and (33) depends only on the independent variables kx, kz, and ωt and on the value of kL, (because $k_x/k \equiv 2\pi/kL$) . For the discussion that follows, the fluid is air (ρ_0 = 1.2 kg/m^3, c_0 = 343 m/s, β_0 = 1.2) and ω = 10 kHz.

A case of comparatively low frequency is illustrated in Figure 2, for which L = 0.20 meter and ϵ = 0.0014166 corresponding to an excitation of 140 dB re 20 μPa at the origin. For comparison, the noninteractive theory, Eqs. (40), and the quasi-planar limit, Eq. (39) are also shown in the figure. The unimportance of the mixing between the oblique waves is apparent, as is the fact that the distortion associated with the planar theory is stronger.

Altering the frequency for the next example would change the overall degree of nonlinearity. For example, the distance for shock formation in the *planar wave is*

$$\sigma = 1/(\epsilon\beta_0 k) \tag{46}$$

Since the degree to which wave interaction is significant depends (nondimensionally) only on the value of kL, the various phenomena shall be explored by changing L. Thus, the next case, illustrated in Figure 3, is for L = 2 meters, with the other parameters unchanged. The quasi-planar approximation is now very close to the new theory.

The situation for a transitional case is shown in Figure 4, which corresponds to L = 0.5 meter. Neither approximation is accurate here. The difference between the axial phase speeds of the planar harmonic created by nonlinearity and the true planar mode is relatively small. This leads to frequency dispersion in combination with the usual amplitude dispersion that is associated with a sawtooth waveform. The effect is asymmetrical between

compression and rarefaction; it is remarkably similar to the near field distortion observed for baffled transducers [16].

The relatively drastic transition from one approximate theory to another resulting from increasing kL by a factor of 10 has a direct explanation. The frequency dispersion phenomenon is attributable to spatial beating described by the last terms in the coordinate transformations, Eqs. (33). The trigonometric identity for the difference of cosines applied to these terms shows that

$$\cos(\omega t - \alpha_i) - \cos\left[\omega t - \alpha_i - (\frac{k}{k_z} - 1)(\alpha_i + \alpha_j)\right]$$

$$= -2 \sin\left[(\alpha_j + \alpha_i)(\frac{k}{k_z} - 1)\right] \sin[\omega t$$

$$+ \frac{1}{2}(\alpha_j - \alpha_i) - \frac{1}{2}(\alpha_j + \alpha_i)\frac{k}{k_z}]; \quad i,j = 1,2, \quad i \neq j \qquad (47)$$

The first sinusoidal factor is independent of time; it governs the wavelength of the beats. When the argument of that sine term is very small compared to π, the factor is well approximately by $(\alpha_j + \alpha_i)(k/k_z - 1)$. Since α_1 and α_2 may be approximated by $k_z z$, small values of the aforementioned argument correspond to cumulative growth of the frequency dispersion effect.

It follows that the prominance of frequency dispersion is indicated by $\pi/[2k_z z(k/k_z - 1)]$. In contrast, the significance of the sawtooth distortion effect is measured by the ratio of the axial distance z to the planar shock distance σ. A comparison of the two nondimensional factors indicates whether frequency dispersion will be noticeable in the presence of sawtooth distortion. Thus, define a beating parameter β according to

26

$$B = \frac{z/\sigma}{\pi/[2kz(k/k_z - 1)]}$$

$$= \frac{2}{\pi} \epsilon\beta_0(kz)^2 \left[\frac{1 - (1 - k_x^2/k^2)^{1/2}}{(1 - k_x^2/k^2)^{1/2}} \right] \tag{48}$$

This parameter is 5.08, 0.05, and 0.798 for Figures 2-4, respectively. Cases where B is substantially greater than unity can be anticipated to be well described by the earlier noninteractive theory for duct modes, whereas values that are much less than unity will closely fit the planar wave approximation.

Another aspect of the distortion process is displayed in Figures 5 and 6, which are waveforms at off-axis locations. The line $x/L = 1/4$ is a node according to linear theory, as well as the quasi-planar nonlinear approximation. However, Figure 5, which corresponds to such a location, shows that only the odd harmonics are nulled in the oblique wave theories. Hence the fundamental frequency of the signal at the "nodes" is twice the excitation frequency. Note that both oblique wave theories indicate that the tendency to form a sawtooth profile is still present.

The nulling of the odd harmonics was explained in the earlier analysis of the plate problem as being a result of self-refraction [4,6]. The rays in the non-interactive theory were shown to be distorted in the direction of the transverse velocity component. This caused the nodal ray to cross the axial line of zero linearlized pressure twice per axial wavelength, thereby setting up the second harmonic signal. It is apparent from Figure 5 that this effect also occurs in the presence of frequency dispersion resulting from interaction of the oblique waves.

A waveform for a general location appears in Figure 6. The even harmonics are more prominent than they were in Figure 4 because the odd harmonics are lessened by the proximity to the nodal line. This effect is accompanied by amplitude dispersion, as evidenced by the tendency to a

sawtooth profile, and by frequency dispersion, as indicated by the asymmetry between compression and rarefaction.

A different perspective is offered by the amplitude and phase distribution curves in Figures 7-9. These curves were obtained by Fourier series decomposition of the computer waveforms into

$$\frac{p}{\rho_0 c_0^2} = \sum_n P_n \sin[n \, \omega(t - t_0) - x_n]; \ x_1 = 0 \tag{49}$$

where t_0 is the arrival time of the fundamental in the interacting oblique wave theory. The amplitudes p_n are displayed for the three nonlinear theories. However the phase lags x_n are displayed only for the latest theory -- they vanish in the other descriptions in which the waveform distorts symmetrically.

Although only three harmonics are displayed in Figures 7-9, their trends are also indicative of higher harmonics. The earlier observation of the increased relative contribution of the even harmonics in the vicinity of the "nodal" line $x = L/4$ is evident in Figures 8 and 9. In addtion, Figure 7 shows that the phase of each harmonic tends to lag behind that of its predecessor by a uniform amount that increases as the signal propagates. This effect was also predicted for sound beams [20], whose waveform in the near field is much like Figure 4.

7. CONCLUSION

The excitation of the true planar mode, which provides a mechanism for the interaction of the oblique waves forming the fundamental symmetric mode, has been shown to be significant for large values of kL. In the limit, multidimensionality is only manifested as sinusoidal variation in the transverse direction, much like the directivity factor for nonuniform

spherical waves in the far field [19].

In the earlier (small kL) theory the modes are formed from obliquely propagating waves whose interaction is only manifested by a change in the distance parameter governing the distortion. If each wave were truly independent, that parameter would have bee, the distance over which the wave had propagated. Instead the distortion of the oblique waves depends on the axial distance. That theory has been shown here to be valid when the underlying assumption of distinct phase speeds is valid. In that case, kL is moderately larger than 2π , so that the scales with which the signal varies in the transverse and axial directions are comparable. The transition from small to large kL is predicted by the present theory to exhibit frequency dispersion that is responsible for distortion of the waveform that is not symmetrical between compression and rarefaction.

The same mechanism can be expected to enter into other situations in a waveguide. For example, suppose two modes are excited. If they have different phase speeds, they superpose according to the noninteractive theory, [10]. If the two modes have identical phase speeds, the modes combine to form a nondispersive group, for which the earlier theory is also valid. In the transitional situation, the two modes have phase speeds that are nearly identical. The interaction of such modes may be anticipated to lead to frequency dispersion phenomena of the type identified here.

ACKNOWLEDGMENTS

REFERENCES

1. A. H. Nayfeh and M. S. Tsai, "Nonlinear acoustic propagation in two-dimensional duct," J. Acoust. Soc. Am. 55(6), 1166-1172, (1976).

2. A. H. Nayfeh, "Nonlinear propagation of a wave packet in a hard-walled circular duct," J. Acoust. Soc. Am. 57(4), 803-809, 1975.

3. P. G. Vaidya and K. S. Wang, "Non-linear propagation of complex sound fields in rectangular ducts. Part I: The self-excitation phenomenon," J. Sound Vib. 50(1), 29-42, 1977.

4. J. H. Ginsberg, "Multi-dimensional non-linear acoustic wave propagation, Part II: The non-linear interaction of an acoustic fluid and plate under harmonic excitation," J. Sound Vib. 40(3), 359-379, 1975.

5. A. H. Nayfeh and S. G. Kelly, "Nonlinear interactions of acoustic fields with plates under harmonic excitations," J. Sound Vib. 60(3), 371-377, 1978.

6. J. H. Ginsberg, "A re-examination of the non-linear interaction between an acoustic fluid and a flat plate undergoing harmonical excitation," J. Sound Vib. 60(3), 449-458 (1978).

7. J. H. Ginsberg, "A new view point for two-dimensional non-linear acoustic wave radiating from a harmonically vibrating flat plate," J. Sound Vib., 63(1), 151-154, 1979.

8. J. H. Ginsberg, "Two-dimensional finite amplitude acoustic waves radiating from a flat plate in arbitrary periodic vibration," Journal De physique, C8, 35-38, 1979.

9. A. Kluwick, "On the non-linear distortion of waves generated by flat plates under harmonic excitations," J. Sound Vib. 74(4), 601-605, 1980.

10. J. H. Ginsberg, "Finite amplitude two-dimensional waves in a rectangular duct induced by arbitrary periodic excitation," J. Acoust. Soc. Am. 65(5), 1127-1133, 1979.

11. J. H. Ginsberg, "Propagation of nonlinear acoustic waves induced by a vibrating cylinder. I. The two-dimensional case," J. Acoust. Soc. Am., 64, 1671-1678 (1978).

12. J. H. Ginsberg, "Propagation of nonlinear acoustic waves induced by a vibrating cylinder. II. The three-dimensional case," J. Acoust. Soc. Am. 64(6), 1671-1687, 1978.

13. A. H. Nayfeh and S. G. Kelly, "Nonlinear propagation of waves induced by an infinite vibrating cylinder," Journal De Physique, 40; 8-13, 1979.

14. S. G. Kelly and A. H. Nayfeh, "Nonlinear propagation on directional cylindrical waves," J. Sound Vib., 79(3), 415-428, 1981.

15. M. F. Hamilton and J. A. Ten Cate, private communication (1984).

16. D. G. Browning and R. H. Mellen, "Finite-Amplitude distortion of 150 kHz acoustic waves in water," J. Acoust. Soc. Am. 44, 644-646, (1968).

17. S. Goldstein, **Lectures in Fluid Mechanics** (Wiley-Interscience, New York, 1960), Chapter 4.

18. A. D. Pierce, **Acoustics**, McGraw-Hill, New York, 1981, Chapter 11.

19. J. C. Lockwood, "Two problems in high-intensity sound," ARL, Univ. Texas at Austin, Rept. No. ARL-TR-71-28, 1971.

20. J. H. Ginsberg, "Nonlinear King integral for arbitrary axisymmetric sound beams at finite amplitudes - II. Derivation of uniformly accurate expression," J. Acoust. Soc. Am. 76(4), 1208-1214, 1984.

31

List of Captions

FIG. 1   Geometry of the oblique waves.

FIG. 2   Waveform on-axis at z = 3.05 m for 140 dB at the origin, L = 0.2 m, ω = 10 kHz.————: Interacting waves;— — —: Noninteractive theory;— — —: Quasi-planar wave.

FIG. 3   Waveform on-axis at z = 3.05 m for 140 dB at the origin, L = 2.0 m, ω = 10 kHz. ————: Interacting waves;— — —: Noninteractive theory;— — —: Quasi-planar wave.

FIG. 4   Waveform on-axis at z = 3.05 m for 140 dB at the origin, L = 0.5 m, ω = 10 kHz. ———— : Interacting waves;— — —: Noninteractive theory; — — —: Quasi-planar wave.

FIG. 5   Waveform at x = 0.125 m, z = 3.05 m for 140 dB at the origin, L = 0.5 m, ω = 10 kHz.———— : Interacting waves;— — —: Noninteractive theory; — — —: Quasi-planar wave.

FIG. 6   Waveform at x = 0.1 m, z = 3.05 m for 140 dB at the origin, L = 0.5 m, ω = 10 kHz. ———— : Interacting waves;— — —: Noninteractive theory;— — —: Quasi-planar wave.

FIG. 7   Axial dependence of frequency response along x = 0 for 140 dB at the origin, L = 0.5 m, ω = 10 kHz. ————: Interacting waves;— — —: Noninteractive theory;   : Quasi-planar wave.

FIG. 8   Axial dependence of frequency response along x = 0.1 m for 140 dB at the origin, L = 0.5 m, ω = 10 kHz. ———— : Interacting waves;— — —: Noninteractive theory;— — —: Quasi-planar wave.

FIG. 9   Transverse dependence of frequency response along z = 3.05 m for 140 dB at the origin, L = 0.5 m, ω = 10 kHz. ————: Interacting waves;— — —: Noninteractive theory;— — —: Quasi-planar wave.

FIG.1

FIG 2

FIG 3

The graph shows axes labeled $\omega t / 2\pi$ (horizontal, ranging from 0.0 to 2.0) and $p/\rho_0 c_0^2 \, (\times 10^3)$ (vertical, ranging from -2.00 to 2.00).

FIG. 4

FIG. 5

FIG.6

Plot axes: $p/\rho_0 c_0^2 (\times 10^4)$ versus $\omega t/2\pi$

$P_n (\times 10^3)$

X_n (degrees)

z(meters)
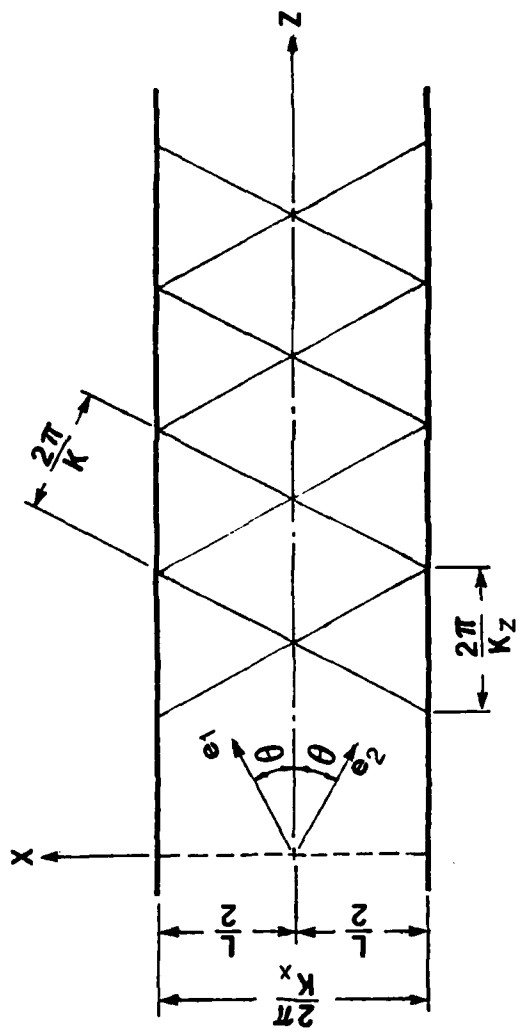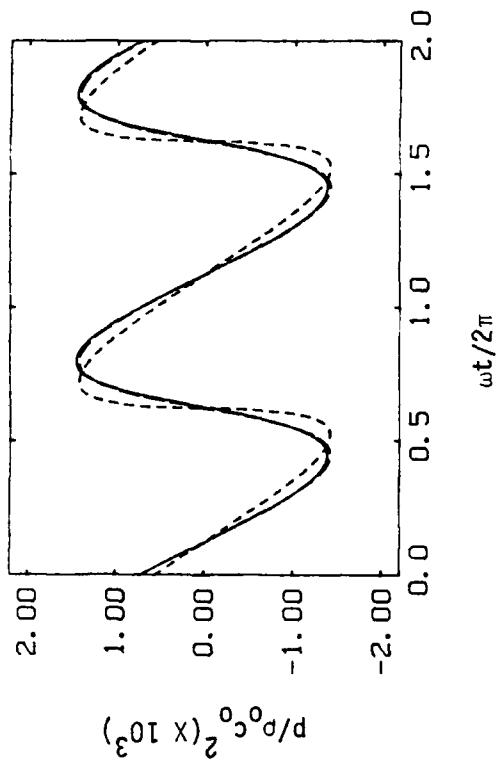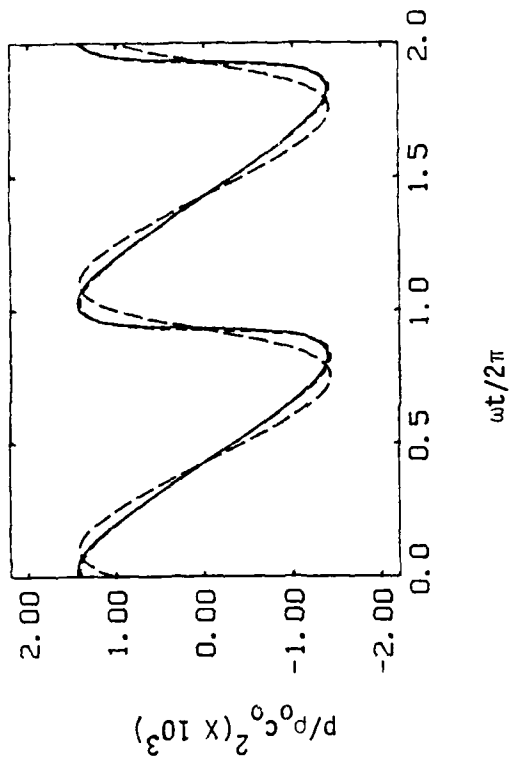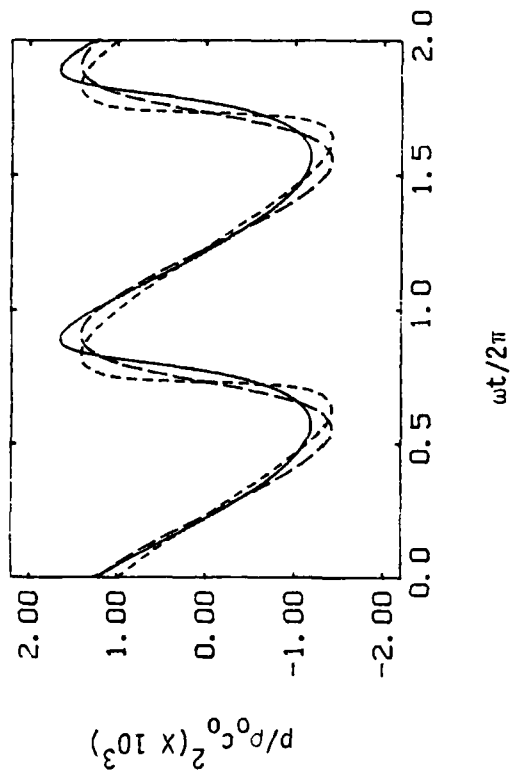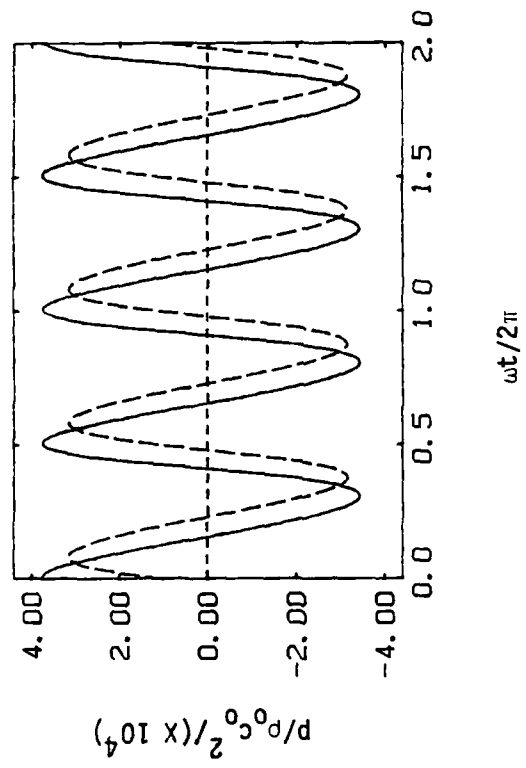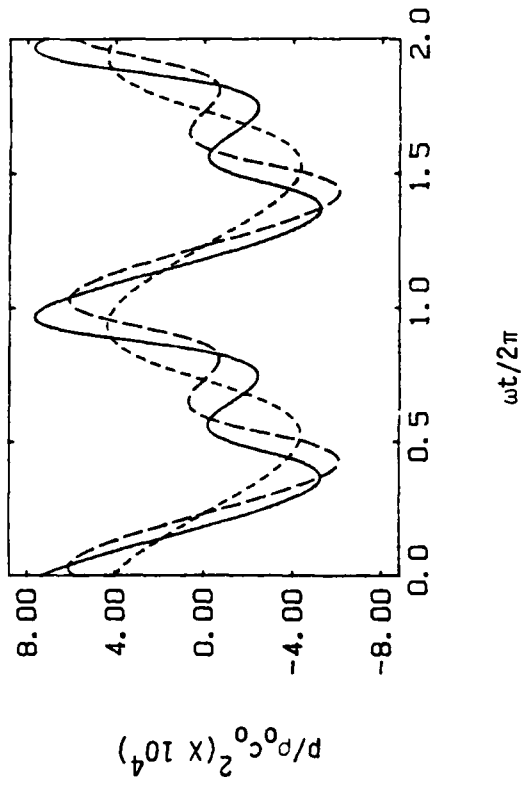
FIG 7

FIG. 8

FIG. 9

SYMPOSIUM IUTAM
AERO ET HYDRO-ACOUSTIQUE

Du 3 au 6 juillet 1985
ECOLE CENTRALE DE LYON
FRANCE

SUBVENTIONNE PAR :
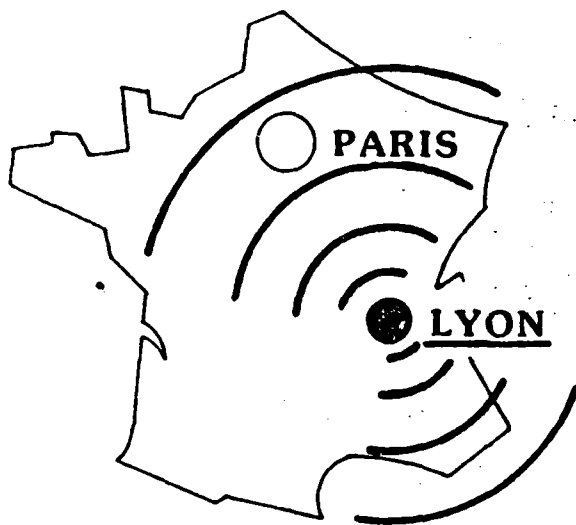
- IUTAM
- CNRS
- DRET
- AUM
- C.G. Rhône
- Ministère Environnement

PARIS

LYON

Avec le Patronage DU GALF

FINITE AMPLITUDE SOUND BEAMS RESULTING FROM NONLINEAR VIBRATION OF
A CIRCULAR MEMBRANE UNDERGOING AXISYMMETRIC RESONANT EXCITATION

J. H. GINSBERG

School of Mechanical Engineering
Georgia Institute of Technology
Atlanta, Georgia

Summary

This paper analyses the interaction between a vibrating circular membrane
contained in an infinite baffle and the resulting sound field radiated
into a fluid medium contained in the half-space above the membrane. The
case of resonant excitation of the membrane leads to nonlinear coupling
between transverse and in-plane displacement. Nonlinearity within the
fluid medium is described by a recent general treatment of finite
amplitude sound beams resulting from boundary motion. The vibratory
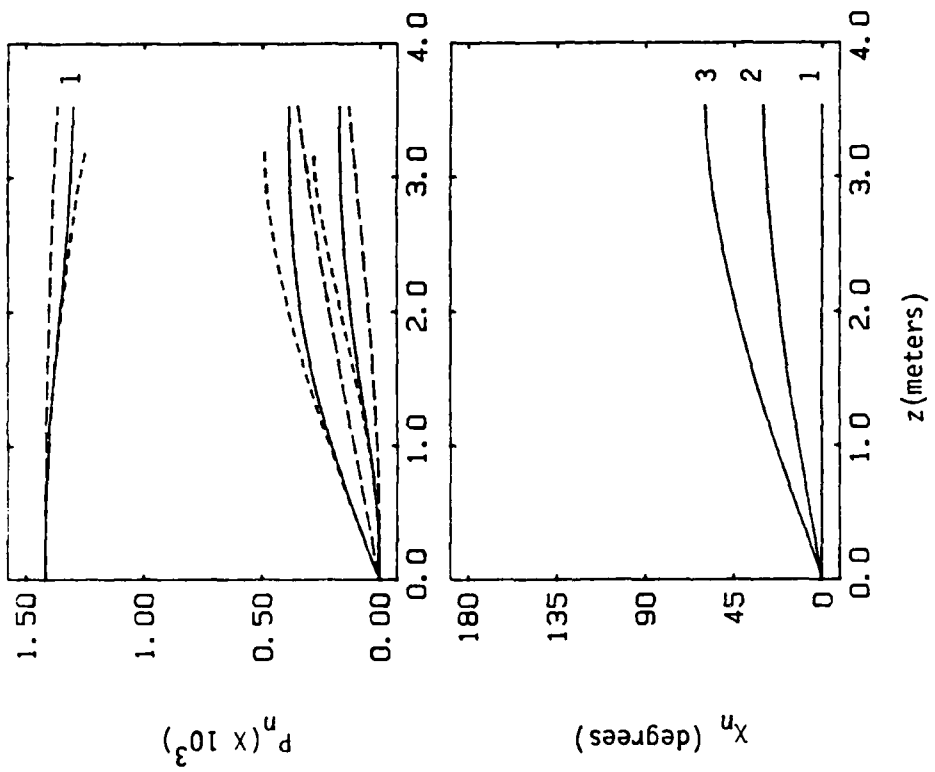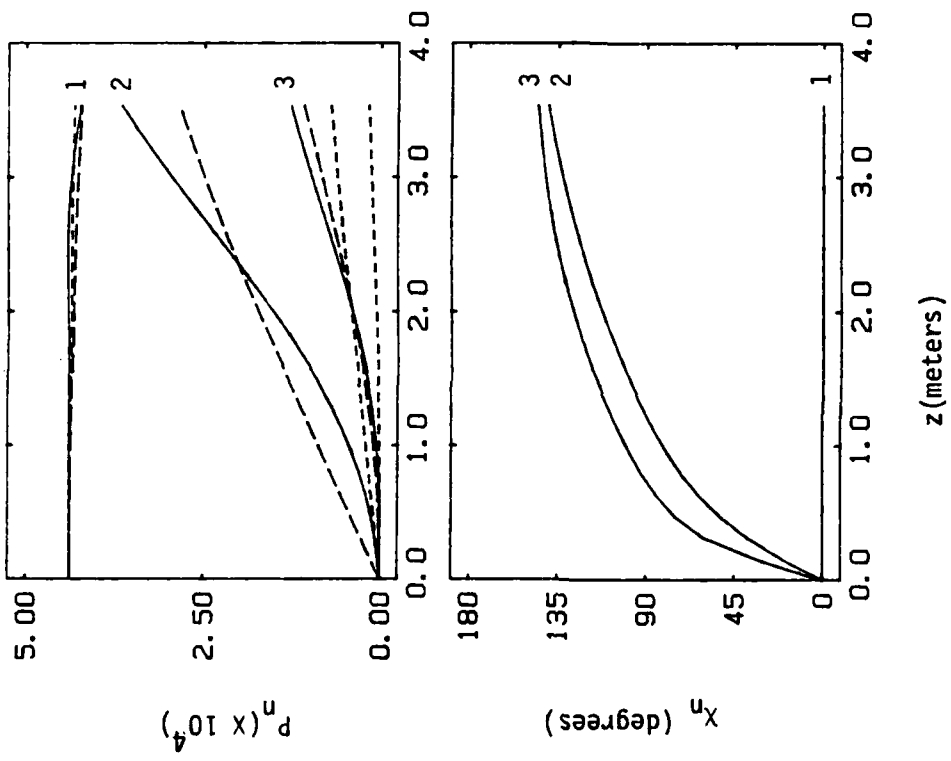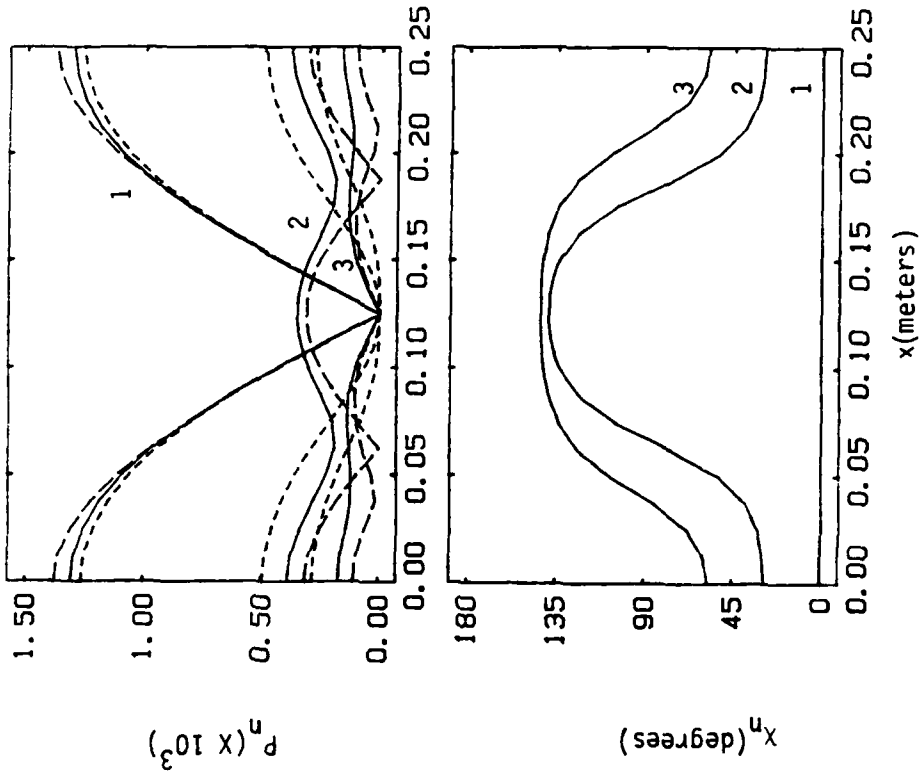response of the membrane is evaluated in a perturbation technique based on
the modes of free vibration. The results give amplitude-frequency rela-
tions for the plate that account for the inertial and damping impedances
of the fluid, as well as expressions that may be solved for the pressure
signal in the fluid.

Finite Amplitude Effects in Acoustic Radiation

Consider a circular membrane of radius a that is fixed at its edges
to an infinite baffle. An excitation at frequency ω close to a natural
frequency is applied on one side, and a fluid medium occupies the half-
space on the other side. The speed of sound and density of the fluid at
ambient conditions are c_0 and ρ_0, respectively. Dimensional cylindrical
coordinates are R/k and z/k within the fluid which occupies z > 0, and
dimensional time is t/ω, where k = ω/c_0. A recent study described the
effects of material and convective nonlinearity on the acoustic radiation
resulting from an arbitrary motion on the boundary [1]. Suppose that the
normal velocity on the boundary is

$$v_z\big|_{z=0} = \frac{1}{2i} \epsilon\, c_0\, f(R)\, \exp(it) + c.c. \tag{1}$$

where $\epsilon \ll 1$ is the acoustic Mach number and $f(R)/R^{1/2}$ is bounded for
large R. Then the pressure at any (R, z), omitting a mean value correc-
tion term, was found to be described by

$$p = \frac{1}{2} \epsilon \rho_0 c_0^2 \int_0^\infty \frac{mV}{\mu} \exp(it - \mu\xi) \, J_0(m\alpha) \, dm + c.c. \qquad (2)$$

In general, c.c. shall denote the complex conjugate of all preceding terms. The parameters m and μ are transverse and axial wavenumbers, respectively, $J_0(\ )$ denotes the Bessel function of zero order, and V is the Hankel transform of the spatial pattern f(R).

$$\mu = i(1 - m^2)^{1/2} \text{ if } m < 1 \quad \& \quad \mu = (m^2 - 1)^{1/2} \text{ if } m > 1$$

$$V = \int_0^\infty R \, f(R) \, J_0(mR) \, dR \qquad (3)$$

The parameters (α, ξ) are strained coordinates defined in implicit form by

$$z = \xi - \pi\epsilon\beta_0\xi \left\{ (mV/\mu) \exp(it) \, \mathrm{erfc}\left[(\mu\xi)^{1/2}\right] + c.c \right\} J_0(n\alpha)$$

$$R = \alpha + \pi\epsilon\beta_0\xi \left\{ (mV/\mu) \exp(it) \, \mathrm{erfc}\left[(\mu\xi)^{1/2}\right] + c.c \right\} J_1(n\alpha) \qquad (4)$$

The evaluation of the response of the fluid-membrane system requires that eqs. (3) and (4) be interfaced with the equations governing the membrane.

Equations of Motion for the Membrane

An elastic membrane undergoing finite deformation due to a resonant excitation was studied by Chobotov and Binder [2]. Several shortcomings of the earlier work shall be corrected here. Small errors associated with using an assumed mode function shall be addressed by employing the exact Bessel function mode. Furthermore, the study here shall describe the situation for resonance of any mode, rather than only the fundamental. The last matter is that the resistive and reactive portions of the fluid impedance will be derived analytically. In Ref. [2] the acoustic impedance was based on a low frequency approximation that did not account for diffraction.

Chobotov and Binder began with a derivation of displacment equations of motion that accounted for in-plane deformation and geometrical nonlinearity. Examination of these equations reveals that the membrane displacements are scaled such that

$$\text{transverse displacement} = \epsilon \frac{w}{k} \; ; \; \text{in-plane displacement} = \epsilon^2 \frac{u}{k} \qquad (5)$$

Based on these definitions and the fact that the acoustic Mach number ε in eq. (1) is very small, the equation for in-plane motion may be rewritten from its original form in [2] as

$$\frac{\partial}{\partial R}\left[\frac{1}{R}\frac{\partial}{\partial R}(Ru)\right] + \frac{1}{2}\frac{\partial}{\partial R}\left(\frac{\partial w}{\partial R}\right)^2 + \frac{(1-\nu)}{2R}\left(\frac{\partial w}{\partial R}\right)^2 = \frac{c_0^2}{c_u^2}\frac{\partial^2 u}{\partial t^2} \tag{6}$$

The corresponding equation for transverse motion is

$$\frac{1}{R}\frac{\partial}{\partial R}\left\{R\frac{\partial w}{\partial R} + \frac{\varepsilon^2}{e_0}\left[R\frac{\partial u}{\partial R}\frac{\partial w}{\partial R} + \nu u\frac{\partial w}{\partial R} + \frac{1}{2}R\left(\frac{\partial w}{\partial R}\right)^3\right]\right\}$$

$$+ \frac{\Gamma}{\varepsilon ka}\left[Q(R)\cos(t) - \frac{p|_{z=0}}{\rho_0 c_0^2}\right] = \frac{c_0^2}{c_w^2}\frac{\partial^2 w}{\partial t^2} \tag{7}$$

In the foregoing $\Gamma = \rho_0 c_0^2 a/\sigma_0 h$ (h is the thickness of the membrane), $Q(R)$ is the radial profile of the excitation applied to the membrane, and

$$c_u = \left[E/\rho(1-\nu^2)\right]^{1/2} \; ; \; c_w = (\sigma_0/\rho)^{1/2} \; ; \; e_0 = (c_w/c_u)^2 \tag{8}$$

Note for later use that $c_w \ll c_u$. In addition, the magnitude of Q is required to be sufficiently small to induce a transverse displacement whose peak velocity actually is a small fraction of c_0.

Vibratory Response

The eigenfunctions for a membrane whose edges are fixed are

$$\Phi_j = J_0(\eta) \quad \text{where} \quad \eta = \lambda_j R/ka \quad \text{and} \quad J_0(\lambda_j) = 0 \tag{9}$$

Some approximate values are $\lambda_1 = 2.405$, $\lambda_2 = 5.520$, $\lambda_3 = 8.654$. Proximity to resonance is specified by $\omega = \lambda_j c_w/a$.

In general, the transverse displacement may be expanded in a series of modes. When the excitation is close to one of the natural frequencies, the corresponding mode may be expected to dominate the response. Since the nonlinear terms in eq. (7) are $O(\varepsilon^2)$, the transverse motion in this case should satisfy

$$w = \Phi_j w_j(t) + \varepsilon^2 \hat{w}(R, t) \tag{10}$$

where $\hat{w}(R,t)$ is orthogonal to Φ_j over the interval $0 \leq R \leq ka$.

Substitution of eq. (10) into eqs. (6) and (7) shows that all derivatives have comparable magnitudes. The largeness of c_u relative to c_w, in combination with the resonance of w, makes it permissible to neglect the inertia of in-plane motion. An expression for u may then be found analytically. Toward this end the $O(1)$ term for w in eq. (10) is substituted into eq. (6). Using the chain rule to replace R by η results in an inhomogeneous ordinary differential equation for u.

$$\frac{\partial}{\partial \eta}\left[\frac{1}{\eta}\frac{\partial}{\partial \eta}(\eta u)\right] = -\frac{\lambda_j}{2a} w_j^2 \left\{\frac{\partial}{\partial \eta}\left[J_1(\eta)^2\right] + \frac{(1-\nu)}{\eta}\left[J_1(\eta)^2\right]\right\} \qquad (11)$$

This equation may be integrated twice, after which the constants of integration are selected so as to satisfy the condition that $u = 0$ at $R = 0$ and $R = ka$. Repeated application of the recursion relations for Bessel functions yields the following expression.

$$u = \frac{\lambda_j}{ka} w_j^2 U$$

$$U = \frac{1}{4}(1 + \nu) J_0(\eta) J_1(\eta) + \frac{1}{4}\nu \eta \left[J_1(\lambda_j)^2 - J_0(\eta)^2 - J_1(\eta)^2\right] \qquad (12)$$

Amplitude-Frequency Relations

The equation for $w_j(t)$ is obtained by substituting eqs. (10) and (12) into eq. (7), then applying orthogonality of $\hat{w}$ with respect to ϕ_j. The result is

$$\frac{1}{2}\left(\frac{\lambda_j}{ka}\right)^2 \left[\lambda_j J_1(\alpha_j)\right]^2 \left[\left(\frac{\omega a}{\lambda_j c_w}\right)^2 \frac{\partial^2 w_j}{\partial t^2} + w_j\right] + \frac{\varepsilon^2}{\varepsilon_0}\left(\frac{\lambda_j}{ka}\right)^4 \delta_j w_j^3$$

$$+ \frac{\Gamma}{\varepsilon ka}\int_0^{\lambda_j} \eta \frac{p|_{z=0}}{\rho_0 c_0^2} J_0(\eta)\, d\eta = \frac{\Gamma}{\varepsilon ka}\cos(t)\cdot\int_0^{\lambda_j} \eta\, Q\, J_0(\eta)\, d\eta \qquad (13)$$

where δ_j is a coefficient of nonlinear elasticity that is found to be

$$\delta_j = \int_0^{\lambda_j}\left\{U\left[(1+\nu) J_1(\eta)^2 - 2\nu J_0(\eta) J_1(\eta)\right] + \frac{1}{2}\eta J_1(\eta)^4\right\} d\eta \qquad (14)$$

values of this parameter for the first three resonances when $\nu = 0.29$ are $\delta_1 = 0.08206$, $\delta_2 = 0.11996$, $\delta_3 = 0.14069$. Chobotov and Binder used the approximate fundamental mode $\phi_1 = 1 - (R/ka)^2$ to obtain $\delta_1 = 0.08424$.

Because of the smallness of the nonlinear term in eq. (13), w_j will

be harmonic in the first order approximation. Let A be the complex amplitude, and let $\bar{w}$ denote the dimensional transverse displacement found from eq. (5).

$$w_j = \frac{A}{2} \exp(it) + c.c. \quad ; \quad \bar{w} = \frac{\varepsilon A}{2k} J_0(\eta) \exp(it) + c.c. + O(\varepsilon^2) \qquad (15)$$

The Hankel transform V of the normal velocity at the membrane may be evaluated by comparing the (dimensional) time derivative of $\bar{w}$ to eq. (1). This defines the shape factor $f(R)$ for $R < ka$. For $R > ka$, $f(R) = 0$ because the baffle is stationary. The transform is found in this manner to be

$$V = - A G \quad ; \quad G = \int_0^{ka} R \, J_0(\lambda_j R/ka) \, J_0(mR) \, dm \qquad (16)$$

The coefficient G, which may be evaluated in closed form, leads to an expression for p according to eq. (3). The acoustic loading applied to the membrane is readily found from that expression, because $\xi = 0$ and $\alpha = R$ at $z = 0$, see eqs. (4).

$$p\big|_{z=0} = - \frac{1}{2} \rho_0 c_0^2 \, \varepsilon A \int_0^\infty \frac{nG}{\mu} \exp(it - \mu z) \, J_0(mR) \, dm + c.c. \qquad (17)$$

The final step leading to the amplitude-frequency relations is to use the method of harmonic balance to equate all terms in the equation of motion that are proportional to $\exp(it)$. (This procedure is equivalent to removing secular terms in singular perturbation schemes.) The equation obtained in this manner relates the amplitude εA to the frequency ω and the generalized modal amplitude Q_j for the excitation.

$$\left[1 + \Gamma (\gamma_d i - \gamma_m) - \left(\frac{\omega a}{\lambda_j c_w}\right)^2 \right] \varepsilon A + \frac{3\delta_j \varepsilon^3 A^2 A^*}{2e_0 [ka J_1(\lambda_j)]^2} = \Gamma \frac{ka}{\lambda_j^2} Q_j \qquad (18)$$

where εA^* denotes the complex conjugate. The coefficients γ_m and γ_d are reactance (added mass) and resistance (damping) impedance coefficients, respectively, resulting from the acoustic radiation.

$$\gamma_d = \frac{2}{ka \, \lambda_j^2 J_1(\lambda_j)^2} \int_0^1 \frac{m \, G^2}{(1 - m^2)^{1/2}} \, dm$$

$$\gamma_m = \frac{2}{ka \, \lambda_j^2 \, J_1(\lambda_j)^2} \int_1^\infty \frac{m \, G^2}{(m^2 - 1)^{1/2}} \, dm \qquad (19)$$

Equivalent expressions were derived by Bouwkamp [3] by using a scattering integral.

The real and imaginary parts of eq. (18) may be solved for the magnitude and phase of ϵA; the latter represents the phase lag of the response relative to the excitation. Then the acoustic signal may be evaluated by substituting the value of ϵA into eqs. (16) to form the Hankel transform V.

Results

Figures 1 and 2 depict the resistance and reactance coefficients as a function of ka. The peaks in γ_m are centered around ka = λ_j for the respective resonances, whereas γ_d rises almost linearly beyond those locations. Suppose that the fluid is water, in which case $c_w/c_0 \ll 1$ ($\sigma_0 \ll \rho_0 c_0^2$ because σ_0 cannot exceed the yield stress). Furthermore, note that ka = $\lambda_j \, c_w/c_0$ when $\omega = \omega_j$, and that ka $\gg 2\pi$ for closely confined sound beams. It follows that resonant excitations at high ka values for beam forming only arise for very high order modes.
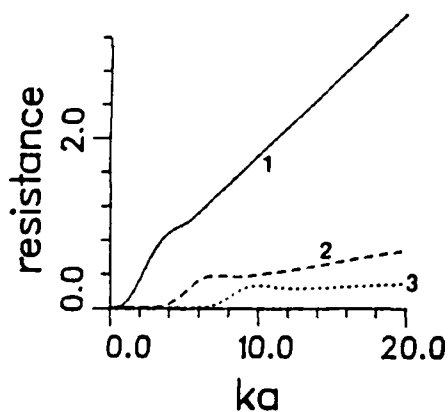

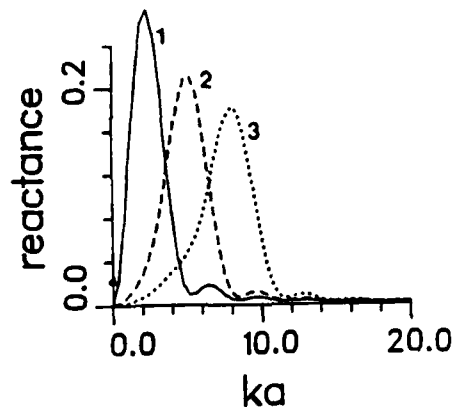Fig. 1. Resistance γ_d for the three lowest modes.

Fig. 2. Reactance γ_m for the three lowest modes.

The dependence of the harmonic amplitudes forming the pressure waveform along the axis of a sound beam is depicted in Figure 3. Only the fundamental frequency, marked #1, is treated by a linearized analysis.

The corresponding result for a piston (uniform velocity) is shown in Figure 4. In both cases ka = 40 and ϵ = 0.00102, which produces a maximum sound pressure level in the piston case of 250 dB re 1 µPa. The fluctuations in the piston case are due to diffraction effects that alternately reinforce and cancel the fundamental frequency in the near field, z < $(ka)^2/2\pi$. Diffraction effects are much less significant for the membrane because the particle velocity is continuous across the edge, so the propagation curves are smoother, and the peak values are lessened.
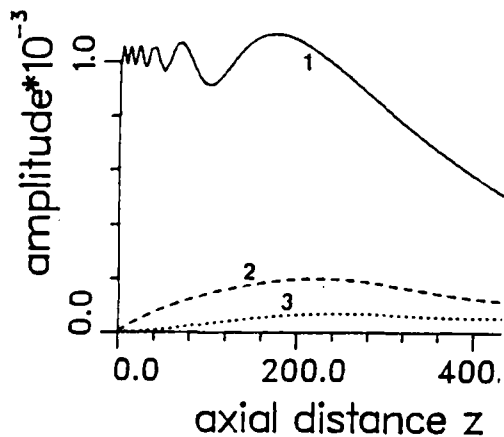

Fig. 3. Range dependence of the amplitude of the three lowest harmonics in a sound beam generated by a membrane, as a fraction of $\rho_0 c_0^2$.
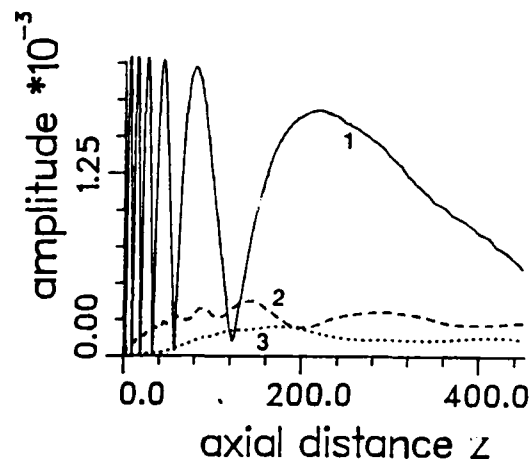
Fig. 4. Range dependence of the amplitude of the three lowest harmonics in a sound beam generated by a piston, as a fraction of $\rho_0 c_0^2$.

References
1. Ginsberg, J. H.: Nonlinear King integral for arbitrary axisymmetric sound beams at finite amplitudes. II. Derivation of uniformly accurate results. J. Acoust. Soc. Am. 76 (1984) 1208 – 1214.

2. Chobotov, V. A. and Binder, R. C.: Nonlinear response of a circular membrane to sinusoidal excitation. J. Acoust. Soc. Am. 36 (1964) 59 – 73.

3. Bouwkamp, C. J.: A contribution to the theory of acoustic radiation. Phillips Research Reports 1 (1946) 251-277.

FINITE AMPLITUDE SOUND BEAMS RESULTING FROM

NONLINEAR VIBRATION OF A CIRCULAR MEMBRANE

UNDERGOING AXISYMMETRIC EXCITATION

J. H. GINSBERG

School of Mechanical Engineering

Georgia Institute of Technology

Atlanta, Georgia 30332, USA

OVERVIEW

Membrane

E, ν : Elasticity

σ_0 : Initial stress

h : Thickness

Resonant Excitation

ω : Frequency

Acoustic fluid

ρ_0 : Ambient density

c_0 : Ambient speed of sound

$k = \omega / c_0$: axial wave number

Fluid

R/k

a

z/k

membrane

transverse displacement

baffle
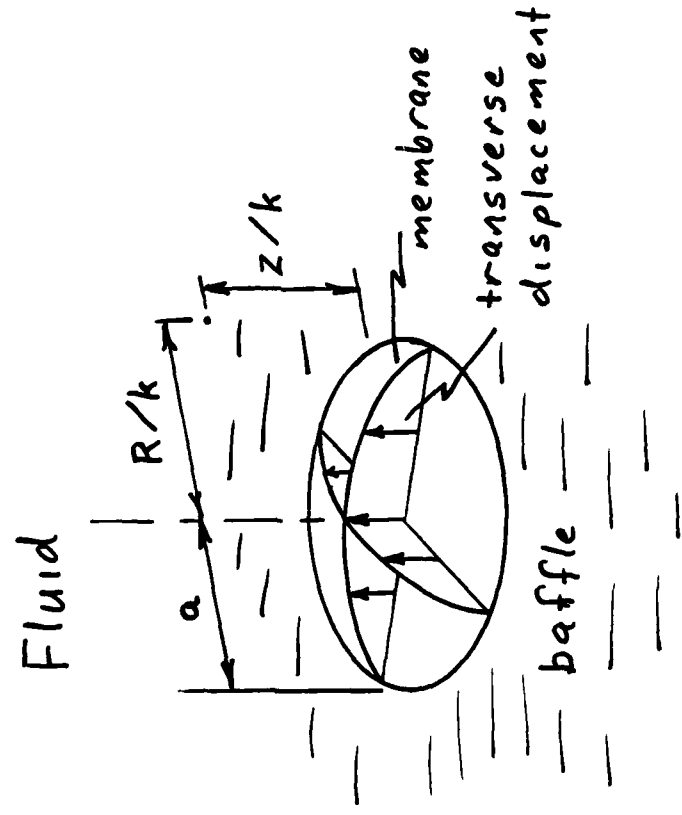
PROBLEM STATEMENT

a) Excitation drives membrane

b) Resonance → finite displacement effects

c) Compatibility between velocity of membrane and fluid

d) High acoustic intensity → material and spatial nonlinearity

e) Fluid impedance on membrane

What is the membrane response?

What are the effects of finite amplitudes on the acoustic radiation?

NONLINEAR SOUND BEAMS

J. H. Ginsberg — J. A. S. A. ....

Governing Equations

$$\bar{v} = c_0 \nabla \phi$$

$$\nabla^2 \phi - \frac{\partial^2 \phi}{\partial t^2} = \frac{\partial}{\partial t}\left[(\beta_0 - 1)\left(\frac{\partial \phi}{\partial t}\right)^2 + \nabla \phi \cdot \nabla \phi \right]$$

$$\frac{\partial \phi}{\partial z}\Big|_{z=0} = \frac{1}{2}\epsilon c_0 f(R)\, exp(it) + c.c.$$

ϵ = acoustic Mach number << 1

Perturbation solution: $\phi = \epsilon \phi_1 + \epsilon^2 \phi_2$

First order – Hankel transform –
  spectrum of transverse wave numbers
Second order – quadratic nonlinearity –
  dual spectrum
Asymptotic integration – growth effects –
  reduction to a single spectrum

Uniform Validity

Require P_2/P_1 bounded for all z

Distort space-time grid for each transverse n

$$p = \frac{1}{2}\varepsilon\rho_0 c_0^2 \int_0^\infty \frac{mV}{\mu} \exp(it - \mu\xi) J_0(m\alpha) \, dm + c.c.$$

where

$$\mu = i(1-m^2)^{1/2} \text{ if } m < 1 \; ; \; \mu = (m^2-1)^{1/2} \text{ if } m > 1$$

$$V = \int_0^\infty R f(R) J_0(mR) \, dR$$

Coordinate straining

$$z = \xi - \pi\varepsilon\beta_0\xi \left\{ \left[\frac{mV}{\mu} \exp(it) \, erfc\left[(\pi\xi)^{1/2}\right] + c.c.\right] J_0(m\alpha)\right\}$$

$$R = \alpha + \pi\varepsilon\beta_0\xi \left\{ \left[\frac{mV}{\mu} \exp(it) \, erfc\left[(\pi\xi)^{1/2}\right] + c.c.\right] J_1(m\alpha)\right\}$$

GENERAL APPROACH

Vicinity of the membrane

$\xi \sim z$ and $\propto \sim R$ when $z = O(1)$ - small

nonlinear effect near the source $\nrightarrow$ use

linear fluid-structure interaction model

Determination of membrane response

If resonance is sharp (high Q), then fluid

impedance is light - use linear acoustics

and nonlinear structural theory

If acoustic impedance is heavy - use linear

acoustic and structural theories

Assume high Q case

Evaluate nonlinear acoustic radiation after

vibration properties are known

MEMBRANE EQUATIONS OF MOTION

Chobotov and Binder, J.A.S.A., 1964

Equilibrium of an sectorial segment

  a) Finite strain and rotation

  b) Force balance in transverse and
     radial directions in deformed
     state

  c) Membrane pre-stress

  d) Linear stress-strain

Scaling - transverse velocity $<<$ c_o

Transverse displacement: ε w/k

Resonant excitation of membrane

$$P_{ext} = \rho_o c_o^2 \, Q(R) \, \cos(t)$$

Resonance $\not\Rightarrow$ in-plane $<<$ transverse

  thus   in-plane displacement: ε^2 u/k

Transverse motion

$$\frac{1}{R}\frac{\partial}{\partial R}\left\{ R\frac{\partial w}{\partial R} + \frac{\epsilon^2}{e_0}\left[R\frac{\partial u}{\partial R}\frac{\partial w}{\partial R} + \nu u\frac{\partial w}{\partial R} + \frac{1}{2}R\left(\frac{\partial w}{\partial R}\right)^3 \right] \right\}$$

$$+ \frac{1}{\epsilon\sigma_0 kh}\left[P_{ext} - P\big|_{z=0} \right] = \frac{c_0^2}{c_w^2}\frac{\partial^2 w}{\partial t^2}$$

In-plane motion

$$\frac{\partial}{\partial R}\left[\frac{1}{R}\frac{\partial}{\partial R}(Ru) \right] + \frac{1}{2}\frac{\partial}{\partial R}\left(\frac{\partial w}{\partial R}\right)^2 + \frac{(1-\nu)}{2R}\left(\frac{\partial w}{\partial R}\right)^2$$

$$= \frac{c_0^2}{c_u^2}\frac{\partial^2 u}{\partial t^2}$$

where $\quad c_u = \left[\frac{E}{\rho(1-\nu^2)}\right]^{1/2}$; $\quad c_w = \left(\frac{\sigma_0}{\rho}\right)^{1/2}$; $\quad e_0 = \frac{c_w^2}{c_u^2}$

VIBRATORY RESPONSE

Linear analysis

Eigenfunctions - $\phi_j = J_o(\lambda_j R/ka)$; $J_o(\lambda_j) = 0$

Natural frequencies - $\omega_j = \lambda_j \, c_w/a$

Chobotov and Binder used $\phi_j = (1 - R^2/k^2 a^2)$

  a) Descriptive of fundamental mode only

  b) Not exact free vibration properties - does
    this affect higher order corrections?

FINITE AMPLITUDE EFFECT

Nonlinearity is $O(\epsilon^2)$

Resonance $\Rightarrow$ $w = w_j(t) \; \Phi_j(R) + O(\epsilon^2)$

Substitute into equation for u

a) Neglect in-plane inertia because $\omega_j \ll$ natural frequency for radial displacement

b) Employ many identities for derivatives and integrals of products of Bessel functions

Integrate o. d. e. for u directly -

satisfy $u = 0$ at $R = 0$ and $R = ka$

$$u = \frac{\lambda_j}{ka} \; w_j^2 \; U$$

where $\eta = \lambda_j R / ka$

$$U = \frac{1}{4}(1+\nu) J_0(\eta) J_1(\eta) + \frac{1}{4} \eta \nu \left[J_1(\lambda_j)^2 - J_0(\eta)^2 - J_1(\eta)^2 \right]$$

COMPLEX AMPLITUDE - FREQUENCY RELATION

Harmonic excitation $\Rightarrow$ $w_j = \frac{1}{2} A \exp(it) + c.c.$

Compatibility

$$\frac{\partial \phi}{\partial z}\Big|_{z=0} = \begin{cases} \frac{1}{2i} \varepsilon c_0 A J_0(\eta) \exp(it) + c.c. \; ; \; R > ka \\ 0 \; ; \; R > ka \end{cases}$$

thus $V = -AG; \quad G = \int_0^{ka} R \, J_0(\lambda_j R/ka) \, J_0(mR) \; dm$

Substitute $p|_{z=0}$, w, and u into d.e. for w

$$\left[1 + \frac{\rho_0 c_0^2}{\sigma_0 kh} \left(\Upsilon_d i - \Upsilon_m \right) - \left(\frac{\omega a}{\lambda_j c_w} \right)^2 \right] \varepsilon A$$

$$+ \delta \frac{3}{2 e_0 [ka \, J_1(\lambda_j)]^2} \; \varepsilon^3 A^2 A^* = \frac{\rho_0 c_0^2 ka^2}{\sigma_0 \lambda_j^2 h} \, Q_j$$

$\qquad\qquad\qquad\qquad\nearrow \qquad\qquad\qquad\qquad\nwarrow$

$\qquad\qquad\text{complex} \qquad\qquad\qquad\quad \text{Hankel transform}$
$\qquad\qquad\text{conjugate} \qquad\qquad\qquad\qquad \text{of } Q(R)$

COEFFICIENTS

Nonlinear elasticity: δ

Fundamental resonance: $j = 1$
Chobotov and Binder $\quad \delta = 0.08424$
Present analysis $\quad \delta = 0.08206$

Acoustic impedances:

Resistance: $Y_d = \dfrac{2}{\lambda_j^2 J_1(\lambda_j)^2} \displaystyle\int_0^1 \dfrac{mG^2}{(1-m^2)^{1/2}}\, dm$
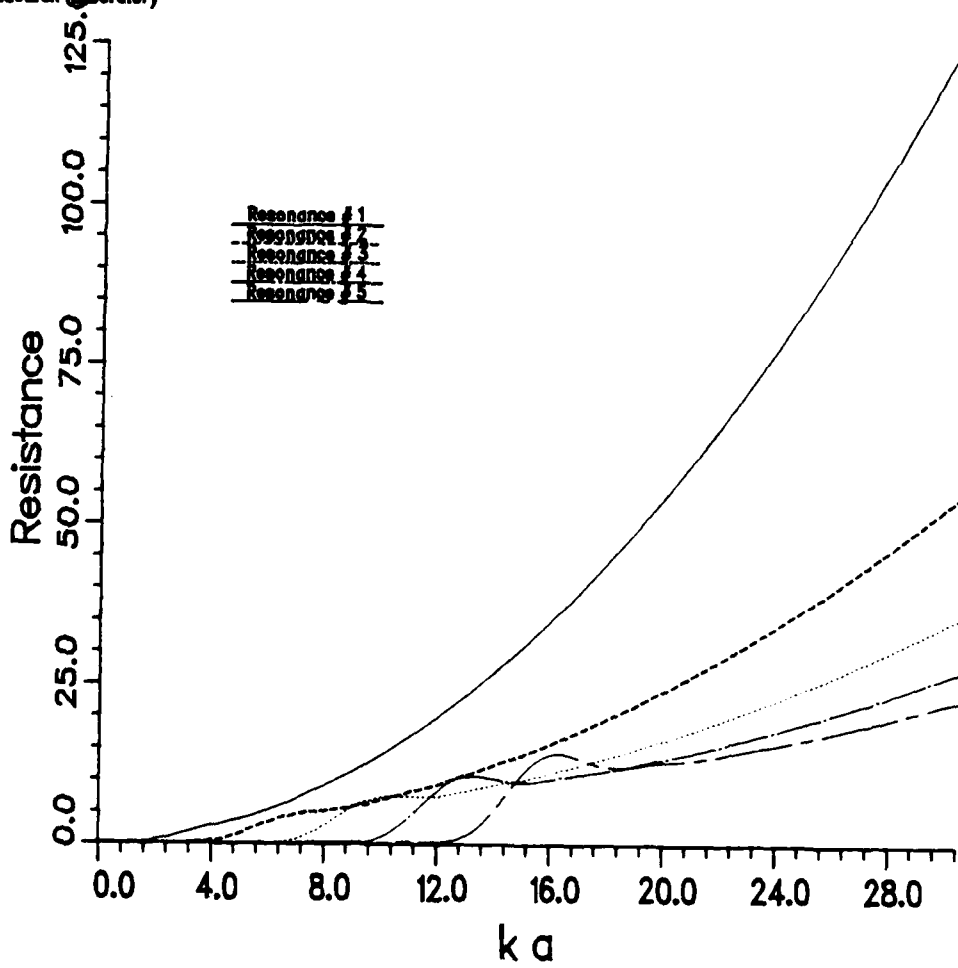
Reactance: $Y_m = \dfrac{2}{\lambda_j^2 J_1(\lambda_j)^2} \displaystyle\int_1^\infty \dfrac{mG^2}{(m^2-1)^{1/2}}\, dm$
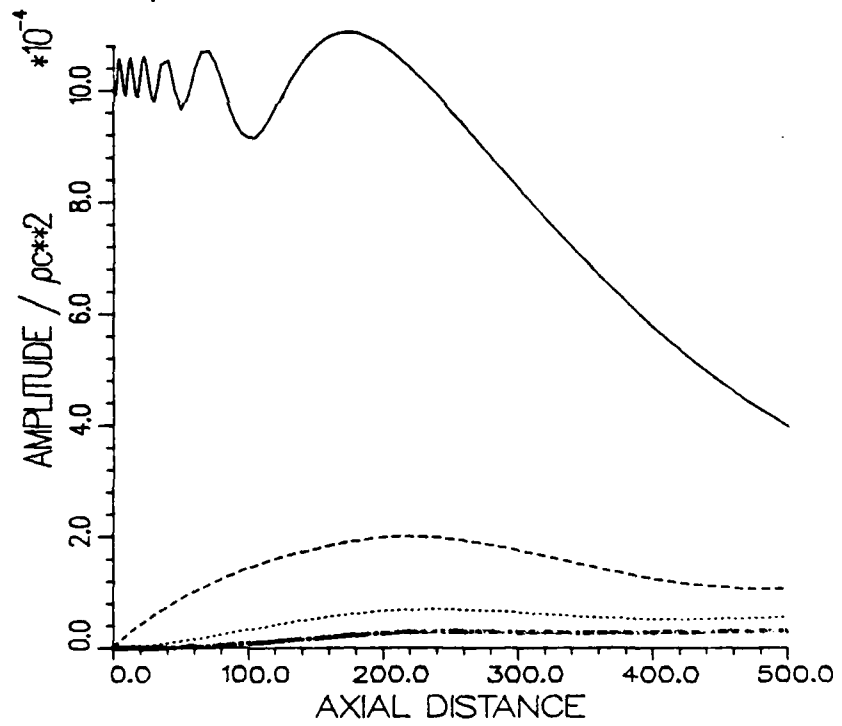
Same impedances previously obtained by
Bouwkamp. J.A.S.A. 1949

Resonant Membrane Transducer

G_T
Acoustics & Dynamics
Research Laboratory

Legend:
- Resonance # 1
- Resonance # 2
- Resonance # 3
- Resonance # 4
- Resonance # 5

Y-axis: Resistance (0.0, 25.0, 50.0, 75.0, 100.0, 125.0)

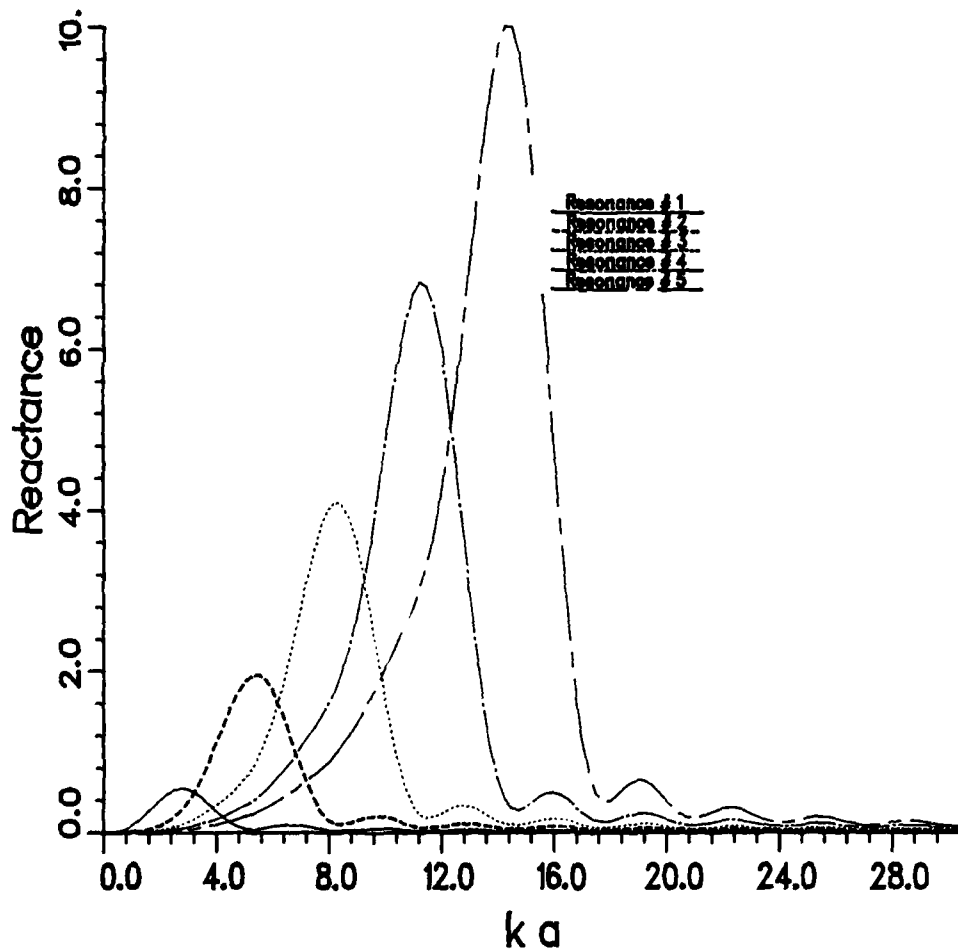X-axis: k a (0.0, 4.0, 8.0, 12.0, 16.0, 20.0, 24.0, 28.0)
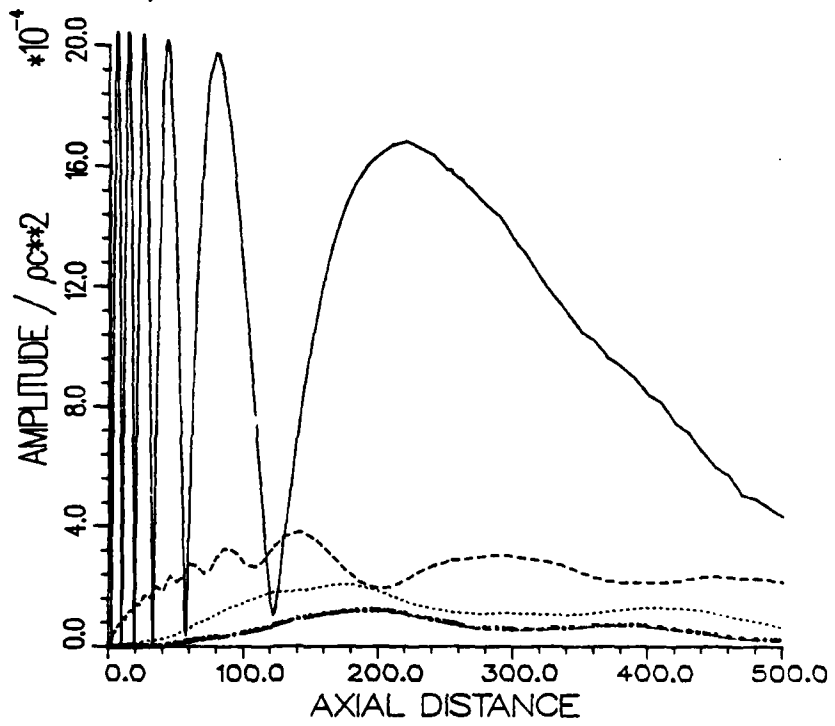
G_T Acoustics & Dynamics Research Laboratory

MEMBRANE, ka = 40

Resonant Membrane Transducer

GT
Acoustics & Dynamics
Research Laboratory

PISTON, ka = 40

OBSERVATION

Resonance $\Rightarrow \omega = \lambda_j c_w/a$

but $c_w \ll c_o$ because $\sigma_o < $ yield stress $\ll E$

Thus $ka = \lambda_j c_w/ c_o$ at resonance

NONLINEAR DISPLACEMENT EFFECTS ARE NOT IMPORTANT FOR MEMBRANES IN WATER EXCEPT FOR VERY HIGH ORDER RESONANCES

THE JOURNAL

of the

Acoustical Society of America

Program of the
110th Meeting

WEDNESDAY MORNING, 6 NOVEMBER 1985   DAVIDSON ROOM A, 9:00 TO 11:30 A.M.

Session S. Physical Acoustics IV: Nonlinear Acoustics

Joseph E. Blue, Chairman

Underwater Sound Reference Detachment, Naval Research Laboratory, P. O. Box 8337, Orlando, Florida 32856

9:30

S3. Fourier series representation of finite amplitude sound beams. Hsu-Chiang Miao and Jerry H. Ginsberg (School of Mechanical Engineering, Georgia Institute of Technology, Atlanta, GA 30332)

An earlier analysis of finite amplitude sound beams derived general expressions from the behavior in the off-axis region [J. H. Ginsberg, J. Acoust. Soc. Am. 76, 1201–1214 (1984)]. An asymptotic analysis of the region very close to the beam axis confirms the earlier result for the velocity potential. The signal is rewritten in a form that makes the contribution of each wavenumber in a continuous spectrum appear to be the sum of two waves traveling transversely, as well as axially. The coordinate transformations required to renormalize this form lead to a temporal Fourier series that is reminiscent of the Fuoini solution for finite amplitude planar waves. The complex amplitude of each harmonic is obtained from an integration over the transverse wavenumber. The computational efficiency of this representation permits extensive evaluation of propagation properties. An example compares the signal derived from a piston to that obtained from the one-dimensional assumption that $p = \rho c v_n$ on the boundary, which has been employed in prior investigations using approximate parabolic equations. [Work supported by ONR, Code 425-UA.]

Hyatt Regency Hotel
Nashville, Tennessee
4–8 November 1985

THE JOURNAL

of the

Acoustical Society of America

**Program of the
110th Meeting**

WEDNESDAY MORNING, 6 NOVEMBER 1985   DAVIDSON ROOM A, 9:00 TO 11:30 A.M.

Session S. Physical Acoustics IV: Nonlinear Acoustics

Joseph E. Blue, Chairman
Underwater Sound Reference Detachment, Naval Research Laboratory, P. O. Box 8337, Orlando, Florida 32856

S4. Finite amplitude acoustic waves generated by a baffled dual frequency transducer. Mosaad A. Foda and Jerry H. Ginsberg (School of Mechanical Engineering, Georgia Institute of Technology, Atlanta, GA 30332)

In a previous presentation [J. Acoust. Soc. Am. Suppl. 1 **75**, S92 (1984)], a nonuniformly accurate expression for the velocity potential was derived using a singular perturbation procedure. The linearized signal was represented by a dual King integral, and the cumulative growth was evaluated asymptotically. In this paper, the renormalization version of the method of strained coordinates is employed to annihilate the secular terms. The result is a uniformly valid expression for the acoustic pressure at all locations preceding the formation of a shock. Additional discussion is devoted to a simpler model that interfaces the dual frequency King integral in the nearfield with nonlinear spherical distortion in the farfield. The results obtained from both descriptions in the case of a parametric array (proximate primary frequencies) agree better than earlier theories with previous measurements performed for a wide range of parameters [Work supported by ONR, Code 425-UA.]

**Hyatt Regency Hotel
Nashville, Tennessee
4–8 November 1985**

FINITE AMPLITUDE ACOUSTIC WAVES GENERATED

BY A BAFFLED DUAL FREQUENCY TRANSDUCER

M. A. FODA

J. H. GINSBERG

SCHOOL OF MECHANICAL ENGINEERING
GEORGIA INSTITUTE OF TECHNOLOGY

ARBITRARY EXCITATION OF TWO PRIMARIES

Cylindrical Coordinate (R, z)

BOUNDARY CONDITION :

$$v_z = \frac{\epsilon}{2i} \left[\epsilon_1 f_1(R) \exp(i\omega_1 t) + \epsilon_2 f_2(R) \exp(i\omega_2 t) \right] + C.C.$$

C.C. denotes Complex Conjugate

where

$$\epsilon_j = \hat{\epsilon}_j / \epsilon$$

$\hat{\epsilon}_j = j^{th}$ frequency component Mach number

ϵ = source Mach number

$f_j(R)$: $R f(R)$ is piecewise continuous and absolutely integrable over $0 \rightarrow \infty$

FIRST ORDER SOLUTION FOR THE VELOCITY POTENTIAL DUAL FREQUENCY KING INTEGRAL

$$\varphi_1 = -\int_0^\infty \left\{ \left[\frac{nV_1}{\mu_n} \exp[w_1(it - \mu_n z)] \right] J_0(w_1 nR) \right.$$

$$\left. + \frac{nV_2}{\mu_n} \exp[w_2(it - \mu_n z)] J_0(w_2 nR) \right\} dn$$

$$+ C.C.$$

(a) Hankel transforms of the transducer vibration are V_1 and V_2

(b) Transverse wave number is n.

(c) Axial wave number is

$$\mu_n = \begin{cases} i(1 - n^2)^{1/2} & ; \ 0 \leq n \leq 1 \ \text{(propagating)} \\ (n^2 - 1)^{1/2} & ; \ n > 1 \ \text{(evanescent)} \end{cases}$$

SECOND ORDER POTENTIAL

Signal at the sum of any two frequencies:

$$\Phi_2 = \Phi_2^{2\omega_1} + \Phi_2^{2\omega_2} + \Phi_2^{\omega_1+\omega_2} + \Phi_2^{\omega_1-\omega_2}$$

$$\Phi_2^{(\omega_j+\omega_\ell)} = \int_0^\infty 2i\left[\tfrac{1}{2}\omega_j\omega_\ell(\omega_j+\omega_\ell)\right]^{\tfrac{1}{2}} n^2 \frac{V_j V_\ell}{\mu_n \mu_n} (\pi\mu_n z)^{\tfrac{1}{2}} \times$$

$$\exp\left[(\omega_j+\omega_\ell)(it-\mu_n z)\right]\left[J_0(\omega_j nR)J_0(\omega_\ell nR) - J_1(\omega_j nR)J_1(\omega_\ell nR)\right] dn$$

$$\underline{\hspace{3cm}} + C.C. + Subdominant\ terms$$

appears only if j≠ℓ

Similar form for difference frequency

The expression for the acoustic pressure is not uniformly accurate

$$P = -\int_0 c_0^2 \left(\epsilon \frac{\partial \Phi_1}{\partial t} + \epsilon^2 \frac{\partial \Phi_2}{\partial t}\right)$$

SECOND ORDER SOURCE TERMS

EQUATION GOVERNING THE SECOND ORDER POTENTIAL

$$\nabla^2 \Phi_2 - \frac{\delta^2 \Phi_2}{\delta t^2} \sim \sum_{j,l} \int_o^\infty \int_o^\infty m \, n \cdots \left\{ \begin{array}{l} J_o(w_j nR) J_o(w_l mR) \\ J_1(w_j nR) J_1(w_l mR) \end{array} \right\} \times$$

$$exp\left[i(w_j \pm w_l)t - (w_j \mu_n \pm w_l \mu_m)z\right] dn \, dm$$

Particular solutions ==> Consist of:
second harmonics, sum and difference frequencies
(1) Form suggested by method of variations of
    parameters
(2) Secularity as m→n
(3) General solution when m≠n must match
    particular solution when m=n
(4) Asymptotic integration by Laplace's method
(5) Procedure as by Ginsberg JASA (1984)

RENORMALIZATION OF THE SIGNAL
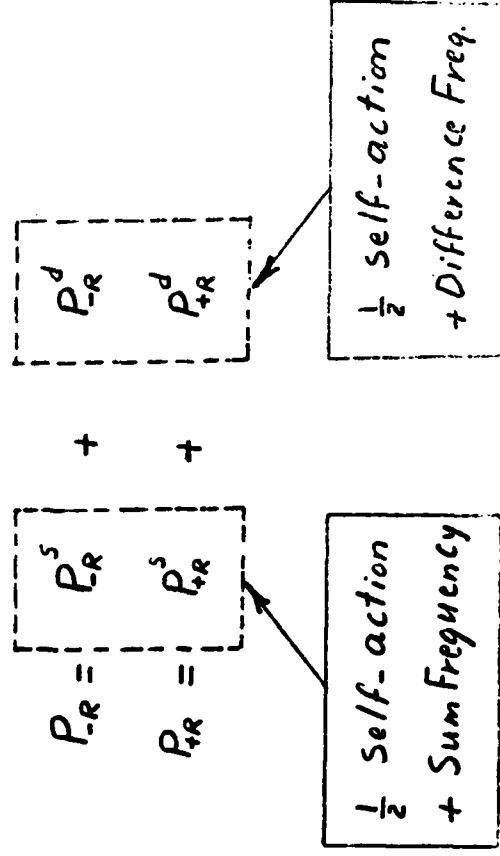
Study behavior off-axis, then match back to R<<1.

Signal off-axis ==> pairs of interacting cylindrical waves: inward and outward.

Each propagates in postive axial direction.

Renormalize each cylindrical wave independently.

Split up cylindrical waves:

$$P_{-R} = \boxed{\begin{array}{c} P^s_{-R} \\ + \\ P^s_{+R} \end{array}} + \boxed{\begin{array}{c} P^d_{-R} \\ \\ P^d_{+R} \end{array}}$$

$$P_{+R} =$$

$$\boxed{\frac{1}{2} \text{ self-action} + \text{SumFrequency}}$$

$$\boxed{\frac{1}{2} \text{ self-action} + \text{Difference Freq.}}$$

Four coordinate transformations.

Match back to forms that are valid for all R.

QUANTITATIVE EVALUATION

(1) Discretize transverse wave number spectrum.
(2) Evaluate coordinate transformations.

Numerical computation is very intensive because:

    (a) Resolution in wave number
    (b) Coordinate transformations
    (c) Resolution in time domain

ALTERNATIVE ALGORITHMS

Farfied of piston transducer: Lockwood (1971) ARL
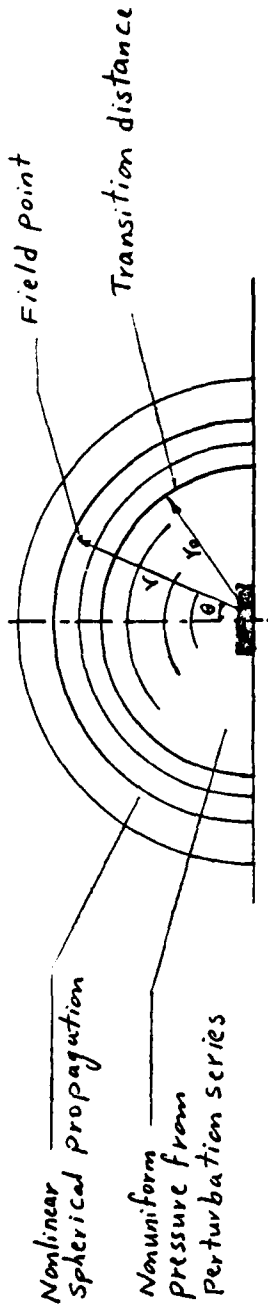
Axisymmetric spherical coordinates (r, θ)

Given : $P(r_o, \theta, t) = \epsilon \sum_i F_i(\theta, \omega_i t)$

then $P(r, \theta, t) = \epsilon \frac{r_o}{r} \sum_i F_i[\theta, \omega_i(t - \alpha - r_o)]$

where : $r = \alpha + \beta \alpha \ln(\alpha / r_o) P$

Solve a single transcendental equation

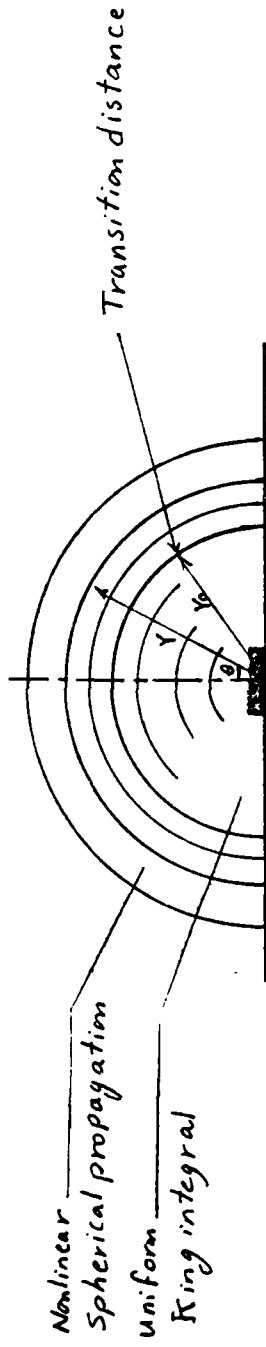# METHOD I - NONUNIFORM SPHERICAL PROPAGATION (NSP)

Nonlinear Spherical propagation

Nonuniform pressure from Perturbation series

Field Point

Transition distance

Interface with spherical model using

$$P(r_o, \theta, t) = \sum \sum_{n,m=0,1,2} (A_{nm})_o \sin[(nw_1 t + mw_2 t) - (\alpha_{nm})_o]$$

(1) Select spherical boundary r_o.

(2) Evaluate signal at the transition distance from the nonuniform pressure expression.

(3) Excitation ==> amplitudes and phases: primaries. 2 nd harmonics. sum and difference frequencies.

(a) No coordinate straining required.

(b) Input frequency response given directly.

(c) Not a thorough description of distortion in the nearfield.

METHOD II - UNIFORM SPHERICAL PROGAGATION (USP)

Nonlinear
Spherical propagation
uniform
King integral

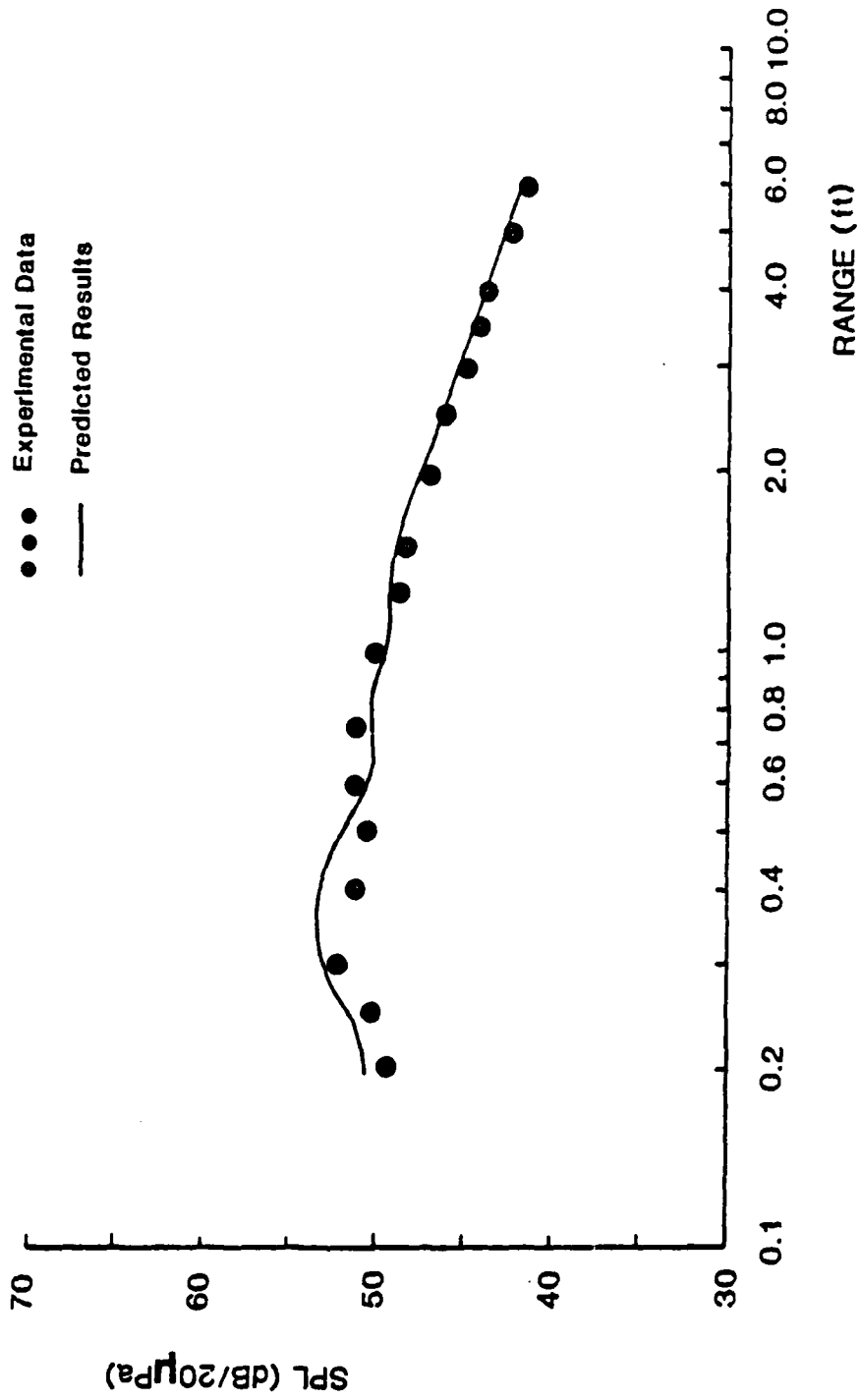*Transition distance*

Interface with spherical model using

$$P(r_o, \theta, t) = \sum \sum_{n,m=0,1,2,\ldots} (A_{nm})_o \sin[(n\omega_1 t \pm m\omega_2 t) - (N_{nm})_o]$$

(1) Employ nonlinear King integral to find the signal at the transition distance r_o.

(2) Two dimensional Fourier series yields frequency response at transition to farfield.

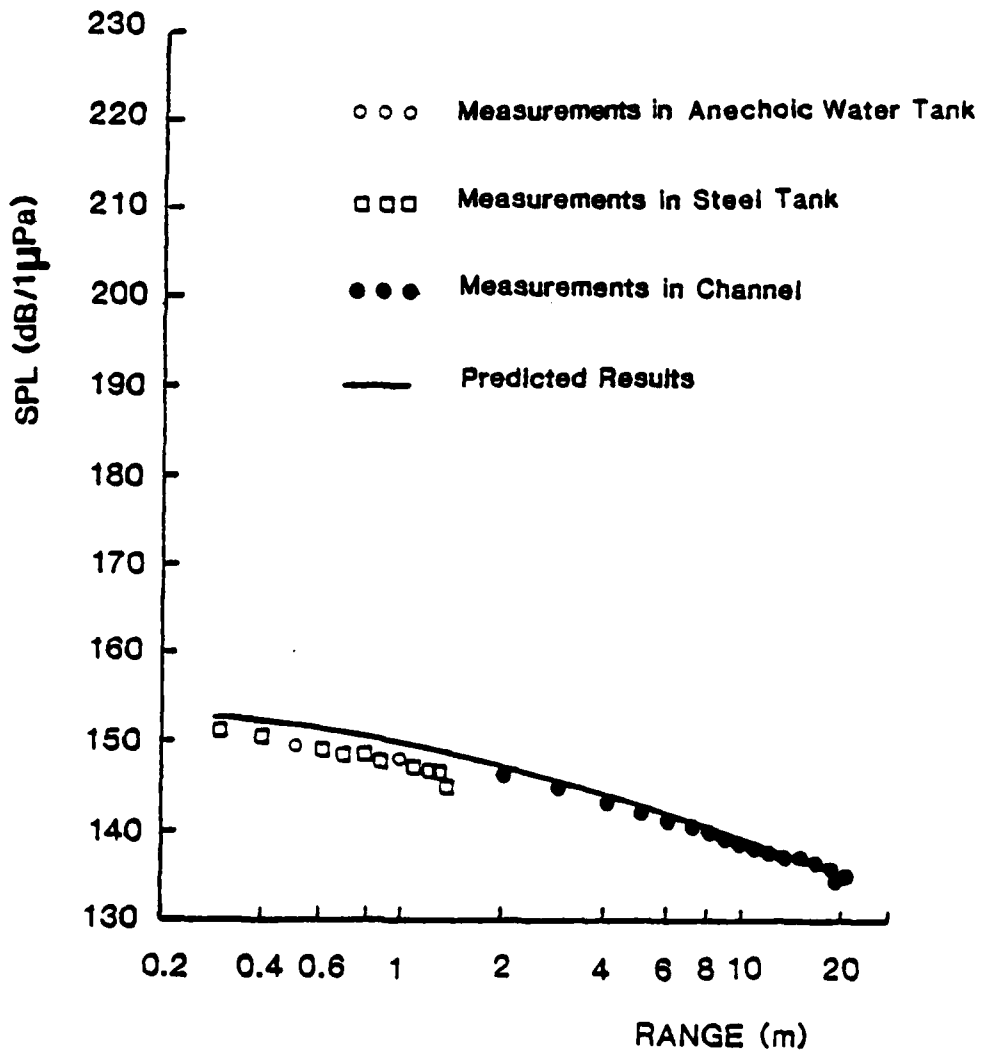(3) Use this signal to generate nonlinear spherical wave at $r > r_o$.

(a) Efficient algorithim.

(b) USP model results are very close to the King integral. *Rayleigh length* $r_o = \frac{1}{2} k_o a^2$
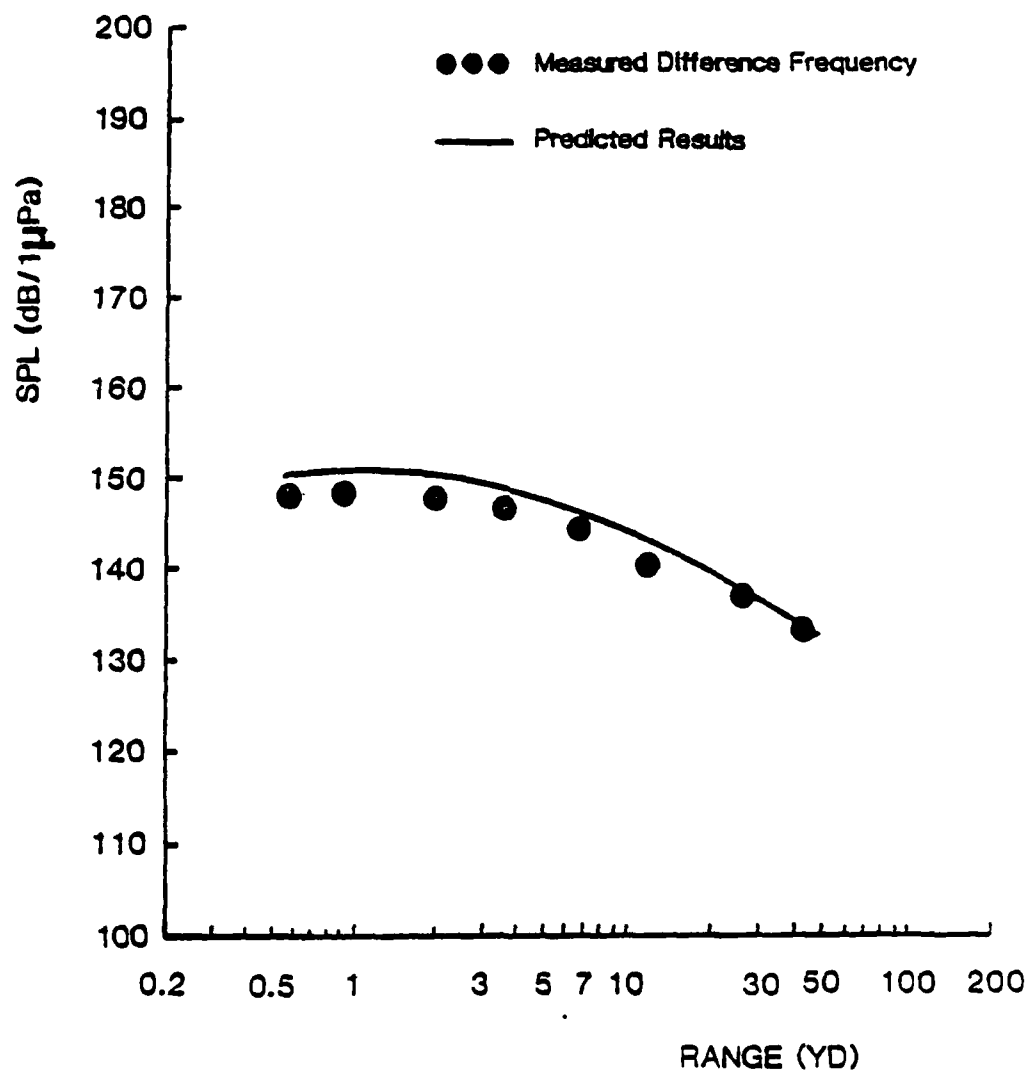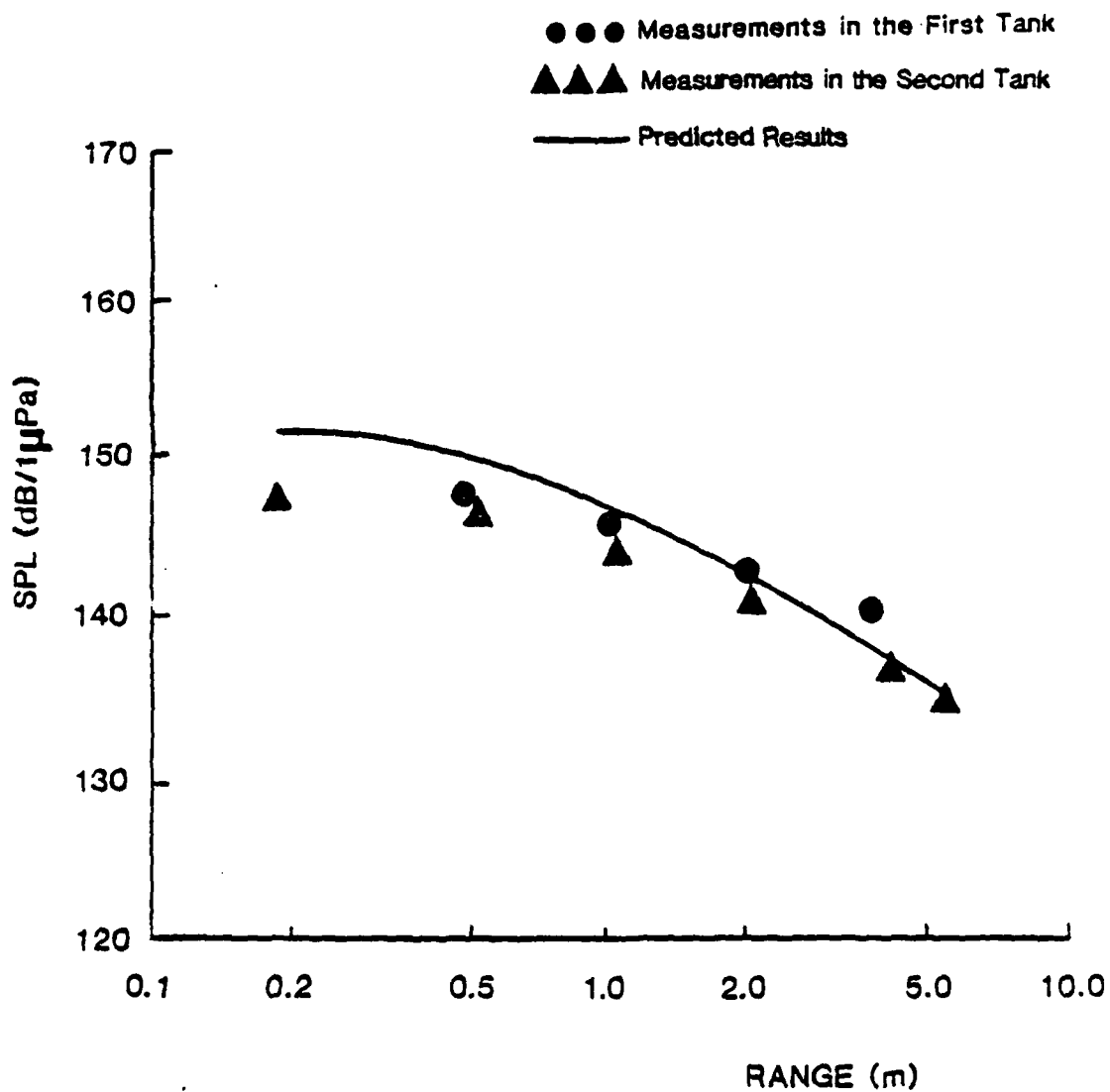
Bennett and Blackstock JASA (1975)

RANGE (ft)

SPL (dB/20μPa)

• • • Experimental Data
—— Predicted Results

Bjorno et al ACUSTICA (1976)

Muir and Willette JASA (1972)

Figure shows a plot with SPL (dB/1μPa) on the vertical axis (ranging from 100 to 200) versus RANGE (YD) on the horizontal logarithmic axis (0.2 to 200). Legend: ●●● Measured Difference Frequency; — Predicted Results.
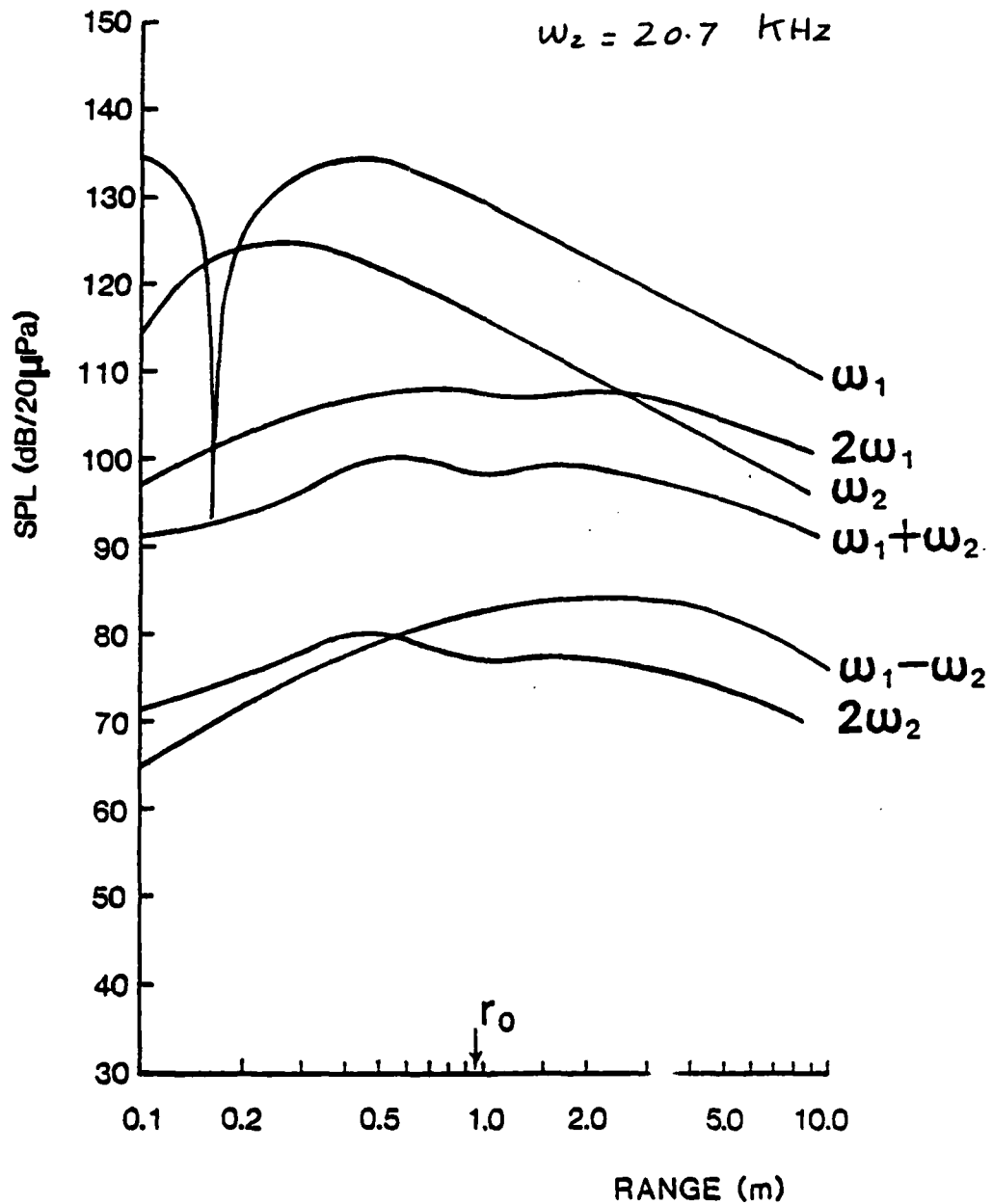
Eller JASA (1974)

Waveform for Bennett and Blackstock Data at z=18m and Primary Frequencies of 25 KHz and 20 KHz
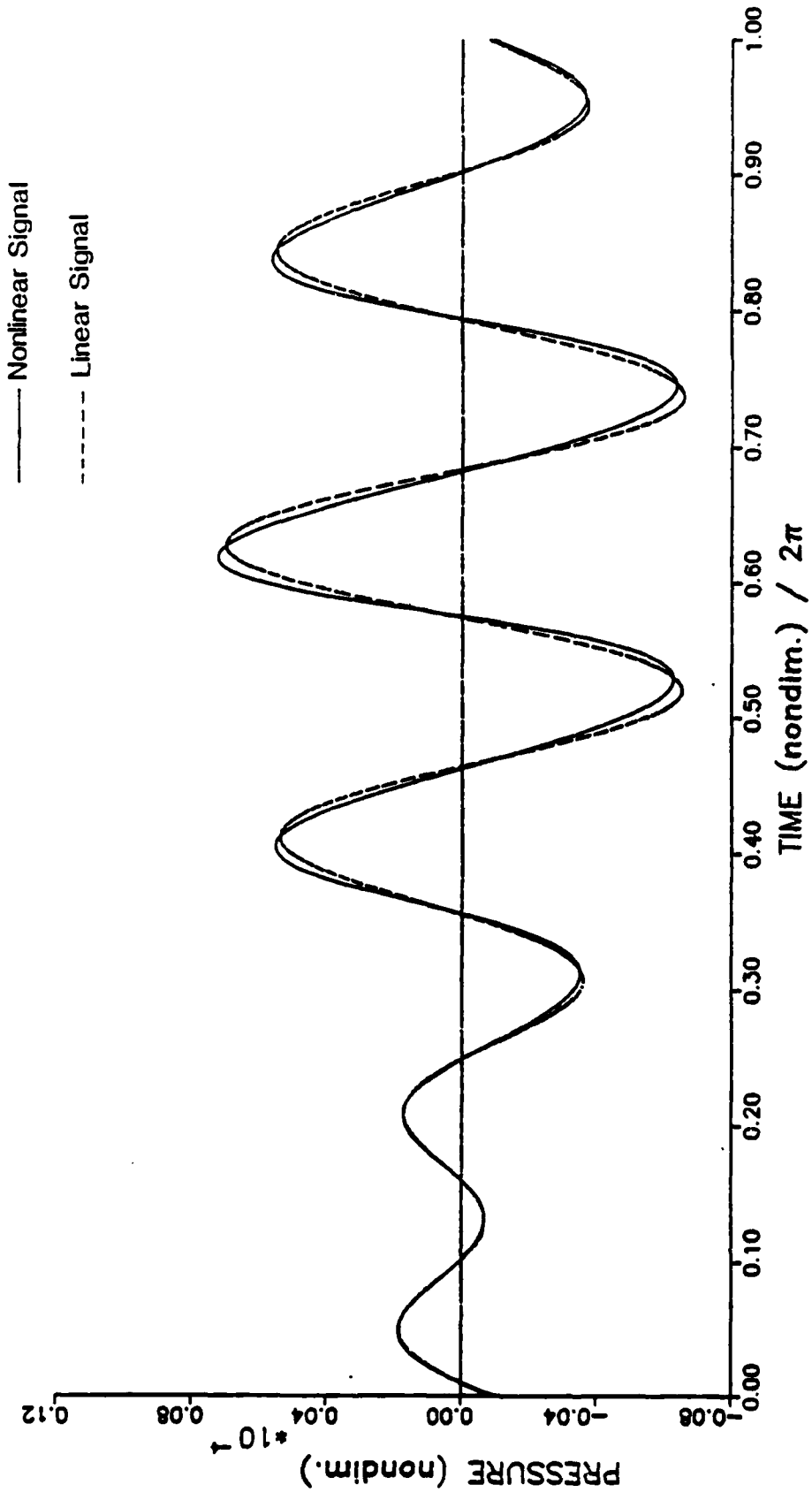
Fundamentals, Second Harmonics, Sum and Difference Frequency Signals, $K_o a = 30$

$\omega_1 = 30.5$ KHz
$\omega_2 = 20.7$ KHz

CONCLUSIONS

(1) General King integral is valid for arbitrary frequencies.

(2) Improved agreement in parametric array configuration between the prediction from the present model and experiments ==> interactions in the Fresnel zone are important.

(3) Computional time for the King integral increases as the propagation distance increases.

(4) Switching from nonlinear King integral to nonlinear spherical wave results in an efficient model.

(5) Experimental work is needed to obtain propagation characteristics, waveforms, and phase measurments for arbitrary frequency combinations.

END

FILMED

3-86

DTIC